

## Manual For Model 205/205a

# Torsional Control System

(Instructor's Edition)

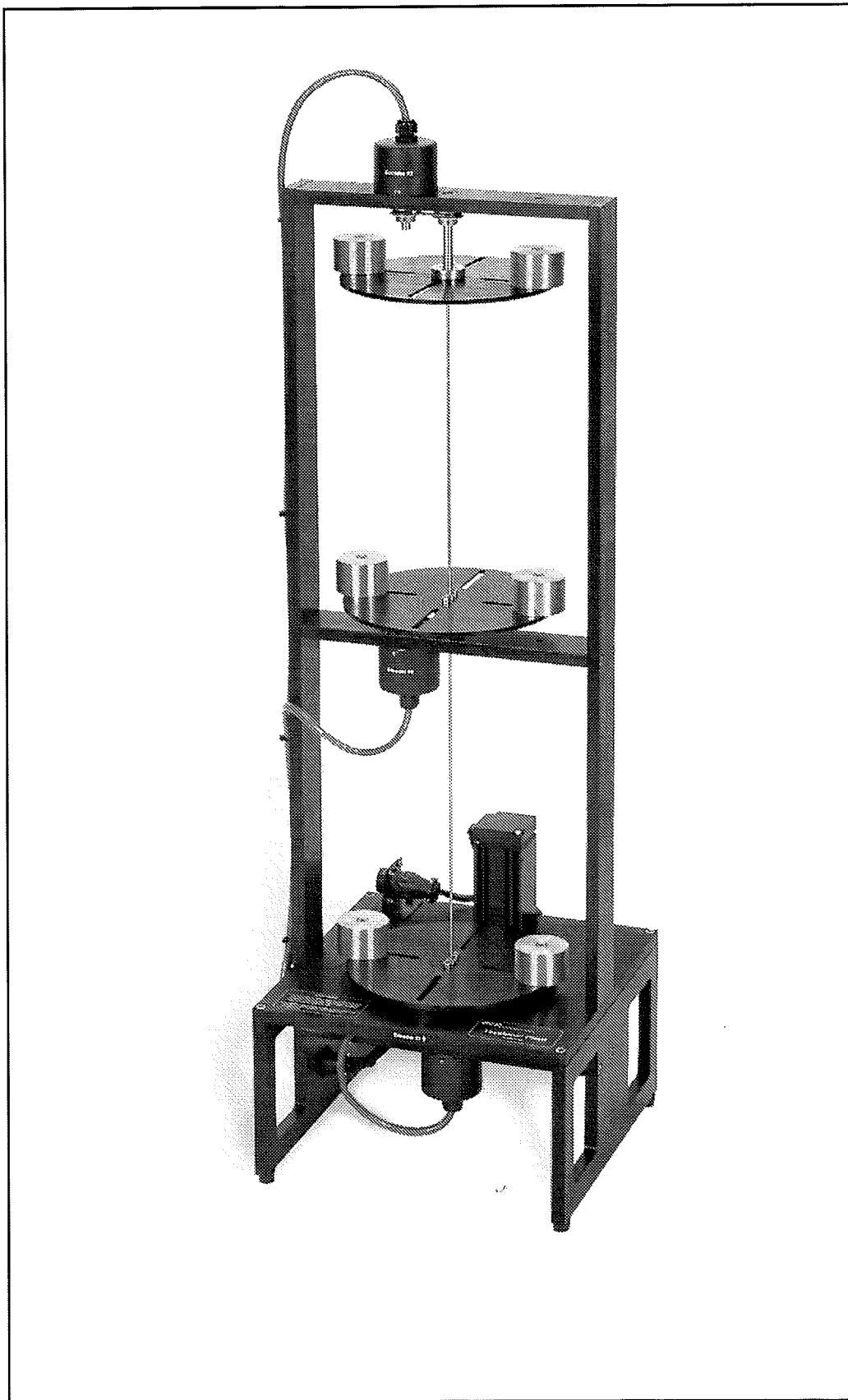
### Important Notice

Section 2.3 of this manual contains important safety information that must be read by all users prior to operating the ECP system.

**Created & Edited By:  
Thomas R. Parks**

This manual is for use in conjunction with ECP experimental systems only and may be reproduced only for that purpose. All other use, dissemination, or reproduction in whole or in part without the written permission of ECP is strictly prohibited.

© COPYRIGHT 1991-1999 by ECP, Educational Control Products. All rights reserved.



**The Model 205a Torsion Spring / Inertia Apparatus**

# CONTENTS

<b>1</b>	<b>Introduction</b>	<b>1</b>
1.1	System Overview	1
1.2	Manual Overview	2
<b>2</b>	<b>System Description &amp; Operating Instructions</b>	<b>3</b>
2.1	ECP Executive Software	3
2.2	Electromechanical Plant	31
2.3	Safety	38
<b>3</b>	<b>Start-up &amp; Self-Guided Demonstration</b>	<b>41</b>
3.1	Hardware Set-up Verification	41
3.2	Demonstration Of ECP Executive Program	43
3.3	Nonintuitive System Behavior	51
<b>4</b>	<b>Real-time Control Implementation</b>	<b>52</b>
4.1	Servo Loop Closure	53
4.2	Command Generation	56
4.3	Servo Motor & Amplifier	60
4.4	Multi-tasking Environment	64
4.5	Sensors	65
4.6	Auxiliary Analog Output	67
<b>5</b>	<b>Plant Dynamic Models</b>	<b>68</b>
5.1	Two Degree of Freedom Plants	68
5.2	Three Degree of Freedom Plants (Model 205a only)	70
<b>6</b>	<b>Experiments</b>	<b>73</b>
6.1	System Identification	73
6.2	Rigid Body PD & PID Control	78
6.3	Disturbance Rejection of Various Controllers	84
6.4	Colocated PD With 2 DOF Plant	86
6.5	Noncolocated PD Plus Notch Filter	88
6.6	Successive Loop Closure / Pole Placement	91
6.7	LQR Control	95
6.8	Practical Control Implementation	98
6.8.1	Effect of Drive Saturation	98
6.8.2	Effect of Discrete-time Sampling	99
6.8.3	Effect of Finite Wordlength & Sensor Quantization	100

<b>A</b>	<b>Dynamic Modeling Details</b>	<b>103</b>
A.1	Dynamics Of Ideal Plant	103
A.2	Practical Plant Model	109
A.3	One Degree Of Freedom Plants	113
A.4	Three Degree of Freedom Plants (Model 205a only)	114

**(Instructor's Manual Only)**

<b>6i</b>	<b>Instructor's Supplement To Experiments</b>	<b>118</b>
6.1i	System Identification	119
6.2i	Rigid Body PD & PID Control	125
6.3i	Disturbance Rejection of Various Controllers	135
6.4i	Colocated PD With 2 DOF Plant	139
6.5i	Noncolocated PD Plus Notch Filter	148
6.6i	Successive Loop Closure / Pole Placement	156
6.7i	LQR Control	164
6.8i	Practical Control Implementation	169
6.8.1i	Effect of Drive Saturation	169
6.8.2i	Effect of Discrete-time Sampling	172
6.8.3i	Effect of Finite Wordlength & Sensor Quantization	174
6.9i	Sensitivity to Parameter Changes	175
6.10i	Effect of Doutput Disturbance On Multi-DOF Systems	177
6.10i	Suggested Further Experiments	180
<b>Ai</b>	<b>Useful Scripts</b>	<b>184</b>
A.1i	Plant Model Builder	184
A.2i	Notch Filter Designer	186
A.3i	Successive Loop Control Designer	186
A.2i	LQR Synthesis	188



## 1 Introduction

Welcome to the ECP line of educational control systems. These systems are designed to provide insight to control system principles through hands-on demonstration and experimentation. Seen in Figure 1.1-1, each consists of an electromechanical plant and a full complement of control hardware and software. The user interface to the system is via a user-friendly, PC window environment which supports a broad range of controller specification, trajectory generation, data acquisition, and plotting features. The systems are designed to accompany introductory through advanced level controls courses and support either high level usage (i.e. direct controller specification and execution) or detailed user-written algorithms.

The electromechanical apparatus may be transformed into a variety of dynamic configurations which represent important classes of "real life" systems. The Model 205 torsional mechanism represents many such physical plants including rigid bodies; flexibility in drive shafts, gearing and belts; and coupled discrete vibration with actuator at the drive input and sensor collocated or at flexibly coupled output (noncollocated). Thus the plant models may range from a simple double integrator to a fourth order<sup>1</sup> case with two lightly damped poles and either two or no zeros.

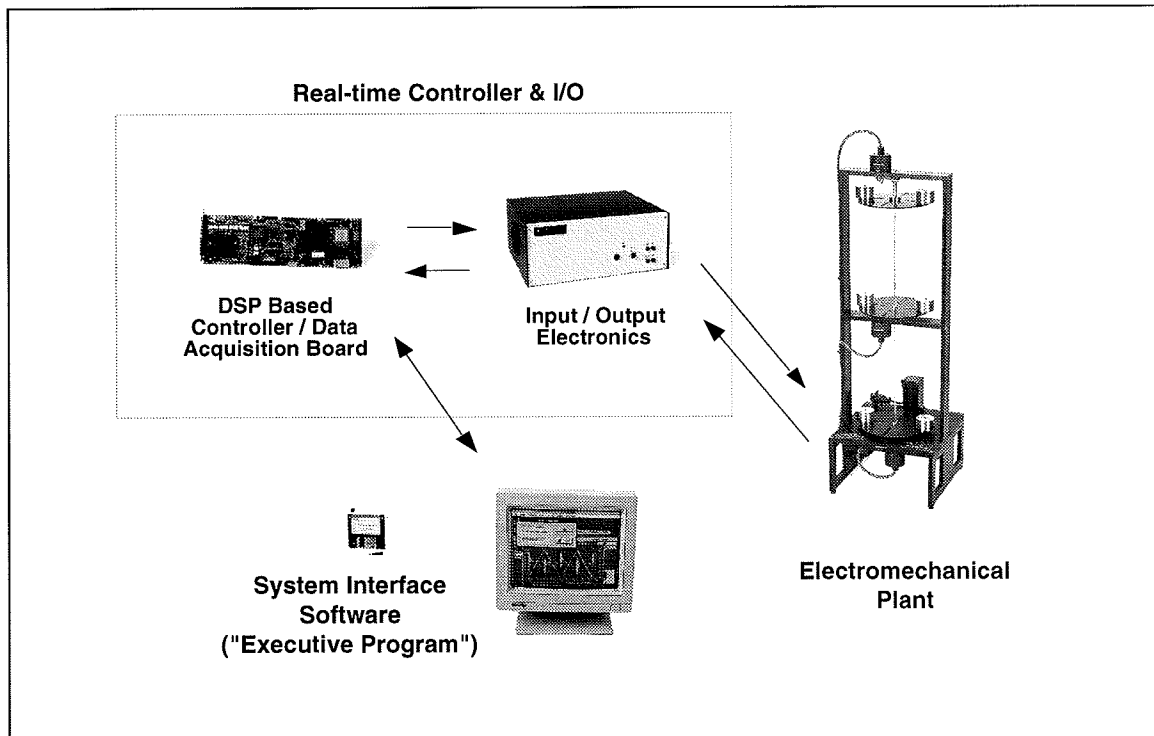


Figure 1.1-1. The Model 205 Experimental Control System

<sup>1</sup> For Model 205a the model order may be as high as six with either four, two, or no zeros.

## 1.1 System Overview

The experimental system is comprised of the three subsystems shown in Figure 1.1-1. The first of these is the electromechanical plant which consists of the torsion mechanism, its actuator and sensors. The design features a brushless DC servo motor, high resolution encoders, adjustable inertias, and reconfigurable plant type.

The next subsystem is the real-time controller unit which contains the digital signal processor (DSP) based real-time controller<sup>1</sup>, servo/actuator interfaces, servo amplifiers, and auxiliary power supplies. The DSP is capable of executing control laws at high sampling rates allowing the implementation to be modeled as continuous or discrete time. The controller also interprets trajectory commands and supports such functions as data acquisition, trajectory generation, and system health and safety checks. A logic gate array performs motor commutation and encoder pulse decoding. Two optional auxiliary digital-to-analog converters (DAC's) provide for real-time analog signal measurement. This controller is representative of modern industrial control implementation.

The third subsystem is the executive program which runs on a PC under the DOS or Windows<sup>TM</sup> operating system. This menu-driven program is the user's interface to the system and supports controller specification, trajectory definition, data acquisition, plotting, system execution commands, and more. Controllers may assume a broad range of selectable block diagram topologies and dynamic order. The interface supports an assortment of features which provide a friendly yet powerful experimental environment.

## 1.2 Manual Overview

The next chapter, Chapter 2, describes the system and gives instructions for its operation. Section 2.3 contains important information regarding safety and is mandatory reading for all users prior to operating this equipment. Chapter 3 is a self-guided demonstration in which the user is quickly walked through the salient system operations before reading all of the details in Chapter 2. A description of the system's real-time control implementation as well as a discussion of generic implementation issues is given in Chapter 4. Chapter 5 presents dynamic equations useful for control modeling. Chapter 6 gives detailed experiments including system identification and a study of important implementation issues and practical control approaches.

---

<sup>1</sup> The system is also available in a PC bus installation form in which the DSP based real-time controller resides in the PC and all other control unit hardware remains in a separate box. This form has faster PC/controller communication rates. (Controller speed is unaffected.)

## **2 System Description & Operating Instructions**

This chapter contains descriptions and operating instructions for the executive software and the mechanism. The safety instructions given in Section 2.3 must be read and understood by any user prior to operating this equipment.

### **2.1 ECP Executive Software**

The ECP Executive program is the user's interface to the system. It is a menu driven / window environment that the user will find is intuitively familiar and quickly learned - see Figure 2.1-1. This software runs on an IBM PC or compatible computer and communicates with ECP's digital signal processor (DSP) based real-time controller. Its primary functions are supporting the downloading of various control algorithm parameters (gains), specifying command trajectories, selecting data to be acquired, and specifying how data should be plotted. In addition, various utility functions ranging from saving the current configuration of the Executive to specifying analog outputs on the optional auxiliary DAC's are included as menu items.

#### 2.1.1 The DOS Version of the Executive Program

##### 2.1.1.1 PC System Requirements

For the ECP Executive (DOS version), you will need at least 2 megabyte of RAM and a hard disk drive with at least 4 megabytes of space. All DOS versions of the Executive program run under any of DOS versions 3.x, 4.x, 5.x, and 6.x. The Executive requires a VGA monitor with a VGA graphics card installed on the PC.

The Executive Program runs best on a 386, 486, or Pentium® based PC with 4 megabytes or more of memory under DOS 5.0 or higher with HIGHMEM.SYS driver included in your CONFIG.SYS file.<sup>1</sup> Also, if the software does not "see" at least 2 megabytes of free RAM, you may find the program executing somewhat slowly since it will use the hard disk as virtual memory.

---

<sup>1</sup>A faster computer, such as a ≥66 Mhz 486 with the real-time controller on the PC bus provides a much more expeditious working environment than a 386 or 286 and/or RS232 controller/PC communication. Real-time control speed, however, is unaffected.

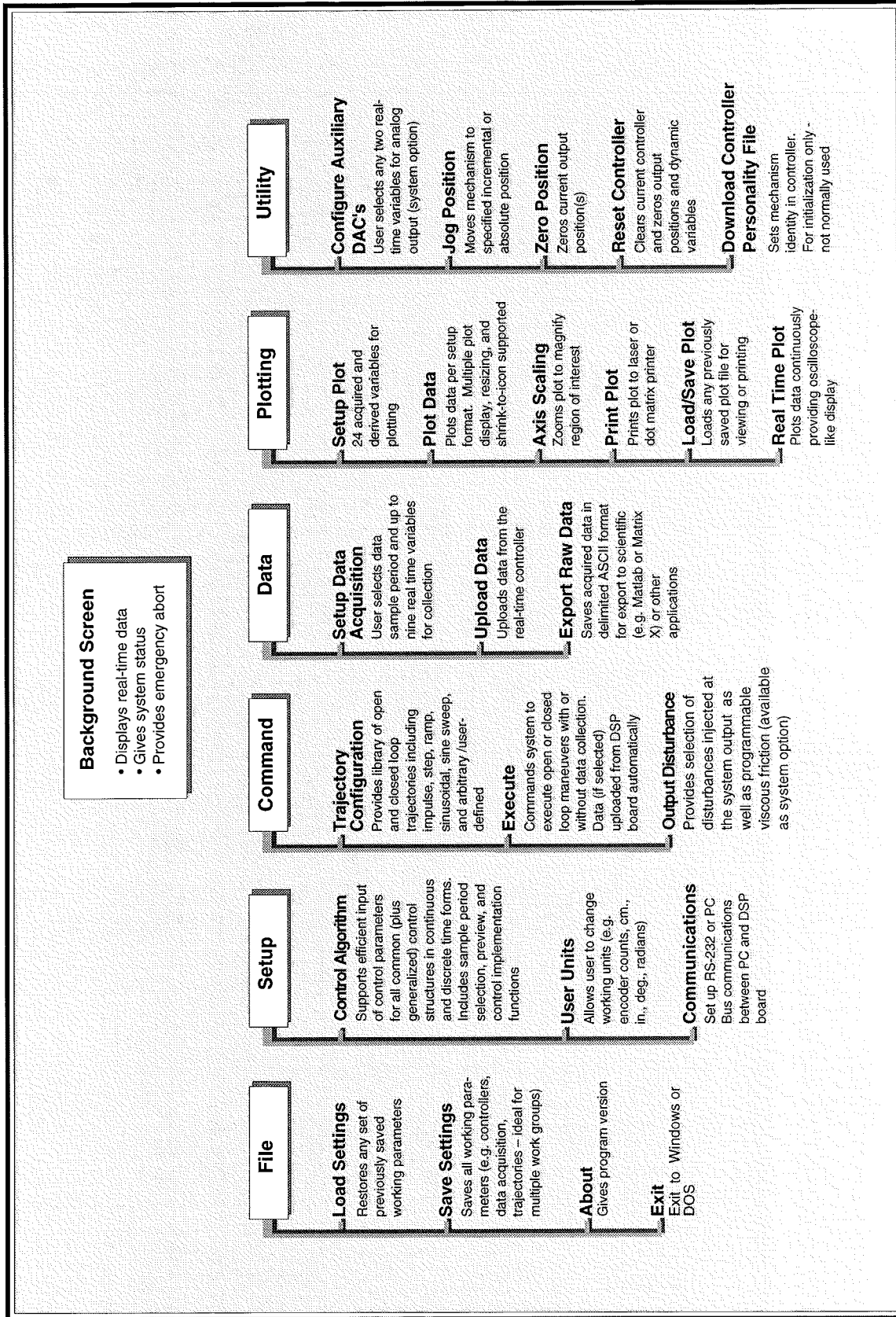


Figure 2.1-1. Structure and Key Features of Executive Program

### 2.1.1.2 Installation Procedure For The DOS Version

The ECP Executive Program consists of several files on a 3.25" 1.44 megabyte distribution diskette in a compressed form. The key files on the distribution diskette are:

```
ECP.EXE
ECP.DAT
ECPBMP.DAT
*.CFG
*.PLT
*.PMC
```

The "ECP\*. \*" files are needed to run the Executive Program. The "\*.CFG" and "\*.PLT" files are some driving function configuration and plotting files that are included for the initial self-guided demonstration. The "\*.PMC" file is the controller Personality File and should only be used in the case of a non curable system fault (see Utility Menu below).

To install the Executive program, it is recommended that you make a dedicated sub directory on the hard disk and enter this sub directory. For example type:

```
>MD ECP
>CD ECP
```

Next insert the distribution diskette in either "A:" or "B:" drive, as appropriate. Copy all files in the distribution diskette to the hard disk under the "ECP" sub directory. For example if the "B:" drive is used:

```
>COPY B:*. * C:
```

Next execute INSTALL.EXE by typing:

```
>INSTALL
```

You will notice some file decompression activities. This completes the installation procedure. You may run the ECP Executive by typing:

```
>ECP
```

The Executive program is window based with pull-down menus and dialog boxes. You may either use the cursor keys on the keyboard or a mouse to make selections from the pull-down menus. Vertical movement within these menus is accomplished by the up and down arrow keys, respectively. To make a selection with the keyboard, simply highlight the desired choice and press <ENTER>. Menu choices with highlighted letters may also be selected by pressing the corresponding function key. (The indicated key for menus; "alt" plus the indicated key within dialog boxes).

Within dialog boxes, movement from one object to the next is accomplished by using the <TAB> and the <SHIFT-TAB> keys. Here, "objects" includes input lines, check boxes, and "radio buttons". As you move from one object to the next, the selected object is highlighted. Pressing <ENTER> will effect the function of the highlighted button (e.g. termination of the dialog box will result if the Cancel button is highlighted).

### 2.1.2 The Windows Version of the Executive Program

#### 2.1.2.1 PC System Requirements

The ECP Executive 16-bit code runs on any PC compatible computer under Windows 3.1x and/or Windows 95. You will need at least 8 megabyte of RAM and a hard disk drive with at least 12 megabytes of space. The 16-bit Windows version of the Executive Program runs best with Pentium® based PC having 16 megabytes or more of memory.

#### 2.1.2.2 Installation Procedure For The Windows Version

The ECP Executive Program consists of several files on two 3.25" 1.44 megabyte distribution diskettes in a compressed form. The key files on the distribution diskettes are:

ECP.EXE  
ECP.DAT  
ECPBMP.DAT  
\*.CFG  
\*.PLT  
\*.PMC

The "ECP\*.\*" files are needed to run the Executive Program. The "\*.CFG" and "\*.PLT" files are some driving function configuration and plotting files that are included for the initial self-guided demonstration. The "\*.PMC" file is the controller Personality File and should only be used in the case of a non curable system fault (see "Utility Menu" below).

To install the Executive program enter the Windows operating system. Then go to the "Run" menu, and simply run the SETUP.EXE file from diskette labeled 1. Follow the interactive dialog boxes of the installation program until completion.

### 2.1.3 Background Screen

The *Background Screen*, shown in Figure 2.1.-1, remains in the background during system operation including times when other menus and dialog boxes are active. It contains the main menu and a display of real-time data, system status, and an *Abort Control* button to immediately discontinue control effort in the case of an emergency.

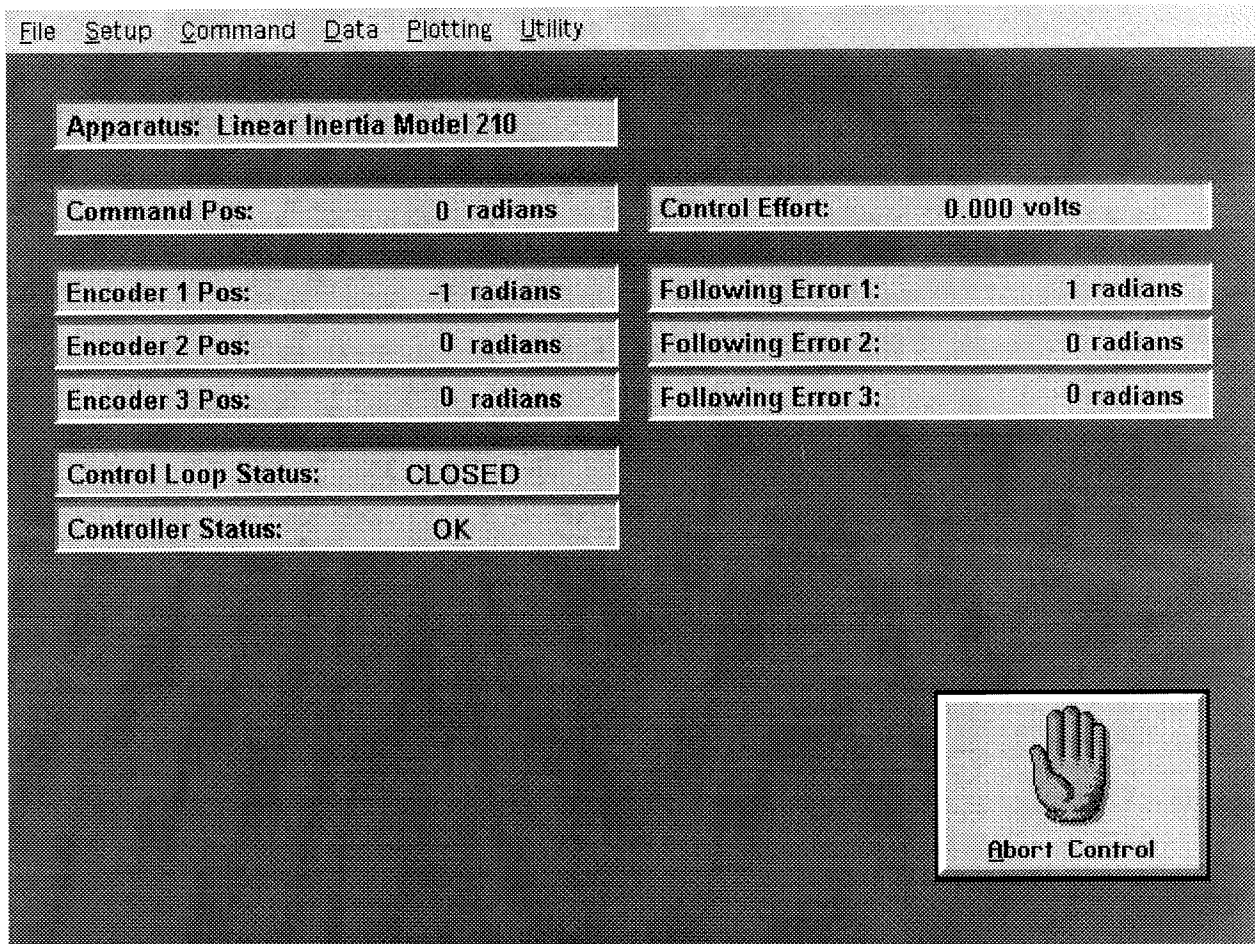


Figure 2.1-1. The Background Screen

#### 2.1.3.1 Real-Time Data Display

In the *Data Display* fields, the instantaneous commanded position, the encoder positions, the following errors (instantaneous differences between the commanded position and the actual encoder positions), and the control effort in volts (on the DAC) are shown.

#### 2.1.3.2 System Status Display

The Control Loop Status ("Open" or "Closed"), indicates "Closed" unless an open loop trajectory is being executed or a "Limit Exceeded" condition has occurred. In either of these cases the Control Loop Status will indicate "Open". The Controller Status will indicate "Active" unless a motor over-speed, a shaft over-deflection, or motor/amplifier over-temperature condition has occurred (see

Section 2.3 for more details). In any of these cases the Controller Status will indicate "Limit Exceeded". The Limit Exceeded indicator will reoccur unless the user takes one of the two following actions depending on the nature of the over-limit cause. Either a stable controller (one that does not cause limiting conditions) must be implemented via the Control Algorithm box under the Setup menu or an acceptable trajectory must be executed under the Command menu. An "acceptable" trajectory is one that does not over-speed the motor, over-deflect the flexible shaft or result in sustained high current to the motor. The controller must be "re implemented" in order to clear the Limit Exceeded condition – see Section 2.1.5.1.1.

The Disturbance Status field will indicate "Active" when the viscous friction disturbance is invoked and/or when a disturbance torque profile is selected during a trajectory execution. It will otherwise indicate "Not Active" unless, due to disturbance motor amplifier over-current or load shaft over-speed, a "Limit Exceeded" condition develops. In this situation the "Limit Exceeded" indication will continue to appear until a new disturbance torque is implemented which does not cause a limit exceeding condition. Note that the disturbance drive is optional for the Model 205 system.

#### 2.1.3.3 Abort Control Button

Also included on the Background Screen is the Abort Control button. Clicking the mouse on this button simply opens the control loop. This is a very useful feature in various situations including one in which a marginally stable or a noisy closed loop system is detected by the user and he/she wishes to discontinue control action immediately. Note also that control action may always be discontinued immediately by pressing the red "OFF" button on the control box. The latter method should be used in case of an emergency.

#### 2.1.3.4 Main Menu Options

The *Main menu* is displayed at the top of the screen and has the following choices:

- File
- Setup
- Command
- Data
- Plotting
- Utility

#### 2.1.4 File Menu

The File menu contains the following pull-down options:

- Load Settings
- Save Settings
- About
- Exit



2.1.4.1 The Load Settings dialog box allows the user to load a previously saved configuration file into the Executive. A configuration file is any file with a ".cfg" extension which has been previously saved by the user using Save Settings. Any "\*.cfg" file can be loaded at any time. The latest loaded "\*.cfg" file will overwrite the previous configuration settings in the ECP Executive *but* changes to an existing controller residing in the DSP real-time control card will not take place until the new controller is "implemented" – see Section 2.1.5.1. The configuration files include information on the control algorithm, trajectories, data gathering, and plotting items previously saved. To load a "\*.cfg" file simply select the Load Settings command and when the dialog box opens, select the appropriate file from the directory.<sup>1</sup> Note that every time the Executive program is entered, a particular configuration file called "default.cfg" (which the user may customize - see below) is loaded. This file must exist in the same directory as the Executive Program in order for it to be automatically loaded.

2.1.4.2 The Save Settings option allows the user to save the current control algorithm, trajectory, data gathering and plotting parameters for future retrieval via the Load Settings option. To save a "\*.cfg" file, select the Save Settings option and save under an appropriately named file (e.g. "pid1dsk.cfg"). By saving the configuration under a file named "default.cfg" the user creates a default configuration file which will be automatically loaded on reentry into the Executive program. You may tailor "default.cfg" to best fit your usage.

2.1.4.3 Selecting About brings up a dialog box with the current version number of the Executive program.

2.1.4.4 The Exit option brings up a verification message. Upon confirming the user's intention, the Executive is exited.

## 2.1.5 Setup Menu

The Setup menu contains the following pull-down options:

- Control Algorithm
- User Units
- Communications

---

<sup>1</sup>Its fastest to simply double-click on the desired file.

2.1.5.1 Setup Control Algorithm allows the entry of various control structures and control parameter values to the real-time controller – see Figure 2.1-2. In addition to feedforward which will be described later, the currently available feedback options are:

- PID
- PI With Velocity Feedback
- PID+Notch
- Dynamic Forward Path
- Dynamic Prefilter/Return Path
- State Feedback
- General Form

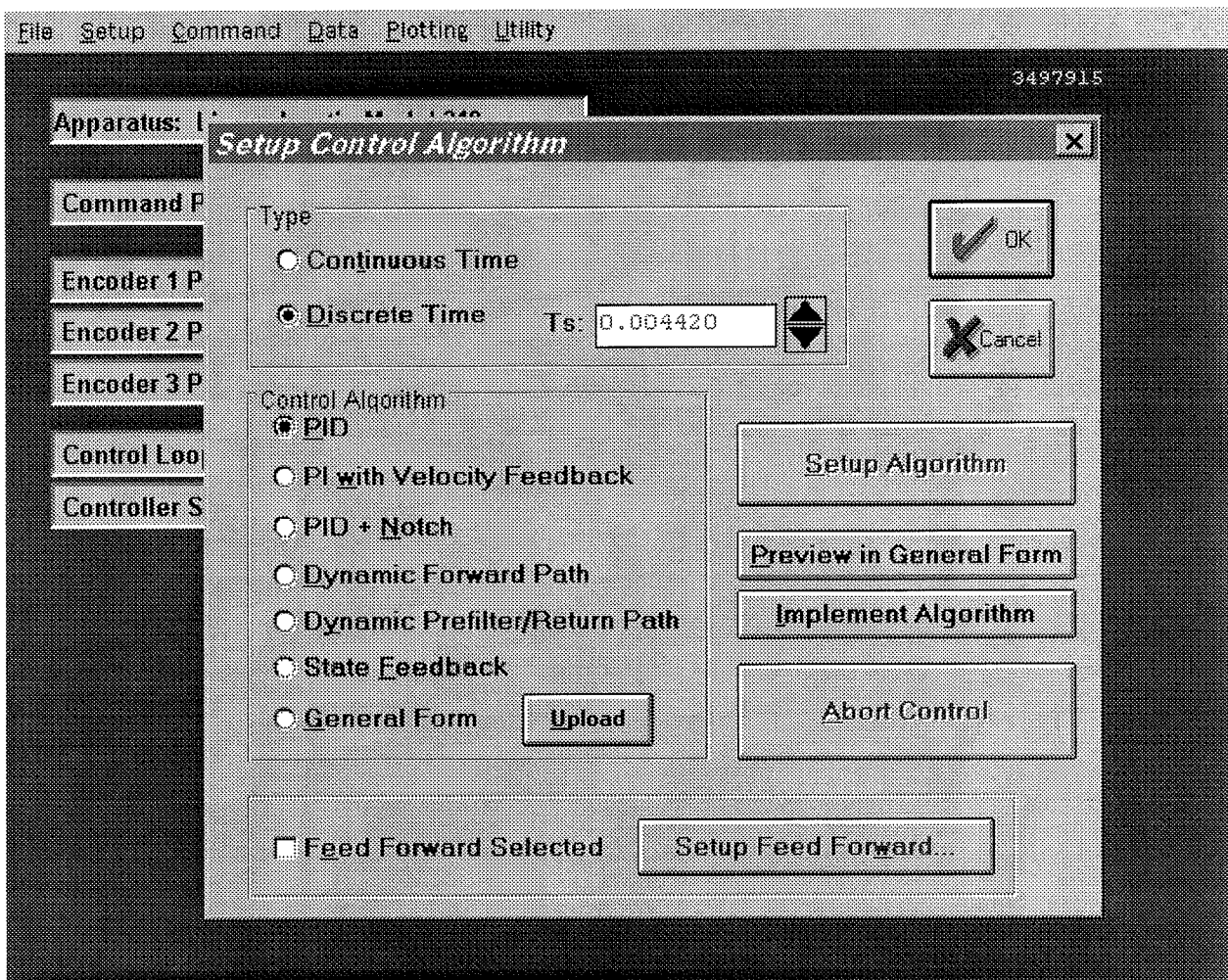


Figure 2.1-2. Setup Control Algorithm Dialog Box

2.1.5.1.1 Discrete Time Control Specification

The user chooses the desired option by selecting the appropriate "radio button" and then clicking on Setup Algorithm. The user must also select the sampling period which is always in multiples of 0.000884 seconds (1.1 KHz is the maximum sampling frequency).<sup>1</sup> To run the selected choice on the real-time controller click on the Implement Algorithm button. The control action will begin immediately. To stop control action and open the loop with zero control effort click on the Abort button. To upload the current controller select General Form then click on the Upload Algorithm button followed by Setup Algorithm. Here you will find the current controller in the form that is actually executed in real-time – see Figure 2.1-3.

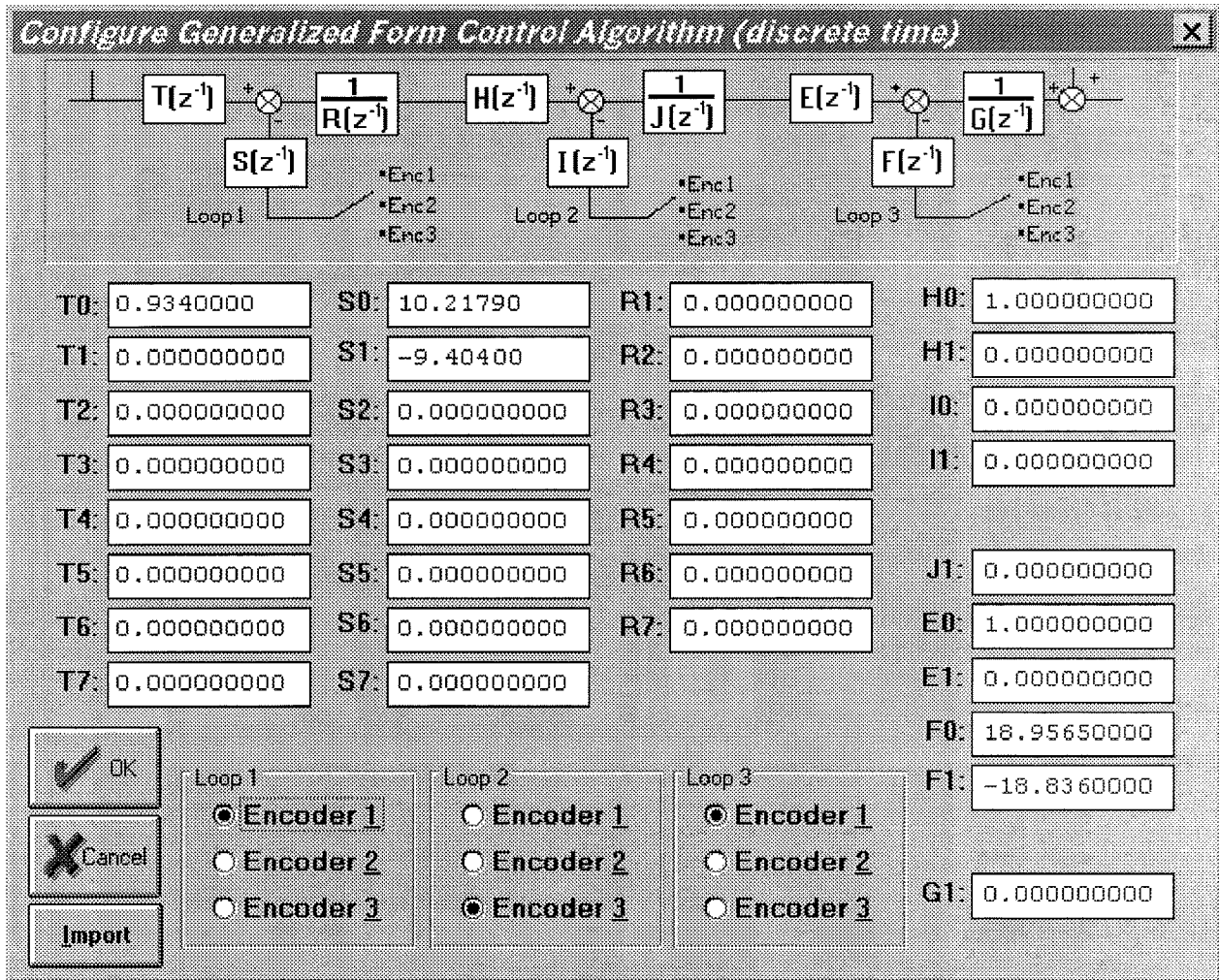


Figure 2.1-3. Dialog Box For Generalized Control Algorithm Input

<sup>1</sup> For many designs, the value  $T_s = .00442$  sec is a good midpoint between the spatial quantization induced noise associated with rate derivation over small sample periods and the phase lag associated with large ones.

A typical sequence of events is as follows: Select the desired servo loop closure sampling time  $T_s$  in multiples of 0.000884 seconds; then select the control structure you wish to implement (e.g. radio buttons for PID, PID+Notch etc.). Select Setup Algorithm to input the gain parameters (coefficients). You must also select the desired feedback channel by choosing the correct encoder(s) used for your particular control design. Exit Setup by selecting OK. Now you should be back in the Setup Control Algorithm dialog box with a selected set of gains for a specified control structure. To download this set of control parameters to the real-time controller click on Implement Algorithm. This action results in an immediate running of your selected control structure on the real-time controller. If you notice unacceptable behavior (instability and/or excessive ringing or noise) simply click on Abort Control which opens up the control loop with zero control effort commanded to the actuator.

To inspect the form by which your particular control structure is actually implemented on the real-time controller, simply click on Preview In General Form. You may edit the algorithm in the General Form box, however when you exit, you must select General Form prior to "implementing" if you want the changes to become effective. (i.e. the radio button will still indicate the box you were in prior to previewing and this one will be downloaded unless General Form is selected).

The Setup Feed Forward option allows the user to add feedforward action to any of the above feedback structures. By clicking on this button a dialog box appears which allows the feedforward control parameters (coefficients) to be entered. To augment the feedforward action to the feedback algorithm the user must then check the Feedforward Selected check-box. Any subsequent downloading (via the Implement Algorithm button) combines the feedforward control algorithm with the selected feedback control algorithm.

**Important Note:** Every time a set of control coefficients are downloaded via Implement Algorithm button, the commanded position as well as all of the encoder positions are reset to zero. This action is taken in order to prevent any instantaneous unwanted transient behavior from the controller. The control action then begins immediately.

**Important Note:** For high order control laws (those using more than 2 or 3 terms of either the R, S, T, K, or L polynomials), it is often important that the coefficients be entered with relatively high precision— say at least 5 to 6 points after the decimal. The real-time controller works with 96-bit real number arithmetic (48-bit integer plus 48-bit fraction). Although the Executive displays the coefficients with nine points after the decimal, it accepts higher precision numbers and downloads them correctly.

#### 2.1.5.1.2 Continuous Time Control Specification

Depending on your course of study, It may be desirable to specify the control algorithm in continuous time form.<sup>1</sup> The method for inputting control parameters is identical to that described

---

<sup>1</sup>An often used rule of thumb is that the continuous time approximation of sampled data systems is acceptably accurate if the sampling frequency is at least 10 times the system bandwidth. (This rule is not always conservative)

for the discrete time case. Again you may preview your controller in the continuous General Form prior to implementing. Upon selecting either Implement Algorithm or Preview in General Form, the algorithm also gets mapped into the discrete General Form where it may be viewed either before (following "Preview") or after (following "Implement") downloading to the real time controller.<sup>1</sup>

Again it is the discrete time general form that is actually executed in real time. The input coefficients are transformed to discrete time using one of the two following substitutions. For polynomials:  $n(s)$ ,  $d(s)$  in PID + Notch;  $s(s)$ ,  $t(s)$ , and  $r(s)$  in Dynamic Forward Path, Dynamic Prefilter / Return Path, and the General Form; and  $k(s)$ ,  $l(s)$  in Feed Forward, the Tustin (bilinear) transform

$$s = \frac{2}{T_s} \frac{1-z^{-1}}{1+z^{-1}}$$

is used. All other cases (first order) use the Backwards Difference method:

$$s = \frac{1-z^{-1}}{T_s}$$

Blocks using the Tustin transform must be proper in  $s$  while those using backwards difference may be improper – e.g. a differentiator.<sup>2</sup>

### 2.1.5.1.3 Importing Controller Specifications From Other Applications

You may import controllers designed using other applications such as Matlab® and Matrix X®.<sup>3</sup> Within each controller specification dialog box is an Import button by which the user download the control gains or coefficients previously saved as an ASCII text file with a extension "\*.par". The format for the file is as shown in Table 2.1-1.

---

however, see Section 6.3.5 & 6.3.5i). Since the attainable closed loop bandwidths for the system are generally less than 10 Hz, sampling rates above 100 Hz usually provide results that are indistinguishable between equivalent continuous and discrete controller designs. I.e. for sampling rates above 100 Hz, the user may generally design and specify the controller in continuous time with no measurable difference in system behavior than if the controller were designed in discrete time.

<sup>1</sup>Note that in previewing the discrete generalized form of a continuous controller you should select Discrete Time . General Form, then Setup Algorithm. If instead the sequence Discrete Time, Preview In General Form, is used, then the selected discrete time algorithm (the one with the red dot next to it and which will not generally contain parameters that correspond to the continuous time design) will be previewed. Subsequent "Implementing" will then download the wrong design.

<sup>2</sup>You may notice the term  $r_1$  in the Continuous Time General Form has a default value 0.0000002 whenever PD, PID, PID+ Notch, or State Feedback are selected. (in this case you would enter the General Form via the Preview In General Form button). This adds a pole at very high frequency and is of no practical consequence to system stability or performance. It is necessary to make the S(s)/R(s) and T(s)/R(s) blocks proper when implementing the differentiator terms in the above mentioned control forms.

<sup>3</sup>This format may be produced in Matlab® using the `fprintf` function.

Table 2.1-1 File Format For Importing Controller Coefficients

Continuous Time Controller Specification				Discrete Time Controller Specification			
Control Algorithm	File Format	Control Algorithm	File Format	Control Algorithm	File Format	Control Algorithm	File Format
PID	{PID_C} kp=n.n kd=n.n ki=n.n	Dynamic Prefilter/ Return Path	{DYNPR_C} t0=n.n : : t7=n.n s0=n.n : : s7=n.n r0=n.n : : r7=n.n	PID	{PID_D} Kp=n.n Kd=n.n Ki=n.n	Dynamic Prefilter/ Return Path	{DYNPR_D} T0=n.n : : T7=n.n S0=n.n : : S7=n.n R1=n.n : : R7=n.n
PID w/ Velocity Feedback	{PID_C} kp=n.n kd=n.n ki=n.n	State Feedback	{STATEF_C} kpf=n.n k1=n.n k2=n.n k3=n.n k4=n.n k5=n.n k6=n.n	PID w/ Velocity Feedback	{PID_D} Kp=n.n Kd=n.n Ki=n.n	State Feedback	{STATEF_D} Kpf=n.n K1=n.n K2=n.n K3=n.n K4=n.n K5=n.n K6=n.n
PID + Notch	{PIDNOTCH_C} kp=n.n kd=n.n ki=n.n n0=n.n n1=n.n n2=n.n d1=n.n : : d4=n.n	General Form	{GENERAL_C} t0=n.n : : t7=n.n s0=n.n : : s7=n.n r0=n.n : : r7=n.n h0=n.n h1=n.n i0=n.n i1=n.n j0=n.n j1=n.n e0=n.n e1=n.n f0=n.n f1=n.n g0=n.n g1=n.n	PID + Notch	{PIDNOTCH_D} Kp=n.n Kd=n.n Ki=n.n N0=n.n : : N4=n.n D1=n.n : : D4=n.n	General Form	{GENERAL_D} T0=n.n : : T7=n.n S0=n.n : : S7=n.n R1=n.n : : R7=n.n H0=n.n H1=n.n I0=n.n I1=n.n J1=n.n E0=n.n E1=n.n F0=n.n F1=n.n G1=n.n
Dynamic Forward Path	{DYNFWD_C} s0=n.n : : s7=n.n r0=n.n : : r7=n.n	Feed Forward	{FF_C} k0=n.n : : k6=n.n l0=n.n : : l7=n.n	Dynamic Forward Path	{DYNFWD_D} S0=n.n : : S7=n.n R1=n.n : : R7=n.n	Feed Forward	{FF_D} K0=n.n : : K6=n.n L1=n.n : : L7=n.n

2.1.5.2 The User Units dialog box provides the user with various choices of angular or linear units. For Model 205 the choices are *counts*, *degrees* and *radians*. There are 16000 counts, 360 degrees and  $2\pi$  radians per revolution of both the load and drive inertia disks. By clicking on the desired radio button the units are changed automatically for trajectory inputs as well as the

Background Screen displays, plotting and jogging activities. Units of *counts* are used exclusively for the examples in this manual.

2.1.5.3 The Communications dialog box is usually used only at the time of installation of the real-time controller. The choices are serial communication (RS232 mode) or PC-bus mode – see Figure 2.1-4. If your system was ordered for PC-bus mode of communication, you do not usually need to enter this dialog box unless the default address at 528 on the ISA bus is conflicting with your PC hardware. In such a case consult the factory for changing the appropriate jumpers on the controller. If your system was ordered for serial communication the default baud rate is set at 34800 bits/sec. To change the baud rate consult factory for changing the appropriate jumpers on the controller. You may use the Test Communication button to check data exchange between the PC and the real-time controller. This should be done after the correct choice of Communication Port has been made. The Timeout should be set as follows:

ECP Executive For Windows with Pentium Computer:	Timeout $\geq$ 50,000
ECP Executive For Windows with 486 Computer:	Timeout $\geq$ 20,000
ECP Executive For DOS with Pentium Computer:	Timeout $\geq$ 150
ECP Executive For Windows with 486 or lower Computer:	Timeout $\geq$ 80

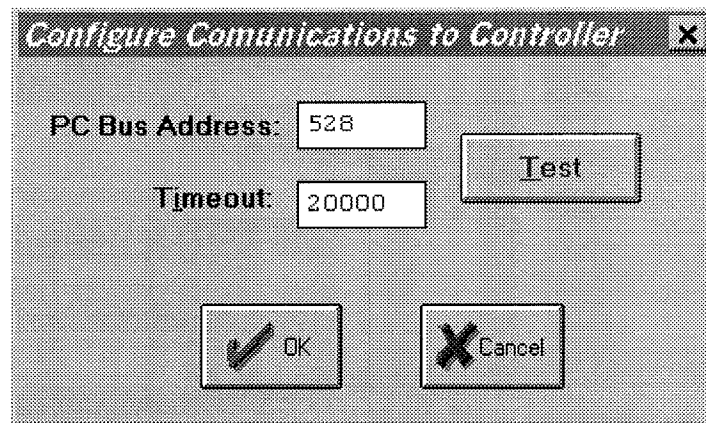


Figure 2.1-4. The Communications Dialog Box

### 2.1.6 Command Menu

The Command menu contains the following pull-down options

- Trajectory . . .
- Disturbance . . .
- Execute . . .

2.1.6.1 The Trajectory Configuration dialog box (see Figure 2.1-5) provides a selection of trajectories through which the apparatus can be maneuvered. These are:

- Impulse
- Step
- Ramp
- Parabolic
- Cubic
- Sinusoidal
- Sine Sweep
- User Defined

A mathematical description of these is given later in Section 4.1.

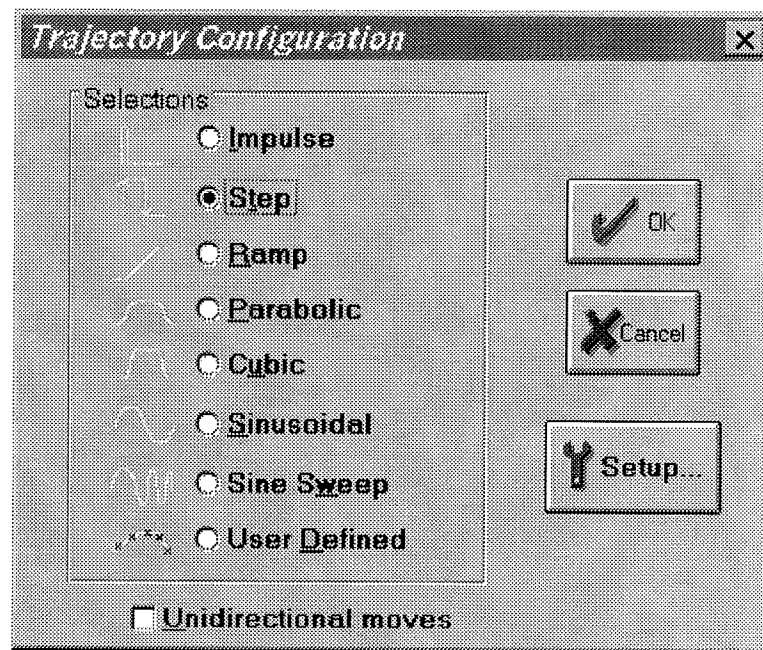
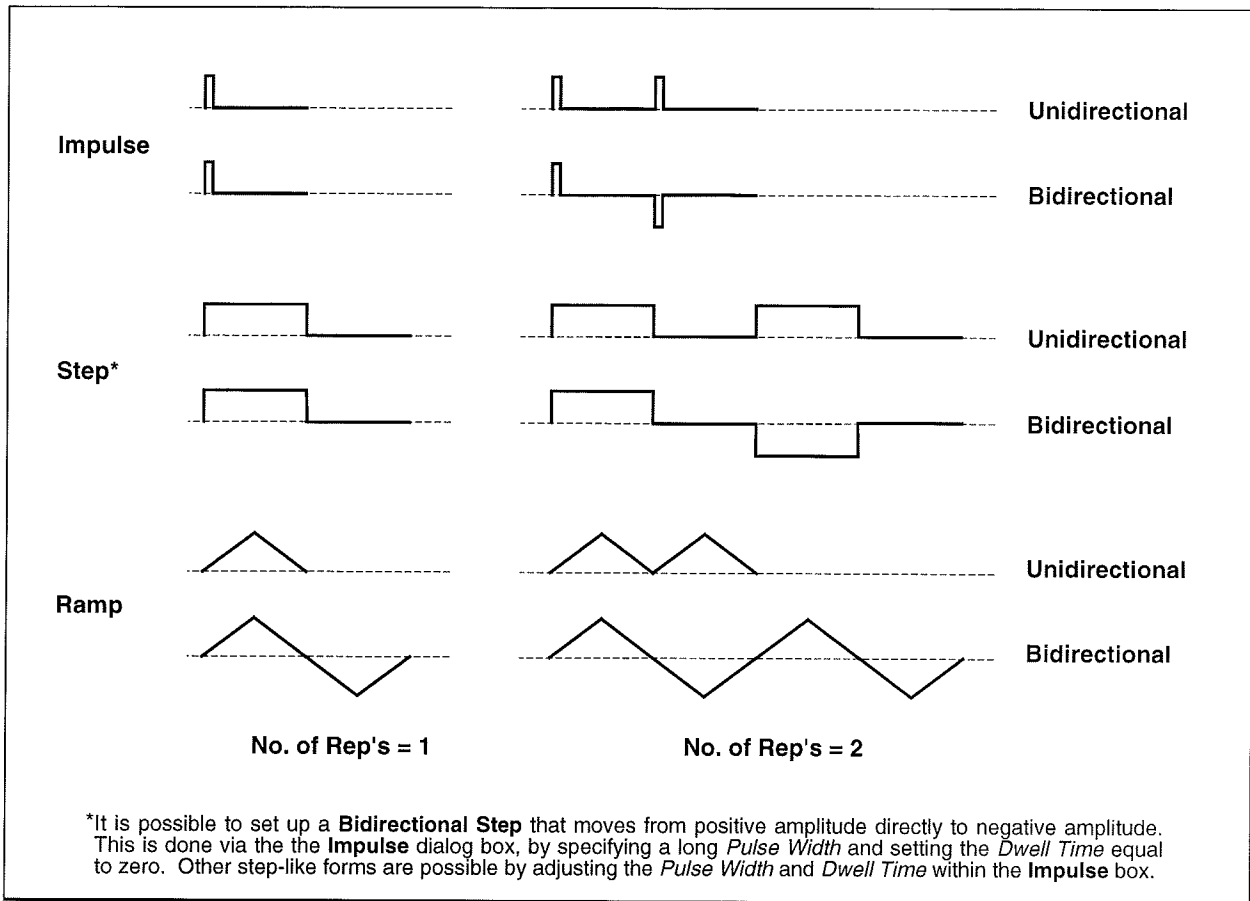


Figure 2.1-5. The Trajectory Configuration Dialog Box

All *geometric* input shapes – Impulse through Cubic – may be specified as Unidirectional or Bi-directional. Examples of these shape types are shown in Figure 2.1-6. The bi-directional option should normally be selected whenever the system is configured to have a *rigid body mode* (one that rotates freely) and the system is operating open loop. This is to avoid excessive speed or displacement of the system.





**Figure 2.1-6. Example Geometric Trajectories**

By selecting the desired shape followed by Setup, one enters a dialog box for the corresponding trajectory. Examples of these boxes are shown in Figure 2.1-7. The amplitude is specified in units consistent with the selected User Units (Setup menu) under closed loop operation and in units of DAC volts (0-5 VDC) under open loop. The closed loop units will change automatically to be consistent with the selected User Units. Amplitudes are always incremental from the value that exists at the beginning of the maneuver (see Execute, Section 2.1.6.3). The characteristic durations of the various shapes are specified in units of milliseconds.

The Impulse, Step, Sinusoidal, Sine Sweep, and User-defined trajectories may be specified as open or closed loop. The remaining shapes are closed loop only.

**Important Note:** It is possible to specify amplitudes and/or abruptly changing shapes that exceed the linear range of the motor and drive electronics or cause large excursions of the mechanism due to system dynamic response. These may result in inaccurate test results and could lead to a hazardous operating condition or over-stressing of the apparatus<sup>1</sup>. If in doubt as to whether the

<sup>1</sup>The system contains safeguards to prevent unsafe operations in most cases. If a hardware or software limit is

drive linear range has been exceeded, you may view Control Effort (either by real-time plotting or via data acquisition/plotting<sup>1</sup>). When specifying an unfamiliar shape the user should generally begin with small amplitudes, velocities, accelerations, and RMS power levels and gradually increase them to suitable safe values. Similarly, when specifying control algorithm parameters, one should begin with conservatively low values; then gradually increase them. See Section 2.3 on safety.

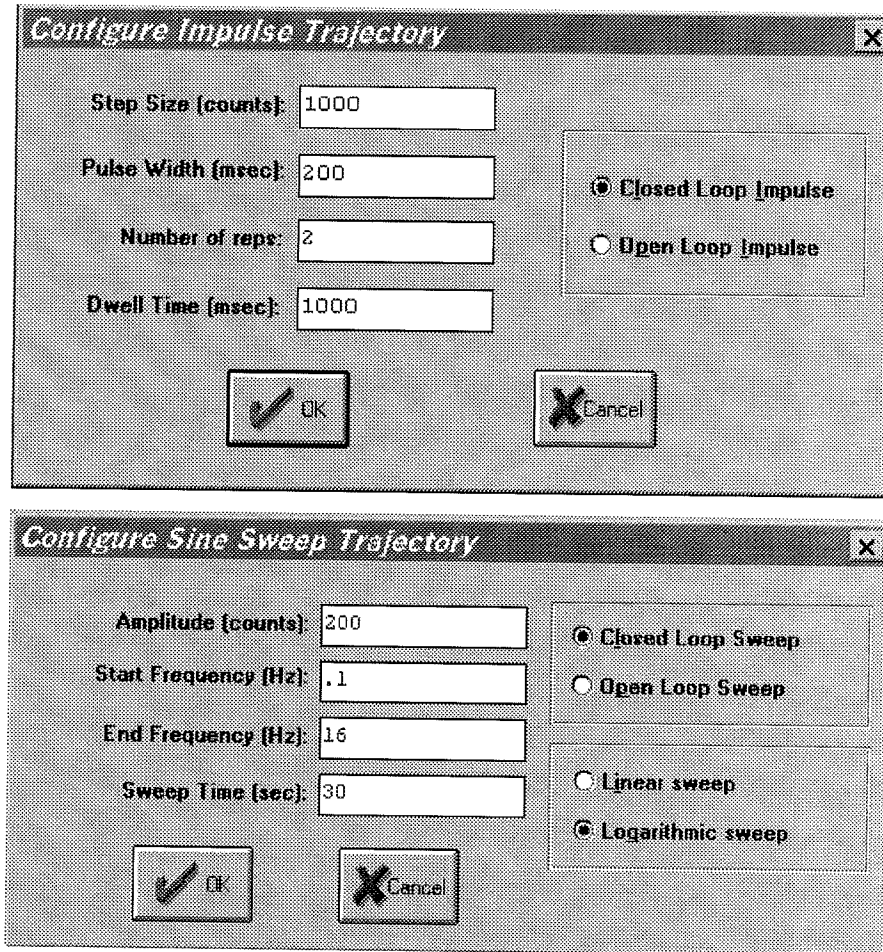


Figure 2.1-7. Example "Setup Trajectory" Dialog Boxes

The Impulse dialog box provides for specification of amplitude, impulse duration, dwell duration, and number of repetitions.<sup>2</sup> The Step box supports specification of step amplitude, duration, and number of repetitions with the dwell duration being equal to the step duration. The Ramp shape

---

exceeded, the Controller Status display on the Background Screen will indicate Limit Exceeded. In this event, the user should Reset Controller (Utility menu), and re-Implement (Command menu) using an appropriate (safe) set of control coefficients.

<sup>1</sup>The software is set to saturate control effort at  $\pm 5$  V. If this amplitude is exceeded, the input shape amplitudes or accelerations as appropriate should be reduced.

<sup>2</sup>If the specified "impulse" duration becomes long enough, the resulting torque becomes more step-like than impulsive. Thus the Setup Impulse dialog box may also be used for Step input shapes where the dwell (zero excitation) period may be specified independently of the step duration.

is specified by the peak amplitude, ramp slope (units of amplitude per second), dwell time at amplitude peaks, and number of repetitions. The Parabolic shape is specified by the peak amplitude, ramp slope (units of ampl./s), acceleration time, dwell time at amplitude peaks, and number of repetitions. In this case, the acceleration (units of ampl./s<sup>2</sup>) results from meeting the specified amplitude, slope, and acceleration period. The Cubic shape is specified by the peak amplitude, ramp slope (units of ampl./s), acceleration time, dwell time at amplitude peaks, and number of repetitions. In this case, the "jerk" (units of ampl./s<sup>3</sup>) results from meeting the specified amplitude, slope, and acceleration period where the acceleration increases linearly in time until the specified velocity is reached.

Note that the only difference between a parabolic input and a cubic one is that during the acceleration/deceleration times, a constant acceleration is commanded in a parabolic input and a constant jerk is commanded in the cubic input. Of course, in a ramp input the commanded acceleration/deceleration is infinite at the ends of a commanded displacement stroke and zero at all other times during the motion. For safety, there is an apparatus-specific limit beyond which the Executive program will not accept the amplitude inputs for each geometric shape.

The Sinusoidal dialog box provides for specification of input amplitude, frequency and number of repetitions.

The Sine Sweep dialog box accepts inputs of amplitude, start and end frequencies (units of Hz), and sweep duration. Both linear and logarithmic frequency sweeps are available. The linear sweep frequency increase is linear in time. For example a sweep from 0 Hz to 10 Hz in 10 seconds results in a one Hertz per second frequency increase. The logarithmic sweep increases frequency logarithmically so that the time taken in sweeping from 1 to 2 Hz for example, is the same as that for 10 to 20 Hz when a single test run includes these frequencies. There is an apparatus-specific amplitude limit beyond which the Executive will not accept the inputs.

**Important Note:** A large open loop amplitude combined with a low frequency may result in an over-speed condition which will be detected by the real-time controller and will cause the system to shut down. In closed loop operations, high frequency, large amplitude tests may result in a shut down condition. For both the open and closed loop cases, even modest commanded amplitude near or at a resonance frequency can cause an excessive shaft deflection.<sup>1</sup> Any of these conditions will cause the test to be aborted and the System Status display in the Background Screen to indicate Limit Exceeded. To run the test again you should reduce the input shape amplitude and then Reset Controller (Utility menu), and re-Implement a stabilizing controller (Command menu). In general, all trajectories that generate either too high a speed, too large a deflection, or excessive motor power will cause this condition – see the safety section 2.3. For a

---

<sup>1</sup>Sweeping through resonances is very useful in visualizing the frequency response dynamics, but must be done at a sufficiently low input amplitude. When viewing open loop sine sweep results, it is often best to view velocity rather than position data to reduce position drift effects. By selecting a relatively long sweep period, the transient effects of frequency change are minimized and the true frequency response is best approximated.

further margin of safety, there is an apparatus-specific amplitude limit beyond which the Executive program will not accept the inputs.

The User Defined shape dialog box provides an interface for the specification of any input shape created by the user. In order to make use of this feature the user must first create an ASCII text file with an extension ".trj" (e.g. "random.trj"). This file may be accessed from any directory or disk drive using the usual file path designators in the filename field or via the Browse button. If the file exists in the same directory as the Executive program, then only the file name should be entered. The content of this file should be as follows:

The first line should provide the number of points specified. The maximum number of points is 923. This line should not contain any other information. The subsequent lines (up to 923) should contain the consecutive set points. For example to input twenty points equally spaced in distance one can create a file called "example.trj" using any text editor as follows

```
20
5
10
15
20
25
30
35
40
45
50
55
60
65
70
75
80
85
90
95
100
```

The segment time which is a time between each consecutive point can be changed in the dialog box. For example if a 100 milliseconds segment time is selected, the above trajectory shape would take 2 seconds to complete ( $100 \times 20 = 2000$  ms). The minimum segment time is restricted to five milliseconds by the real-time controller. When Open Loop is selected, the units of the trajectory are assumed to be DAC bits ( $+16383 = 4.88$  V,  $+16383 = -4.88$  V). In Closed Loop mode, the

units are assumed to be the position displacement units specified under User Units (Setup menu). The shape may be treated by the system as a discrete function exactly as specified, or may be smoothed by checking the Treat Data As Splined box. In the latter case the shapes are cubic spline fitted between consecutive points by the real-time controller. Obviously a user-defined shape may also cause over-speed or over-deflection of the mechanism if the segment time is too long or the distance between the consecutive points is too great.

2.1.6.2 The Disturbance Configuration dialog box (see Figure 2.1.-5a) provides a selection of disturbance torque profiles for the disturbance motor. This motor and servo drive is optional on the Model 205 system. If your system does not include this option, this dialog box will not be accessible. The available disturbances are:

- Viscous Friction
- Step
- Sinusoidal (time)
- Sinusoidal (theta)
- User Defined

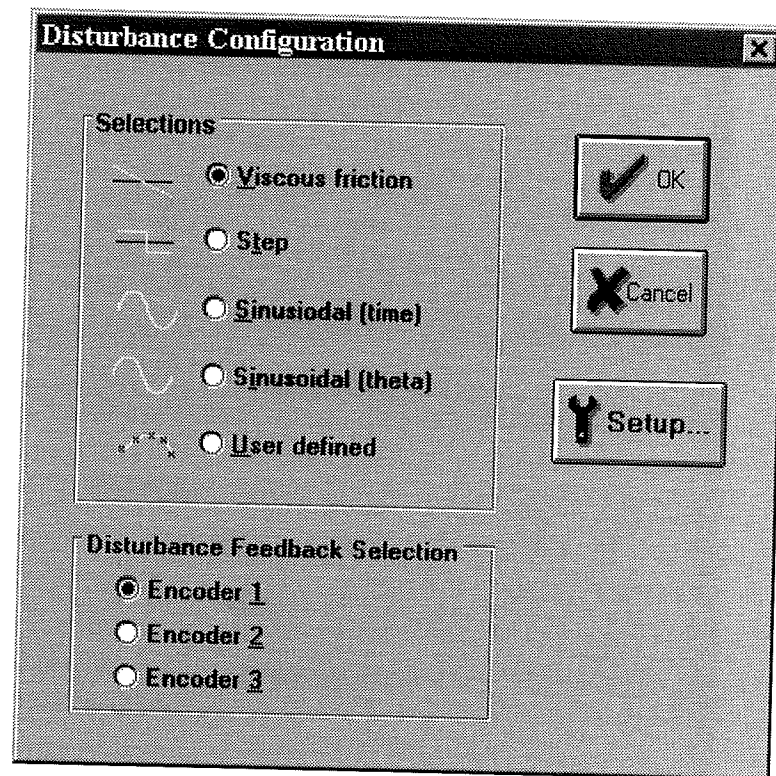


Figure 2.1-6. The Disturbance Configuration Dialog Box

By selecting the desired disturbance profile followed by Setup, one enters a corresponding dialog box.

The Viscous Friction box allows the user to input a disturbance signal proportional to the angular speed of the disturbance disk (i.e. the one that the disturbance motor is attached to) as sensed by the corresponding disk encoder. It is important to properly specify the corresponding encoder number (inertia disk location) in the Disturbance Configuration dialog box for the viscous friction function to work properly. The Amplitude entry is the magnitude of the viscous coefficient in units of volts/radian/second. Once the disturbance motor is calibrated this entry translates to a certain number of N-m/rad/sec. The user has a choice of implementing the viscous disturbance either directly through this dialog box or later prior to running a trajectory in the Execute dialog box. The maximum amplitude of viscous disturbance is limited to 5 volts/radian/second.

The Step disturbance dialog box allows the user to input the parameters for a square wave torque disturbance. The entries in this dialog box are identical to the Open Loop Step trajectory discussed above.

The Sinusoidal (time) option allows the user to input a torque disturbance to the desired disk via the disturbance motor in the form of a sinusoidal function of time. The entries in this dialog box are identical to the Open Loop Sinusoidal trajectory discussed above.

The Sinusoidal (theta) option specifies a sinusoidal torque as a function of disk position. This allows the simulation of spatially dependent disturbances such as motor cogging torque. The amplitude of the disturbance torque is entered in terms of volts. The user must enter the number of torque cycles per revolution of the disturbance disk (maximum number is limited to 100). In addition, the period of time for which this disturbance is active must be specified. It is important to properly specify the encoder (inertia disk) corresponding to the current disturbance drive location in the Disturbance Configuration dialog box for the Sinusoidal (theta) function to work properly.

The User Defined disturbance box provides the interface for the input of any form of disturbance trajectory created by the user. In order to make use of this feature the user must first create an ASCII text file with an extension .trj (e.g. random.trj). The format is identical to the User Defined trajectories discussed in the previous section. Note that the maximum number of points are still 100 and the first entry must be the number of points in a particular file. The units of inputs are in DAC bits (+16383 = 4.88 V, -16383 = -4.88 V). After the calibration of the disturbance motor, the exact ratio between a DAC bit and the actual disturbance torque on the load shaft may be determined.

During the active period of any of the above disturbance profiles the Disturbance Status will normally indicate "Active". It is, however, possible that the disturbance motor enters the "Limit Exceeded" condition either as a result of over current or over speed. To return to the "Active" condition, the user must modify the disturbance parameters and implement the disturbance torque again via the Execute dialog box (note that the Viscous friction disturbance may also be implemented within its own dialog box).

The following rules apply to disturbance implementation:

1. You must have selected a disturbance (and verified its parameters) under the Disturbance Configuration dialog box and checked "Include XXX Disturbance" when Executing a trajectory.
2. The disturbance will only be active while the trajectory is executing. If the trajectory terminated before the specified disturbance duration, the disturbance will also terminate. (You may of course input a trajectory of zero amplitude to study the effects of the disturbance alone)
3. The only exception to rules 1 and 2 is viscous damping which may be invoked either via its own dialog box (under Disturbance Configuration) or when a trajectory is executed (by checking Include Viscous Friction before Executing). Viscous friction may run simultaneously with other disturbances. Note that Viscous Friction, if implemented, will remain in effect until either it is removed in its own dialog box, or a new trajectory is run without checking Include Viscous Friction.
4. Disturbance control effort is limited to  $\pm 4.88V$ .
5. For the Viscous Friction and the Sinusoidal (theta) options, the checked Encoder number under the Disturbance Feedback Selection must match the physical location of the Disturbance motor.

2.1.6.3 The Execute dialog box (see Figure 2.1-7) is entered after a trajectory is selected. Here the user commands the system to execute the current specified trajectory and may also choose viscous friction and an output disturbance (system option). The user may select either Normal or Extended Data Sampling. Normal Data Sampling acquires data for the duration of the executed trajectory. Extended Data Sampling acquires data for an additional 5 seconds beyond the end of the maneuver. Both the Normal and Extended boxes must be checked to allow extended data sampling. (For the details of data gathering see Section 2.1.7.1 Setup Data Acquisition).

After selecting disturbance and data gathering options, the user normally selects Run. The real-time controller will begin execution of the specified trajectory. Once finished, and provided the Sample Data box was checked, the data will be uploaded from the DSP board into the Executive (PC memory) for plotting, saving and exporting. At any time during the execution of the trajectory or during the uploading of data the process may be terminated by clicking on the Abort button. Finally, if the disturbance torque profile has a time period longer than the selected trajectory period, it will be terminated at the end of the trajectory profile.

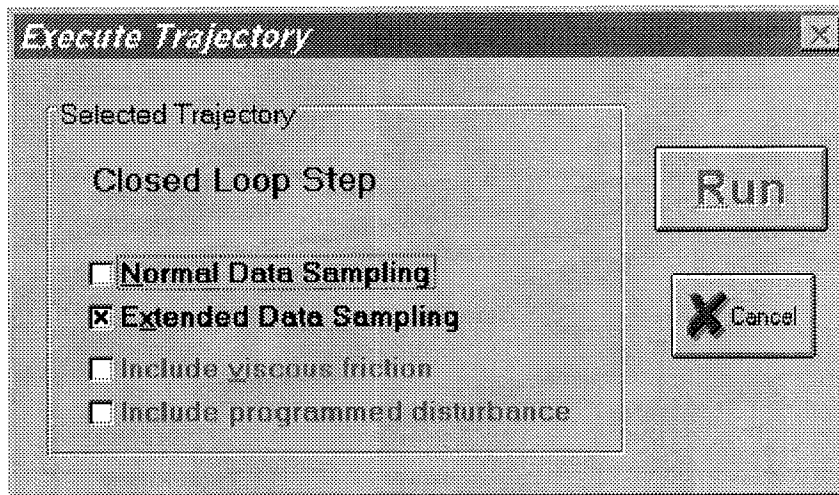


Figure 2.1-7. The Execute Dialog Box



### 2.1.7 Data Menu

The Data menu contains the following pull-down options

- Setup Data Acquisition
- Upload Data
- Export Raw Data

2.1.7.1 Setup Data Acquisition allows the user to select one or more of the following data items to be collected at a chosen multiple of the servo loop closure sampling period while running any of the trajectories mentioned above – see Figures 2.1-8 and 4.1-1:

- Commanded Position
- Encoder 1 Position
- Encoder 2 Position
- Encoder 3 Position
- Control Effort (output to the servo loop or the open loop command)
- Disturbance Effort (disturbance motor command [system option])
- Node A (input to the H polynomial in the Generalized Control Algorithm)
- Node B (input to the E polynomial in the Generalized Control Algorithm)
- Node C (output of the 1/G polynomial in the Generalized Control Algorithm)
- Node D (output of the feedforward controller which is added to the node C value to form the combined regulatory and tracking controller).

In this dialog box the user adds or deletes any of the above items by first selecting the item, then clicking on the Add Item or Delete Item button. The user must also select the data gather sampling period in multiples of the servo period. For example, if the sample time ( $T_s$  in the Setup Control Algorithm) is 0.00442 seconds and you choose 5 for your gather period here, then the selected data will be gathered once every fifth sample or once every 0.0221 seconds. Usually for trajectories with high frequency content (e.g. Step, or high frequency Sine Sweep), one should choose a low data gather period (say 10 ms). On the other hand, one should avoid gathering more often (or more data types) than needed since the upload and plotting routines become slower as the data size increases. The maximum available data size (no. variables x no. samples) is 33,586.

2.1.7.2 Selecting Upload Data allows any previously gathered data to be uploaded into the Executive. This feature is useful when one wishes to switch and compare between plotting previously saved raw data and the currently gathered data. Remember that the data is automatically uploaded into the executive whenever a trajectory is executed and data acquisition is enabled. However, once a previously saved plot file is loaded into the Executive, the currently gathered data is overwritten. The Upload Data feature allows the user to bring the overwritten data back from the real-time controller into the Executive.

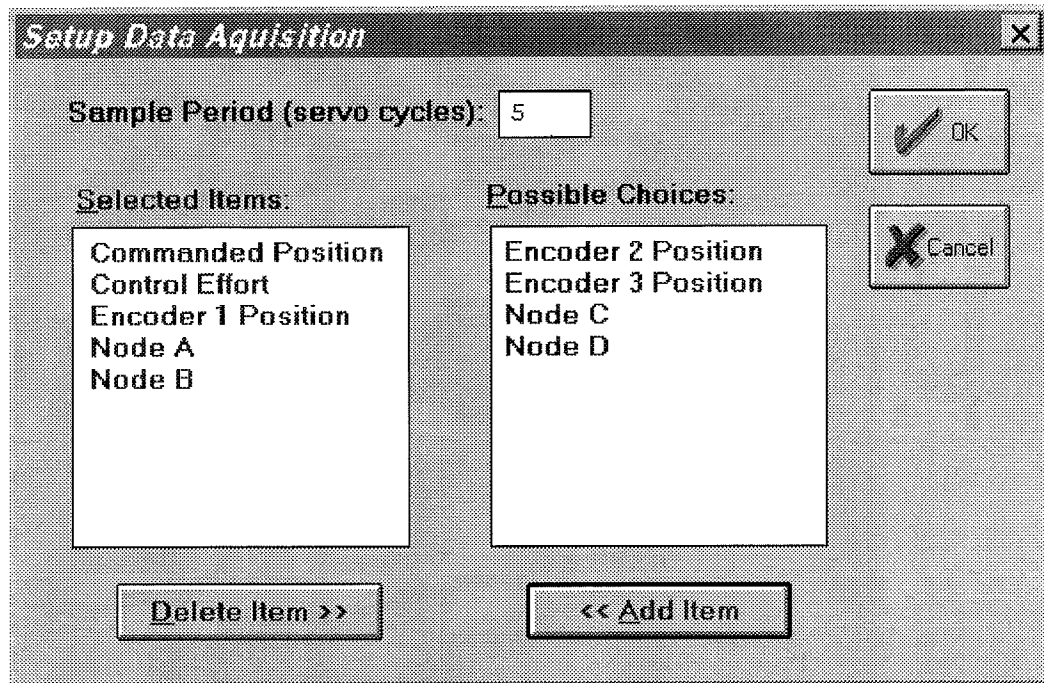


**Figure 2.1-8. The Setup Data Acquisition Dialog Box**

2.1.7.3 The Export Raw Data function allows the user to save the currently acquired data in a text file in a format suitable for reviewing, editing, or exporting to other engineering/scientific packages such as Matlab®.<sup>1</sup> The first line is a text header labeling the columns followed by bracketed rows of data items gathered. The user may choose the file name with a default extension of ".text" (e.g. 1qrstep.txt). The first column in the file is sample number, the next is time, and the remaining ones are the acquired variable values. Any text editor may be used to view and/or edit this file.

### 2.1.8 Plotting Menu

The Plotting menu contains the following pull-down options

- Setup Plot
- Plot Data
- Axis Scaling
- Print Plot
- Load Plot Data
- Save Plot Data
- Real Time Plotting
- Close Window

<sup>1</sup>The bracketed rows end in semicolons so that the entire file may be read as an array in Matlab by running it as a script once the header is stripped i.e. the script should be: <array name>= [exported data file]. Variable values over time are the columns of this array; the rows are the variable value set at successive sample numbers.

2.1.8.1 The Setup Plot dialog box (see Figure 2.1-9) allows up to four acquired data items to be plotted simultaneously – two items using the left vertical axis and two using the right vertical axis units. In addition to the acquired raw data, you will see in the box plotting selections of velocity and acceleration for the position and input variables acquired. These are automatically generated by numerical differentiation of the data during the plotting process. Simply click on the item you wish to add to the left or the right axis and then click on the Add to Left Axis or Add to Right Axis buttons. You must select at least one item for the left axis before plotting is allowed – e.g. if only one item is plotted, it must be on the left axis. You may also change the plot title from the default one in this dialog box.

Items for comparison should appear on the same axis (e.g. commanded vs. encoder position) to ensure the same axis scaling and bias. Items of dissimilar scaling or bias (e.g. control effort in volts and position in counts) should be placed on different axes.

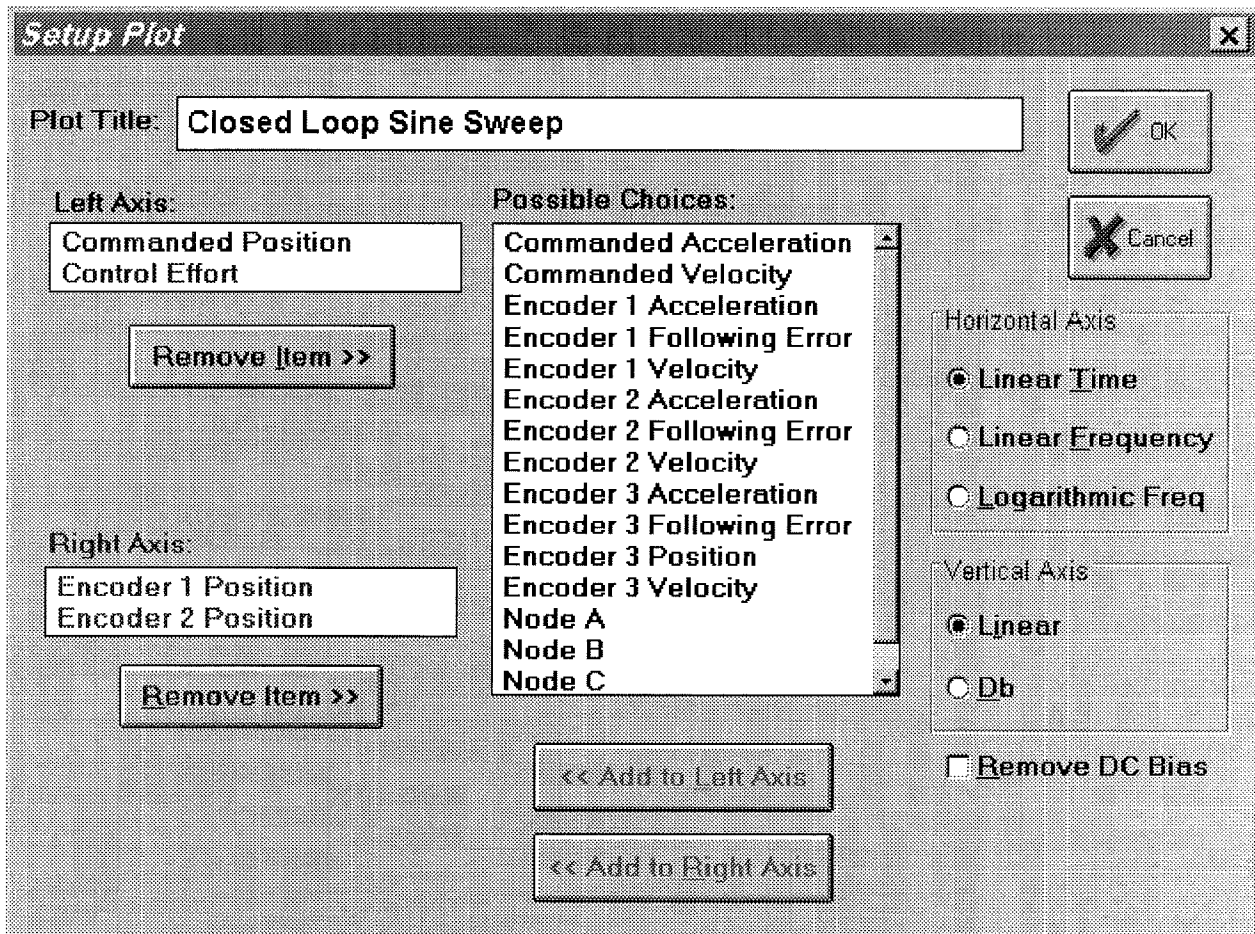


Figure 2.1-9 The Setup Plot Dialog Box

When the current data (either from the last test run or from a previously saved and loaded plot file) is from a Sine Sweep input, several data scaling/transformation options appear in the Setup Plot box. These include the presentation of data with horizontal coordinates of time, linear frequency (i.e. the frequency of the input) or logarithmic frequency. The vertical axis may be plotted in linear or Db (i.e.  $20 \cdot \log_{10}(\text{data})$ ) scaling. In addition, the Remove DC Bias option subtracts the average of the final 50 data points from the data set of each acquired variable. This generally gives a more representative view of the frequency response of the system, particularly when plotting low amplitude data in Db. Sine Sweep must be selected in the Trajectory Configuration dialog box in order for these options to be available in Setup Plot. Examples of sine sweep (frequency response) data plotted using two of these options is given later in Figure 3.2-6.

2.1.8.2 Plot Data generates a plot of the selected items. By clicking on the upper blue border of the plots, they may be dragged across the screen. The view size may be maximized by clicking on the up arrow of the upper right hand corner. It can also be shrunk to an icon by clicking on the down arrow of the upper left hand corner. It can be expanded back to the full size at any time by double-clicking on the icon. Also more than one plot may be tiled on the Background Screen. This function is very useful for comparing several graphs. By clicking on any point within the area of a desired plot it will appear over the others. Plots may be arbitrarily shaped by using the cursor to "drag" the edges of the plot. The corners allow you to resize height and width simultaneously (position cursor at corner and begin "dragging" when cursor becomes a double arrow). Finally by double clicking on the top left hand corner of a plot screen one can close the plot window. A typical plot as seen on screen is shown in Figure 2.1-10.

2.1.8.3 Axis Scaling provides for scaling or "zooming" of the horizontal and vertical axes for closer data inspection – both visually and for printing. This box also provides for selection or deselection of grid lines and data point labels. When Real-time Plotting is used (see Section 2.1.8.7), the data sweep / refresh speed and amplitudes may be adjusted via the Axis Scaling box.

2.1.8.4 The Print Data option provides for printing a hard copy of the selected plot on the current PC system printer. The plots may be resized prior to printing to achieve the desired print format

2.1.8.5 The Load Plot Data dialog box enables the user to bring into the Executive previously saved ".plt" plot files. Note that such files are not stored in a format suitable for use by other programs. The ".plt" plot files contain the sampling period of the previously saved data. As a result, after plotting any previously saved plot files and before running a trajectory, you should check the servo loop sampling period  $T_s$  in the Setup Control Algorithm dialog box. If this number has been changed, then correct it. Also, check the data gathering sampling period in the Data Acquisition dialog box, this too may be different and need correction.

2.1.8.6 The Save Plot Data dialog box enables the user to save the data gathered by the controller for later plotting via Load Plot Data. The default extension is ".plt" under the current directory. Note that ".plt" files are not saved in a format suitable for use by other programs. For this purpose the user should use the Export Raw Data option of the Data menu.

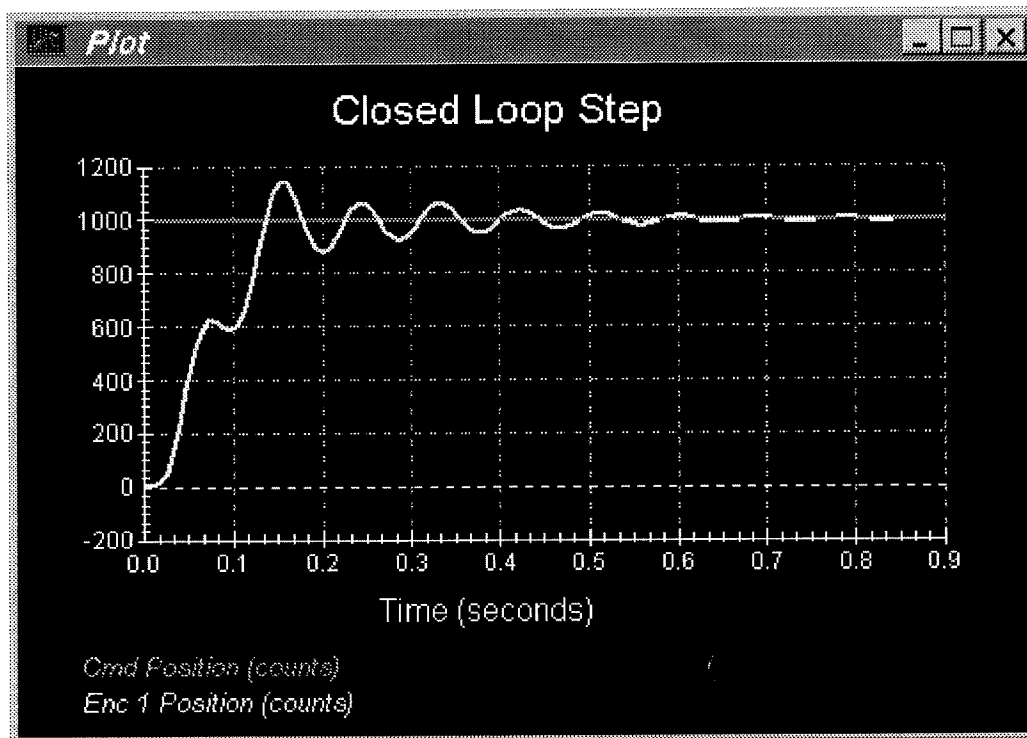


Figure 2.1-10. A Typical Plot Window

2.1.8.7 The Setup Real Time Plotting dialog box enables the user to view data in real time as it is being generated by the system. Thus the data is seen in an oscilloscope-like fashion. Unlike normal (off-line) plotting, real-time plotting occurs continuously whether or not a particular maneuver (via Execute, Command Menu) is being executed<sup>1</sup>. The setup for real-time plotting is essentially identical to that for normal plotting (see Section 2.1.8.1). Because the expected data amplitude is not known to the plotting routine, the plot will first appear with the vertical axes scaled to full scale values of 1000 of the selected variable units. These should be rescaled to appropriate values via Axis Scaling. The sweep or data refresh rate may also be changed via Axis Scaling when real-time plotting is underway. A slow sweep rate is suitable for slow system motion or when a long data record is to be viewed in a single sweep. The converse generally holds for a fast sweep rate.

The data update rate is approximately 50 ms and is limited by the PC/DSP board communication rate. Therefore, frequency content above about 5 Hz is not accurately displayed due to numerical aliasing. The real-time display however is very useful in visually correlating physical system motion with the plotted data and is valid for most practical system frequencies. The data acquired via the data acquisition hardware (for normal plotting) may be sampled at much higher rates (up to 1.1 KHz) and hence should be used when quantitative high speed measurements are desired.

<sup>1</sup> In some cases, you will need to "drag" the Executing Input Shape box out of the way to see the plot during the maneuver. This is practical for longer duration maneuvers.

2.1.8.8 The Close Window option allows the currently marked plot window to close. This can also be done by double clicking on the top left hand corner of the plot window.

### 2.1.9 Utility Menu

The Utility menu contains the following pull-down options:

- Configure Optional auxiliary DACs
- Jog Position
- Zero Position
- Reset Controller
- Rephase Motor
- Down Load Controller Personality File

2.1.9.1 The Configure Auxiliary DACs dialog box (see Figure 2.1-11) enables the user to select various items for analog output on the two optional analog channels in front of the ECP Control Box. Using equipment such as an oscilloscope, plotter, or spectrum analyzer the user may inspect the following items continuously in real time:

- Commanded Position
- Encoder 1 Position
- Encoder 2 Position
- Encoder 3 Position
- Control Effort
- Node A
- Node B
- Node C
- Node E

The scale factor which divides the item can be less than 1 (one). The DACs analog output is in the range of +/- 10 volts corresponding to +32767 to -32768 counts. For example to output the commanded position for a sine sweep of amplitude 2000 counts you should choose the scale factor to be 0.061 ( $2000/32767=0.061$ ) This gives close to full +/- 10 volt reading on the analog outputs. In contrast, if the numerical value of an item is greater than +/- 32767 counts, for full scale reading, you must choose a scale factor of greater than one. Note that the above items are always in counts (not degrees or radians) within the real time controller and since the DAC's are 16-bit wide, + 32767 counts corresponds to +9.999 volts, and -32768 counts corresponds to -10 volts.

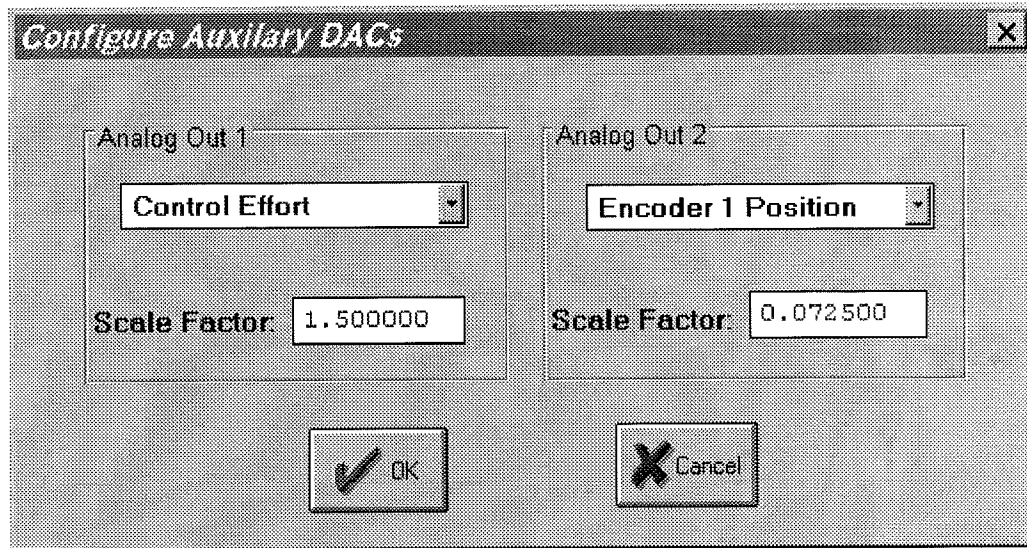


**Figure 2.1-11. The Configure Auxiliary DACs Dialog Box**

2.1.9.2 The Jog Position option enables the user to move the mechanism to a different commanded position. In contrast to displacements executed under the Trajectory dialog box, during a Jog command no data is acquired for plotting purposes. Since this motion is effected via the current controller, one can only jog under closed loop control with a stable controller. By selecting the appropriate radio button either incremental and absolute displacements may be carried out. The jogging feature allows the user to return to a known position after the execution of the various forms of open and closed loop trajectories.

2.1.9.3 The Zero Position option enables the user to reinitialize the current position as the zero position. Note that if following errors exists, then the actual positions may be other than zero even though the commanded position is at zero (since the action is similar to commanding an instantaneous zero set point, a sudden small jerk in position may occur).

2.1.9.4 The Reset Controller option allows the user to reset the real-time controller. Upon Power up and after a reset activity, the loop is closed with zero gains and there it behaves in the same way as in the open loop state with zero control effort. Thus the user should be aware that even though the Control Loop Status indicates "closed loop", all of the gains are zeroed after a Reset. In order to implement (or re implement) a controller you must go to the Setup Control Algorithm box.

2.1.9.5 The Rephase Motor option enables a user to simply rephase a brushless motor's commutation phase angle. This feature is not used by the current Model 205 system since its motors use absolute sensors for commutation.

2.1.9.6 The Download Controller Personality File is an option which should not be used by most users. In a case where the real-time controller irrecoverably malfunctions, and after consulting ECP, a user may download the personality file if a ".pmc" file exists. In the case of Model 205, this file is named "m205xxx.pmc". This downloading process takes a few seconds.

## 2.2 Electromechanical Plant

### 2.2.1 Design Description

The plant, shown in Figure 2.2-1, consists of two (Model 205) or three (Model 205a) disks supported by a torsionally flexible shaft which is suspended vertically on anti-friction ball bearings. The shaft is driven by a brushless servo motor connected via a rigid belt (negligible tensile flexibility) and pulley system with a 3:1 speed reduction ratio. An encoder located on the base of the shaft measures the angular displacement,  $\theta_1$  of the first disk,  $J_1$ . The second disk is connected to its encoder by a rigid belt / pulley with a 1:1 speed ratio. As shown in Figure 2.2-2a this disk and encoder may be moved from the upper shaft location to the middle location for Model 205. For Model 205a, there is an encoder at each disk location (Figure 2.2-2b)

Figures 2.2-2a & b also show the variety of plant types that are supported by each model. Mathematical modeling and parameter identification of these plants are given in Chapters 5 and 6.

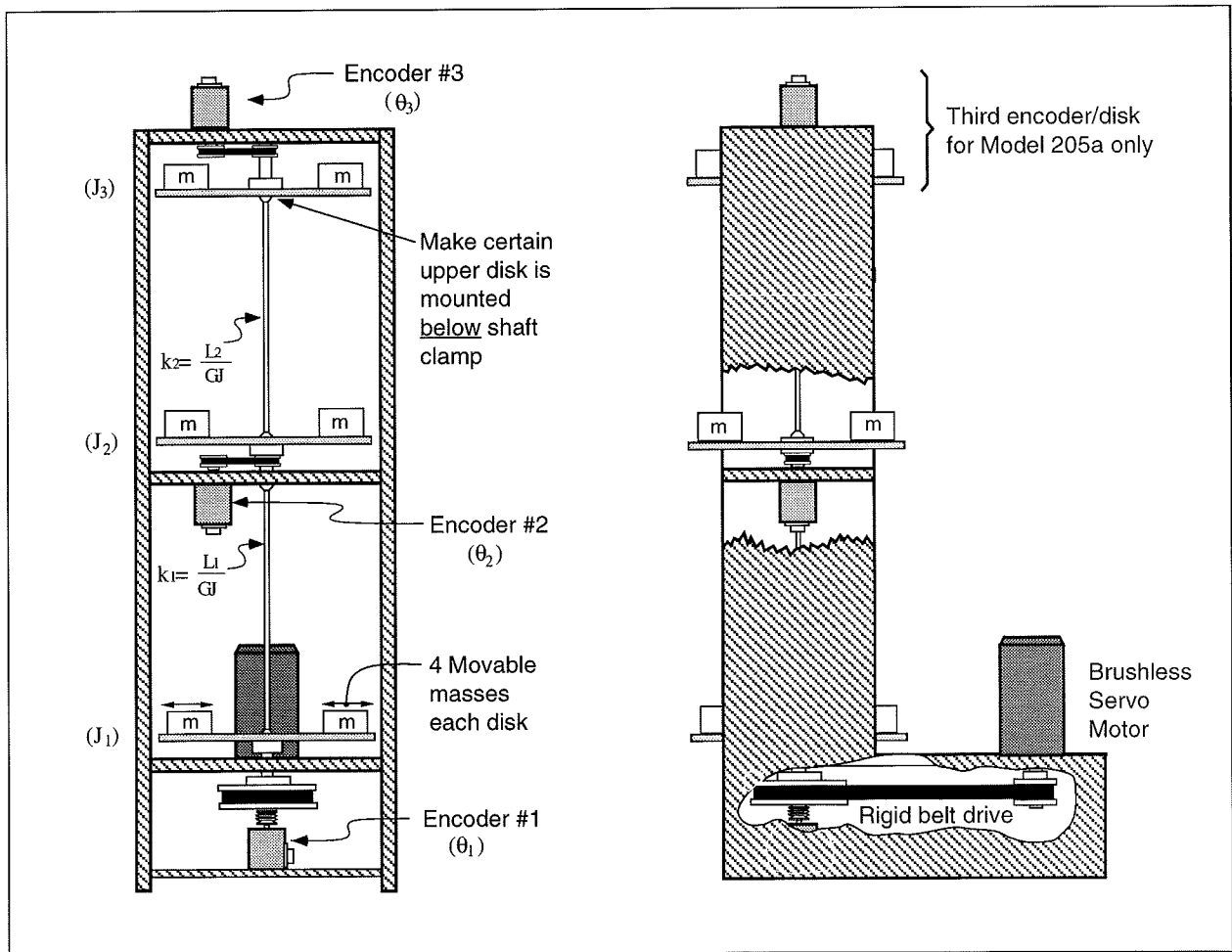


Figure 2.2-1. Torsion Spring / Inertia Apparatus



<p>Spring / Inertia / Encoder Configurations</p>		<p>Free-clamped, 2 DOF</p>
<p>OR</p>	<p>Free-free, 2 DOF</p>	
	<p>Free-clamped</p>	
	<p>Rigid body</p>	

Figure 2.2-2a. Plant configurations for Model 205

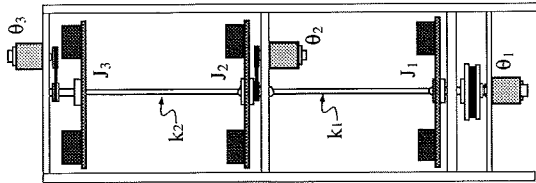
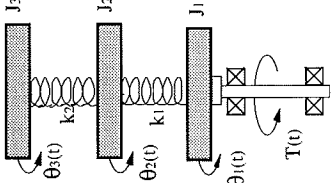
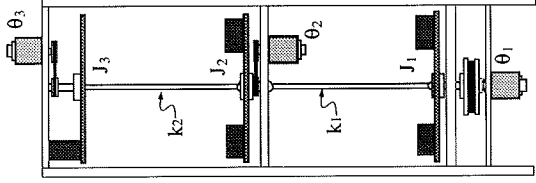
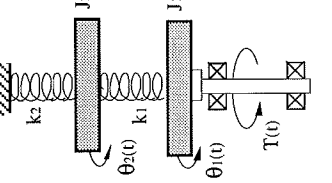
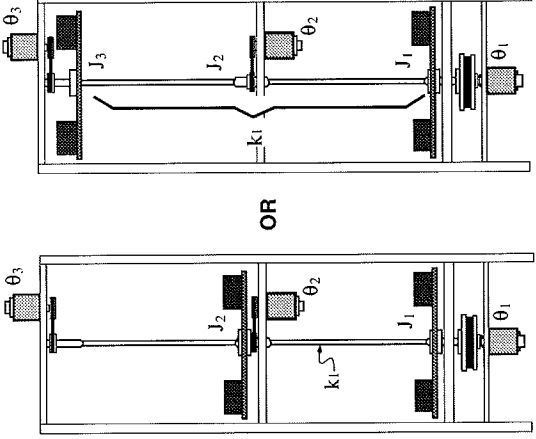
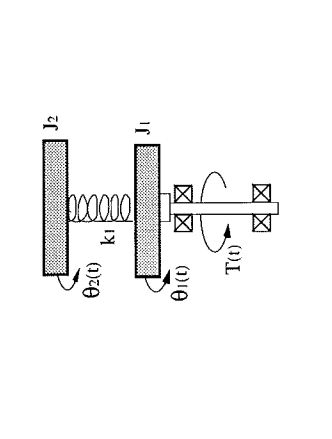
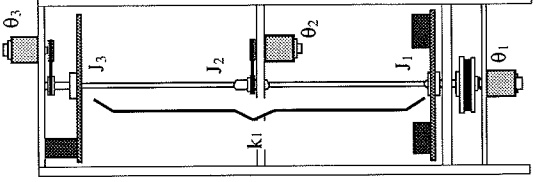
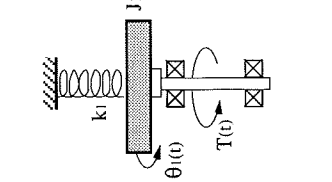
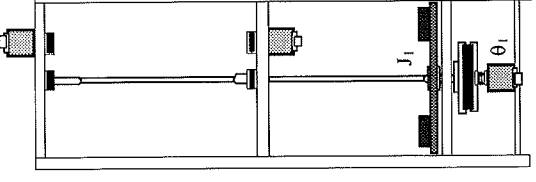
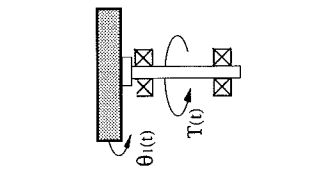
Spring / Inertia / Encoder Configurations	Plant Model					OR					
											

Figure 2.2-2b. Plant configurations for Model 205a

2.2.2 Changing Plant Configurations and Parameter Values

As shown in Figure 5.2.2-2, the plant may be placed in a variety of free and clamped configurations with 1, 2, and 3 (Model 205a) degrees of freedom (DOF). For 1 and 2 DOF plants, the torsional spring constant  $k_1$  may be halved by choice of disk location. Changing configurations often requires removing or replacing inertia disks. Although these operations are straightforward, it is recommended that they be performed by a qualified technician. It is important to keep each pair of half-disks together in matched sets (see inscribed letters on disk edges). By aligning the concentric markings, the proper relative alignment of the two halves is assured. For operating safety, be sure to firmly tighten (but not excessively so) the bolts that fasten the disks to the shaft clamps.

The user may change inertia values by changing the number of masses and/or their location on a given disk. Figure 2.2-3 gives instructions for physically changing inertias.

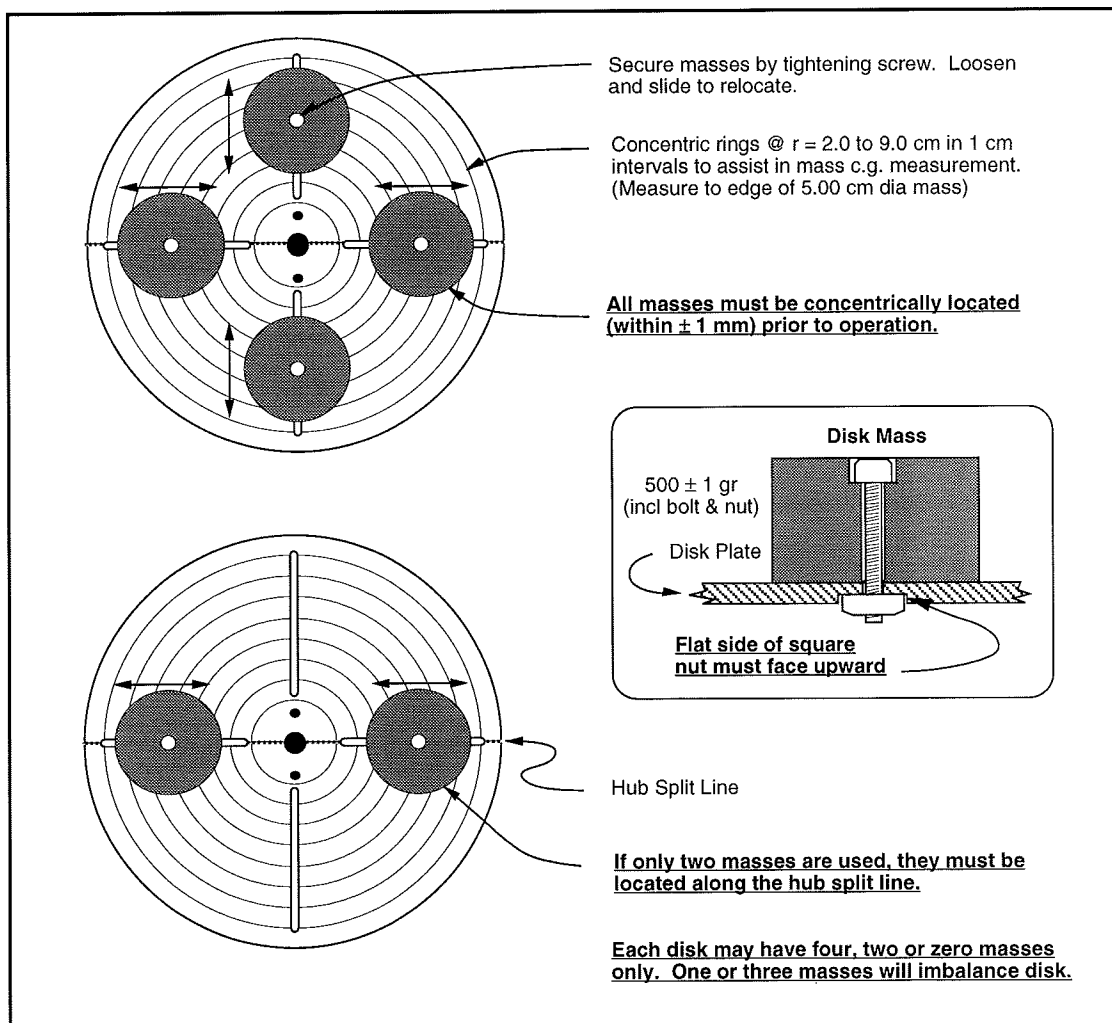


Figure 2.2-3. Guidelines For Changing Or Adjusting Disk Masses

The user should verify that the disks, belts, and pulleys are properly aligned and secured and rotate freely prior to operation.

For Model 205 (2 disk only) the second disk is nominally located at the upper shaft position. If the disk is moved to the middle position, the encoder will be oriented upside down and the polarity of its signal will be reversed. A negative unity gain in the encoder feedback branch (e.g.  $S(z)$ ,  $I(z)$ , or  $F(z)$ ) must be downloaded via the general form to provide stable (negative feedback) closed loop control. This must be done every time a controller involving encoder #2 (at the mid-shaft location) is implemented. For Model 205a no polarity correction is necessary.

### 2.2.3 The Optional Disturbance Drive

The drive is calibrated at the factory to output approximately 1.2 N-m/V as applied to the inertia disk. Here “V” is the input voltage to the motor amplifier and may be specified via the executive program, or applied externally in the case the user is supplying control hardware inputs (e.g. the system was purchased in the “Plant Only” configuration.) \

When the drive is driven in response to the motion at a specific disk – e.g. in the “viscous friction” or torque proportional to  $\sin(\theta)$  modes – the motion is sensed via the encoder at the adjacent disk. The particular disk must be specified in the Disturbance Configuration dialog box. The “viscous friction” is applied as a torque (motor current) proportional to and in the opposite direction of the rate as measured via the encoder at the specified inertia disk.)

Instructions for positioning, adjusting, and stowing the drive are given in Figure 2.2-4.

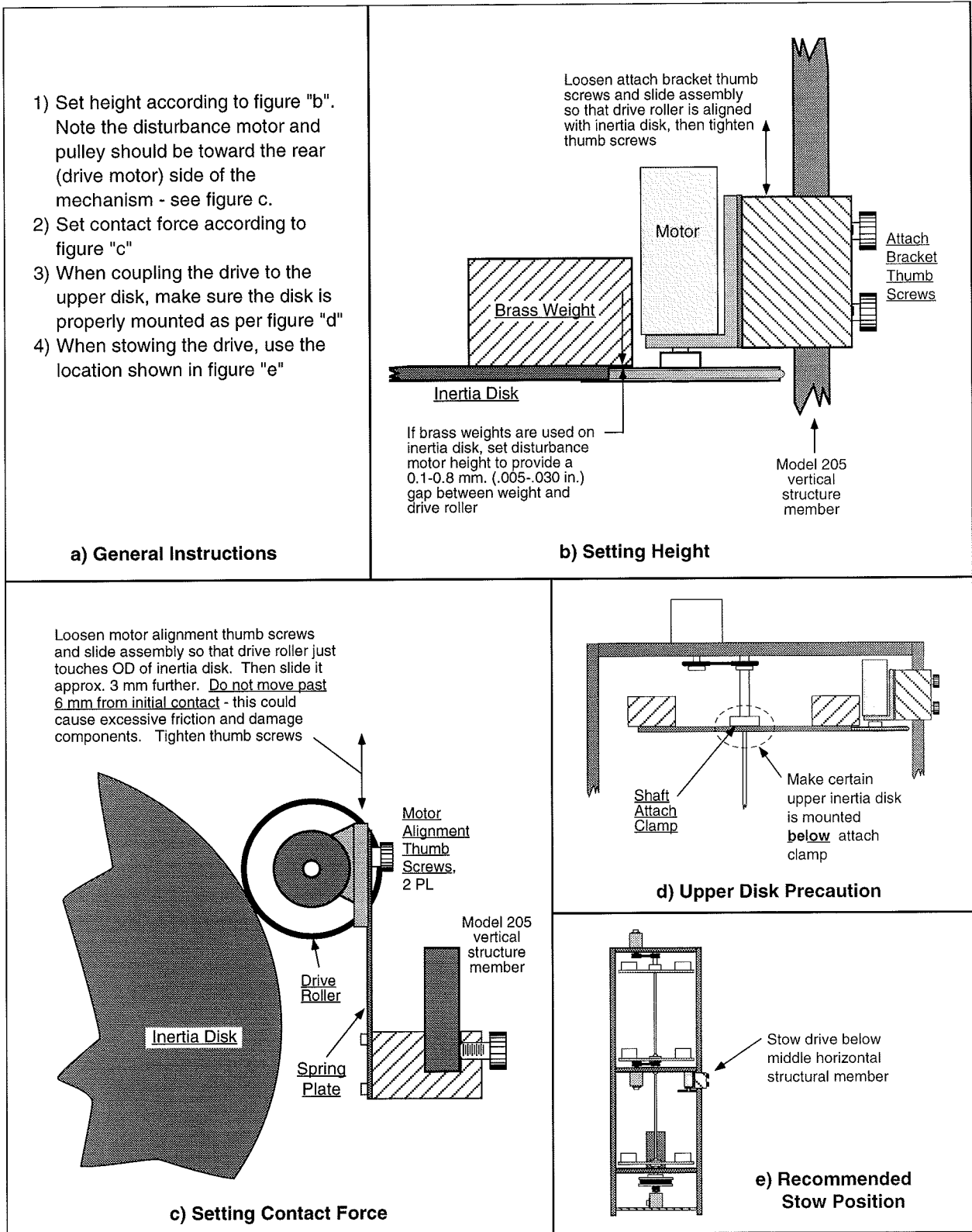


Figure 2.2-4. Guidelines For Positioning & Stowing the Disturbance Drive

## 2.3 Safety

The following are safety features of the system and cautions regarding its operation. This section must be read and understood by all users prior to operating the system. If any material in this section is not clear to the reader, contact ECP for clarification before operating the system.

**Important Notice: In the event of an emergency, control effort should be immediately discontinued by pressing the red "OFF" button on front of the control box.**

### 2.3.1 Hardware

A relay circuit is installed within the Control Box which automatically turns off power to the Box whenever the real-time Controller (within the PC) is turned on or off. Thus for the PC bus version<sup>1</sup> of the real-time Controller the user should turn on the computer prior to pressing on the black ON switch. This feature is implemented to prevent uncontrolled motor response during the transient power on/off periods. The power to the Control Box may be turned off at any time by pressing the red OFF switch.

Although not recommended, it will not damage the hardware to apply power to the Control-Box even when the PC is turned off. However, doing so does not result in motor activation as the motor current amplifier will be disabled. The *amplifier enable* signal input to the Control Box is connected to the real-time Controller via the 60-pin flat ribbon cable. This input operates in a normally closed mode. When power to the real-time Controller is off, this input becomes open which in turn disables the motor amplifier.

The recommended procedure for **start up** is as follows:

- First :** Turn on the PC with the real-time Controller installed in it.
- Second:** Turn on the power to Control Box (press on the black switch).

The recommended **shut down** procedure is:

- First:** Turn off the power to the Control Box.
- Second:** Turn off the PC..

---

<sup>1</sup>The majority of this section (2.3.1) pertains to the PC bus installation of the real-time controller. For the controller box/RS-232 version, the control box should generally be powered on before entering the executive software.

**FUSES:** There are two 3.0A 120V slow blow fuses within the Control Box. One of them is housed at the back of the Control Box next to the power cord plug. The second one is inside the box next to the large blue colored capacitor.

### 2.3.2 Software

The Limit Exceeded indicator of the Controller Status display indicates either one or more of the following conditions have occurred:

- Over speed of the motor
- Excessive deflection (twisting) of the torsion shaft
- Excessive drive motor power

The real-time Controller continuously monitors the above limiting conditions in its background routine (intervals of time in-between higher priority tasks). When one if these conditions occurs, the real-time Controller opens up the control loop with a zero torque command sent to the actuator. The Limit Exceeded indicator stays on until a new set of (stabilizing) control gains are downloaded to the real-time Controller via the Implement Algorithm button of the Setup Control Algorithm dialog box, or a new trajectory is executed via the Command menu. Obviously the new trajectory must have parameters that do not cause the Limit Exceeded condition.

The Limit Exceeded indicator of the Disturbance Motor Status display indicates either one or both of the following conditions have occurred:

- Over speed of the disturbance motor.
- Excessive disturbance motor power

Also included is a *watch-dog timer*. This subsystem provides a fail-safe shutdown to guard against software malfunction and under-voltage conditions. The use of the watch-dog timer is transparent to the user. This shutdown condition turns on the red LED on the real-time Controller card, and will cause the control box to power down automatically. You may need to cycle the power to the PC in order to reinitialize the real-time Controller should a watch-dog timer shutdown occur.

### 2.3.3 Safety Checking The Controller

While it should generally be avoided, in some cases it is instructive or necessary to manually contact the mechanism when a controller is active. This should always be done with caution and never in such a way that clothing or hair may be caught in the apparatus. By staying clear of the mechanism when it is moving or when a trajectory has been commanded, the risk of injury is greatly reduced. Being motionless, however, is not sufficient to assure the system is safe to

contact. In some cases an unstable controller may have been implemented but the system may remain motionless until perturbed – then it could react violently.

In order to eliminate the risk of injury in such an event, you should always safety check the controller prior to physically contacting the system. This is done by lightly grasping a slender, light object with no sharp edges (e.g. a ruler without sharp edges or an unsharpened pencil) and using it to slowly move either the load or drive disk from side to side. Keep hands clear of the mechanism while doing this and apply only light force to the disk. If the disk does not spin up or oscillate then it may be manually contacted – but with caution. This procedure must be repeated whenever any user interaction with the system occurs (either via the Executive Program or the Controller Box) if the mechanism is to be physically contacted again.

#### 2.3.4 Warnings

**WARNING #1: Stay clear of and do not touch any part of the mechanism while it is moving, while a trajectory has been commanded (via Execute, Command menu), or before the active controller has been safety checked – see Section 2.3.3.**

**WARNING #2: The following apply at all times except when motor drive power is disconnected (consult ECP if uncertain as to how to disconnect drive power):**

- a) Stay clear of the mechanism while wearing loose clothing (e.g. ties, scarves and loose sleeves) and when hair is not kept close to the head.
- b) Keep head and face well clear of the mechanism.

**WARNING #3: Verify that the masses and inertia disks are secured per section 2.2 of this manual prior to powering up the Control Box or transporting the mechanism.**

**WARNING #4: Do not take the cover off or physically touch the interior of the Control Box unless its power cord is unplugged (first press the "Off" button on the front panel) and the PC is unpowered or disconnected.**

**WARNING #5: The power cord must be removed from the Control box prior to the replacement of any fuses.**



### 3. Start-up & Self-guided Demonstration

This chapter provides an orientation "tour" of the system for the first time user. In Section 3.1 certain hardware verification steps are carried out. In Section 3.2 a self-guided demonstration is provided to quickly orient the user with key system operations and Executive program functions. Finally, in Section 3.3, certain system behaviors which may be nonintuitive to a first time user are pointed out .

All users must read and understand Section 2.3, Safety, Before performing any procedures described in this chapter.

#### 3.1 Hardware Setup Verification

At this stage it is assumed that

- a) The ECP Executive program has been successfully installed on the PC's hard disk (see Section 2.1.2).
- b) The actual printed circuit board (the real-time Controller) has been correctly inserted into an empty slot of the PC's extension (ISA) bus (this applies to the PC bus version only).
- c) The supplied 60-pin flat cable is connected between the J11 connector (the 60-pin connector) of the real-time Controller and the JMACH connector of the Control Box<sup>1</sup>.
- d) The other two supplied cables are connected between the Control Box and the Torsion apparatus;
- e) The apparatus has the three disks securely installed (Model 205a, two disks for Model 205) with no weights fastened to any disks and all clamps removed. (i.e. the plant should be set up as shown in Figure 2.2-1 except with no masses on the disks. This is the configuration the mechanism is shipped in.)
- f) You have read the safety Section 2.3. All users must read and understand that section before proceeding.

Please check the cables again for proper connections.

---

<sup>1</sup>This applies to the PC-bus installation only. For the controller in the Control Box, the RS-232 cable must be connected between the Control Box and the PC.

### 3.1.1 Hardware Verification (For PC-bus Installation)

**Step 1:** Switch off power to both the PC and the Control Box.

**Step 2:** With power still switched off to the Control Box, switch the PC power on. Enter the ECP program by double clicking on its icon (or type ">ECP" in the appropriate directory under DOS). You should see the Background Screen (see Section 2.1.3). Gently rotate the drive or load disk by hand. You should observe some following errors and changes in encoder counts. The Control Loop Status should indicate "CLOSED" and the Controller Status should indicate "ACTIVE". If this is the case skip Step 3 and go to Step 4.

**Step 3:** If the ECP program cannot find the real-time Controller (a pop-up message will notify you if this is the case), try the Communication dialog box under the Setup menu. Select PC-bus at address 528, and click on the test button. If the real-time Controller is still not found and you are using the ECP Executive for DOS, try increasing the time-out in increments of 20 up to a maximum of 300. If you are using the ECP Executive for Windows, try increasing the time-out in increments of 5000 up to a maximum of 80000. If this doesn't correct the problem, switch off power to your PC and then take its cover off. With the cover removed check again for the proper insertion of the Controller card. Switch the power on again and observe the two LED lights on the Controller card. If the green LED comes on all is well; if the red LED is illuminated, you should contact ECP for further instructions. If the green LED comes on, turn off power to your PC, replace the cover and turn the power back on again. Now go back to the ECP program and you should see the positions change as you gently rotate the disks.

**Step 4:** Make sure that you can rotate the disks freely. Now connect the power cord to the Control Box and press the black "ON" button to turn on the power to the Control Box. You should notice the green power indicator LED lit, but the motor should remain in a disabled state. Do not touch the disks whenever power is applied to the Control Box since there is a potential for uncontrolled motion of the disks (see the warnings in Section 2.3) unless the controller has been safety checked.

This completes the hardware verification procedure. Please refer again to Section 2.3 for future start up and shut down procedures.

### 3.2 Demonstration of ECP Executive Program

This section walks the user through the salient functions of the system. By following the instructions below you will actually implement a controller, maneuver the system through various trajectories, and acquire and plot data. The procedures given in this section are for Model 205a (3 disk) but also apply to Model 205 except where noted. The data plots shown are for Model 205a. The corresponding plots for Model 205 are given in Section 3.2.1 immediately following this section.

**Step 1: Loading A Configuration File.** With the power to the Control box turned off, enter the ECP Executive program. You should see the Background Display. Turn on power to the Control Box (press on the black button). Now enter the File menu, choose Load Setting and select the file `default.cfg`. This configuration file is supplied on the distribution diskette and should have been copied into the ECP directory by now. In fact, it would have been loaded into the Executive automatically (see Section 2.1.4.1) upon startup. This particular `default.cfg` file contains the controller gain parameters and other trajectory, data gathering and plotting parameters specifically saved for the activities within this section.

Note again that this file has been created to operate with a plant with three disks with no extra (brass) weights attached. (For Model 205 the file is for an upper and lower disk only with no weights attached.)

**Step 2: Implementing The Controller.** Now enter the Setup menu and choose Setup Control Algorithm. You should see the sampling time  $T_s = 0.004420$  seconds, Discrete Time control type, and State Feedback control selected. Select Setup Algorithm; you should see for Model 205a the following gains:  $k_{pf}=0.935$ ,  $k_1=1.0074$ ,  $k_2=4.9957$ ,  $k_3=-0.07867$ ,  $k_4= 5.27106$ ,  $k_5=0.00533$  and  $k_6=5.510$ . (For Model 205, the gains are  $k_{pf}=0.930$ ,  $k_1=0.780$ ,  $k_2=3.416$ ,  $k_3=0.150$ ,  $k_4=7.350$ .) This controller was designed using linear quadratic regulator (LQR) synthesis techniques with all error weighting on encoder 3 (encoder 2 for Model 205, i.e. the noncollocated encoder at the top of the apparatus).

Exit this dialog box and select Implement Algorithm. The control law is now downloaded to the real-time Controller. Use a ruler to verify that control action is in effect on the lower disk (see Sect. 2.3.3, "Safety Checking The Controller") If you do not notice any motor power, click on the Implement Algorithm button again until you notice the servo loop closed. Now select Upload Algorithm, then General Form and Setup Algorithm. You should see the general form of the real-time algorithm with some non-zero coefficients. These coefficients correspond to the state feedback gains mapped to a form suitable for execution via the general form algorithm. Note that the general form algorithm is the only structure that actually runs in real-time. All other structures (e.g. PID, dynamic filters, etc.) are translated to the general form by the Executive prior to implementation.

**Step 3: Setting Up Data Acquisition.** Enter the Data menu and select Setup Data Acquisition. In this box make sure that the following four items are selected: Commanded Position and Encoders 1,2, & 3 (Encoders 1 & 2 only for Model 205). *Data sample period* should be 2 which means that data will be collected every second servo cycle (in this case every  $2 * 0.00442 = 0.00884$  seconds).

**Step 4: Executing A Step Input Trajectory & Plotting.** Enter the Command menu and select Trajectory. In this box select Step and then Setup. You should see *step size* = 1000, *dwell time* = 1000 ms and *no. of repetitions* = 1. If not, change the values to correspond to this parameter set. Exit this box and go to the Command menu. This time select Execute and with the Sample Data check box checked run the trajectory. You should have noticed a step move of 1000 counts, a dwell of 1 second and a return step move. Wait for the data to be uploaded from the real-time Controller to the Executive program running on the PC. Now enter the Plotting menu and choose Setup Plot. Select Encoder 3 (Encoder 2 for Model 205) and Commanded Position for plotting (left axis) and select Plot Data.

You should see a plot similar to the one shown in Figure 3.2-1. Replace Encoder 3 with 2 via the Setup Plot box and then with Encoder 1, plotting the data each time. Similar plots to the ones shown in Figures 3.2-2 and 3.2-3 should be seen. Note that all plot screens may be repositioned by dragging the plot frame bar using the mouse. A plot screen may be minimized or "shrunk" by clicking on the left most button on the top right hand corner. By double clicking on a minimized plot screen it may be expanded again. In general, to limit the program memory usage, one should avoid minimizing more than 8 to 10 plot screens on the Background screen. It is best to close unwanted plot screens rather than minimize them. You can re-size the plots using the cursor to "drag" any edge of the plot frame (position cursor at corner and begin "dragging" when cursor becomes double arrow).

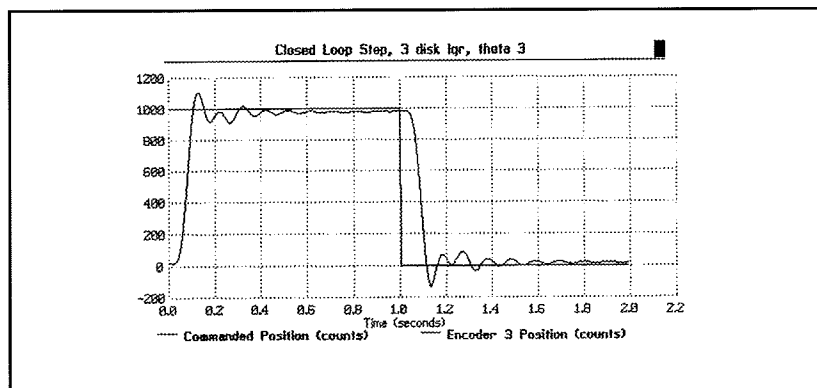


Figure 3.2-1 Step Response at Encoder 3

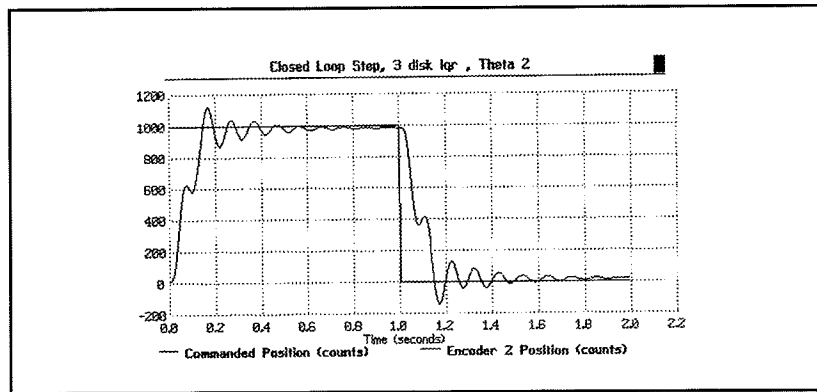


Figure 3.2-2 Step Response at Encoder 2

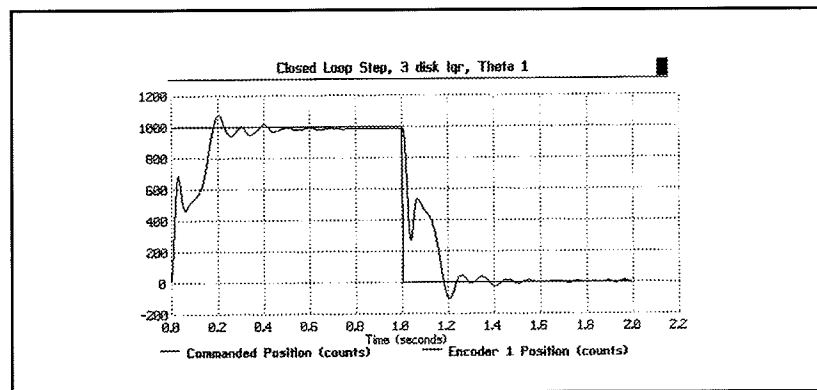


Figure 3.2-3 Step Response at Encoder 1

**Step 5: Tracking Response.** Return to Trajectory and select Ramp and then Setup to enter the *Ramp* dialog box. You should see *distance* = 10000 counts, *velocity* = 10000 counts/s, *dwell time* = 10 ms and *no. of repetitions* = 1. If not, change the values to this set. Exit this box and go to the Command menu. Again select Execute and with Sample Data checked, run the trajectory. You should have noticed the ramp move of 10000 counts followed by an immediate return ramp move. Now enter the Plotting menu and choose Setup Plot. Select Encoder 3 and Commanded Position for plotting and then plot the data. You should see a plot similar to the one shown in Figure 3.2-4. Replacing Encoder 3 with 1 and replotting should result in a response similar to Figure 3.2-5. (Encoder 3 tracks best due to the lqr design objective with error weighting on disk 3). You may save the ramp response under anyname.plt using the Save Plot Data option. Any plot data thus saved may be reloaded from the disk using the Load Plot Data option for future inspection, plotting or printing. To print simply choose the Print Data menu option and select the appropriate printer before the printing command. Alternatively, any set of collected data may be exported as an ASCII text file by the use of the Export Data option of the Data menu.

Now close all plot windows.

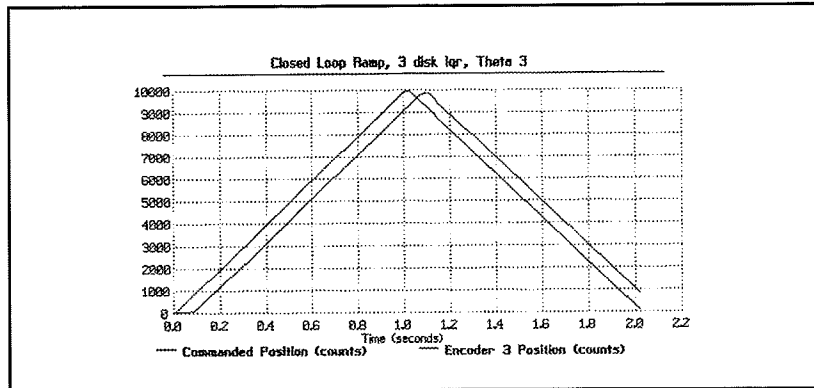


Figure 3.2-4 Ramp Response at Encoder 3

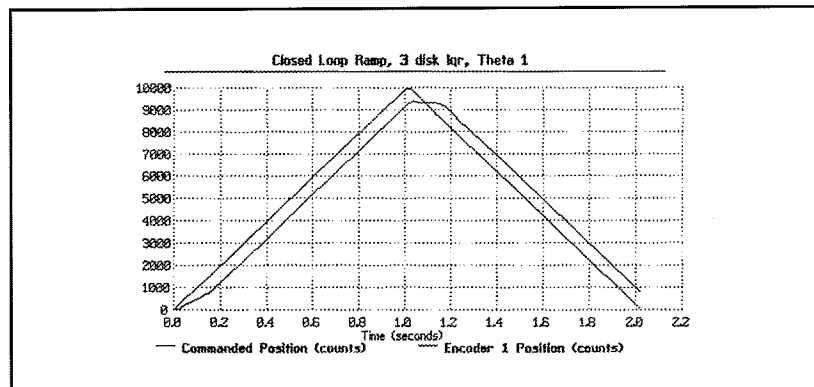


Figure 3.2-5 Ramp Response at Encoder 1

**Step 7: Frequency Response.** Again enter Trajectory and select Sine Sweep then Setup. You should see the *amplitude* = 100 counts, *max. freq.* = 20 Hz, *min. freq.* = 1 Hz, *sweep time* = 29.5 sec., and *Linear Sweep* selected. Again, if different, change the values to correspond this set. Exit this box and go to the Command menu and Execute with Sample Data checked. While running this trajectory, you should notice sinusoidal motion with increasing frequency for about thirty seconds. Now enter the Plotting menu and choose Setup Plot. This time select only Encoder 3 (Encoder 2 for Model 205) for plotting and choose Linear Time and Linear amplitude scaling for the horizontal and vertical axes; then plot the data. You should see a plot similar to the one shown in Figure 3.2-6a. Now replace Encoder 3 with 2 and then with 1. Plots similar to the ones shown in Figures 3.2-6b&c should be seen. Now return to the Sine sweep trajectory box and select with all else unchanged. Execute this maneuver and plot the data using Logarithmic Frequency and Db axis scaling. Now the plots should appear similar to those shown in Figure 3.2-6d-f.<sup>1</sup>

<sup>1</sup> The Logarithmic frequency / Db data may be also plotted from the linear sweep which results in fewer cycles at low frequency and more at high frequency.

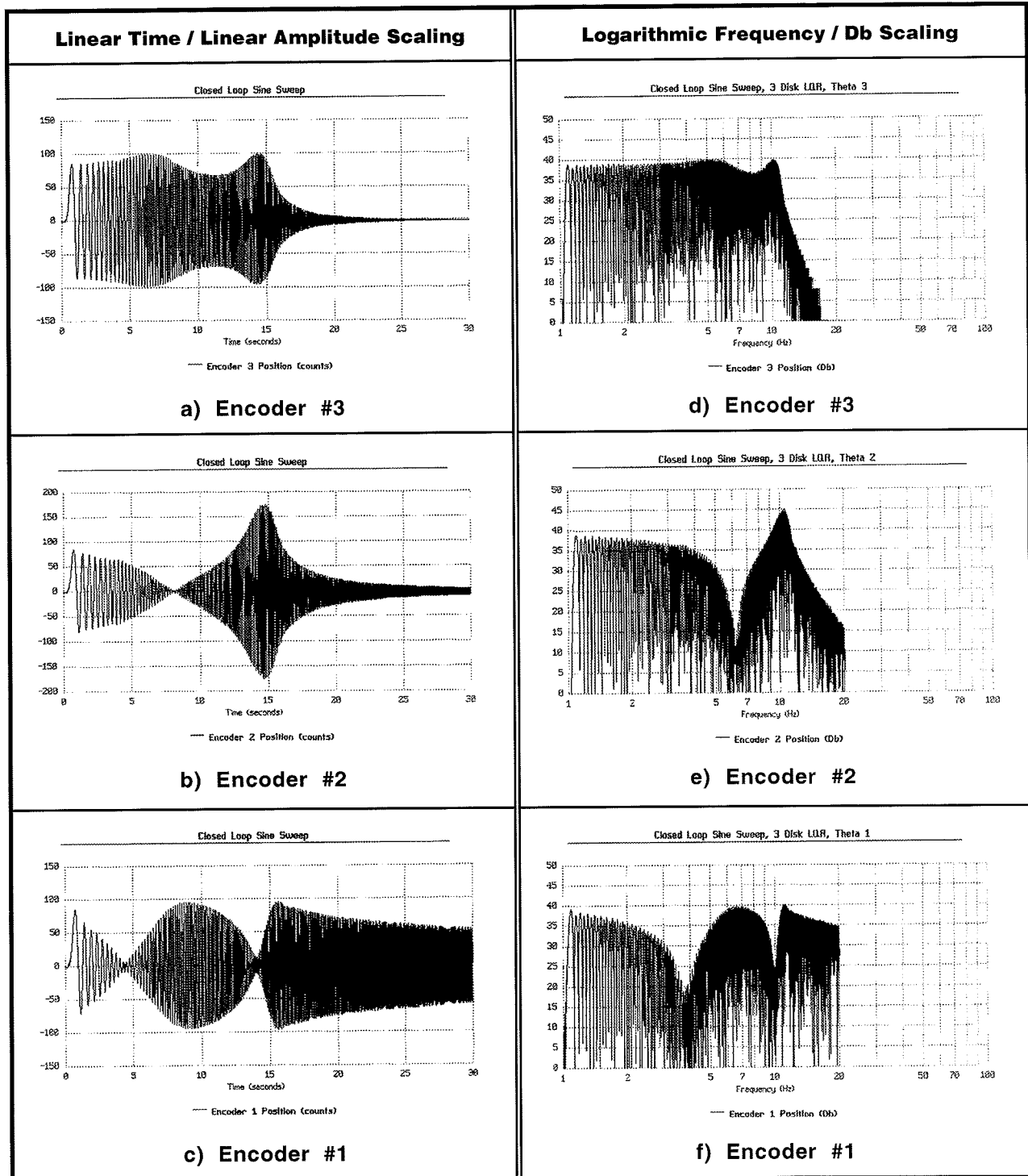


Figure 3.2-6i Sine Sweep (Frequency) Response Data With Various Trajectory / Plotting Options

The linear time / amplitude depiction shows the data in a manner that more intuitively represents for most students the physical motion of the system as witnessed. The  $\text{Log}(w)$  / Db scaling presents the data in a way that leads to physical understanding of the Bode magnitude plots commonly found in the literature. The resonances and anti-resonances (lightly damped poles and zeros) seen

in these responses agree with their transfer function models. That is, the resonances (poles) are common to all outputs, and disks 1, 2, & 3 have zero, one, and two zero pairs respectively. The high frequency attenuation is greater with disk number reflecting the respective two, four, and six pole excesses. Similarly insightful properties of open loop systems are found by measuring their sine sweep responses.

This completes the basic self-guided tour of the Model 205a system. For users with the Disturbance Drive option, the tour is continued in Section 3.2.2. It is advised that the user read all material in Chapters 2 and 3 before further operation of the equipment.

3.2.1 Plot Results For Model 205

The plots resulting from the self-guided tour for Model 205 are as follows.

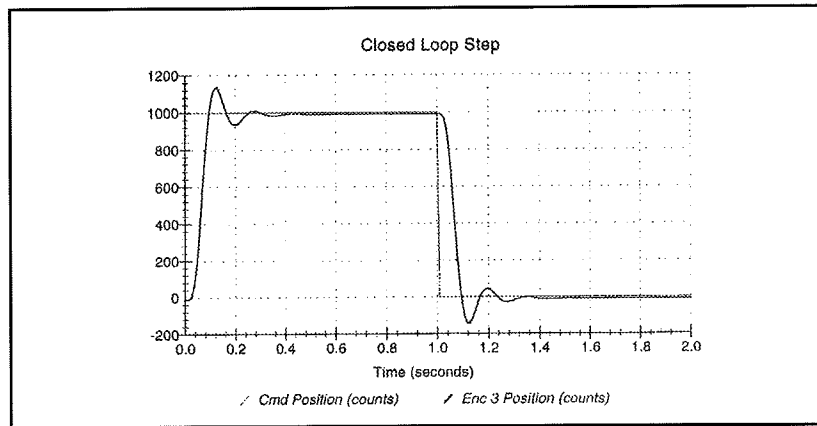


**Figure 3.2-7 Step Response at Encoder 2**

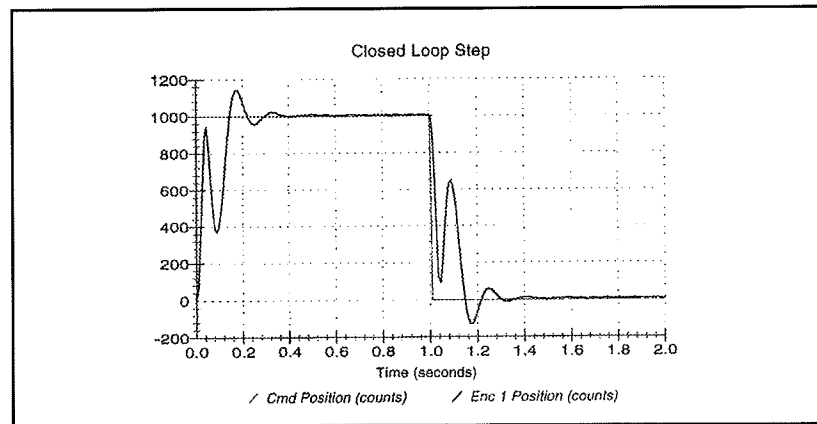


**Figure 3.2-8 Step Response at Encoder 1**



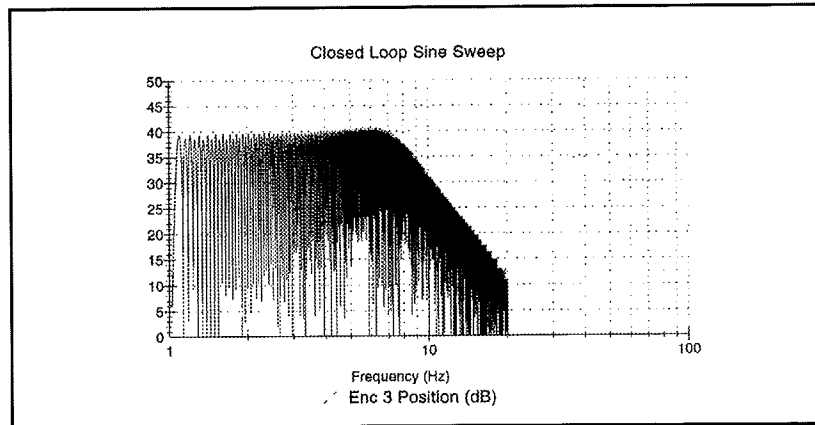


**Figure 3.2-9 Sine Sweep Response at Encoder 2**

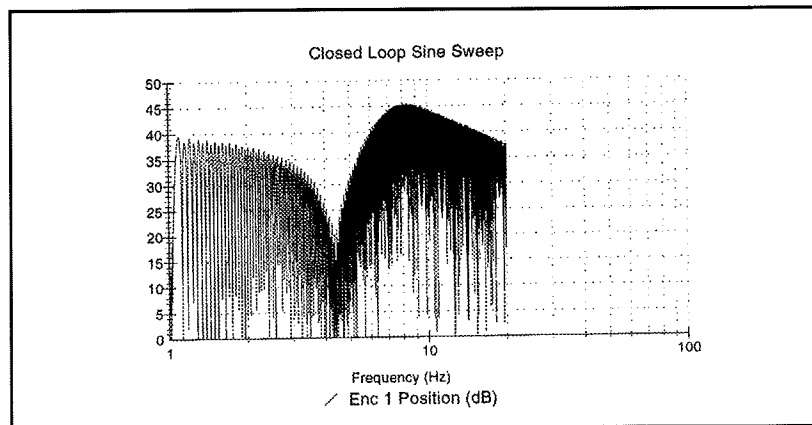


**Figure 3.2-10 Sine Sweep Response at Encoder 1**

The ramp following results appear similar to those in Figures 3.2-4,5 and are not shown here.

This completes the self-guided tour of the Model 205 system. For users with the Disturbance Drive option, the tour is continued in the next section. It is advised that the user read all material in Chapters 2 and 3 before further operation of the equipment.

### 3.2.2 Using The Optional Disturbance Drive

The optional disturbance drive is useful in studying the important system properties of regulation performance and disturbance rejection at any of the system outputs (inertia disks). It may also be used to apply viscous friction at any of these locations. The data shown below is for Model 205a (three disk) but is also representative of that for the basic Model 205.

### Step 1: Disturbance Rejection During System Regulation

Attach the disturbance Drive to the upper disk as per Section 2.2.3. Implement the controller according to Section 3.2 Step #2. (This is the default controller shipped with the system. If you have been following the Self Guided Tour until now, you should simply need to select Implement Algorithm in the Setup Control Algorithm dialog box.) The system should now be regulating (in closed loop control with a zero valued reference input). Enter the Disturbance Configuration dialog box and select Sinusoidal (time). Specify an amplitude of 1 V, frequency of 1 Hz, and 5 Repetitions. Enter Trajectory Configuration. Setup a Step input with *distance* = 0 counts, *dwell time* = 2000 ms and *no. of repetitions* = 1. This will provide a zero amplitude input for gathering data during the disturbance. Execute this trajectory via the Command menu making sure that Include Sinusoidal Disturbance is checked. Plot the data to find a disturbance response similar to Figure 3.2-11. Note that the response is greater at  $\theta_3$ , and that the  $\theta_1$  and  $\theta_3$  responses are roughly  $90^\circ$  out of phase.

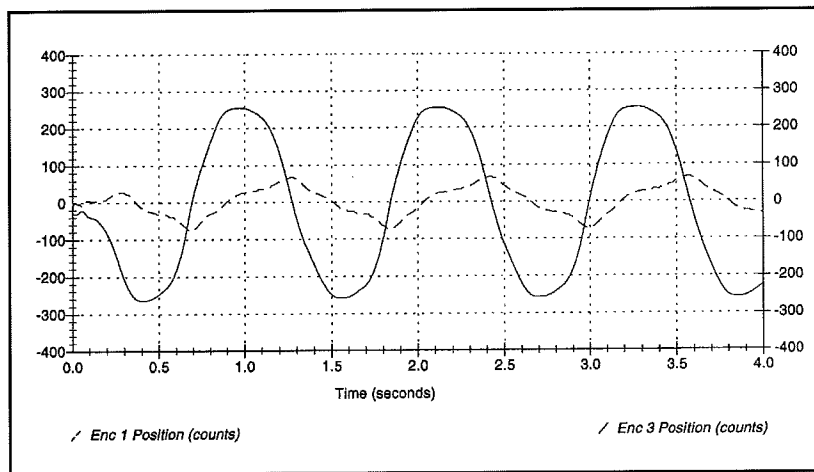


Figure 3.2-11 Disturbance Transmission During Regulation At Encoders 1 & 3

### Step 2: Disturbance Transmission During Tracking

Return to Trajectory Configuration and setup a Ramp input with *distance* = 20000 counts, *velocity* = 5000 counts/s, *dwell time* = 10 ms and *no. of repetitions* = 1. Execute this shape and plot the data to find a response similar to Figure 3.2-12. The effect of the disturbance is clearly seen in the  $\theta_3$  output.

You may wish to try other combinations of disturbances and trajectories and at the various inertia disk locations. Viscous friction may be applied simultaneously with disturbances.

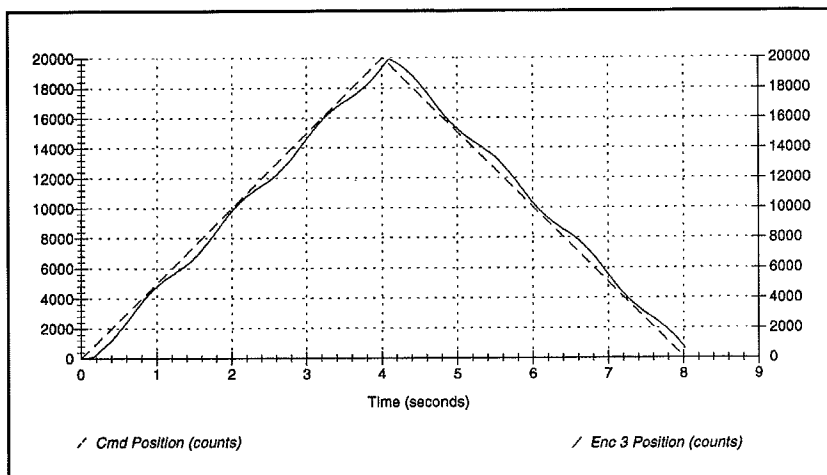


Figure 3.2-12 Disturbance Transmission At Encoder 3 During Tracking

### 3.3 Nonintuitive System Behavior

An explanation of system functionality which may be nonintuitive to first time (or first few time) users is given below.

**Point 1:** Upon PC power up, the control loop is closed but all gains are cleared to zero. As a result, even though the status display indicates CLOSED LOOP, the control effort is zero indicating that there is no torque command to the actuator. With zero gains, the closed loop system behaves like an open loop one. This initialization of the gains to zero also takes place every time the real-time controller is Reset under the Utility menu.

**Point 2:** Even though the parameters for a particular control algorithm may exist within the Executive, the real-time Controller does not carry them until the Implement Algorithm button of the Setup Control Algorithm dialog box is activated. Then control is implemented immediately

**Point 3:** The **Limit Exceeded** message comes on as a result of either motor over-speed, shaft over-deflection or drive over-current. In any case the message does not clear until a stable set of control gains are downloaded and if necessary a less abrupt trajectory is requested (see Section 2.1.3 ). This condition may also occur when the following takes place. With the control loop closed, the power to the Control Box is turned off and the disks are rotated manually and then the power is turned back on again. In this case the uncontrolled motion of the disks may cause the limiting conditions.

## 4. Real-Time Control Implementation

A functional overview of the control system is shown in Figure 4.0-1. The system is comprised of three subsystems: The mechanism including motor and sensors, the real-time controller / drive electronics, and the user/system (“Executive”) interface software.

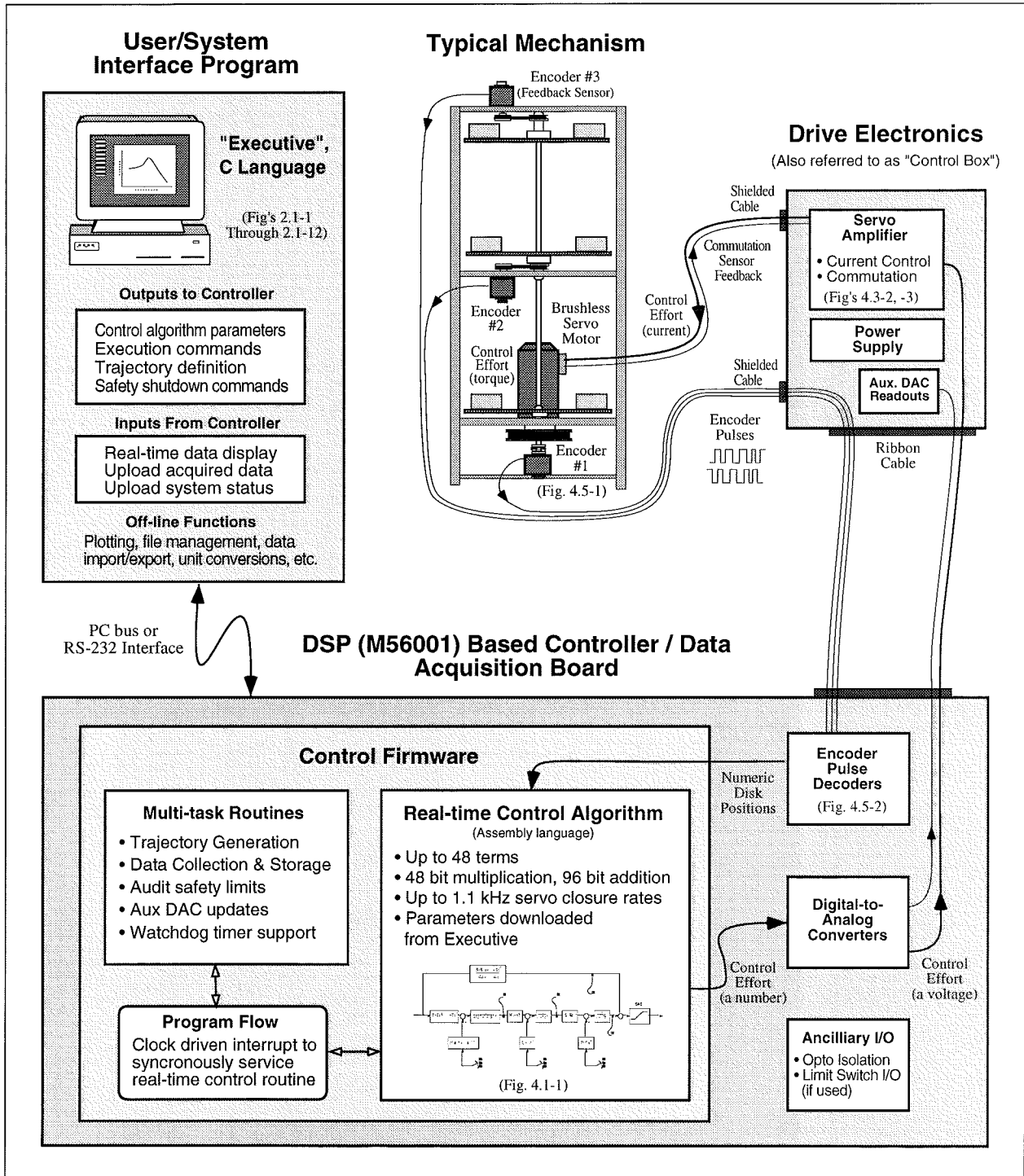


**Figure 4.0-1. Overview of Real-time Control System.**  
This architecture is consistent with modern industrial control implementation.

An brief survey of the system architecture is afforded by tracing the data flow as the system is operated. The user specifies the control algorithm in the Executive program and downloads it (via "Implement Algorithm") to the DSP based real-time controller board. The DSP immediately executes the algorithm at the specified sample rate. This involves reading the reference input<sup>1</sup> and feedback sensor (optical encoders) values, computing the algorithm, and outputting the digital control effort signal to the digital-to-analog converter (DAC).

The DAC converts the resulting stream of digital words to an analog voltage which is transformed to a current by the servo amplifier and then to a torque by the motor. The mechanism transforms the motor input to motion at the desired output according to the plant dynamics (i.e. equations of motion). These plant outputs are sensed by the encoders which output a stream of pulses<sup>2</sup>. The pulses are decoded by a counter on the DSP board and made available as a digital position word to the real-time control algorithm.

When the user specifies a trajectory and subsequently commands the system to "Execute" the maneuver, the trajectory parameters are downloaded to the controller board. The DSP generates corresponding reference input values for use by the real-time control algorithm. Throughout the maneuver, any data specified by the user is captured and stored in memory on the board. On completion of the maneuver, the data is uploaded to PC memory where it is available for plotting and storage.

Details of these and other significant system functions are given in the remainder of this chapter.

#### 4.1 Servo Loop Closure

Servo loop closure involves computing the control algorithm at the sampling time. The real-time Controller executes the General Form equation of the control law at each sample period  $T_s$ . This period can be as short as 0.000884 seconds (approx. 1.1 KHz) or any multiple of this number. The Executive program's Setup Control Algorithm dialog box allows the user to alter the sampling period. All forms of control laws are automatically translated by the Executive program to the General Form prior to downloading ("implementing") to the Controller. The General Form, shown in Figure 4.1-1, uses 96-bit real number (48-bit integer and 48-bit fractional) arithmetic for computation of the control effort. The control effort is saturated in software at +/- 16384 to represent +/- 5 volts on the 16-bit DACs whose range is +/- 10 volts. The +/-5 volt limitation is due to the actuator 's amplifier input voltage scaling.

---

<sup>1</sup> Since no trajectory is being input at this point, the system is regulating about a reference input value of zero.

<sup>2</sup> Each pulse corresponds to a small displacement (1/16,000 revolution in this case) at the plant output.

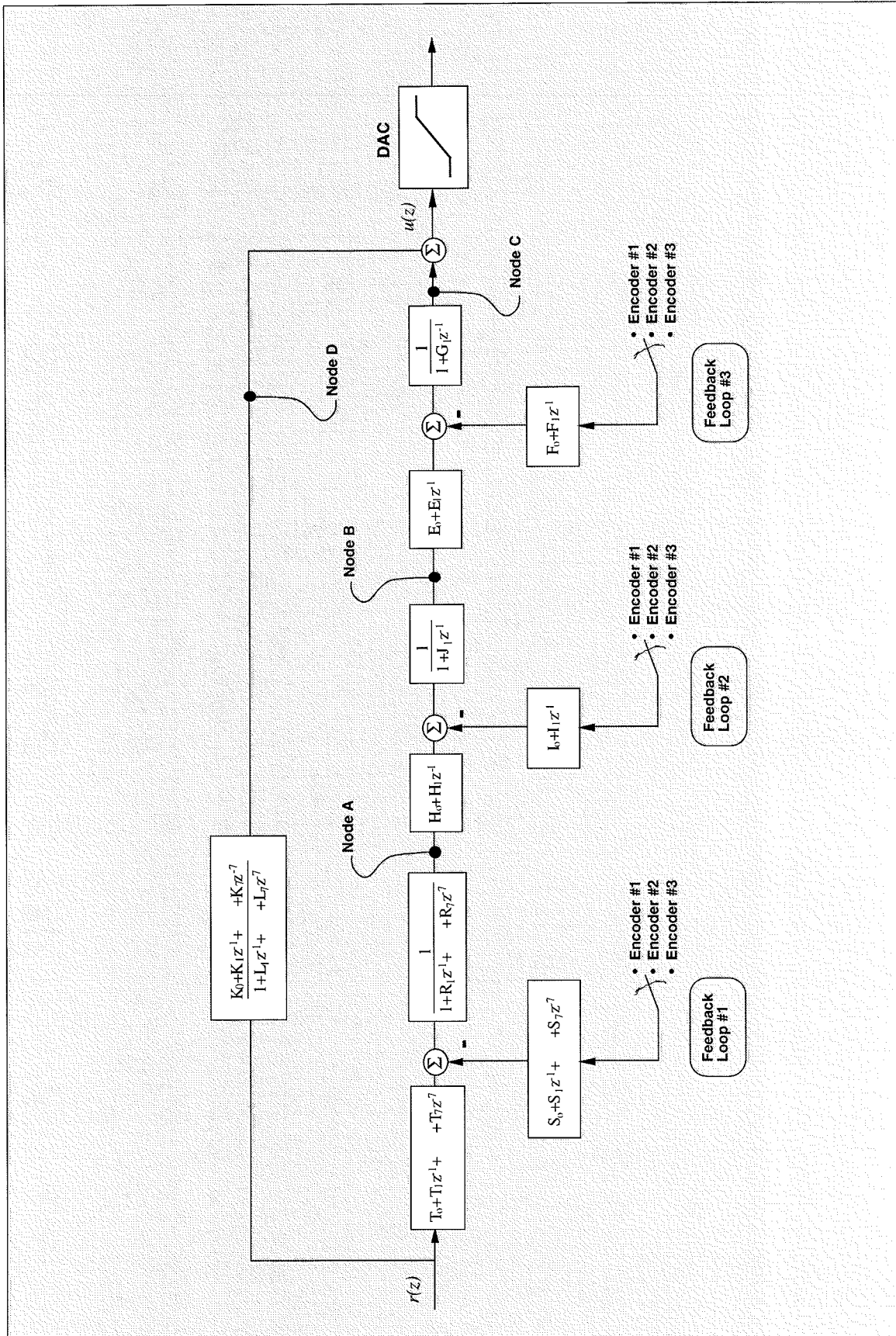


Figure 4.1-1. General Form Of The ECP Control Algorithm

Referring to Figure 4.1-1, the control equations are as follows:

$$R(q^{-1})\text{nodeA}(k) = T(q^{-1}) * c_p(k) - S(q^{-1}) * f_{b1}(k)$$

Here T, S, and R are seventh order polynomials of the unit time shift operator q, and the letter k represents the k<sup>th</sup> sampling period for k=0, 1, 2, ... . The variable nodeA is an intermediate value of the overall control law equation which is stored in the memory and may be acquired by the user through the Data Acquisition feature of the Executive program. The variable c<sub>p</sub>(k) is the commanded position which is generated by the real-time Controller as described in the next section. The variable f<sub>b1</sub>(k) may be from any of the three possible feedback sensors depending on the state of software loop switch 1.

Next the intermediate loop is computed as follows

$$J(q^{-1}) * \text{nodeB}(k) = H(q^{-1}) * \text{nodeA}(k) - I(q^{-1}) * f_{b2}(k)$$

Here again nodeB is an intermediate value stored in the memory and f<sub>b2</sub> is the sensor feedback selected via loop switch 2. J, H, and I are second order polynomials. For the inner loop we have

$$G(q^{-1}) * \text{nodeC}(k) = E(q^{-1}) * \text{nodeB}(k) - F(q^{-1}) * f_{b3}(k)$$

NodeC is the contribution to the value of the control effort generated by the overall regulator and f<sub>b3</sub> is the sensor feedback selected via loop switch 3. G, E, and F are second order polynomials. For the feedforward loop we have

$$L(q^{-1}) * \text{nodeD}(k) = K(q^{-1}) * c_p(k)$$

In this case nodeD is the contribution to the value of the control effort generated by the feedforward terms, L and K are sixth order polynomials.

The combined regulatory and tracking controller generates the control effort as:

$$\text{control effort}(k) = \text{nodeC}(k) + \text{nodeD}(k)$$

The general control structure described above supports the implementation of a broad range of specific control forms.

## 4.2 Command Generation

*Command generation* is the real-time generation of motion trajectories specified by the user. The parameters of these trajectories are downloaded to the real-time Controller through the Executive program via the Trajectory Configuration dialog box. This section describes the trajectories generated in the current control version.

### 4.2.1 Step Move

Figure 4.2-1a shows a step move demand. The desired trajectory for such a move can be described by

$$\begin{aligned}c_p(t) &= c_p(0) + C && \text{for } t > 0 \\c_v(t) &= 0 && \text{for } t > 0 \\c_v(0) &= \infty\end{aligned}$$

Where  $c_p(t)$  and  $c_v(t)$  represent commanded position and velocity at time  $t$  respectively and  $C$  is the constant step amplitude. Such a move demand generates a strong impulsive torque from the control actuator. The response of a mechanical system connected to the actuator would depend on the dynamic characteristics of the controller and the system itself. However, in a step move, the instantaneous velocity and its derivatives are not directly controllable. Usually step moves are used only for test purposes; more gentle trajectories are nearly always used for practical maneuvers.

### 4.2.2 Ramp Move

A ramp demand is seen in Figure 4.2-1b. The trajectory can be described by

$$\begin{aligned}c_p(t) &= c_p(0) + V * t && \text{for } t > 0 \\c_v(t) &= V && \text{for } t > 0 \\c_a(0) &= \infty\end{aligned}$$

where  $c_a(0)$  represents commanded acceleration at time zero and  $V$  is a constant velocity. Relative to a step demand, a ramp demand is more gentle, however the acceleration is still impulsive. The commanded velocity is a known constant during the maneuver.



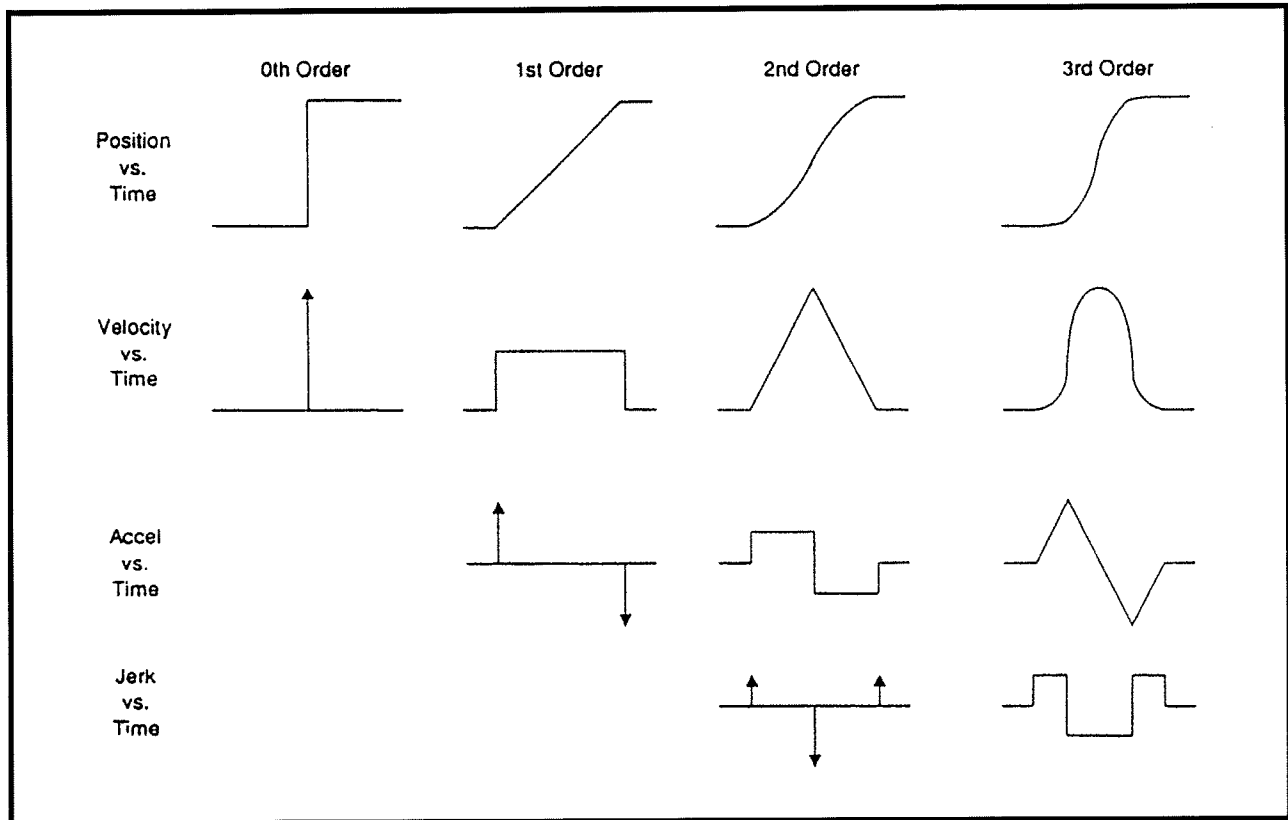


Figure 4.2-1. Geometric Command Trajectories Of Increasing Order

4.2.3 Parabolic Move

Figure 4.2-1c shows a parabolic move demand. Its trajectory can be expressed as:

$$\begin{aligned}
 c_p(t) &= c_p(0) + c_v(0) \cdot t + \frac{1}{2} A \cdot t^2 && \text{for } t > 0 < \frac{1}{2} t_f \\
 c_v(t) &= c_v(0) + A \cdot t && \text{for } t > 0 < \frac{1}{2} t_f \\
 c_a(t) &= A && \text{for } t > 0 < \frac{1}{2} t_f \\
 c_j(0) &= \infty
 \end{aligned}$$

where  $c_j(t)$  represents commanded jerk at time  $t$  and  $A$  is a constant acceleration, and  $t_f$  is the final destination time. Relative to a ramp demand, a parabolic demand is more gentle, however the rate of change of acceleration (jerk) is still impulsive. Note that the commanded acceleration is a known constant during the maneuver. The second half of a parabolic demand uses  $-A$  for deceleration.

4.2.4 Cubic Move

Figure 4.2-1d shows a cubic demand which can be described by

$$\begin{aligned}c_p(t) &= c_p(0) + c_v(0)*t + 1/2 c_a(0)*t^2 + 1/6 J*t^3 && \text{for } t > 0 < 1/4 t_f \\c_v(t) &= c_v(0) + c_a(0)*t + 1/2 J*t^2 && \text{for } t > 0 < 1/4 t_f \\c_a(t) &= c_a(0) + J*t && \text{for } t > 0 < 1/4 t_f \\c_j(0) &= J\end{aligned}$$

where  $J$  represents a constant jerk. Relative to all the above demands, a cubic demand is more gentle. The commanded acceleration is linearly changing during the three sections of the maneuver. The second half of a cubic demand uses  $-J$  and the third part uses  $J$  again for the jerk input.

#### 4.2.5 The Blended Move

Any time a ramp, a parabolic or a cubic trajectory move is demanded the real-time Controller executes a general blended move to produce the desired reference input to the control algorithm. The move is broken into five segments as shown in the velocity profile of Figure 4.2-2. For each section a cubic (in position) trajectory is planned. Five distinct cubic equations can describe the forward motion. After the dwell time, the reverse motion can be described by five more cubic trajectories. Each cubic has the form:

$$c_{p_i}(t) = c_{p_i}(0) + V_i*t + 1/2 A_i*t^2 + 1/6 J_i*t^3 \quad i = 1, \dots, 5$$

Using a known set of trajectory data (i.e. the requested total travel distance, acceleration time  $t_{acc}$ , and the maximum speed  $v_{max}$ , for each move), the constant coefficients  $V_i$ ,  $A_i$ , and  $J_i$  are determined for each segment of the move by the real-time Controller. This function is known as the "motion planning" task. Note that for a parabolic profile  $J_i=0$ , and for a ramp profile  $A_i$  is also zero which further simplifies the task. Having determined the coefficients for each section, the real-time Controller uses these values at the servo loop sampling periods to update the commanded position (reference input). For example if the segment is a cubic ( $J \neq 0$ ):

$$\begin{aligned}c_a(k) &= c_a(k-1) + J*T_s \\c_v(k) &= c_v(k-1) + c_a(k)*T_s \\c_p(k) &= c_p(k-1) + c_v(k)*T_s\end{aligned}$$

where  $T_s$  is the sampling period and  $c_a(k)$ ,  $c_v(k)$ ,  $c_p(k)$  represent commanded acceleration, velocity and position at the  $k^{th}$  sampling period.

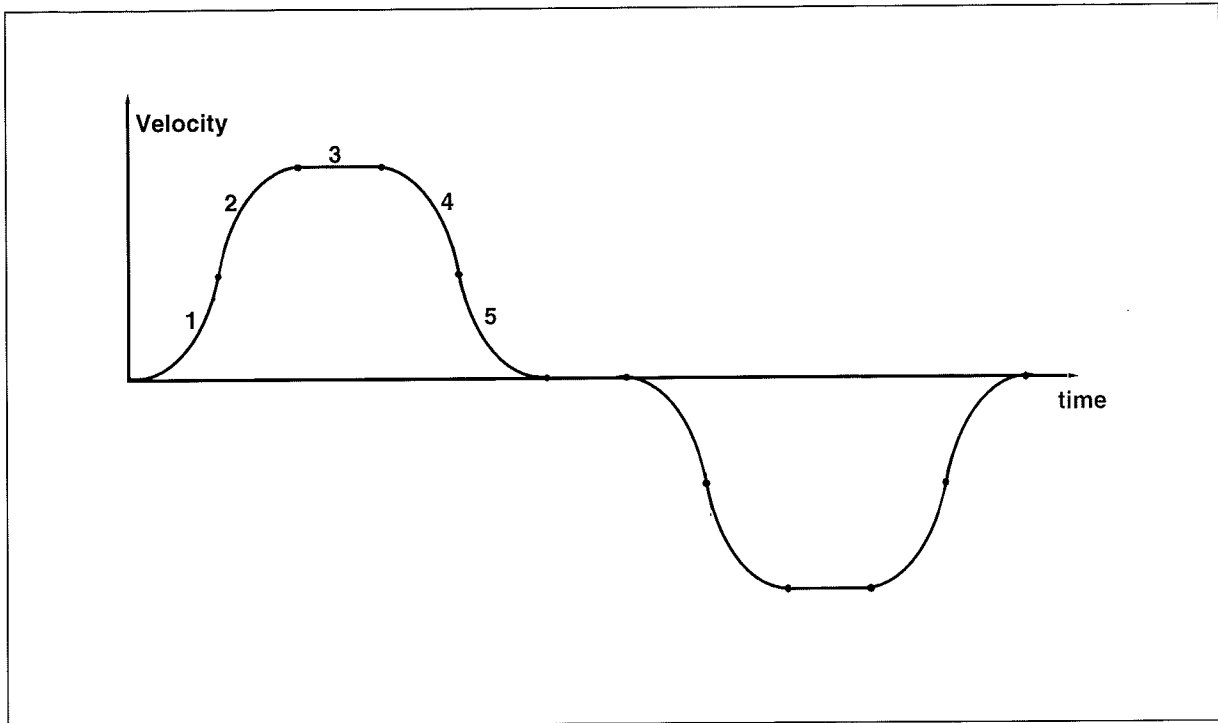


Figure 4.2-2 Velocity Profile for General Blended Move

4.2.6 Sinusoidal Move

The sinusoidal move is generated using the following equation:

$$c_p(k) = R * \sin(\theta(k))$$

where R is the amplitude,  $\theta(k) = \omega * k * T_p$  for  $k=0,1,\dots$ , and  $\omega$  is the commanded frequency in Hz.  $T_p$  is set to five milliseconds (i.e. k is incremented every 5 ms.). To further smooth out the trajectory, a cubic spline is fitted between the points as follows:

$$c_p'(k) = (c_p(k-1) + 4 * c_p(k) + c_p(k+1)) / 6$$

For the linear sine sweep,  $\omega(k) = \alpha * T_p$ , where  $\alpha$  is a constant determined by the difference between the maximum and the minimum frequency divided by the sweep time

$$\alpha = (\omega_{max} - \omega_{min}) / \text{sweep time}$$

For the logarithmic sweep

$$\omega = \omega_{min} * 10^{(B-A) * (k * T_p) / \text{sweep time}}$$

where A and B are defined according to

$$A \triangleq \log_{10}(\omega_{min}), B \triangleq \log_{10}(\omega_{max})$$

### 4.3 Brushless Motor Commutation and Torque Control

The main advantage of a DC brushless motor (otherwise known as a *permanent magnet synchronous* motor) over the conventional DC brush motor is the elimination of both brush friction associated wear.

Figure 4.3-1 shows a cross sectional view of a typical DC brushless motor. In contrast to the conventional DC brush motor, the permanent magnets are fixed to the rotor. The phase windings (typically 3 phases) are distributed in slots of the stator. This arrangement also provides for greater heat dissipation ( $i^2R$ ), which in turn leads to improved life and typically greater volume-to-power ratios for brushless motors than for brush motors.

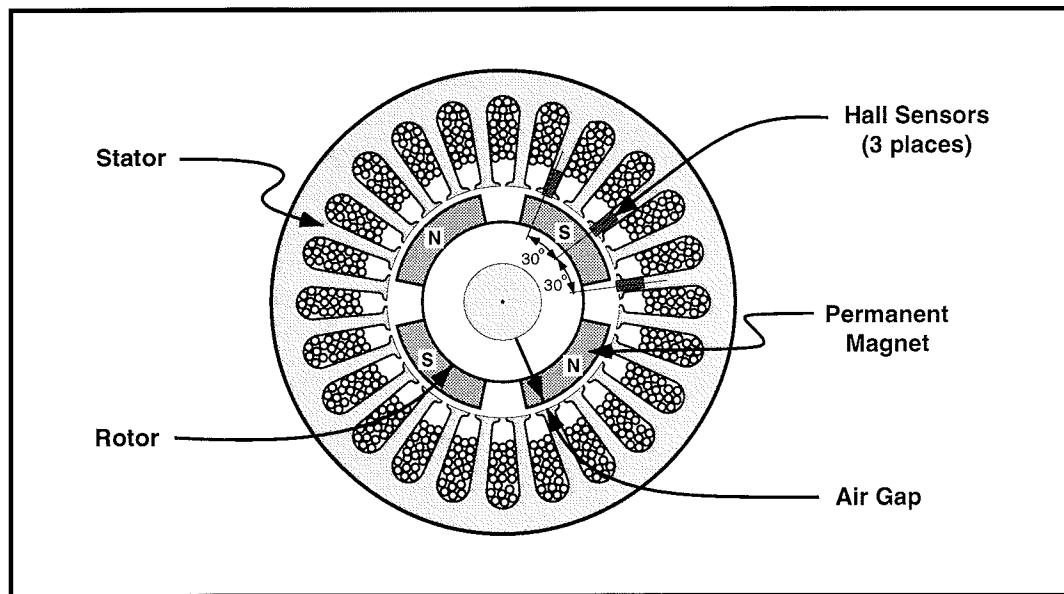


Figure 4.3-1. Cross-section of a Typical DC Brushless Motor. (Four pole type shown)

In any continuously rotating motor, to provide continuous torque the current must be successively altered or switched depending on the absolute position of the rotor. In a DC brush motor, this switching is implemented mechanically by the commutator. In a DC brushless motor, a rotor positioning sensor is used and the commutation procedure is done electronically. We will consider two different types of commutation procedures for DC permanent magnet brushless motors: rectangular and sinusoidal.

#### 4.3.1 Rectangular (Hall-Effect) Commutation

Figure 4.3-2 shows a simplified schematic of the drive system(s) used in this mechanism. This is a typical drive scheme for a 4-pole 3-phase star-wound brushless motor with Hall-effect (rectangular) commutation. The three Hall-effect sensors are positioned on the stator. The sensed magnetic field switches between the adjacent north/south poles as the rotor rotates. This switching sequence is then used to direct the commanded motor current to individual winding phases (Figure 4.3-3). A simple electronic logic circuit is used for the generation of the switching steps (six steps per electrical cycle or 12 steps per mechanical cycle for a 4-pole motor). Analog high bandwidth *proportional plus integral* (PI) current feedback loops are then used on two of the three phases to

assure almost instantaneous response of the actual winding current following any commanded current changes. The third phase does not require a current feedback loop because (as per Kirchoff's law) the current in the third phase is the negative of the sum of the current in the other two phases.

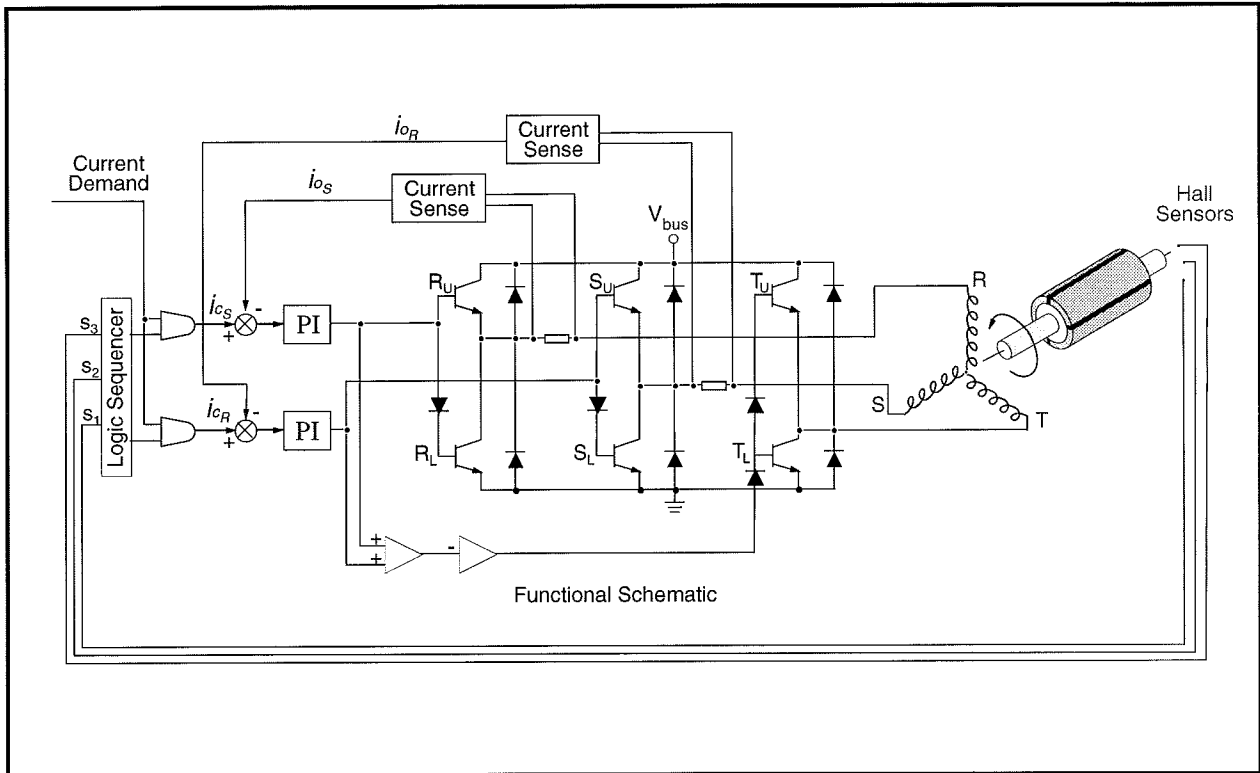


**Figure 4.3-2 Simplified Schematic of Hall-effect Commutated DC Brushless Motor Drive System**

We assume that, due to the relatively high bandwidth of the current loops, nearly instantaneous matching of the commanded current (torque) and the actual current occurs.<sup>1</sup> With the rectangular drive scheme shown in Figure 4.3-3b, at any position only two of the three phases are operational so that the current in the third phase is zero. Consider a 60 electrical degree interval  $0 \leq \theta \leq 60$ . The torque input from phase R is

$$T_R = K_t I_R \sin\theta \tag{4.3-1}$$

and

$$I_R = -I_T \text{ with } I_S = 0$$

where  $K_t = Z \cdot B_p \cdot r \cdot l$  is the torque constant per phase in N-m.  $Z$  is the number of turns per winding,  $r$  is the inside radius of the stator in meters, and  $l$  is the active length of conductors in meters.  $B_p$  is the peak air gap flux density in Teslas.

<sup>1</sup>We qualify the validity of this assumption later when we discuss the PI current loops.

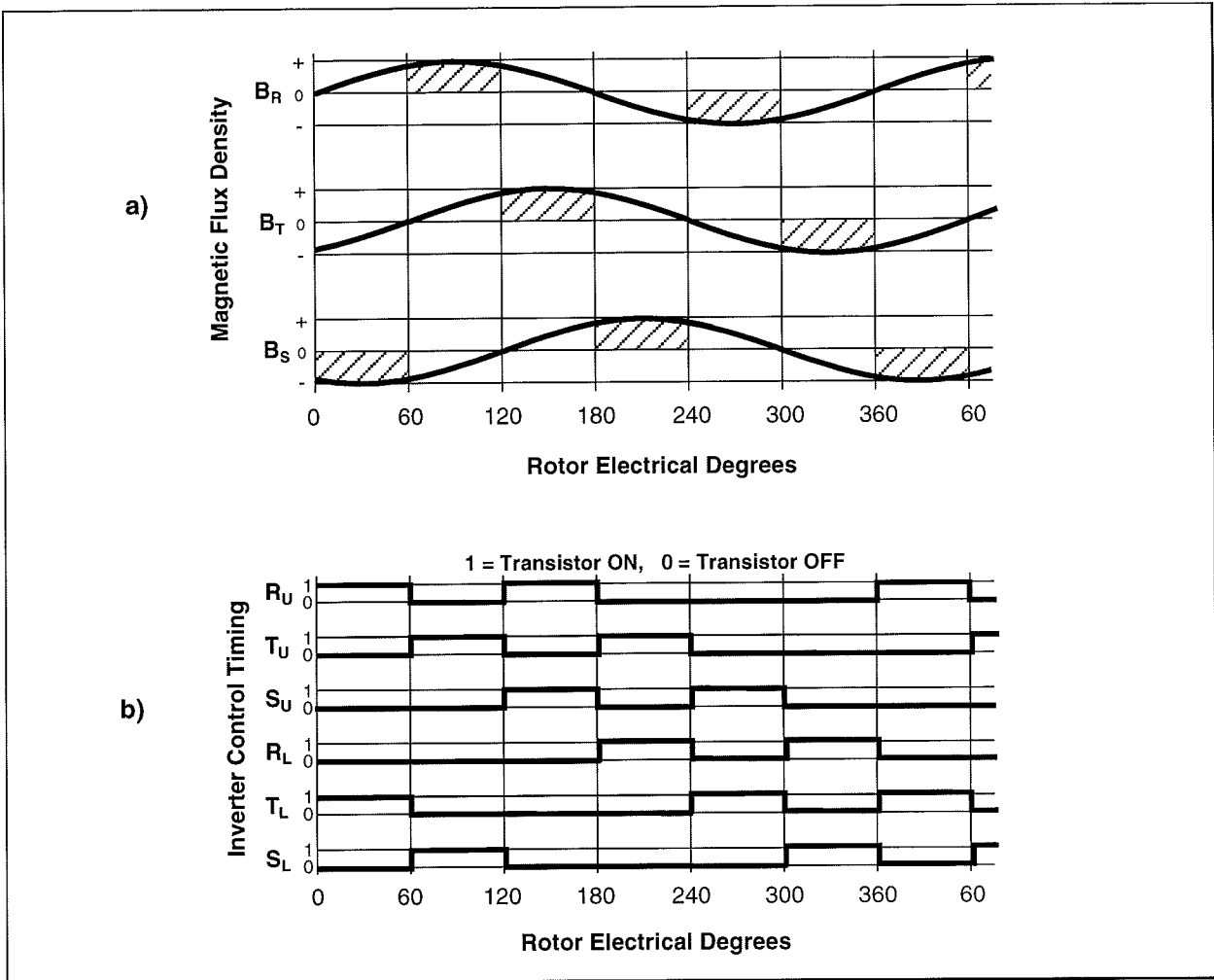


**Figure 4.3-3 Hall-effect Commutation Timing Diagram**

To produce positive torque, the flux density must be negative for phase T. This is the case for a sinusoidally wound motor (see Figure 4.3-3a):

$$\begin{aligned}
 T_T &= K_t I_R \sin(\theta+240) && (4.3-2) \\
 &= K_t I_R (0.5\sin\theta+0.886\cos\theta) \quad \text{for } 0 \leq \theta \leq 60
 \end{aligned}$$

The total torque is given by the addition of  $T_T$  and  $T_R$  over the interval  $0 \leq \theta \leq 60$ :

$$T = T_R + T_T = K_t(1.5\sin\theta+0.886\cos\theta)*I_R \quad (4.3-3)$$

Equation 4.3-3 shows that the effective torque constant,  $K_t(1.5\sin\theta+0.886\cos\theta)$ , changes as a function of rotor angle producing a torque ripple as much as 13% for rectangular commutation. This torque ripple can be treated as a disturbance which, in most practical applications, is reduced by closing outer velocity and position loops around the current loop.

### 4.3.2 Sinusoidal Commutation

For a motor with sinusoidally wound stator coils the air gap flux densities are:

$$\begin{aligned} B_R &= B_p \sin \theta \\ B_S &= B_p \sin(\theta+120) \\ B_T &= B_p \sin(\theta+240) \end{aligned} \quad (4.3-4)$$

Where  $B_R$ ,  $B_S$ , and  $B_T$  are the per phase flux densities for the motor phases R, S, and T respectively and  $B_p$  is the peak value in Tesla. If we assume that the PI controllers around the current loop maintain the phase currents in phase with the air gap flux densities, then the current in each phase in terms of the peak current  $I_p$  are given by

$$\begin{aligned} I_R &= I_p \sin \theta \\ I_S &= I_p \sin(\theta+120) \\ I_T &= I_p \sin(\theta+240) \end{aligned} \quad (4.3-5)$$

From equation 4.3-4 and 4.3-5, the instantaneous torque being produced in each phase is

$$\begin{aligned} T_R &= K_t I_p \sin^2 \theta \\ T_S &= K_t I_p \sin^2(\theta+120) \\ T_T &= K_t I_p \sin^2(\theta+240) \end{aligned} \quad (4.3-6)$$

The total torque is the sum of the above torque components, which is given by

$$\begin{aligned} T &= T_R + T_S + T_T \\ &= K_t I_p (\sin^2 \theta + \sin^2(\theta+120) + \sin^2(\theta+240)) \\ &= 3/2 K_t I_p \end{aligned} \quad (4.3-7)$$

Equation 4.3-7 shows that "perfect" sinusoidal commutation of a "perfectly" sinusoidally wound motor provides for a ripple free torque constant. In practice, however, a small amount of torque ripple may exist due to imperfections in the windings and the current loop elements and misalignment of the rotor position sensor. Note that for this method of commutation, a high resolution absolute position sensor is required.

### 4.3.3 Proportional Plus Integral (PI) Current Loop

Each phase of the motor winding coil is characterized by its resistance  $R$  and its inductance  $L$ . If we assume that the per-phase back emf of motor is negligible in the high torque / low speed region of operation, then the block diagram shown in Figure 4.3-4 represents the per-phase PI loop for two of the three phases. (There is no need for PI loop on the third phase, as the sum of the total current must be zero in a star winding circuit).

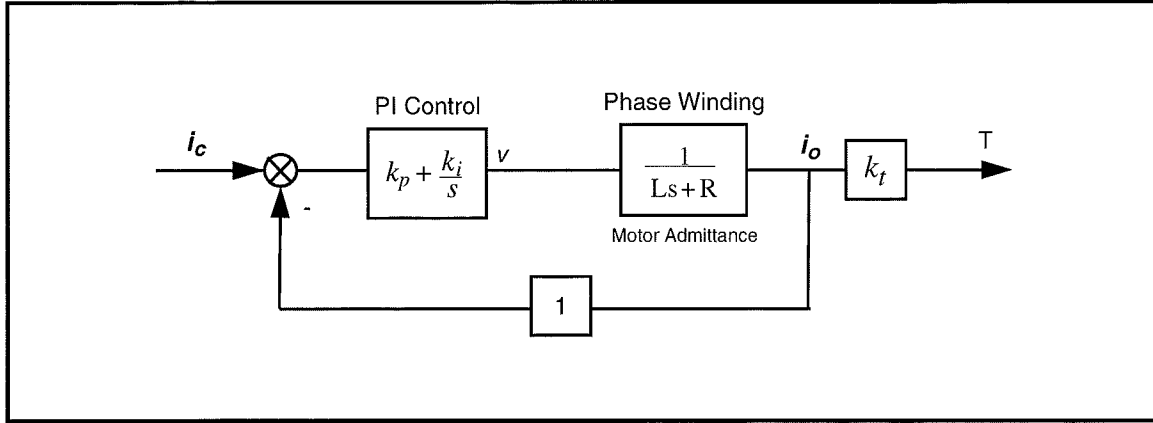


Figure 4.3-4 Simplified Block Diagram of Analog PI Controller (applies to each motor winding phase)

This is a second order system with the transfer function

$$\frac{i_o(s)}{i_c(s)} = \frac{(k_p/L)s + k_i/L}{s^2 + (R + k_p/L)s + k_i/L} \tag{4.3-8}$$

having natural frequency

$$\omega_n = \sqrt{\frac{k_i}{L}} \tag{4.3-9}$$

and damping ratio

$$\zeta = \frac{k_p + R}{2\sqrt{k_i L}} \tag{4.3-8}$$

By choosing the appropriate values for  $k_i$  and  $k_p$ , very high bandwidths for closed loop current (torque) response may be achieved (>500 Hz). In comparison to the achievable bandwidths for the outer velocity and/or position loops, the bandwidth of the current loop is generally about two orders of magnitude greater. This means that the current (torque) response is essentially instantaneous and therefore its dynamics may usually be ignored. Note also that the addition of the integrator has made this closed loop system a type one system. This, in turn, results in zero steady state error and a unity DC gain.

#### 4.4 Multi-Tasking Environment

Digital control implementation is intimately coupled with the hardware and software that supports it. Nowhere is this more apparent than in the architecture and timing used to support the various data processing routines. A well prioritized time multi-tasking scheme is essential to maximizing the performance attainable from the processing resources.

The priority scheme for the ECP real-time Controller's multi-tasking environment is tabulated in Table 4.4-1. The highest priority task is the trajectory update and servo loop closure computation which takes place at the maximum rate of 1.131 KHz (minimum sampling period is 0.000884 seconds). In this case, the user may reduce the sampling rate through the Executive Program via changes to  $T_s$  in the Setup Control Algorithm dialog box.



The trajectory planning task has the third highest priority and is serviced at a maximum rate of 377 Hz. Here the parameters for a new trajectory need not be calculated every time this task is serviced by the real-time Controller. Whenever a new trajectory is required (i.e. the current trajectory is near its completion) this task is executed. The lower priority tasks are system house keeping routines including safety checks, interface and auxiliary analog output.

**Table 4.4-1 The Multi-Tasking Priority Scheme of the Real-Time Controller**

Priority	Task Description	Service Frequency
1	Servo Loop Closure & Command Update	1.1 KHz
2	Trajectory Planning	377 Hz
3	Background Tasks including User Interface, Auxiliary DAC Update, Limit checks etc.	Background (In time between other tasks)

The higher priority tasks always prevail over lower ones in obtaining the computational power of the DSP. This multi-tasking scheme is realized by a real-time clock which generates processor interrupts.

#### 4.5 Sensors

There are two incremental rotary shaft encoders used in the Model 205. Each has a resolution of 4000 pulses per revolution. These encoders measure the incremental displacement of the motor and the load shaft.

The encoders are an optical type whose principle of operation is depicted in Figure 4.5-1. A low power light source is used to generate two 90 degrees out of phase sinusoidal signals on the detectors as the moving plate rotates with respect to the stationary plate. These signals are then squared up and amplified in order to generate quadrate logic level signals suitable for input to the programmable gate array on the real-time Controller. The gate array uses the A and B channel phasing to decode direction and detects the rising and falling edge of each to generate 4x resolution – see Figure 4.5-2.<sup>1</sup> The pulses are accumulated continuously within 24-bit counters (hardware registers). The contents of the counters are read by the DSP once every servo (or commutation) cycle time and extended to 48-bit word length for high precision numerical processing. Thus the accumulation of encoder pulses provides an angular position measurement (signal) for the servo routines.

<sup>1</sup>I.e. the disk encoder resolution effectively becomes 16,000 counts per revolution.

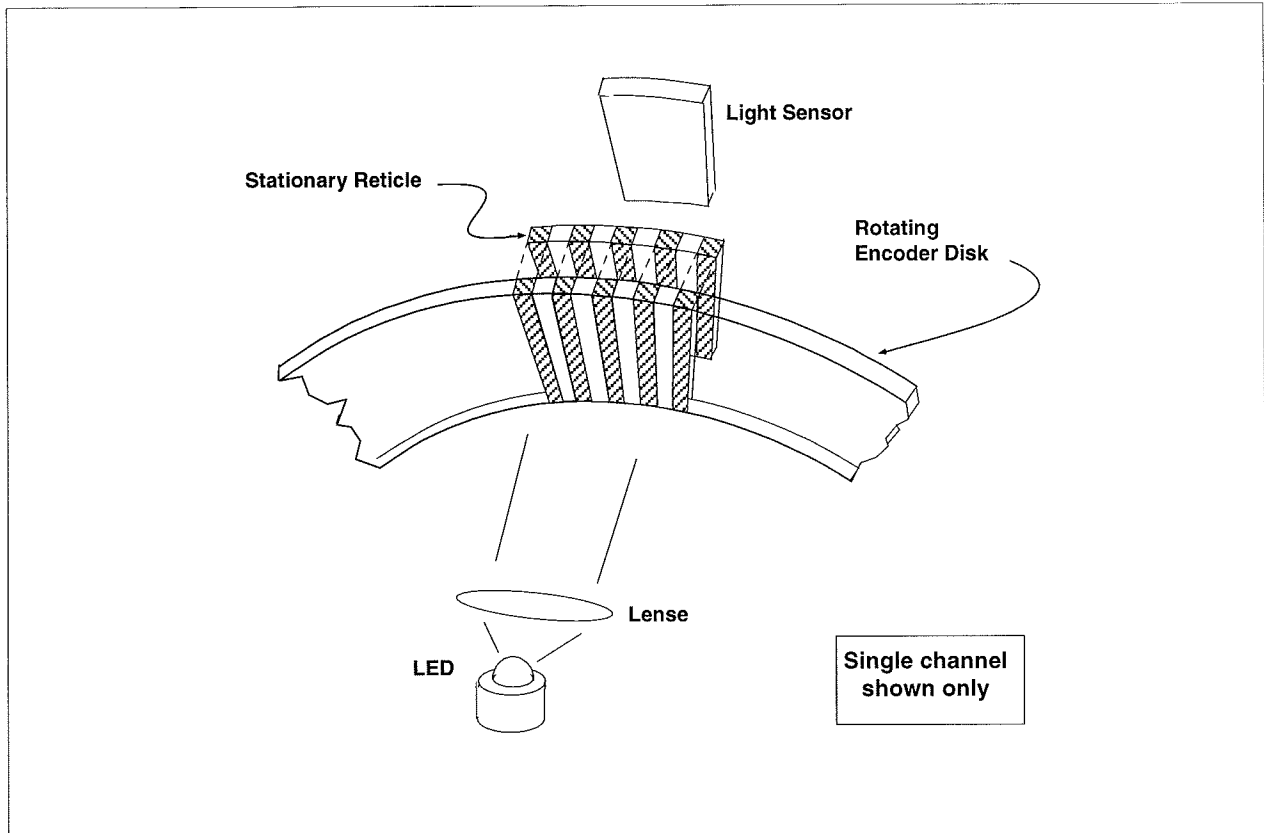


Figure 4.5-1 The Operation Principle of Optical Incremental Encoders

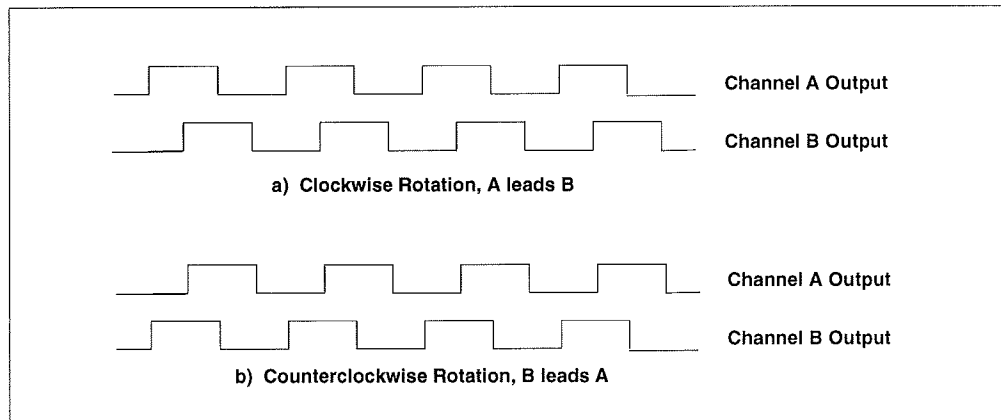


Figure 4.5-2. Optical Encoder Output

#### 4.6 Auxiliary Analog Output (System Option)

A system option provides two analog output channels in the Control Box which are connected to two 16-bit DACs which physically reside on the real-time Controller. Each analog output has the range of +/- 10 volts (-32768 to +32767 counts) with respect to the analog ground. The outputs on these DACs are updated by the real-time Controller as a low priority task. However, for virtually all trajectories (e.g. for sine sweep up to approx. 25 Hz) the update rate is sufficiently fast for an oscilloscope or other analog equipment to inspect the various internal Controller signals. See the section on the Executive Program's Utility menu for the available signals to output on these DACs.

## 5. Plant Dynamic Models

This Chapter provides time and Laplace domain expressions which are useful for linear control implementation and are used in the experiments described later in this manual. Details of the development of these equations as well as their motivation and additional equation forms are provided in Appendix A.

### 5.1 Two Degree of Freedom Plants

The most general form of the two degree of freedom torsional system is shown in Figure 5-1a where friction is idealized as being viscous. Using the free body diagram of Figure 5-1b and summing torques acting on  $J_1$  we have via the rotational form of Newton's second law:

$$J_1 \ddot{\theta}_1 + c_1 \dot{\theta}_1 + k_1 \theta_1 - k_1 \theta_2 = T(t) \quad (5.1-1)$$

Similarly from Figure 5-1c for  $J_2$ :

$$J_2 \ddot{\theta}_2 + c_2 \dot{\theta}_2 + (k_1 + k_2) \theta_2 - k_1 \theta_1 = 0 \quad (5.1-2)$$

These may be expressed in a state space realization as:

$$\begin{aligned} \dot{x} &= Ax + BT(t) \\ Y &= Cx \end{aligned} \quad (5.1-3)$$

where:

$$X = \begin{bmatrix} \theta_1 \\ \dot{\theta}_1 \\ \theta_2 \\ \dot{\theta}_2 \end{bmatrix}, \quad A = \begin{bmatrix} 0 & 1 & 0 & 0 \\ -k_1/J_1 & -c_1/J_1 & k_1/J_1 & 0 \\ 0 & 0 & 0 & 1 \\ k_1/J_2 & 0 & -(k_1+k_2)/J_2 & -c_2/J_2 \end{bmatrix},$$

$$B = \begin{bmatrix} 0 \\ 1/J_1 \\ 0 \\ 0 \end{bmatrix}, \quad C = \begin{bmatrix} C_1 & 0 & 0 & 0 \\ 0 & C_2 & 0 & 0 \\ 0 & 0 & C_3 & 0 \\ 0 & 0 & 0 & C_4 \end{bmatrix}$$

and  $C_i = 1$  ( $i=1,2,3,4$ ) when  $X_i$  is an output and equals 0 otherwise.

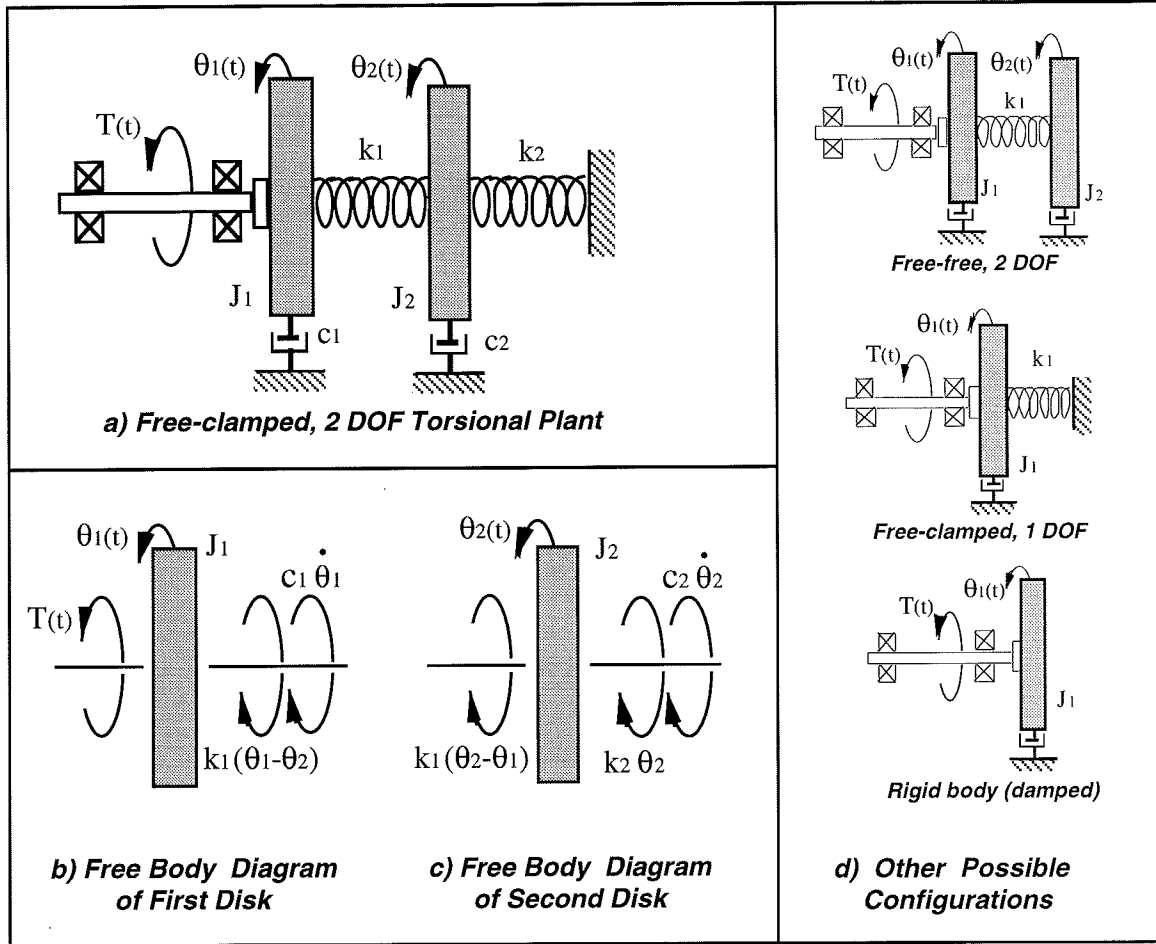


Figure 5-1 Two DOF Plant Models

By Laplace transform of Eq's (5.1-1,-2) and assuming zero valued initial conditions we may solve for the transfer functions:

$$\frac{\theta_1(s)}{T(s)} = \frac{J_2 s^2 + c_2 s + k_1 + k_2}{D(s)} \tag{5.1-4}$$

$$\frac{\theta_2(s)}{T(s)} = \frac{k_1}{D(s)} \tag{5.1-5}$$

where:

$$D(s) = J_1 J_2 s^4 + (c_1 J_2 + c_2 J_1) s^3 + (J_1(k_1 + k_2) + J_2 k_1 + c_1 c_2) s^2 + (c_1(k_1 + k_2) + c_2 k_1) s + k_1 k_2 \tag{5.1-6}$$

which may also be expressed in the form:

$$\frac{\theta_1(s)}{T(s)} = \frac{K_1 (s^2 + 2\zeta_z \omega_z s + \omega_z^2)}{(s^2 + 2\zeta_{p1} \omega_{p1} s + \omega_{p1}^2)(s^2 + 2\zeta_{p2} \omega_{p2} s + \omega_{p2}^2)} \quad (5.1-7)$$

$$\frac{\theta_2(s)}{T(s)} = \frac{K_2}{(s^2 + 2\zeta_{p1} \omega_{p1} s + \omega_{p1}^2)(s^2 + 2\zeta_{p2} \omega_{p2} s + \omega_{p2}^2)} \quad (5.1-8)$$

where the  $\omega_i$ 's and  $\zeta_i$ 's are the natural frequencies and damping ratios respectively, and the gains  $K_1$  &  $K_2$ , are nominally equal to  $1/J_1$  and  $k_1/J_1 J_2$  (but often may be measured more directly).

For the case  $k_2 = 0$  ( $\omega_l = 0$ ), a damped rigid body motion exists and Eq's (5.1-7,-8) become:

$$\frac{\theta_1(s)}{T(s)} = \frac{K_1 (s^2 + 2\zeta_z \omega_z s + \omega_z^2)}{s(s + c^*)(s^2 + 2\zeta_{p2} \omega_{p2} s + \omega_{p2}^2)} \quad (5.1-9)$$

$$\frac{\theta_2(s)}{T(s)} = \frac{K_2}{s(s + c^*)(s^2 + 2\zeta_{p2} \omega_{p2} s + \omega_{p2}^2)} \quad (5.1-10)$$

The equations describing the single DOF plant may be obtained from the above or found in Appendix A.

## 5.2 Three Degree of Freedom Plants (Model 205a only)

The time domain equations of motion for the three DOF torsional plant are (see Appendix A, Figure A-4):

$$J_1 \ddot{\theta}_1 + c_1 \dot{\theta}_1 + k_1 \theta_1 - k_1 \theta_2 = T(t) \quad (5.2-1)$$

$$J_2 \ddot{\theta}_2 + c_2 \dot{\theta}_2 + (k_1 + k_2) \theta_2 - k_1 \theta_1 - k_2 \theta_3 = 0 \quad (5.2-2)$$

$$J_3 \ddot{\theta}_3 + c_3 \dot{\theta}_3 + k_2 \theta_3 - k_2 \theta_2 = 0 \quad (5.2-3)$$

which may be expressed in a state space realization:

$$\begin{aligned} \dot{x} &= Ax + BT(t) \\ Y &= Cx \end{aligned} \quad (5.2-4)$$

$$X = \begin{bmatrix} \theta_1 \\ \dot{\theta}_1 \\ \theta_2 \\ \dot{\theta}_2 \\ \theta_3 \\ \dot{\theta}_3 \end{bmatrix}, \quad A = \begin{bmatrix} 0 & 1 & 0 & 0 & 0 & 0 \\ -k_1/J_1 & -c_1/J_1 & k_1/J_1 & 0 & 0 & 0 \\ 0 & 0 & 0 & 1 & 0 & 0 \\ k_1/J_2 & 0 & -(k_1+k_2)/J_2 & -c_2/J_2 & k_2/J_2 & 0 \\ 0 & 0 & 0 & 0 & 0 & 1 \\ 0 & 0 & k_2/J_3 & 0 & -k_2/J_3 & -c_3/J_3 \end{bmatrix},$$

$$B = \begin{bmatrix} 0 \\ 1/J_1 \\ 0 \\ 0 \\ 0 \\ 0 \end{bmatrix}, \quad C = \begin{bmatrix} C_1 & 0 & 0 & 0 & 0 & 0 \\ 0 & C_2 & 0 & 0 & 0 & 0 \\ 0 & 0 & C_3 & 0 & 0 & 0 \\ 0 & 0 & 0 & C_4 & 0 & 0 \\ 0 & 0 & 0 & 0 & C_5 & 0 \\ 0 & 0 & 0 & 0 & 0 & C_6 \end{bmatrix}$$

with the output notation as in Eq (5.1-3).

The Laplace transformation of Eq's (5.2-1,-2 & -3) yields (zero valued initial conditions):

$$\frac{\theta_1(s)}{T(s)} = \frac{N_1(s)}{D(s)} \tag{5.2-6}$$

$$\frac{\theta_2(s)}{T(s)} = \frac{N_2(s)}{D(s)} \tag{5.2-7}$$

$$\frac{\theta_3(s)}{T(s)} = \frac{N_3}{D(s)} \tag{5.2-8}$$

where:

$$N_1(s) = J_2 J_3 s^4 + [J_2 c_3 + J_3 c_2] s^3 + [J_2 k_2 + c_2 c_3 + J_3 k_1 + J_3 k_2] s^2 + [c_2 k_2 + c_3 k_1 + c_3 k_2] s + k_1 k_2 \tag{5.2-9}$$

$$N_2(s) = k_1 [J_3 s^2 + c_3 s + k_2] \tag{5.2-10}$$

$$N_3(s) = k_1 k_2 \tag{5.2-11}$$

$$D(s) = J_1 J_2 J_3 s^6 + [J_1 J_2 c_3 + J_1 J_3 c_2 + J_2 J_3 c_1] s^5 + [J_1 (J_2 k_2 + J_3 k_1 + J_3 k_2 + c_2 c_3) + J_2 (J_3 k_1 + c_1 c_3) + J_3 c_1 c_2] s^4 + [J_1 (c_2 k_2 + c_3 k_1 + c_3 k_2) + J_2 (c_1 k_2 + c_3 k_1) + J_3 (c_1 k_1 + c_1 k_2 + c_2 k_1) + c_1 c_2 c_3] s^3 + [(J_1 + J_2 + J_3) k_1 k_2 + c_1 (c_2 k_2 + c_3 k_1 + c_3 k_2) + c_2 c_3 k_1] s^2 + [(c_1 + c_1 + c_1) k_1 k_2] s \tag{5.2-12}$$

which may also be expressed as:

$$\frac{\theta_1(s)}{T(s)} = \frac{K_1 (s^2 + 2\zeta_{z1}\omega_{z1}s + \omega_{z1}^2)(s^2 + 2\zeta_{z2}\omega_{z2}s + \omega_{z2}^2)}{s(s + c^*)(s^2 + 2\zeta_{p2}\omega_{p2}s + \omega_{p2}^2)(s^2 + 2\zeta_{p3}\omega_{p3}s + \omega_{p3}^2)} \quad (5.2-13)$$

$$\frac{\theta_2(s)}{T(s)} = \frac{K_2 (s^2 + 2\zeta_z\omega_zs + \omega_z^2)}{s(s + c^*)(s^2 + 2\zeta_{p2}\omega_{p2}s + \omega_{p2}^2)(s^2 + 2\zeta_{p3}\omega_{p3}s + \omega_{p3}^2)} \quad (5.2-14)$$

$$\frac{\theta_3(s)}{T(s)} = \frac{K_3}{s(s + c^*)(s^2 + 2\zeta_{p2}\omega_{p2}s + \omega_{p2}^2)(s^2 + 2\zeta_{p3}\omega_{p3}s + \omega_{p3}^2)} \quad (5.2-15)$$

where again the  $\omega_i$ 's and  $\zeta_i$ 's are the respective natural frequencies and damping ratios, and the ordered gains  $K_i$  are nominally equal to  $1/J_1$ ,  $k_1/J_1J_2$  and  $k_1k_2/J_1J_2J_2$  respectively.

Parameter identification to establish the explicit plant transfer functions or state space realizations for Models 205 & 205a is covered in Section 6.1.



## 6. Experiments

This chapter outlines experiments which identify the plant parameters, implement a variety of control schemes, and demonstrate many important control principles. The versatility of this software / hardware system allows for a much broader range of experimental uses than will be described here and the user is encouraged to explore whatever topics and methodologies may be of interest – subject of course to your school and laboratory guidelines and the safety notations of this manual. The safety portion of this manual, Section 2.4, must be read and understood by any user prior to operating this equipment.

The instructions in this chapter begin at a high level of detail so that they may be followed without a great deal of familiarity with the PC system interface and become more abbreviated in details of system operation as the chapter progresses. To become more familiar with these operations, it is strongly recommended that the user read Chapter 2 in its entirety prior to undertaking the operations described here. Remember here, as always, it is recommended to save data and control configuration files regularly to avoid undue work loss should a system fault occur.

### 6.1 System Identification

This section gives a procedure for identifying the plant parameters applicable to Eq's (5.1-1 through 5.1-8). The approach will be to use certain fundamental properties of lightly damped second order systems to indirectly measure the inertia, spring, and damping constants of the plant by making measurements of the plant while set up in a pair of classical spring-mass configurations.

#### Procedure:

1. For Model 205a, clamp the center disk to put the mechanism in the configuration shown in Figure 6.1-1a using the 1/4" bolt, square nut, and clamp spacer. Only light torqueing on the bolt is necessary. For Model 205 (2 disk) use one half of the lower disk to clamp the shaft at the center location.
2. Secure four 500g masses on the upper and lower disks (upper disk only for Model 205) as shown in the figure. Verify that the masses are secured per Section 2.2.2 and that each is at a center distance of 9.0 cm from the shaft center-line.

- With the controller powered up, enter the Control Algorithm box via the Set-up menu and set  $T_s = 0.00442$ . Enter the Command menu, go to Trajectory and select Step, Set-up. Select Open Loop Step and input a step size of 0 (zero), a duration of 4000 ms and 1 repetition. Exit to the Background Screen by consecutively selecting OK. This puts the controller board in a mode for acquiring 8 sec of data on command but without driving the actuator. This procedure may be repeated and the duration adjusted to vary the data acquisition period.

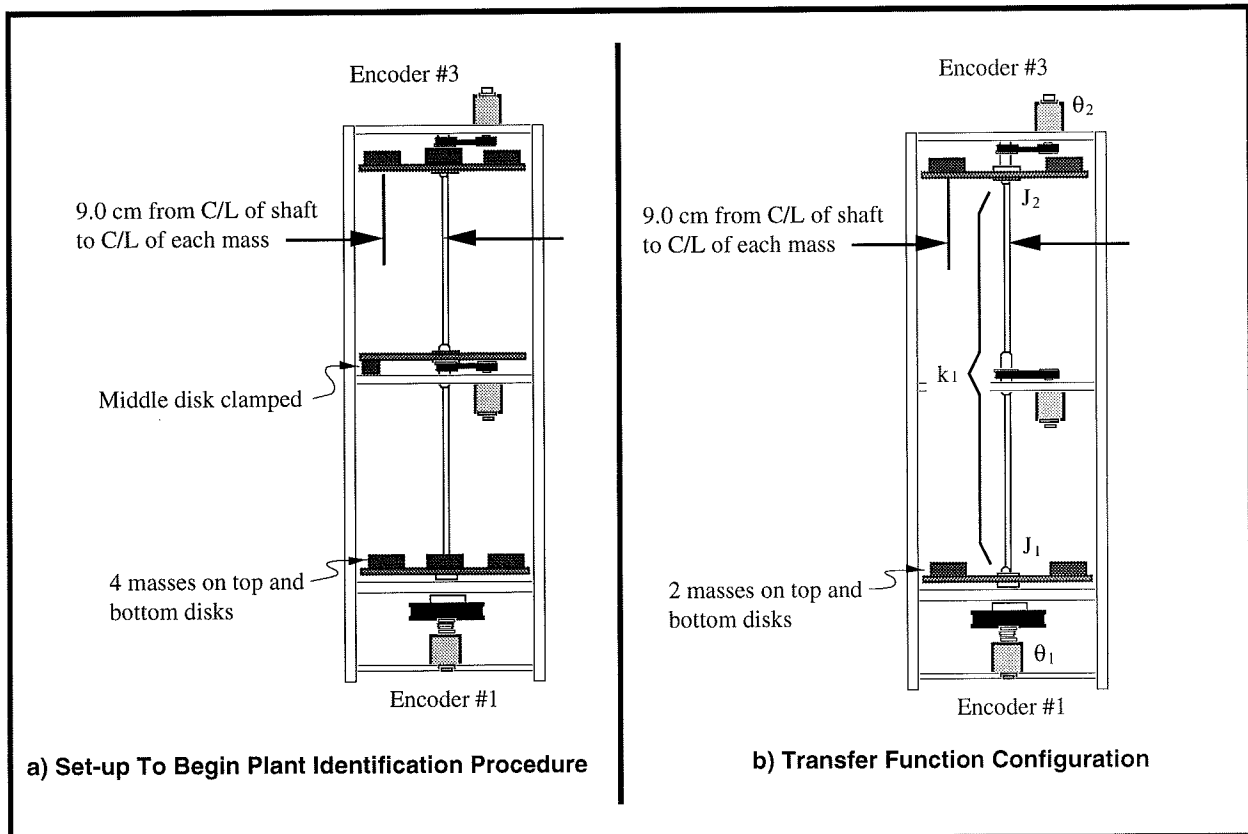


**Figure 6.1-1 Configurations For Plant Identification** (Model 205a shown)

- Go to Set up Data Acquisition in the Data menu and select Encoder #1 and Encoder #3 (for Model 205a, Encoder #1 and Encoder #2 for Model 205) as data to acquire and specify data sampling every 2 (two) servo cycles, i.e. every  $2 T_s$ 's. Select OK to exit. Select Zero Position from the Utility menu to zero the encoder positions.
- Select Execute from the Command menu. Prepare to manually displace the upper disk approximately 20 deg. Exercise caution in displacing the inertia disk; displacements beyond 40 deg may damage and possibly break the flexible drive shaft. (Displacements beyond 25 deg will trip a software limit which disables the controller indicated by "Limit Exceeded" in the Controller Status box in the Background Screen. To reset, simply reselect Execute from the Command menu.) With the upper disk displaced approximately 20 deg ( $\leq 1000$  encoder counts as read on the Background Screen display) in either direction, select Run from the Execute box and release the disk approximately 1 second

later. The disk will oscillate and slowly attenuate while encoder data is collected to record this response. Select OK after data is uploaded.

6. Select Set-up Plot from the Plotting menu and choose Encoder #3 position (for Model 205a, or Encoder #2 for Model 205); then select Plot Data from the Plotting menu. You will see the upper disk time response.
7. Choose several consecutive cycles (say 5 to 10) in the amplitude range between 100 and 1000 counts (This is representative of oscillation amplitudes during later closed loop control maneuvers. Much smaller amplitude responses become dominated by nonlinear friction effects and do not reflect the salient system dynamics) Divide the number of cycles by the time taken to complete them being sure to take beginning and end times from the same phase of the respective harmonic cycles.<sup>1</sup> Convert the resulting frequency in Hz to radians/sec. This *damped frequency*,  $\omega_d$ , approximates the *natural frequency*,  $\omega_n$ , according to:

$$\omega_{n_{d31}} = \frac{\omega_{d_{d31}}}{\sqrt{1-\zeta_{d31}^2}} \approx \omega_{d_{d31}} \quad (\text{for small } \zeta_{d31}) \quad (6.1-1)$$

where the "d31" subscript denotes disk #3, trial #1. (Close the graph window by clicking on the left button in the upper right hand corner of the graph. This will collapse the graph to icon form where it may later be brought back up by double-clicking on it.)

8. Remove the four masses from the third (upper) disk and repeat Steps 5 through 7 to obtain  $\omega_{n_{d32}}$  for the unloaded disk. If necessary, repeat Step 3 to reduce the execution (data sampling) duration.
9. Measure the reduction from the initial cycle amplitude  $X_o$  to the last cycle amplitude  $X_n$  for the  $n$  cycles measured in Step #8. Using relationships associated with the *logarithmic decrement*:

$$\frac{\zeta_{d32}}{\sqrt{1-\zeta_{d32}^2}} = \frac{1}{2\pi n} \ln\left(\frac{X_o}{X_n}\right) \rightarrow \zeta_{d32} \approx \frac{1}{2\pi n} \ln\left(\frac{X_o}{X_n}\right) \quad (\text{for small } \zeta_{d32}) \quad (6.1-2)$$

find the damping ratio  $\zeta_{d32}$  and show that for this small value the approximations of Eq's (6.1-1, -2) are valid.

10. Repeat Steps 5 through 9 for the lower disk, disk #1. Here in Step 6 you will need to remove Encoder #3 position (#2 for Model 205) and add Encoder #1 position to the plot set-up. Hence obtain  $\omega_{n_{d11}}$ ,  $\omega_{n_{d12}}$  and  $\zeta_{d12}$ . How does this damping ratio compare with that for the upper disk?
11. Use the following information pertaining to each mass piece to calculate the portion of each disk's inertia attributable to the four masses for the "d31" and "d11" cases.

mass (incl. bolt & nut) = 500g ( $\pm$  5g)  
 dia = 5.00 cm ( $\pm$  0.02 cm)

<sup>1</sup>You may "zoom" the plot via Axis Scaling for more precise measurement in various areas. For an even greater precision, the data may be examined in tabular numerical form – see Export Raw Data, Section 2.1.7.3.

12. Calling this inertia  $J_m$  (i.e. that associated with the four masses combined), use the following relationships to solve for the unloaded disk inertia  $J_{d3}$ , and upper torsional shaft spring  $k_{d3}$ .

$$k_{d3}/(J_m + J_{d3}) = (\omega_{nd31})^2 \quad (6.1-3)$$

$$k_{d3}/J_{d3} = (\omega_{nd32})^2 \quad (6.1-4)$$

Find the damping coefficient  $c_{d3}$  by equating the first order terms in the equation form:

$$s^2 + 2\zeta\omega_n s + \omega_n^2 = s^2 + c/J_s + k/J \quad (6.1-5)$$

Repeat this for the lower unloaded disk inertia (this includes the reflected inertias of the motor, belt, and pulleys), spring and damping  $J_{d1}$ ,  $c_{d1}$  and  $k_{d1}$  respectively.<sup>1</sup>

Now all dynamic parameters have been identified! Values for  $J_1$  and  $J_2$  for any configuration of masses may be found by adding the calculated inertia contribution of the masses to that of the unloaded disk<sup>2</sup>.

The following is necessary to establish the hardware gain for control modeling purposes.

#### Procedure:

13. Remove the entire upper disk, unfasten the mid-shaft disk and clamp and replace the four masses on the lower disk (only) at the 9.0 center distance following the guidelines of Step 2. Verify that the masses are secure and that the disk rotates freely. Hook up the drive power to the mechanism.
14. In the Trajectory window deselect Unidirectional moves (i.e. enabling bi-directional inputs) select Step, Set-up. Choose Open Loop Step, and input *1.00 Volts, 500 ms, 2 reps*. Execute this open loop step via the Execute menu. (For higher open loop voltages, this move may trip a software speed limit which disables the controller indicated by "Limit Exceeded" in the Controller Status box in the "desk top". Again, to reset, simply reselect Execute from the Execute menu.) Go to Set-up in the Plot Data menu and select Encoder #1 velocity for plotting.
15. Plot this data and observe four velocity profile segments with nominal shapes of: linear increase (constant acceleration), constant (zero acceleration<sup>3</sup>), linear decrease (deceleration), and constant. Obtain the acceleration,  $\theta_{1e}$ , (counts/s<sup>2</sup>) by carefully measuring the velocity difference and dividing by the time difference (500 ms) through the positive-sloped linear segment.<sup>4,1</sup> Repeat this

<sup>1</sup>Steps 11 and 12 may be done later, away from the laboratory, if necessary.

<sup>2</sup>In plant configurations where a disk is used in the center location, the inertia and damping parameters may be assumed to be the same as for the upper disk.

<sup>3</sup> Some small deceleration will exist due to friction.

<sup>4</sup>For more precise measurement you may "zoom in" on this region of the plot using Axis Scaling in the Plotting menu.

for the negative-sloped segment. Calculate the average magnitude of the positive and negative accelerations for use in obtaining  $k_{hw}$  below.

16. Save any files or plots of interest. Exit the executive program and power down the system.

### Transfer Function Calculation

The so-called hardware gain,  $k_{hw}$ ,<sup>2</sup> of the system is comprised of the product:

$$k_{hw} = k_c k_a k_t k_p k_e k_s \quad (6.1-6)$$

where:

$k_c$ , the DAC gain, = 10V / 32,768 DAC counts

$k_a$ , the Servo Amp gain, = approx. 2 (amp/V)

$k_t$ , the Servo Motor Torque constant = approx. 0.1 (N-m/amp)

$k_p$ , the Drive Pulley ratio = 3 (N-m @ disk / N-m @ Motor)

$k_e$ , the Encoder gain, = 16,000 pulses /  $2\pi$  radians

$k_s$ , the Controller Software gain, = 32 (controller counts / encoder or ref input counts)<sup>3</sup>

In Step 15, we obtained the acceleration  $\ddot{\theta}_{1e}$  (counts/s<sup>2</sup>) of a known inertia,  $J_I = J_m + J_{dl}$  with a known voltage applied at the DAC. Thus by neglecting the relatively small friction:

$$\text{Applied Torque} = J_I \ddot{\theta}_1 = J_I \ddot{\theta}_{1e} / k_e \quad (6.1-7)$$

and we have a direct measurement of the four-term product  $k_a k_t k_e k_p$ . i.e.:

$$1.00V k_a k_t k_p = \text{Applied Torque in Step 15} \quad (6.1-8)$$

Use (6.1-6 through 6.1-8) to solve for  $k_{hw}$  using the specified values for  $k_c$  and  $k_s$ .

For control purposes it is generally desirable to put the transfer function in denominator-monic form (leading term in D(s) has unity coefficient).

Construct a denominator-monic plant model suitable for control design for the case of two 500g weights on each of the upper & lower disks with each mass centered at 9.0 cm from the shaft

<sup>1</sup> It is possible to read the accelerations directly by plotting Encoder #1 acceleration. This data, obtained by double numerical differentiation, is typically somewhat noisy however. The student may want to verify this by observing the acceleration plot

<sup>2</sup>It contains software gain also. This software gain,  $k_s$  is used to give higher controller-internal numerical resolution and improves encoder pulse period measurement for very low rate estimates.

<sup>3</sup>The "controller counts" are the counts that are actually operated on in the control algorithm. i.e. The system input (trajectory) counts and encoder counts are multiplied by 32 prior to control law execution.

center-line – see Figure 6.1-1b. Use the results of this section and equations (5.1-4 through 5.1-6) to generate these transfer functions where the hardware gain multiplies the numerator for each transfer function.

**Questions / Exercises:**

- A. Report the measured properties and derived parameter values:  
 $J_m, J_{d1}, J_{d2}, J_{d3}, c_{d1}, c_{d2}, c_{d3}, k_{d1}, k_{d3},$  and  $k_{hw}$
- B. Construct a denominator-monic plant model suitable for control design for the case of two 500g weights on the upper most & lower disks with each mass centered at 9.0 cm from the shaft center-line – see Figure 6.1-1b. Use the results of this section and equations (5.1-4 through 5.1-6) to generate these transfer functions where the hardware gain multiplies the numerator for each transfer function.
- C. What are the units of  $k_{hw}$ ?

## 6.2 Rigid Body PD & PID Control

This experiment demonstrates some key concepts associated with proportional plus derivative (PD) control and subsequently the effects of adding integral action (PID). This control scheme, acting on plants modeled as rigid bodies finds broader application in industry than any other. It is employed in such diverse areas as machine tools, automobiles (cruise control), and spacecraft (attitude and gimbal control). The block diagram for forward path PID control of a rigid body is shown in Figure 6.2-1a where friction is neglected.<sup>1</sup> Figure 6.2-1b shows the case where the derivative term is in the return path. Both implementations are found commonly in application and –as the student should verify – have identical characteristic roots. They therefore have identical stability properties and vary only in their response to dynamic inputs.

The closed loop transfer functions for the respective cases are:

$$c(s) = \frac{\theta(s)}{r(s)} = \frac{(k_{hw}/J)(k_d s^2 + k_p s + k_i)}{s^3 + (k_{hw}/J)(k_d s^2 + k_p s + k_i)} \quad (6.2-1a)$$

$$c(s) = \frac{\theta(s)}{r(s)} = \frac{(k_{hw}/J)(k_p s + k_i)}{s^3 + (k_{hw}/J)(k_d s^2 + k_p s + k_i)} \quad (6.2-1b)$$

<sup>1</sup>The student may want to later verify that for the relatively high amount of control damping in the scheme that follows – induced via the parameter  $k_d$  – that the plant damping is very small.

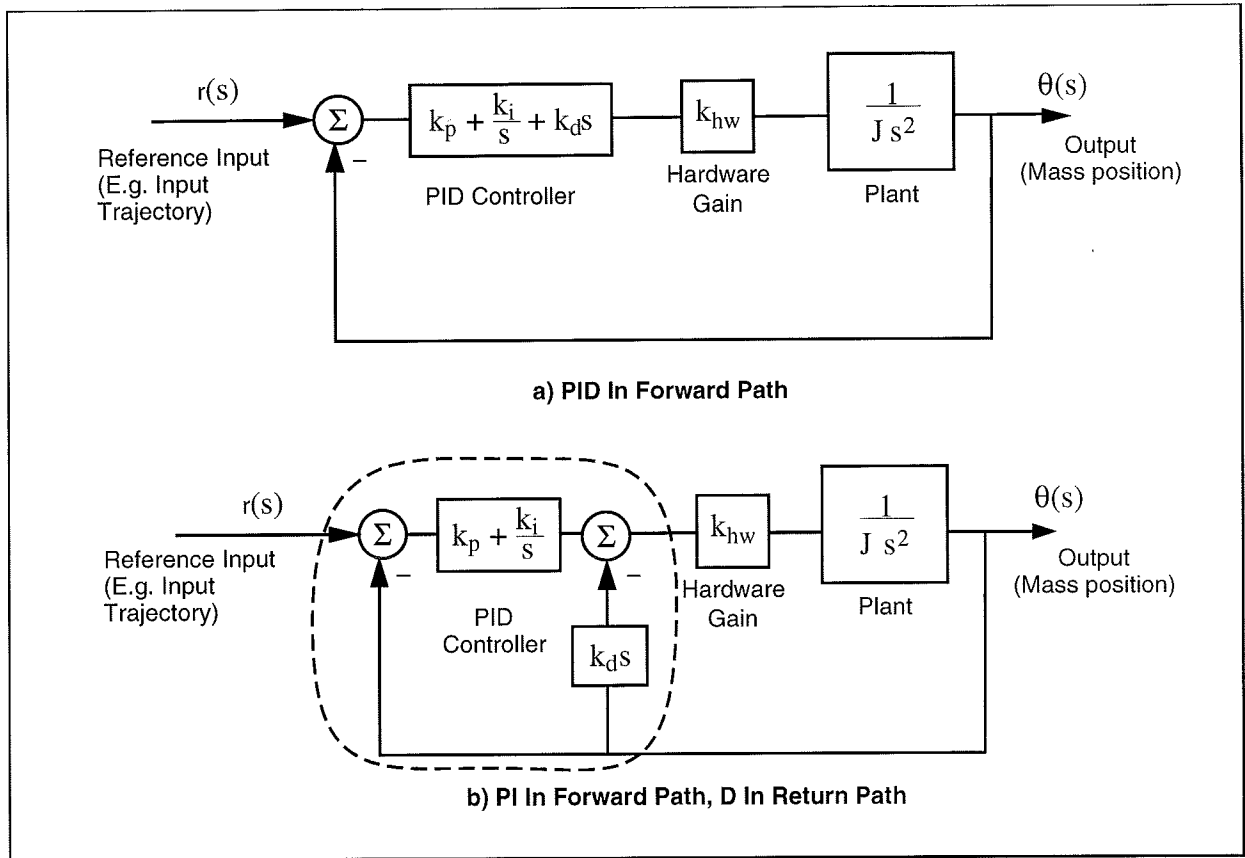


Figure 6.2-1. Rigid Body PID Control – Control Block Diagram

For the first portion of this exercise we shall consider PD control only ( $k_i=0$ ). For the case of  $k_d$  in the return path the transfer function reduces to:

$$c(s) = \frac{k_p k_{hw} / J}{s^2 + (k_{hw} / J)(k_d s + k_p)} \tag{6.2-2}$$

By defining:

$$\omega_n \triangleq \sqrt{\frac{k_p k_{hw}}{J}} \tag{6.2-3}$$

$$\zeta \triangleq \frac{k_d k_{hw}}{2J \omega_n} = \frac{k_d k_{hw}}{2\sqrt{J k_p k_{hw}}} \tag{6.2-4}$$

we may express:

$$c(s) = \frac{\omega_n^2}{s^2 + 2\zeta \omega_n s + \omega_n^2} \tag{6.2-5}$$

The effect of  $k_p$  and  $k_d$  on the roots of the denominator (damped second order oscillator) of Eq (6.2-2) is studied in the work that follows.

Procedure :Proportional & Derivative Control Actions

1. Using the results of Section 6.1 construct a model of the plant with two mass pieces at 9.0 cm radial center distance on the bottom disk – both other disks removed. You may neglect friction.
2. Set-up the plant in the configuration described in Step 1.
3. From Eq (6.2-3) determine the value of  $k_p$  ( $k_d=0$ ) so that the system behaves like a 1 Hz spring-inertia oscillator.
4. Set-up to collect Encoder #1 and Commanded Position information via the Set-up Data Acquisition box in the Data menu. Set up a closed-loop step of 0 (zero) counts, dwell time = 5000 ms, and 1 (one) rep (Trajectory in the Command menu).
5. Enter the Control Algorithm box under Set-up and set  $T_s=0.00442$  s and select Continuous Time Control. Select PI + Velocity Feedback (this is the return path derivative form) and Set-up Algorithm. Enter the  $k_p$  value determined above for 1 Hz oscillation ( $k_d$  &  $k_i = 0$ , do not input values greater than  $k_p = 0.08$ <sup>1</sup>) and select OK.

In this and all future work, be sure to stay clear of the mechanism before doing the next step. Selecting Implement Algorithm immediately implements the specified controller; if there is an instability or large control signal<sup>2</sup>, the plant may react violently. If the system appears stable after implementing the controller, first displace the disk with a light, non sharp object (e.g. a plastic ruler) to verify stability prior to touching plant

Select Implement Algorithm, then OK.

6. Select Execute under Command. Prepare to manually rotate the lower disk roughly 60 deg. Select Run, rotate about 60 deg. and release disk. Do not hold the rotated disk position for longer than 1-2 seconds as this may cause the motor drive thermal protection to open the control loop.
7. Plot encoder #1 output (see Step 6 Section 6.1). Determine the frequency of oscillation. What will happen when proportional gain,  $k_p$ , is doubled? Repeat Steps 5 & 6 and verify your prediction. (Again, for system stability, do not input values greater than  $k_p = 0.08$ ).
8. Determine the value of the derivative gain,  $k_d$ , to achieve  $k_d k_{hw} = 0.1$  N-m/(rad/s)<sup>3</sup>. Repeat Step 5, except input the above value for  $k_d$  and set  $k_p$  &  $k_i = 0$ . (Do not input values greater than  $k_d = 0.1$ ).
9. After checking the system for stability by displacing it with a ruler, manually move the disk back and forth to feel the effect of viscous damping provided by  $k_d$ . Do not excessively coerce the disk as this will again cause the motor drive thermal protection to open the control loop.

<sup>1</sup>Here due to friction the system, which is ideally quasi-stable (characteristic roots on the  $j\omega$  axis), remains stable for small  $k_p$ . For larger values, the time delay associated with sampling may cause instability.

<sup>2</sup>E.g. a large error at the time of implementation.

<sup>3</sup>For the discrete implementation you must divide the resulting value by  $T_s$  for the controller input value. Here, since the PD controller is improper, the backwards difference transformation:  $s = (1-z^{-1})/T_s$  is used.



- Repeat Steps 8 & 9 for a value of  $k_d$  five times as large (Again,  $k_d \leq 0.1$ ). Can you feel the increased damping?

### PD Control Design

- From Eq's (6.2-3,-4) design controllers (i.e. find  $k_p$  &  $k_d$ ) for a system natural frequency  $\omega_n = 1$  Hz, and three damping cases: 1)  $\zeta = 0.2$  (under-damped), 2)  $\zeta = 1.0$  (critically damped), 3)  $\zeta = 2.0$  (over-damped).<sup>1</sup>

### Step Response

- Implement the underdamped controller (via PI + Velocity Feedback) and set up a trajectory for a 2500 count closed-loop Step with 2000 ms dwell time and 1 rep.
- Execute this trajectory and plot the commanded position and encoder position (Plot them both on the same vertical axis so that there is no graphical bias.)
- Repeat Steps 12 & 13 for the critically damped and over-damped cases. Save your plots for later comparison.

### Frequency Response

Review the discussion at the end of this section regarding the use of various sine sweep data scaling options prior to completing Step 16.

- Implement the underdamped controller from Step 11. Set up a trajectory for a 400 count closed-loop Sine Sweep from 0.1 Hz to 20 Hz of 60 seconds duration with Logarithmic Sweep checked. (You may wish to specify Encoder #1 data only via Set-up Data Acquisition. This will reduce the acquired data size.)
- Execute the trajectory and plot the Encoder 1 frequency response using Linear Time and Linear amplitude for the horizontal and vertical axes. The data will reflect the system motion seen as the sine sweep was performed. Now plot the same data using Logarithmic Frequency and Db amplitude. By considering the amplitude (the upper most portion of the data curve) you will see the data in the format commonly found in the literature for Bode magnitude plots. Can you easily identify the resonance frequency and the high frequency (>5 Hz) and low frequency (<0.8 Hz) gain slopes? (i.e. in Db/decade).
- Repeat Step 16 for the critically damped and overdamped cases.

### Adding Integral Action

- Now compute  $k_i$  such that  $k_i k_{hw} = 3$  N-m/(rad-sec).<sup>2</sup> Implement a controller with this value of  $k_i$  and the critically damped  $k_p$  &  $k_d$  parameters from Step 11. (Do not input  $k_i > 0.4$ .<sup>3</sup> Be certain that the following error seen in the background window is within 20 counts prior to implementing.(if not chose Zero Position from the Utility menu). Execute a 2500 count closed-loop step of 2000 ms duration (1 rep). Plot the encoder #1 response and commanded position.

<sup>1</sup>Recall that for discrete implementation, you must divide the  $k_d$  values by  $T_s$  for controller input.

<sup>2</sup>For discrete implementation you must multiply the resulting value of  $k_i$  by  $T_s$  before inputting into the controller.

<sup>3</sup>For discrete implementation, do not input  $k_i > 0.4 * T_s$ .

19. Increase  $k_i$  by a factor of two, implement your controller (do not input  $k_i > 0.4$ ) and plot its step response. Manually displace the disk by roughly 5 deg. Can you feel the integral action increasing the restoring control torque with time? (Do not hold for more than 5 seconds to avoid excessive torque build-up.) What happens when you let go?

**Questions:**

- A. What is the effect of the system hardware gain,  $k_{hw}$ , the inertia, and the control gains,  $k_p$  and  $k_d$  on the natural frequency and damping ratio? Derive the transfer function for the torsional inertia/spring/damper system shown in Figure 6.2-2. How do the viscous damping constant,  $c$ , and the spring constant  $k$  correspond to the control gains  $k_d$  and  $k_p$  in the PD controlled rigid body of Figure 6.2-1b?
- B. Describe the effects of natural frequency and damping ratio on the characteristic roots of Eq's 6.2-1. Use an S-plane diagram in your answer to show the effect of changing  $\zeta$  from 0 to  $\infty$  for a given  $\omega_n$ .
- C. Compare the step response and frequency response plots for the under-, critical, and overdamped cases ( $k_i = 0$ ). Discuss how the resonance (if present), and *bandwidth*<sup>1</sup> seen in the frequency response data correlate with features of the step responses.
- D. What is the general shape of the frequency response amplitude (i.e. amplitude vs. time) of the three plots obtained in Step 16 (linear time / linear amplitude) at amplitudes well below and above  $\omega_n$ ? What is the shape when viewing the same data plotted with  $\log(\omega)$  / Db scaling? Explain your answer in terms of the asymptotic properties of the closed loop transfer functions as  $\omega$  tends to zero and infinity.
- E. Review the two step response plots obtained by adding integral action (Steps 18 & 19) with the previous critically damped and the critically damped plot ( $k_i = 0$ ) of Step 14. What is the effect of the integral action on steady state error?

Static or Coulomb friction may be modeled as some disturbance torque acting on the output as shown in Figure 6.2-3. Assume that this torque to be step function<sup>2</sup>, and use the final value theorem to explain the effect of such a step on the PD controlled system with and without the addition of integral action.

How does integral action effect overshoot (again, compare with the critically damped plot of Step 14). Why?

<sup>1</sup> For the purposes here, consider *bandwidth* to be the frequency in the sine sweep data at which the system attenuates below 1/2 (-6Db) of its low frequency amplitude

<sup>2</sup> In practice, friction and its effect on system response are much more complex. This assumption however is valid in discussing the effect of the integrating term.

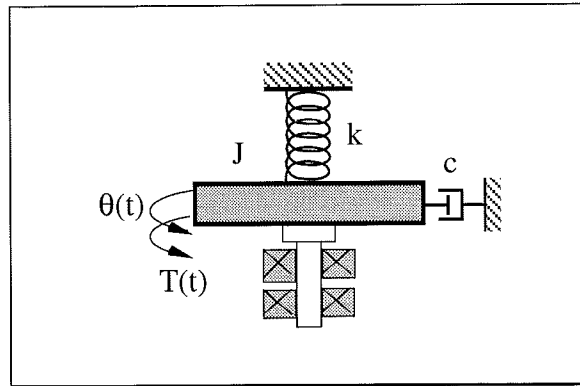


Figure 6.2-2. Torsional Inertia/Spring/Damper

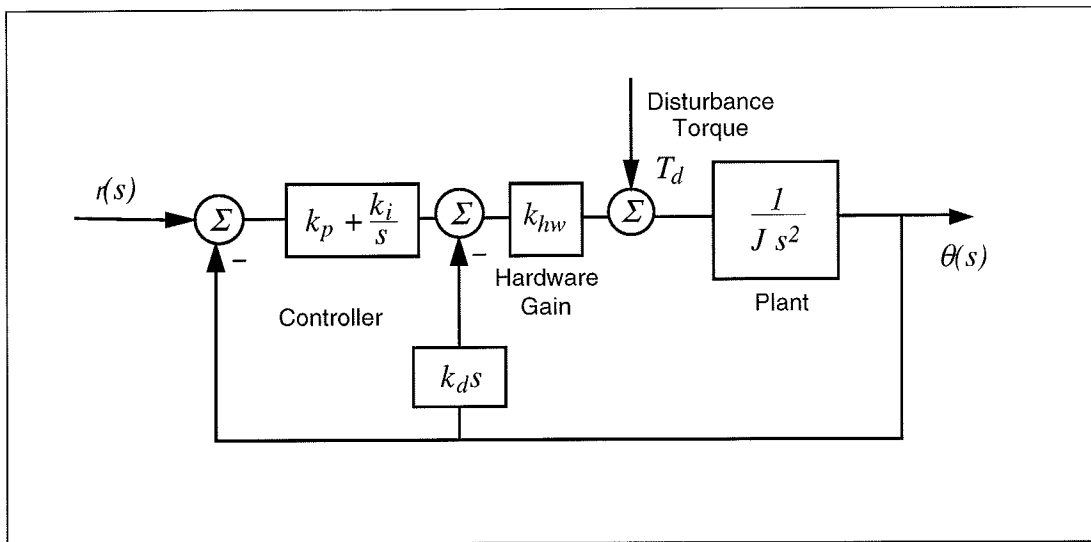


Figure 6.2-3. Friction Modeled as Disturbance Torque at Output

Viewing Sine Sweep (Frequency Response) Plots

Much insight into frequency response behavior is afforded by viewing the above plots in the various data scaling functions available in the Setup Plot dialog box. By viewing the Linear Time - Linear Amplitude modes the data appears as the system motion was viewed during the sine sweep. Note the large range in amplitudes as frequency changes. In Linear Frequency - Linear Amplitude mode the amplitude is as before but the data is shown in with frequency of oscillation as the horizontal coordinate so that amplitude may be associated with a particular frequency.

In Logarithmic Frequency - Linear Amplitude mode the frequency is distributed logarithmically (the sine sweep was executed this way in our case). This is an appropriate frequency scaling function in many cases because magnitude changes of linear systems occur as powers (e.g.  $\omega$ ,  $\omega^{-1}$ ,  $\omega^{-2}$ , etc.) of the excitation frequency and hence often occur over a large dynamic range of frequency. For example the change between 0.1 and 0.2 Hz may be greater than that between 9 and 10 Hz but would be difficult to ascertain in a linear frequency distribution between say 0.1 and 10 Hz because they would constitute only 1% of the plot length. Similarly, phase changes are symmetrically shaped in a logarithmic frequency distribution.

In Logarithmic Frequency - Db mode the frequency is distributed logarithmically and the magnitude is in Db. This method of data presentation, once the user is familiar with it, quickly affords much information about the system. The response magnitude asymptotically tends toward straight lines whose slope is associated with the salient system dynamics (i.e. the powers of  $\omega$  mentioned above).

In ECP systems, the Db magnitude (see Eq. 6.2-6) of each data point is taken so that the upper bound of the trace represents the cycle-to-cycle maximum amplitude. In virtually all other plots that the engineer may encounter, peak Db magnitude is shown as a pure function of frequency - i.e. it is a single curve on the plot. Thus the mapping of actual test data into the frequency-Db format, as done here, affords physical insight into the meaning of these important analytical and design tools.

$$Db(x) = 20 \log(x) \quad (6.2-6)$$

The methods of Log  $\omega$  - Db magnitude scaling, and Log  $\omega$  - linear phase scaling are widely used in industrial and academic practice.

The Remove DC bias check box subtracts the average of the last 50 data points from all points on the curve to provide results that are centered about zero at high frequency. It generally provides better appearance to plots that have low amplitude in the high frequency section (e.g. all  $\theta_1$  and  $\theta_2$  sine sweeps in this manual) and is necessary in many cases to obtain useful Db data at high frequency. It may provide misleading results, however, if the bias of the original data or the amplitude in the final 50 points is large.

### 6.3 Disturbance Rejection of Various 1 DOF Plant Controllers

In this experiment, we consider the performance of three distinct controller designs in rejecting low and higher frequency disturbances. The plant should be setup as per the previous experiment (two 500g. mass pieces at 9.0 cm radial center distance on the bottom disk – both other disks removed).

#### Procedure :

##### Setup Disturbance Apparatus

1. Connect the disturbance apparatus to the lower disk as per the instructions of Section 2.2
2. The three controllers are as follows:
  - a) PD control with  $\omega_n \approx 2$  Hz and  $\zeta \approx 1$ , and feedback at Encoder #1. I.e. use your design from Step 11 in the previous section.
  - b) Same as "a" plus added integral action:  $k_i k_{hw} / J = 2400$ .
  - c) Same as "a" plus a cascaded lead/lag filter with the following specifications: Zero at 0.2 Hz, Pole at 1.0 Hz, DC gain = 1.

Design the lead/lag filter for controller "c". (Hence find  $n_o$ ,  $n_l$ ,  $d_o$ , and  $d_l$  in  $F(s) = (n_o + n_l s) / (d_o + d_l s)$ )

3. Set up a time dependent sinusoidal disturbance (Sinusoidal (time)) of 1.0 volt, 0.1 Hz, 3 repetitions. (You should reduce the data acquisition sampling frequency to say once every 10-20 servo cycles to avoid an unnecessarily large data file). Input the  $k_p$  and  $k_d$  values for controller "a" under PID control using Encoder #1 for feedback with  $T_s = 0.00442$  s. Perform a closed loop step of 0 (zero) count amplitude, 15000 ms duration, and 1 repetition. This sets the system up to acquire data during closed loop regulation for a total of 30 s. Execute this regulation for controllers "a" and "b" above making sure to check the box labeled "Include sinusoidal disturbance" when commanding the system. Plot and save the disturbance effort and encoder #1 data.
4. Input controller "c" via PID + Notch in the Setup Control Algorithm box. Execute the same regulation with disturbance as in Step 3, again plotting and saving your data.
5. Repeat Steps 3 and 4 with the disturbance frequency increased to 2.0 Hz with 30 repetitions. You may reduce the step duration to 10 s and increase the data acquisition frequency to every 5-10 servo cycles.

**Questions:**

- A. Consider the block diagram of Figure 6.3-1. Derive the open loop transfer function

$$\frac{N_{ol}(s)}{D_{ol}(s)} = K(s) k_{hw}P(s) \quad (6.3-1)$$

and closed loop transfer function  $x_l(s) / T_d(s)$  for each controller.

- B. Plot the Bode response for the open and closed loop transfer functions in each of the three controller cases. Explain the disturbance attenuation characteristics of each controller in terms of their Bode response.

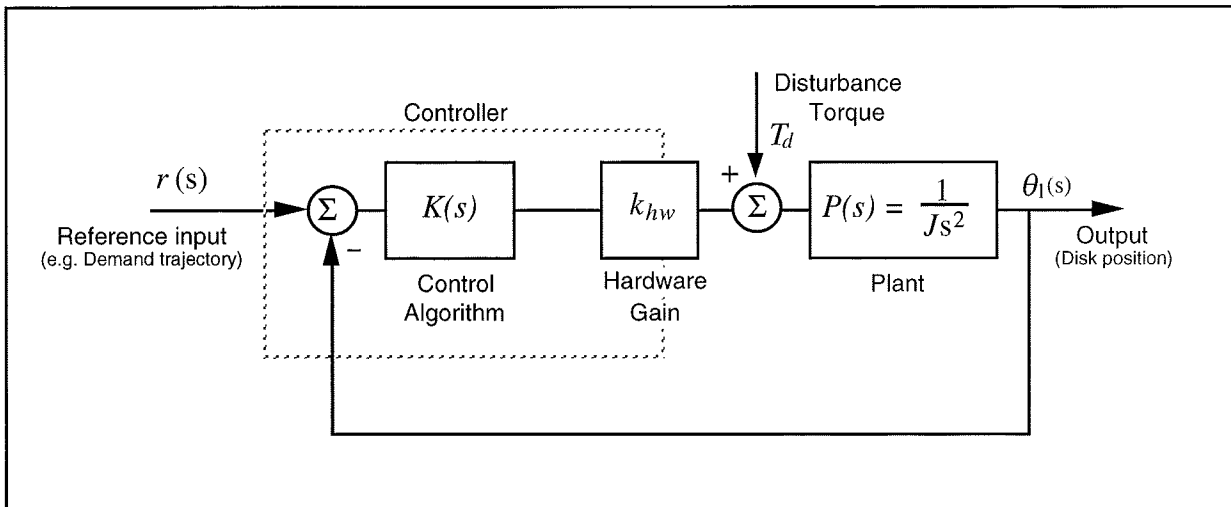


Figure 6.3-1 Disturbance Torque Input To Rigid Body Control Scheme

#### 6.4 Collocated PD Control With 2 DOF Plant

In this experiment we consider PD control of a 2-disk system where the controlled output,  $\theta_1$ , is of the lower disk. Such a scheme is referred to as *collocated* since the sensor output is rigidly coupled to the actuator input.

The addition of the spring and second inertia increases the plant order by two and adds an oscillatory mode to the plant dynamics. This may be thought of, in a sense, as a dynamic disturbance to the rigid body plant studied in Section 6.2. The collocated PD control implemented here is the approach most commonly used in industry. It may be practically employed when there is flexibility between the actuator and some inertia, and the location of objective control being near the actuator. If the location of objective control is at the distant inertia, however, this method has its limitations.

The approach in this experiment will be to design the controller by interactively changing the PD gains and observing their effect on the physical system.

##### Procedure :

1. Set-up the system with two masses on the upper and lower disk as shown in Figure 6.1b.
2. Implement the critically damped controller from Step 11 of Section 6.2 being sure that encoder #1 is selected for control. Set-up data acquisition for encoders 1 & 3 (Model 205a, 1&2 for Model 205) and for commanded position and gather data every 5 servo cycles. Execute a 1000 count step response and plot the result for commanded position and encoder #1.

3. Now iteratively adjust the gains  $k_p$  &  $k_d$  and plot results to obtain an improved response. Make your gain adjustments gradually (not more than 50% at a time) and note the effects of increasing or reducing each of them. Do not input  $k_p > 1$  or  $0.02 < k_d < 0.2$ . Attempt to achieve performance goals for the lower disk of  $\leq 400$  ms rise time (0-90% amplitude) and  $\leq 10\%$  overshoot in the lower disk (encoder #1) without excessive oscillation. Save your best step response plot. Manually displace the upper and lower disks and note their relative stiffness. (The lower disk stiffness is entirely due to the control system.)
4. For your last iteration in Step 3, plot and save the step response of the two disks. What is the predominant characteristic of the top disk motion? Can you give an explanation for the difference in the responses of the two disks in terms of their closed loop transfer functions?
5. Now using the existing values of  $k_p$  &  $k_d$  as starting points, iteratively reduce gains and plot  $\theta_2$  results to provide a well-behaved step response with  $\leq 10\%$  overshoot, without excessive oscillation, and as fast a rise time as possible. Save your final plot and record the corresponding gains. Manually displace the lower and upper disks and note their stiffness. Are they generally more or less stiff than for the controller of Step 3? How does the steady state error compare with the high gain controller from Step 3?

**Questions:**

A. Calculate the poles of the closed-loop transfer functions:  $\theta_1(s)/r(s)$  and  $\theta_2(s)/r(s)$  for your final controllers in Steps 3 & 5 respectively. How close to the imaginary axis (& right half plane) are the most lightly damped poles in each case? How close are the complex poles of  $\theta_1(s)/r(s)$  to its zeros in each case? Explain your answer in terms of the root loci for this system for gain ratios of  $k_d/k_p = 0.05, 0.10, 0.17,$  and  $0.25$ .

B. Calculate the closed loop transfer function in the form:

$$\frac{\theta_2(s)}{r(s)} = \frac{(N(s))_{\text{forward path}} / D_{ol}(s)}{1 + N_{ol}(s)/D_{ol}(s)} \quad (6.4-1)$$

Use  $N_{ol}$  and  $D_{ol}$  to obtain the open loop Nyquist or Bode responses resulting from your high and low gain controllers from Steps 3 & 5 respectively. What are the associated phase and gain stability margins? What are these margins for  $\theta_1(s)/r(s)$ ? Explain.

C. Referring to Figure 6.4-1, the transfer function between the torque disturbance and the first disk hub angle is:

$$\frac{\theta_1(s)}{T_d(s)} = \frac{N_1(s)}{D(s) + k_{hw}(k_p + k_d s) N_1(s)} \quad (6.4-1)$$

where  $N_1(s)$  is the numerator in the right hand side of Eq(5.1-4).

Use the final value theorem to find this expression for a constant

disturbance torque. The inverse of this expression is called the *static servo stiffness*. What is the static servo stiffness of your final controllers from Steps 3 & 5 for the first disk? What is the equivalent expression for the second disk (i.e. defining static stiffness at the second disk as the torque required to displace the disk one radian) and what is its value for the two controllers? Recalling Section 6.2, what is the static stiffness with integral action in the controller (i.e.  $k_i \neq 0$ )?

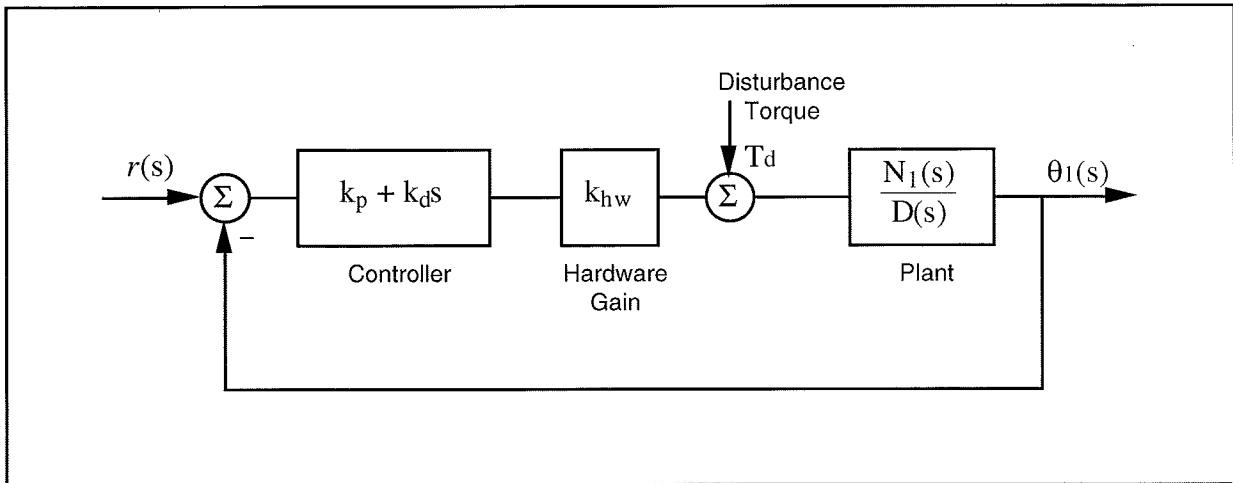


Figure 6.4-1. Disturbance Torques On PD Controlled 2-DOF Plant

### 6.5 Noncollocated PD Plus Notch Filter Control

In this experiment a control scheme is implemented which first closes the collocated loop with simple rate feedback to dampen the oscillatory mode. Then a notch filter is designed to further attenuate the transmission of signals at the damped mode frequency (i.e. nearly canceling the poles with zeros). Finally, PD control is used to achieve certain performance goals. As in the previous section, these gains are found through interactively changing their values and observing the resulting closed loop behavior.

#### Procedure :

1. The plant studied here is that of the two previous exercises, i.e. the one shown in Figure 6.1-1b. Consider the block diagram of Figure 6.5-1. Use root locus techniques to find the rate feedback gain,  $k_v$ , that causes the greatest damping in the complex roots of the inner loop  $\theta_1(s)/r^*(s)$ .



- Implement this gain as the f1 coefficient in the General Form controller specification box. Be sure that you select encoder #1 for feedback loop #3 before exiting the box and implementing. Attempt to manually excite the oscillatory mode via the upper disk and notice the damping effect of velocity feedback.

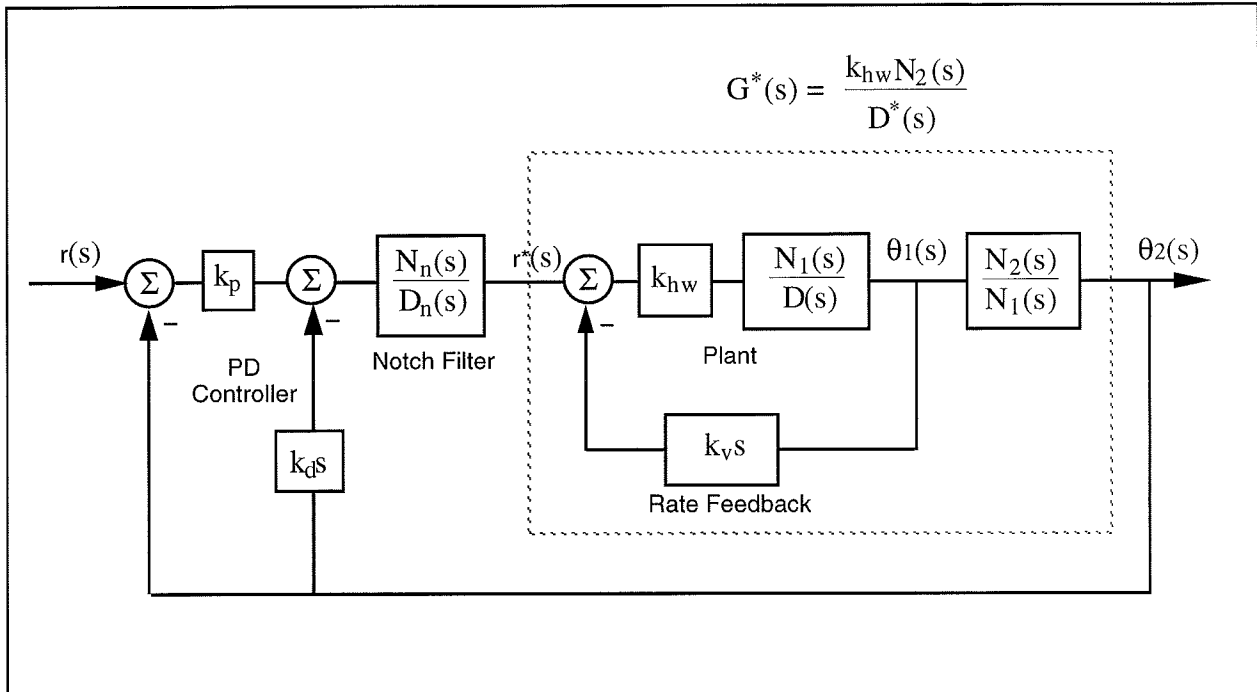


Figure 6.5-1. Control Structure For Section 6.5 Experiment

- We may now design for the new "plant"  $G^*(s)$  where  $N_2(s)$  is as before, and:

$$D^*(s) = D(s) + k_v s N_1(s) \tag{6.5-1}$$

Design a notch filter,  $N_n(s)/D_n(s)$  with two poles at 10.0 Hz and 70.7% damping ( $\zeta = \sqrt{2}$ ), two poles at 40.0 Hz and 70.7% damping and with two zeros at the poles of  $D^*(s)$ . Utilize a monic form of the denominator (highest order term in  $D_n(s)$  has coefficient of 1) and normalize the notch filter transfer function to have unity DC gain.<sup>1</sup>

- Select some initial PD gains for control of  $\theta_2$ . Use values of  $k_p = 0.01$ ,  $k_d = 0.001$  initially. Do not exceed  $k_p = 0.1$  and  $k_d = 0.02$  in any subsequent run. Since this control scheme uses multiple loop feedback, the Executive program requires that it be implemented via the general control algorithm form. A shortcut to controller coefficient entry is as follows: Input your notch filter coefficients and proportional controller gain,  $k_p$ , via the dialog box PID + Notch. Be certain to enter these coefficients in the proper order and to high

<sup>1</sup>For discrete time design, convert your notch filter design to the z domain using the Tustin (bilinear) transformation:

$$s = \frac{2}{T_s} \frac{1-z^{-1}}{1+z^{-1}}$$

numerical precision (e.g. 8 decimal places). Exit and select Preview In General Form. You will see the P + notch controller in the form that it is implemented in the generalized controller form.<sup>1</sup>

In the General Form window, enter the  $f_1$  coefficient calculated in Step 1 (i.e.  $k_v$ ), and enter as  $i_1$  the desired derivative gain,  $k_d$ . Make sure that Encoder #1 is selected for Loop #3 and Encoder #3 is selected for Loops #1&2 (the above for Model 205a, for Model 205 select Encoder #2 for Loop #1). You should verify that these entries appropriately represent the control structure of the controller in Figure 6.5-1. Exit the box and make sure that General Form is selected; then Implement. Now check performance of the control using step trajectories of 1000 counts.

5. Iteratively change PD gains by repeating Step 4 to obtain performance goals of 0.4 sec rise time (0-90% of final amplitude) and overshoot less than 15%. Do not exceed  $k_p=0.10$  or  $k_d=0.01$ . You may notice a trend here that for relatively high values of  $k_d$  the system transmits excessive noise and may appear "twitchy". As  $k_p$  becomes large, the system becomes oscillatory and further increases lead to instability. Does increase in noncollocated derivative action necessarily reduce the step response oscillations?
6. Record your best performance step response. Manually displace the disks and note the relative static stiffness of the upper disk under this control.

#### Questions:

- A. Report your calculated values for  $k_v$ ,  $N_n(s)$ ,  $D_n(s)$ , and your selected values of  $k_p$ ,  $k_d$ . Submit your step response plot. Does it meet the performance goals of Step 5?
- B. Calculate the closed-loop transfer function  $\theta_2(s)/r(s)$  including all elements in the block diagram of Figure 6.5-1. You may express this in terms of the polynomials  $D(s)$ ,  $N_1(s)$ ,  $N_n(s)$ , etc. rather than expanding each term fully. Use the equation

$$\frac{\theta_2(s)}{r(s)} = \frac{(N(s))_{\text{forward path}} / D_{ol}(s)}{1 + N_{ol}(s) / D_{ol}(s)} \quad (6.5-2)$$

and determine the phase and gain margins of your system design via Bode or Nyquist plots. What would happen if you doubled your gains  $k_p$  and  $k_d$ ? What if you quadrupled them?

- C. For this design, determine the static stiffness at  $\theta_1$  and  $\theta_2$  for  $T_{d1}$  and  $T_{d2}$  applied at  $J_1$  and  $J_2$  respectively (i.e.  $T_{d1}/\theta_1$  and  $T_{d2}/\theta_2$ ). What are

<sup>1</sup> $r(s)$  will be the same as  $D_n(s)$  and  $s(s)$  &  $t(s)$  will be identical and equal to  $k_p N_n(s)$ . Upon selecting Preview In General Form the algorithm is also converted to discrete time form (by the Tustin transform for  $N_n$  and  $D_n$ , backwards difference for any derivative terms). In this way the discrete time equivalent controller may be viewed in the discrete time General Form controller box.

the “cross” static stiffnesses (i.e.  $T_{d2}/\theta_1$  and  $T_{d1}/\theta_2$ )? How do the relative stiffness of the upper and lower disk compare in each case? How does the static stiffness of this design compare with those of the last section? Based on these results would you expect relatively high or low steady state errors for this design.

## 6.6 Successive Loop Closure / Pole Placement Design For 2 DOF Plant

In this experiment we first close a position loop about the collocated ( $\theta_1$ ) position with a relatively high bandwidth (close tracking) PD control. We then make the assumption that the lower disk closely follows its internal demand  $r^*(s)$  so that for designing a controller for  $\theta_1$ , the "plant" is approximated by the transfer function  $\theta_2(s)/\theta_1(s)$  (i.e.  $N_2/N_1(s)$ ). The block diagram for this approach is given in Figure 6.6-1.

The design and control implementation in this section proceeds as follows

1. High bandwidth PD control of  $\theta_1$
2. Low pass filter augmentation to attenuate signal noise due to high PD gains
3. Outer loop control via pole placement methodology

### 6.6.1 PD Control Of The Lower Disk

1. Setup the plant in the configuration of Figure 6.1-1b.

#### PD Control Design & Implementation

1. Using Eq's (6.2-3, -4) design the PD control gains such that  $\omega_n = 10$  Hz, and  $\zeta = 0.707$  when considering only  $J_1$  acting as a rigid body.
2. Set the sampling rate to  $T_s = 0.002652$  seconds and implement your gains via the PID control algorithm box. You should notice some system noise associated with the high derivative gain term. After safety checking the controller (See Section 2.3) displace the upper and lower disks and notice their relative stiffness. Discontinue the control via Abort Control.

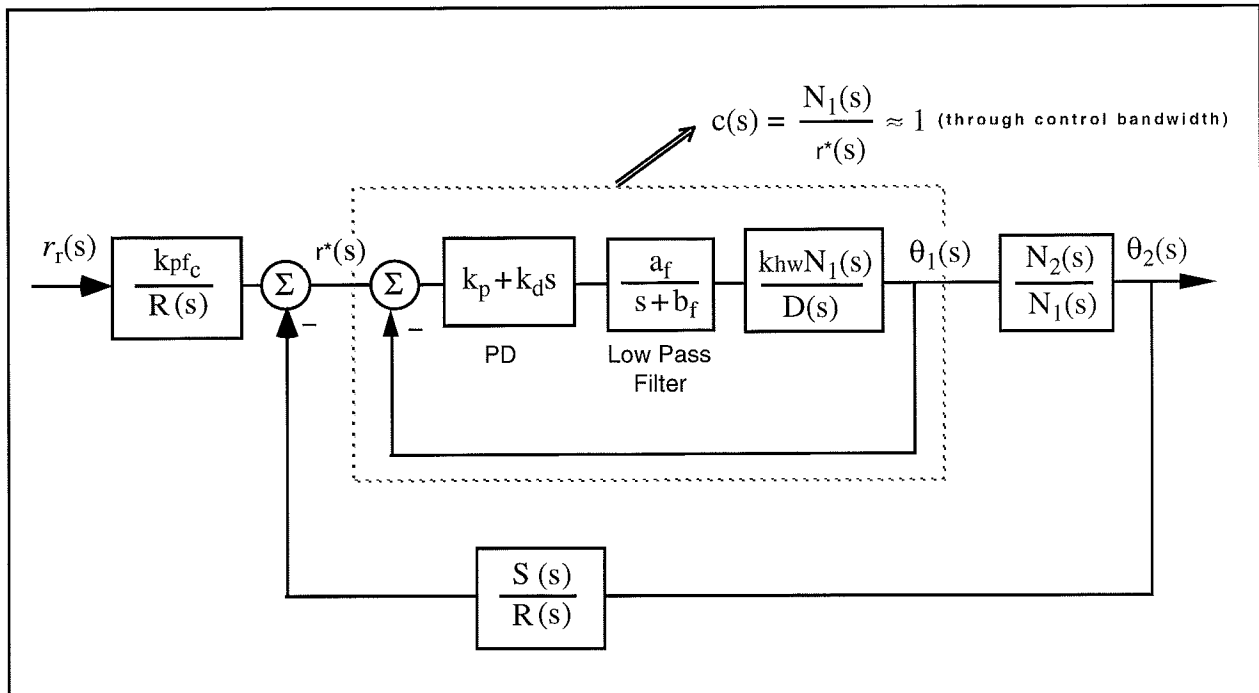


Figure 6.6-1. Control Structure For Successive Loop Closure with High Gain Inner Loop

#### Low Pass Filter Design & Implementation

3. Solve for the constants  $a_f$ , and  $b_f$  such the filter has a pole at  $s = -240$  (approximately 40 Hz) and has unity DC gain.
4. Calculate the numerator and denominator of the controller associated with the cascade of the PD and low pass filter blocks. These will have the form

$$\text{PD*Filter} = \frac{e_0 + e_0s}{g_0 + g_1s} \quad (6.6-1)$$

5. In the Generalized Form box, enter the following.
  - a. Enter your calculated  $e_i$ 's and  $g_i$ 's
  - b. Select Encoder #1 for Loop #2. (the other loops may have any encoder selected at this point)
  - c. Set the following equal to 1:  $t_0, h_0, i_0$ ,
  - d. Verify that  $r_I = 0.0000002$ <sup>1</sup>
  - e. Verify that all other coefficients = 0

It is important to take care and assure that all parameters are properly set before leaving the Generalized Form dialog box and implementing control.

<sup>1</sup> This small value is needed to provide a proper transfer function for bilinear transformation and subsequent discrete control implementation whenever T/R and S/R are used to implement a differentiator. Its small value results in a pole many decades beyond the system bandwidth and is of no practical implication to system modeling or performance. This coefficient may be set to zero here, but should generally remain.

6. Exit the dialog box, verify that the Generalized Form button is selected, and Implement control. You should notice a reduction in audible signal noise. Safety check the controller and manually displace the disks. They should behave as before in Step 2.

### 6.6.2 Pole Placement Control of $\theta_2(s)/\theta_1(s)$

Having closed a relatively high bandwidth ( $\approx 10$  Hz) loop about the first disk, we utilize the fact that the transfer function of Eq. 6.2-5 has near unity input/output gain (and near zero phase) through the bandwidth ( $\approx 2.5$  Hz) that we will attempt to attain in the overall control of  $\theta_2$ . Thus for the control of  $\theta_2$  we consider the outer loop in the block diagram of Figure 6.6-1.

Now the plant to be controlled is:

$$\frac{\theta_2(s)}{\theta_1(s)} = \frac{N_2}{N_1} \triangleq \frac{N^*(s)}{D^*(s)} \quad (6.6-2)$$

The numerical values of the parameters in this expression were determined in Experiment #1.

We now seek to find a controller  $S(s)/R(s)$  which will result in a prescribed set of closed loop poles. The closed loop denominator will have the form:

$$D_{cl}(s) = D^*(s)R(s) + N^*(s)S(s) \quad (6.6-3)$$

which may be expressed as<sup>1</sup>

$$D_{cl}(s) = (d_2s^2 + d_1s + d_0)(r_1s + r_0) + (n_0)(s_1s + s_0) \quad (6.6-4)$$

where the  $d_i$ 's and  $n_i$ 's are the respective coefficients of the denominator and numerator of the right hand side of Eq. (6.6-2). Their values are known from the plant model Eq's (5.1-4,-5) (or Eq's (5.1-7,-8)).

By linear system theory, for coprime  $N^*(s)$ ,  $D^*(s)$  with  $N^*(s)/D^*(s)$  proper, there exists an  $(n-1)^{\text{th}}$  order  $S(s)$ ,  $R(s)$  which when convolved as per Eq. (6.6-3) form an arbitrary  $(2n-1)^{\text{th}}$  order  $D_{cl}(s)$  where  $n$  is the order of  $D^*(s)$ .

Here we shall solve for the desired denominator:

---

<sup>1</sup>The notation here is the obvious one.

$$D_{cl}(s) = \left(s + 5\pi \frac{(1+j)}{\sqrt{2}}\right) \left(s + 5\pi \frac{(1-j)}{\sqrt{2}}\right) (s + 5\pi) \quad (6.6-5)$$

I.e. closed loop poles at -2.5, and  $-1.77 \pm j1.77$ Hz.<sup>1</sup>

### Pole Placement Design

7. Determine the coefficients of the controller polynomials  $S(s)$  and  $R(s)$  by equating coefficients in the expanded forms of Eq's 6.6-4 and 6.6-5.
8. Calculate the scalar prefilter gain  $k_{pf}$  by referring to Figure 6.6-1. The goal is to have the output  $\theta_2(s)$  scaled equal to the input  $r_r(s)$ . Hint: Consider the system in static equilibrium. Set  $\theta_2 = 1$  and  $r_r = 1$  and solve for  $k_{pf}$  using only the constant terms in all control blocks.

### Control Implementation

9. In the Executive program, set-up to collect Encoder #1, Encoder #3 and Commanded Position information<sup>2</sup> via Set-up Data Acquisition with data sampling every two sample periods. Setup a closed loop step trajectory of 1000 counts, 2000 ms duration and 1 repetition.
10. Return to the General Form Algorithm box and verify that the PD controller, low pass filter and all other coefficients are entered as given in Step 5 above. Enter the coefficients for  $S(s)$  and  $R(s)$  determined in Step 1. Enter the value  $k_{pf}$  calculated in Step 8 as to. Make sure that Encoder #3 is selected for Loop #1 (for Model 205a, Encoder #2 for Model 205) and Encoder #1 for Loop #2. Select OK to exit to the controller selection dialog box.
11. While staying clear of the mechanism select Implement Algorithm. If the mechanism reacts violently you have implemented an unstable controller or otherwise improperly entered the control coefficients and you will need to repeat the above steps as appropriate. You should first Reset Controller (Utilities menu) before attempting to re-implement control. If the system is well behaved, and after safety checking the controller, you may disturb the upper and lower disks lightly. Notice the relative stiffness of the two disks and how the lower disk moves in opposition to (i.e. regulation of) disturbances of the upper disk.

You may notice some "twitching" or buzzing due to noise in the system. This often occurs in such high gain systems, but has been mitigated via the low pass filter. If the noise is excessive or there is any possibility that the equipment is at risk discontinue control immediately.

12. Execute the Step input previously programmed, and plot the Encoder 1, Encoder #2, and Commanded Position data. Save your plot. How does the response at  $\theta_2$  compare with designs previously tested? Describe the motion of  $\theta_1$  and how it shapes the response at  $\theta_2$ .

<sup>1</sup> This has poles of magnitude  $|s| = 2.5$  Hz that lie at 135, 180, and 225 deg. It is similar to a third order Butterworth polynomial but somewhat more damped.

<sup>2</sup>You may also select Control Effort if you wish to later observe this value .

**Questions:**

- A. Report your calculated values for  $k_p$ ,  $k_d$ ,  $a_f$ ,  $b_f$ ,  $e_0$ ,  $e_1$ ,  $g_0$ ,  $g_1$ ,  $s_0$ ,  $s_1$ ,  $r_0$ ,  $r_1$ , and  $k_{pf}$
- B. Determine an expression for the closed-loop transfer function  $\theta_2(s)/r_r(s)$  including all elements in the block diagram of Figure 6.6-1. You may express this in terms of the polynomials  $D(s)$ ,  $N_1(s)$ ,  $R(s)$ , etc. rather than expanding each term fully. Determine  $\theta_2(s)/r_r(s)$  using the assumption  $c(s)=1$ . Compare the simulated frequency response of the full and reduced order transfer functions. In which regions are the two similar in magnitude and phase and in which are they different? Are they similar throughout the final system closed loop bandwidth? Is the assumption of unity gain in  $c(s)$  valid for the purposes here?
- C. Determine the phase and gain margins for the outer loop considering the full expression for the closed inner loop  $c(s)$  (i.e. consider  $c(s)$  to be a single block in the outer loop block diagram). Determine the phase and gain margins of the outer loop using the  $c(s) = 1$  assumption. How do the two compare?
- D. For this design, determine the static stiffness at  $\theta_1$  and  $\theta_2$  for  $T_{d1}$  and  $T_{d2}$  applied at  $J_1$  and  $J_2$  respectively (i.e.  $T_{d1}/\theta_1$  and  $T_{d2}/\theta_2$ ). What are the “cross” static stiffnesses (i.e.  $T_{d2}/\theta_1$  and  $T_{d1}/\theta_2$ )? How do the relative stiffness of the upper and lower disk compare in each case?

**6.7 LQR Control**

In this experiment a linear quadratic regulator is implemented using full state feedback. The plant used is again that of Figure 6.1-1b. The states chosen are the disk angles and rates according to the model of Eq (5.1-3) with the output taken as  $\theta_2$ , i.e.

$$C = [ 0 \ 0 \ 1 \ 0 ] \quad (6.7-1)$$

LQR Design:

1. Construct a state space model of the plant using the realization of Eq (5.1-3) and measured parameter values from Section 6.1.
2. The following notation shall be used for LQ optimization:

Feedback law:

$$u = -Kx \quad (6.7-2)$$

where

$$K = [ K_1 \ K_2 \ K_3 \ K_4 ] \quad (6.7-3)$$

Perform LQR synthesis via the Riccati equation solution<sup>1</sup> or numerical synthesis algorithms to find the controller  $K$  which minimizes the cost function (scalar control effort):

$$J = \int (x'Qx + u^2r)dt \quad (6.7-4)$$

In this synthesis choose  $Q=C'C$  so that the error at the intended output,  $\theta_2$ , is minimized subject to the control effort cost. Perform synthesis for control effort weight values:  $r = 100, 10, 1.0, 0.01, \text{ and } 0.001$ . Calculate the closed loop poles for each case as the eigenvalues of  $[A-BK]$

- 3) From this data, select a control effort weight to put the lowest pole frequency between 2.75 and 3.25 Hz. Use one of the above obtained  $K$  values if it meets this criteria, or interpolate between the appropriate  $r$  values and perform one last synthesis iteration. Do not use  $K_1$  or  $K_3$  values greater than 1, or  $K_2$  or  $K_4$  values greater than 0.12.<sup>2</sup>

### Control Implementation

Important Note: For Model 205a, (3 encoders),  $\theta_2$  is measured via Encoder #3.

The design gains  $K_2 + K_3$  are therefore input as  $k_5$  and  $k_6$  in the Executive's State Feedback box.

- 4) Implement your controller via the State Feedback box under Control Algorithm.<sup>3</sup> For tracking, the prefilter gain  $K_{pf}$  must be set equal to  $K_1 + K_3$ . You may wish to select Preview In General Form to see how these parameters are mapped into the generalized algorithm.
- 5) Execute a 1000 count step and plot the result. How do the rise time, overshoot, servo stiffness, and steady state errors compare with previous controllers?

#### **Questions / Exercises:**

- A. Report your calculated values of the closed loop poles for the various values of  $r$  in Step 2 and for your final design. Report the values of  $K$ , for your final design.
- B. Calculate the closed-loop transfer function  $\theta_2(s)/r_r(s)$  including all elements in the block diagram of Figure 6.7-1b (lower subfigure). You may express this in terms of the polynomials  $D(s)$ ,  $N_1(s)$ ,  $N_2$ , and  $K_i$  ( $i = 1,2,3,4$ ). Determine the phase and gain margins for

<sup>1</sup>See for example Kwakernaak and Sivan, "Linear Optimal Control Systems", Wiley & Sons, 1972.

<sup>2</sup> $K_1$  and  $K_3$  scale control effort proportional to position errors,  $K_2$  and  $K_4$  scale control effort proportional to the respective velocities. Excessive values of  $K_1$  or  $K_3$  can lead to low stability margin and in the presence of time delays, instability. Large  $K_2$  or  $K_4$  cause excessive noise propagation and lead to "twitching" of the system. - see Section 6.8

<sup>3</sup>If using discrete time implementation, be sure to divide your  $K_2$  and  $K_4$  values by  $T_s$  before entering them.



the system by considering the open loop “numerator” to be all terms in the closed loop denominator except  $D(s)$ <sup>1</sup>.

C. For this design, determine the static stiffness at  $\theta_1$  and  $\theta_2$  for  $T_{d1}$  and  $T_{d2}$  applied at  $J_1$  and  $J_2$  respectively (i.e.  $T_{d1}/\theta_1$  and  $T_{d2}/\theta_2$ ). What are the “cross” static stiffnesses (i.e.  $T_{d2}/\theta_1$  and  $T_{d1}/\theta_2$ )? How do the relative stiffness of the upper and lower disk compare in each case?

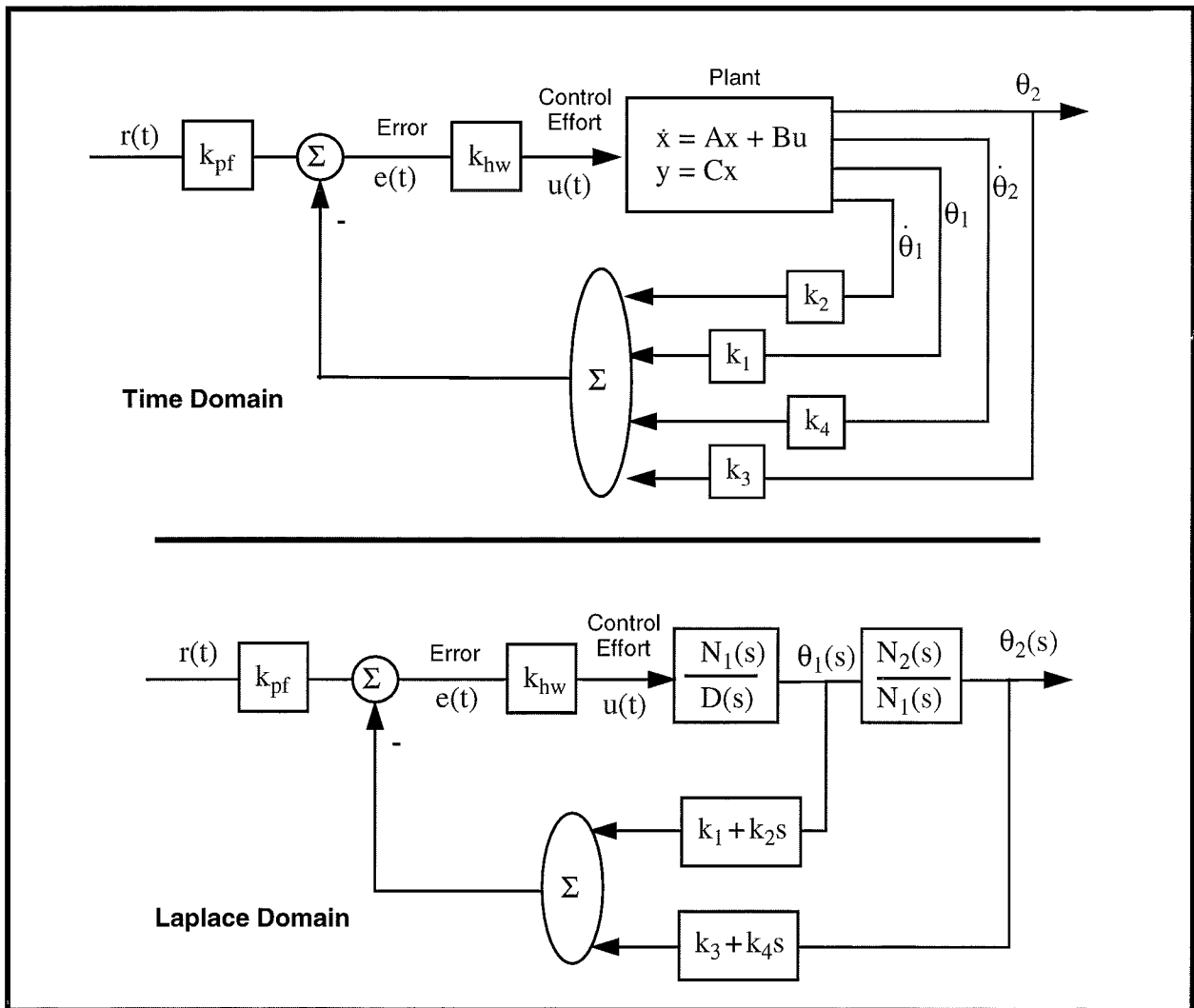


Figure 6.7-1. Representations of the Full State Feedback System

<sup>1</sup> This yields the margins as if the additional phase lag or gain were to occur in the control input (i.e.  $k_{hw}$  block), or uniformly among the outputs. This is not necessarily the case in practice, but does provide a general measure of stability margin.

## 6.8 Practical Control Implementation

This section demonstrates non-ideal behaviors that affect many controls applications, and gives guidelines for mitigating their effects. These are: drive saturation, sensor quantization, and discrete time sampling. Other effects include drive flexibility which is addressed in detail in the above experiments, and various forms of disturbances which may be studied using the optional disturbance drive.

### 6.8.1 Effect of Drive Saturation

*Saturation* is when the output of a device is held at some positive (negative) value for all input values above (below) some limit. This is illustrated in Figure 6.8-1 which depicts the input/output relationship for an otherwise linear device. Saturation may occur due to the control effort signal exceeding the range or capability of the DAC, servo amplifier, or even the sustainable magnetic field of the actuator. In practice however the amplifier and actuator are usually selected to accept full scale DAC voltage or the control electronics are programmed such that the DAC output saturates below control magnitudes that would saturate or damage other drive components.<sup>1</sup>

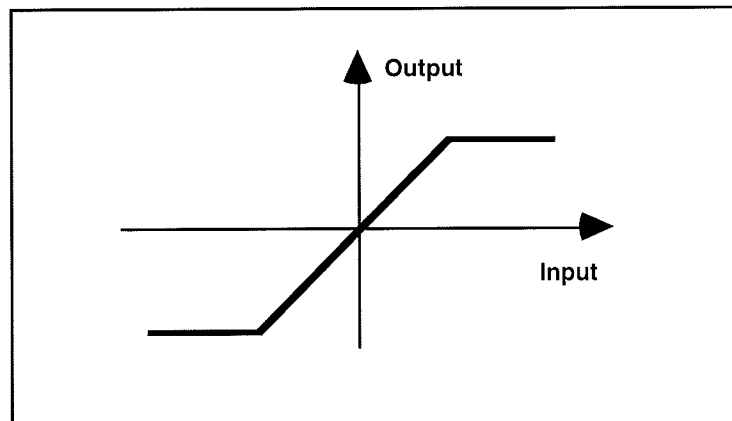


Figure 6.8-1. Linear Device Saturation

### Qualitative Changes in Step Response For High Bandwidth Controller /

- 1 Remove all disks from the apparatus except the bottom disk. Secure two 500 g. brass weights at a 9.0 cm. radial distance from the torsion shaft centerline. Implement the following parameters under PID control (not PI with Velocity

<sup>1</sup>In either case, the DAC is generally programmed to saturate below or at its full scale output. Without programmed saturation the DAC, which typically accepts two's-complement input numbers, would output full scale voltage of reverse polarity upon exceeding its input range. This would clearly be problematic!

Feedback):  $T_s = 0.002652$  s.,  $k_p = 0.4$ ,  $k_d = 0.030$ ,  $k_i = 0$ . The student should verify that these gains correspond to approximately  $\omega_n = 4$  Hz and  $\zeta = 1.0$ <sup>1</sup>.

- 2 Setup to acquire Encoder 1, Commanded Position, and Control Effort every 1 servo cycle. Perform a 50 count step maneuver, then a 1,000 count step, and finally a 16,000 count step. Plot and save your data.

**Questions / Exercises:**

- A. Compare the 50 count and 1000 count step responses and associated control effort for the forward path differentiator DAC saturation tests. Plot the simulated ideal step response for a forward and return path differentiated PD controlled system (e.g. for the return path case plot the response of the system of Eq. 6.2-5 using  $\omega_n=4$  Hz,  $\zeta=1$ ). Which ideal response does the experimental data follow more closely for the 50 and 1000 count amplitudes? Why?
- B. Compare the speed and shape of the 16,000 count response in the DAC saturation tests with the 1000 count one. What is the shape of the motion in the first 150 ms (approximately) for the 16,000 count maneuver? Why?
- C. Describe in what way the following factors affect whether and to what extent a given set of drive hardware will reach its torque limit or saturate: controller bandwidth, commanded acceleration, commanded amplitude.

### 6.8.2 Effect of Discrete-time Sampling

With modern high speed data processing capability, sampling rates are often high enough that control may be analyzed and implemented using continuous time analytical methods. In cases where either the objective control bandwidth is high, the control processor is otherwise heavily burdened, or economic considerations require lower speed processing capability, the sample rate may be sufficiently low that its effect is significant.

Of particular interest is the phase lag due to the time delay associated with sampled data systems. Such time delays propagate from signal sampling and holding in ADC conversion of analog feedback sensors (not the case for the Model 205 system) and in the control algorithm itself. Further time delay and phase lag results from DAC conversion of control effort and in the analog servo amplifier. While a detailed analysis of the associated time delay is beyond the scope of this exercise, the phase lag associated with discrete time sampling is on the order of that of a pure time delay of length equal to the sample period,  $T_s$ . Such a delay, denoted here as  $\phi(s)$ , is expressed in the Laplace domain as:

$$\phi(s) = e^{-sT_s} \quad (6.8-1)$$

<sup>1</sup> The natural frequency and damping ratio will vary depending on the particular system's  $k_{hw}$ .

In the frequency domain, its phase angle is:

$$\arg(\phi(j\omega)) = -T_s\omega \quad (6.8-2)$$

where  $T_s$  is in seconds, and  $\arg(\phi(j\omega))$  and  $\omega$  are in consistent angular units.

#### Procedure

3. Set up the mechanism with the lower disk only attached and with no weights. as per Step 1 above. Verify that the Data Acquisition function is set to sample data every  $1 T_s$ . Implement the following parameters under PI with Velocity Feedback:  $k_p = 0.02$ ,  $k_d = 0.003$ . Use Encoder #1 for feedback and set  $T_s = 0.00442$  s. These gains correspond to approximately  $\omega_n = 2$  Hz and  $\zeta = 1.0$  for this reduced inertia. Perform a 4000 count step. Gradually increase the sample period and repeat the procedure until significant oscillations occur and the system exhibits near instability. Do not implement sampling periods greater than 75 ms. Do not increase sample period after once oscillation amplitudes of 2000 counts peak-to-peak have been observed. Record the highest value of  $T_s$  prior to instability. Plot the step response and note the oscillation frequency.
4. Repeat Step 3 for  $\omega_n \approx 10$  Hz and  $\zeta \approx 1.0$  ( $k_p = 0.5$ ,  $k_d = 0.02$ ). . Increase sample rates by one increment (0.000884 s.) at a time only. Do not implement sampling periods greater than 15 ms in this case. Do not implement again once a limit cycle oscillation has been identified.

#### **Exercise:**

- D. Compute the continuous-time Bode phase margin of the two (2 & 10 Hz) systems and note the associated critical frequency (the frequency where the open loop gain curve crosses 0 Db). Using this information and the approximation for sampling related phase lag from Eq. (6.8-2) to explain the instability. Explain the difference in instability inducing sample rate for the two systems. How does the oscillation frequency compare with the critical frequency? Explain.

### 6.8.3 Effect of Finite Wordlength & Sensor Quantization

Numerical quantization occurs by necessity in all control systems that contain digital control elements. Such effects (also known as finite word-length effects) include coefficient and data quantization, DAC and ADC resolution, signal dynamic range, and round-off noise. These can have profound consequences with respect to system stability and performance. High dynamic

order controllers require particular care in providing robust algorithmic treatment and high data fidelity.<sup>1</sup>

Consider the effect of the position measurement quantization of the feedback encoders. The discrete encoder position measurement may be operated on by high bandwidth control law terms such as the backwards differentiator in discrete-time PD control which can result in quantization noise. The backwards differentiator approximates angular rate as

$$\omega_n \cong \frac{\theta_n - \theta_{n-1}}{T_s} \quad (6.8-3)$$

where  $\theta_n$  is the current encoder measurement and  $\theta_{n-1}$  is the one immediately prior. Calling the encoder measurement resolution  $\Delta_\theta$ ,<sup>2</sup> the backwards difference rate quantum,  $\Delta_\omega$ , becomes

$$\Delta_\omega = \frac{\Delta_\theta}{T_s} \quad (6.8-4)$$

The associated incremental control torque  $T_{\Delta_\omega}$  is

$$T_{\Delta_\omega} = k_d \Delta_\omega k_{hw} = \frac{k_d \Delta_\theta k_{hw}}{T_s} \quad (6.8-5)$$

As  $T_{\Delta_\omega}$  becomes large, a single encoder pulse (which can occur at infinitesimal rates) can cause relatively high instantaneous control effort. This propagates through the system causing high frequency motion in the sensed position further causing high instantaneous torque – i.e. noise is propagated.

From Eq.(6.8-5) torque (or control effort) quantization increases with reduced encoder resolution.<sup>3</sup> For a given encoder, the torque quantization and hence torque noise increases with increased derivative<sup>1</sup> gain and with reduced sampling period.

### Procedure

5. Remove all disks from the apparatus except the bottom disk. Secure two 500 g. brass weights at a 9.0 cm. radial distance from the torsion shaft centerline. Input the following parameters under PI with Velocity Feedback:  $k_d = 0.01$ ,  $k_p$

<sup>1</sup>The DSP controller and imbedded control firmware provide very high data and parameter resolution including a 16 bit DAC, and 48 bit multiplication with 96 bit products. These combined with internal data scaling for numerical conditioning make this system immune to many quantization related problems.

<sup>2</sup> For the units used in this manual, the resolution is the angular size in radians per encoder pulse, i.e.  $2\pi/16,000$  for the encoders on the Model 205 apparatus.

<sup>3</sup>Eq.(6.8-5) should not be viewed as a predictor of noise onset. Many other effects such as system bandwidth, mechanical flexibility, and nonlinear behavior all influence noise propagation and generally have a different effect at different sampling frequency. For a given system and controller, however, high frequency torque (or control effort) quantization is often a dominant factor in noise propagation.

$= 0$ ,  $k_i = 0$  (i.e. the controller will implement a pure backwards differentiator)  
Set  $T_s = 0.00442$  s. Before proceeding, note the following:

If at any time in this experiment excessive noise occurs, shut down open the control loop immediately via Abort Control. Any sustained operation with high frequency noise (and/or high torque) can cause loosening or other damage to drive components.

6. Implement the control and displace the lower disk with a ruler and note if any noise occurs. Reduce  $T_s$  by one increment (0.000884 s) and re-implement, displace the drive disk and check for noise. Repeat this procedure (one  $T_s$  increment at a time) until quantization noise is clearly detected. Abort control immediately upon hearing noise and do not repeat at a lower sample period. Note the last sample period.
7. Repeat Steps 1 and 2 for  $k_d = 0.05$ .

**Question:**

- E. Is the relationship between derivative gain, sampling period, and torque noise implied by Eq.(6.8-5) generally consistent with the results of Steps 6 and 7?

---

<sup>1</sup>Or more generally with increased high bandwidth gain.

## Appendix A. Dynamic Modeling Details

### A.1 Dynamics of Ideal Plant

#### A.1.1 Equations Of Motion

An idealized approximation of the torsional plant is shown in Figure A-1a where friction is neglected. Using the free body diagram of Figure A-1b and summing torques acting on  $J_1$  we have via Newton's second law (in its rotational form)

$$T(t) - k_1(\theta_1 - \theta_2) = J_1 \ddot{\theta}_1$$

or:

$$J_1 \ddot{\theta}_1 + k_1(\theta_1 - \theta_2) = T(t) \tag{A.1-1}$$

Similarly from Figure A-1c for  $J_2$ :

$$J_2 \ddot{\theta}_2 + (k_1 + k_2)\theta_2 - k_1\theta_1 = 0 \tag{A.1-2}$$

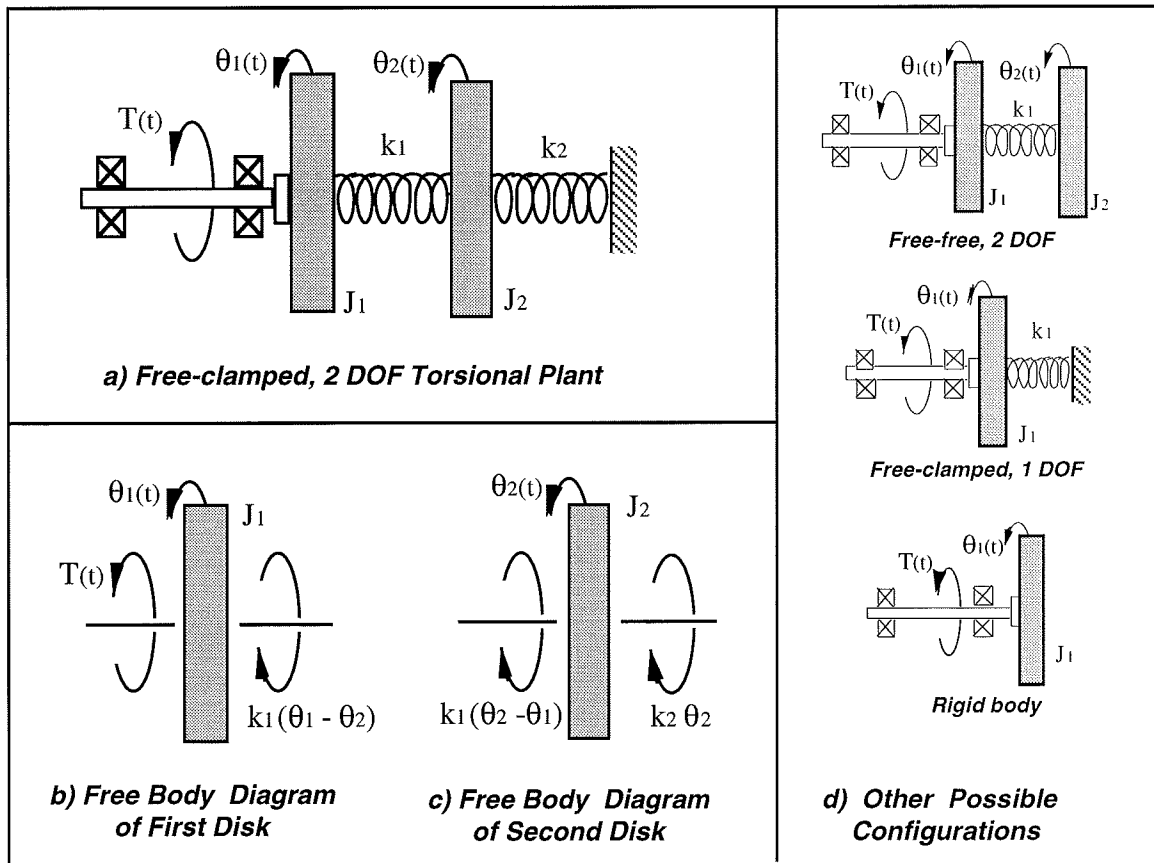


Figure A-1 Idealized Plant Models

or in matrix notation:

$$J\ddot{\theta} + k\theta = T \tag{A.1-3}$$

where

$$\theta = \begin{bmatrix} \theta_1 \\ \theta_2 \end{bmatrix}, \quad J = \begin{bmatrix} J_1 & 0 \\ 0 & J_2 \end{bmatrix}, \quad k = \begin{bmatrix} k_1 & -k_1 \\ -k_1 & k_1+k_2 \end{bmatrix}, \quad T = \begin{bmatrix} T \\ 0 \end{bmatrix} \tag{A.1-4}$$

### A.1.2 State Space Realization

A state space realization which is useful in several control approaches to this system follows directly from Eq A.1-4. i.e.:

$$\begin{aligned} \dot{x} &= Ax + BT(t) \\ Y &= Cx \end{aligned} \tag{A.1-20}$$

where:

$$X = \begin{bmatrix} \theta_1 \\ \dot{\theta}_1 \\ \theta_2 \\ \dot{\theta}_2 \end{bmatrix}, \quad A = \begin{bmatrix} 0 & 1 & 0 & 0 \\ -k_1/J_1 & 0 & k_1/J_1 & 0 \\ 0 & 0 & 0 & 1 \\ k_1/J_2 & 0 & -(k_1+k_2)/J_2 & 0 \end{bmatrix},$$

$$B = \begin{bmatrix} 0 \\ 1/J_1 \\ 0 \\ 0 \end{bmatrix}, \quad C = \begin{bmatrix} C_1 & 0 & 0 & 0 \\ 0 & C_2 & 0 & 0 \\ 0 & 0 & C_3 & 0 \\ 0 & 0 & 0 & C_4 \end{bmatrix}$$

and  $C_i = 1$  ( $i=1,2,3,4$ ) when  $X_i$  is an output and equals 0 otherwise.

### A.1.3 Modal Frequencies and Shapes

Several important dynamic properties are best illustrated by considering a modal representation of the plant. The homogeneous ( $T(t)=0$ ) solutions of Eq's A.1-1,-2 are harmonic and have the general form:

$$\theta_i = \chi_i C \cos(\omega t + \phi) \quad (i=1,2) \tag{A.1-30}$$

Substituting Eq A.1-30 into Eq A.1-3 yields an *eigenvalue problem* in the form:

$$\begin{bmatrix} k_1 - J_1 \omega^2 & -k_1 \\ -k_1 & k_1 + k_2 - J_2 \omega^2 \end{bmatrix} \begin{Bmatrix} \chi_1 \\ \chi_2 \end{Bmatrix} = 0 \tag{A.1-31}$$

which has a nontrivial solution if and only if



$$\begin{vmatrix} k_1 - J_1 \omega^2 & -k_1 \\ -k_1 & k_1 + k_2 - J_2 \omega^2 \end{vmatrix} = J_1 J_2 \omega^4 - [k_1 J_2 + (k_1 + k_2) J_1] \omega^2 + k_1 k_2 = 0 \quad (\text{A.1-32})$$

For the two degrees of freedom system this characteristic equation may be solved explicitly via the quadratic solution. E.g. for the case of  $J_1 = J_2$ ,  $k_1 = k_2$ :

$$\omega^2 = \frac{k_1}{J_1} \left[ \frac{3 \pm \sqrt{5}}{2} \right] \quad (\text{A.1-33})$$

For  $J_1 = 2J_2$ ,  $k_1 = 2k_2$ :

$$\omega^2 = \frac{k_1}{J_1} [2 \pm \sqrt{3}] \quad (\text{A.1-34})$$

Or, in general:

$$\omega^2 = \frac{k_1}{J_1} \left[ \frac{1}{2} + a\beta \pm \sqrt{\frac{1}{4} + b\beta + c\beta^2} \right] \quad (\text{A.1-35})$$

where:

$$a = \frac{1 + \alpha}{2}, \quad b = \frac{1 - \alpha}{2}, \quad c = \frac{1 + \alpha^2}{4} \quad (\text{A.1-36})$$

and:

$$\alpha = k_2/k_1 \quad (\text{A.1-37a})$$

$$\beta = J_1/J_2 \quad (\text{A.1-37b})$$

For the case  $k_2 = 0$  ( $\alpha = 0$ ):

$$\omega^2 = \frac{k_1}{J_1} [0, 1 + \beta] \quad (\text{A.1-38})$$

The  $\omega^2 = 0$  solution corresponds to the *rigid body mode* in which  $J_1$  and  $J_2$  move with constant angular velocity.

The normalized characteristic roots may be plotted as functions of the mass and stiffness ratios  $\alpha$  &  $\beta$  as shown in Figure A-2. The actual modal frequencies are readily found by multiplying the values read from the figure by the ratio  $[k_1/J_1]^{1/2}$ .

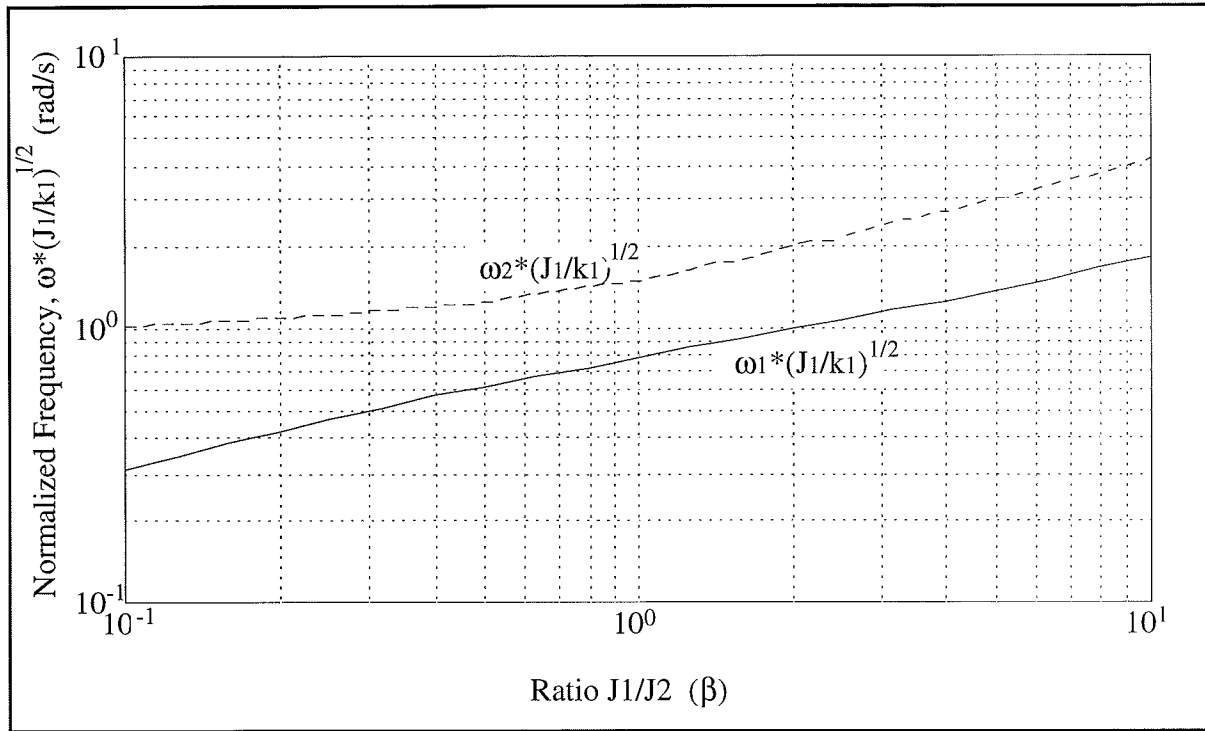


Figure A-2 Dependence of  $\omega_1$  and  $\omega_2$  on  $\beta$ .  $\alpha = 1$

The *mode shapes* (or the relative amplitudes and directions of  $\theta_1$  &  $\theta_2$  when the plant is oscillating at the modal frequencies) are found by solution of Eq. A.1-31 as:<sup>1</sup>

$$\frac{\chi_2}{\chi_1} = \frac{k_1 - J_1 \omega^2}{k_1} \tag{A.1-39}$$

where the constant C of Eq A.1-30 scales both amplitudes and therefore the amplitude  $\chi_1$  is arbitrary.

The special cases considered above yield:

For  $J_1=J_2, k_1=k_2$ : 
$$\frac{\chi_2}{\chi_1} = \frac{-1 \pm \sqrt{5}}{2} \tag{A.1-40}$$

For  $J_1=2J_2, k_1=2k_2$ : 
$$\frac{\chi_2}{\chi_1} = -1 \pm \sqrt{3} \tag{A.1-41}$$

For  $J_1=J_2/\beta, k_2=0$ : 
$$\frac{\chi_2}{\chi_1} = 1, -\beta \tag{A.1-42}$$

<sup>1</sup>Eq A.1-31 is over-determined in that two equations exist for one unknown. Another solution is  $\chi_2/\chi_1 = k_1/(k_1+k_2 - J_2\omega^2)$  which yields identical  $\chi_2/\chi_1$  values for solutions  $\omega^2$  to Eq A.1-32 (or -35).

Eq. A.1-42 shows that with  $k_2$  absent, there is one mode called the *rigid body mode* in which  $\theta_1$  &  $\theta_2$  move in unison and an oscillatory mode in which the coordinate amplitude ratio is proportional to the respective inertias.

#### A.1.4 Modal Coordinate State Space Representation

It may be shown via orthogonality properties that the system motion may at any time be expressed as a linear combination of the mode shapes, i.e.: (Ref Mierovitch, Greenwood)

$$\theta_i(t) = \sum_{j=1}^2 \chi_{ij} q_j(t) \quad i = 1, 2 \quad (\text{A.1-50})$$

where  $\chi_{ij}$  is the amplitude  $(C\chi_i)_j$  (see Eq. (A.1-30)) associated with the  $j$ th mode which has been normalized by:

$$\chi' J \chi = I \quad (\text{A.1-51})$$

with

$$\chi = \begin{bmatrix} \chi_{11} & \chi_{12} \\ \chi_{21} & \chi_{22} \end{bmatrix} \quad (\text{A.1-52})$$

Here  $I$  is the identity matrix. For our case, Eq.(A.1-51) results in:

$$\chi_{1j} = (C\chi_1)_j = \frac{1}{\sqrt{J_1 + J_2 (\chi_{21}/\chi_{11})^2}} \quad (\text{A.1-53})$$

and  $\chi_{2j}$  is found via multiplying  $\chi_{1j}$  by the amplitude ratio Eq.(A.1-39) for the  $j$ th mode.

The variables  $q_j(t)$  in Eq.(A.1-50) are called *modal coordinates*. Eq.(A.1-50) shows that  $q_j(t^*)$  may be thought of as the amount that the  $j$ th mode shape contributes to the system motion at some time  $t^*$ .

The equations of motion may then be expressed as (e.g. via modal decoupling or from orthogonality and Lagrange's equation<sup>1</sup>):

$$\ddot{q}_j(t) + \omega_j^2 q_j(t) = \chi_{1j} T(t) \quad (j=1, 2) \quad (\text{A.1-54})$$

which may be realized in state space form using Eq.(A.1-50) as

<sup>1</sup>See for example "Elements Of Vibration Analysis", L. M. Mierovitch, McGraw-Hill Book Co., 1975; or "Principles Of Dynamics", D. T. Greenwood, Prentice-Hall Inc., 1965.

$$\begin{aligned}\dot{q} &= Aq + BT(t) \\ \theta &= Cq\end{aligned}\tag{A.1-55}$$

where:

$$q = \begin{bmatrix} q_1 \\ \dot{q}_1 \\ q_2 \\ \dot{q}_2 \end{bmatrix}, \quad A = \begin{bmatrix} 0 & 1 & 0 & 0 \\ -\omega_1^2 & 0 & 0 & 0 \\ 0 & 0 & 0 & 1 \\ 0 & 0 & -\omega_2^2 & 0 \end{bmatrix},$$

$$B = \begin{bmatrix} 0 \\ \chi_{11} \\ 0 \\ \chi_{12} \end{bmatrix}, \quad C = \begin{bmatrix} \chi_{11} & 0 & \chi_{12} & 0 \\ \chi_{21} & 0 & \chi_{22} & 0 \end{bmatrix}$$

and  $\theta$  is as per Eq.(A.1-4) (The outputs  $\theta_i$  are obtainable by shifting the first and third columns in  $C$  one column to the right.)

### A.1.5 Transfer Functions

The plant transfer functions are found via the Laplace transform of Eq's(A.1-1,-2) which yield:

$$\frac{\theta_1(s)}{T(s)} = \frac{J_2 s^2 + k_1 + k_2}{D(s)}\tag{A.1-60}$$

$$\frac{\theta_2(s)}{T(s)} = \frac{k_1}{D(s)}\tag{A.1-61}$$

where:

$$D(s) = J_1 J_2 s^4 + (J_1(k_1 + k_2) + J_2 k_1) s^2 + k_1 k_2\tag{A.1-62}$$

Note that  $\theta_1/T$  has two imaginary zeroes at  $\omega = \pm j((k_1 + k_2)/J_2)^{1/2}$  resulting in a pole excess of two.  $\theta_2/T$  has no zeroes and hence a four pole excess. The roots to  $D(s)$  are imaginary and of magnitude given by Eq.(A.1-32 or A.1-35). The system is type zero (no zero valued roots to  $D(s)$ ) except for the case  $k_2 = 0$  (implies rigid body mode present) which is type two.

An expanded transfer function form may be obtained through partial fraction methodology applied to Eq's (A.1-61,-62), or equivalently by Laplace transform of Eq.(A.1-54) combined per Eq.(A.1-50):

$$\frac{\theta_1(s)}{T(s)} = \frac{\chi_{11}^2}{s^2 + \omega_1^2} + \frac{\chi_{12}^2}{s^2 + \omega_2^2}\tag{A.1-63}$$

$$\frac{\theta_2(s)}{T(s)} = \frac{\chi_{11}\chi_{21}}{s^2 + \omega_1^2} + \frac{\chi_{12}\chi_{22}}{s^2 + \omega_2^2} \tag{A.1-64}$$

## A.2 Practical Plant Model

### A.2.1 Equations Of Motion

While the expressions obtained in Section A.1 are useful in understanding the predominant dynamic behavior, they neglect certain non-ideal effects which are in some cases significant.<sup>1</sup> Among these are torques associated with motor cogging<sup>2</sup> and Coulomb (or static) and viscous friction from the pulleys, and bearings. From Figure A-3, a more precise approximation of the system motion is:

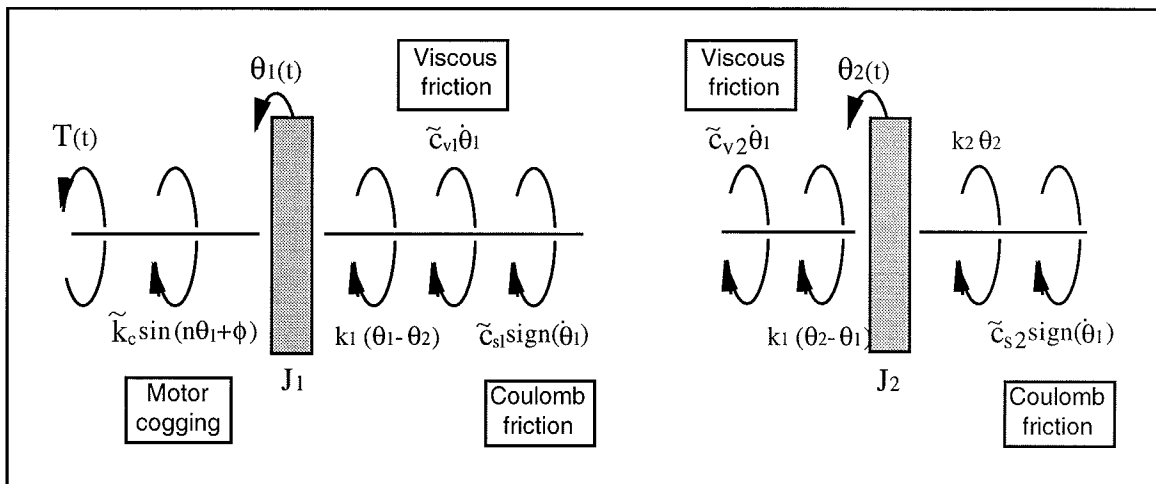


Figure A-3 Free Body Diagram Including Friction and Nonlinearities

<sup>1</sup>It is important to keep in mind the difference between the physical system and mathematical approximations of its behavior. Virtually no physical system follows a mathematical model exactly. In some cases even the dominant dynamic behavior evades mathematical description. It is very often possible, however to model the system sufficiently well for control purposes. The system here is relatively amenable to modeling with the ideal linear behavior dominating the plant dynamics. The generation of a plant model that is of minimal complexity but which represents the salient plant dynamics through the ensuing control bandwidth is central to effective control implementation.

<sup>2</sup>Motor cogging produces the torque "bumps" felt when rotating the motor under a zero torque command (amplifier active) and is associated with brushless motor phasing and rotor magnet / stator field interaction. While this is not a true sinusoid, it may be approximated by  $k_c \sin(n\theta_1 + \phi)$  where  $n$  is equal to the drive pulley diameter ratio times the number of motor poles, i.e.  $n = 2 \times 3$  for Model 205/205a.

$$J_1 \ddot{\theta}_1 + \tilde{c}_{v1} \dot{\theta}_1 + \tilde{k}_c \sin(n\theta_1 + \phi) + \tilde{c}_{s1} \text{sign}(\dot{\theta}_1) + k_1(\theta_1 - \theta_2) = T(t) \quad (\text{A.2-1})$$

$$J_2 \ddot{\theta}_2 + \tilde{c}_{v2} \dot{\theta}_2 + \tilde{c}_{s2} \text{sign}(\dot{\theta}_2) + (k_1 + k_2)\theta_2 - k_1\theta_1 = 0 \quad (\text{A.2-2})$$

which has nonlinear terms.

Reductions in the complexity of this model may be made. When at rest and with no acting torques, the cogging torque will tend to place the system in a point of stable equilibrium. If we define  $\theta_1=0$  at such a point, then if Coulomb friction is small,  $\phi \approx 0$ . By linearization (e.g. the first two Taylor's series terms) about  $\theta_1=0$  we have that for small angles (say  $|\theta_1| \leq 10$  deg) the cogging torque is approximated as:

$$\tilde{k}_c \sin(n\theta_1 + \phi) \cong \tilde{k}_c n \theta_1 \triangleq k_c \theta_1 \quad (\text{A.2-3})$$

An approximation of the Coulomb friction which is satisfactory in many cases is obtained by equating the resulting torque to that supplied by viscous friction when operating at some nominal speed  $\dot{\theta}_{in}$ . From a system stability point of view, it is conservative to use a value  $\dot{\theta}_{in}$  at or near the highest expected operating speed (top speed is generally specified as a design requirement) so that the actual associated damping or energy dissipation is generally greater. So doing and combining with other viscous terms gives:

$$\tilde{c}_{si} \text{sign}(\dot{\theta}_i) \cong c_{vi}^* \dot{\theta}_{i_{max}} \quad (i=1, 2) \quad (\text{A.2-4})$$

$$c_i \cong \tilde{c}_{vi} + c_{vi}^* \quad (i=1, 2) \quad (\text{A.2-5})$$

The above result in simplified equations of motion:

$$J_1 \ddot{\theta}_1 + c_1 \dot{\theta}_1 + (k_c + k_1)\theta_1 - k_1\theta_2 = T(t) \quad (\text{A.2-6})$$

$$J_2 \ddot{\theta}_2 + c_2 \dot{\theta}_2 + (k_1 + k_2)\theta_2 - k_1\theta_1 = 0 \quad (\text{A.2-7})$$

While the approximation of Eq.(A.2-3) is relatively accurate for  $|\theta_1| \leq 4$  deg, it is altogether invalid for angles much beyond this range. Further, the associated torque is small compared to the spring torques and may be considered to be a small disturbance which will be largely rejected under most closed loop control schemes. While the values of  $c_1$  &  $c_2$  will generally not be large for the system here, they are retained as they directly effect such salient plant characteristics as resonant amplitude and stability margins. Based on these considerations, we obtain the following simplified equations.

$$J_1 \ddot{\theta}_1 + c_1 \dot{\theta}_1 + k_1 \theta_1 - k_1 \theta_2 = T(t) \quad (\text{A.2-8})$$

$$J_2 \ddot{\theta}_2 + c_2 \dot{\theta}_2 + (k_1 + k_2) \theta_2 - k_1 \theta_1 = 0 \quad (\text{A.2-9})$$

which may be expressed in a state space form:

$$\begin{aligned} \dot{x} &= Ax + BT(t) \\ Y &= Cx \end{aligned} \quad (\text{A.2-10})$$

where:

$$X = \begin{bmatrix} \theta_1 \\ \dot{\theta}_1 \\ \theta_2 \\ \dot{\theta}_2 \end{bmatrix}, \quad A = \begin{bmatrix} 0 & 1 & 0 & 0 \\ -k_1/J_1 & -c_1/J_1 & k_1/J_1 & 0 \\ 0 & 0 & 0 & 1 \\ k_1/J_2 & 0 & -(k_1+k_2)/J_2 & -c_2/J_2 \end{bmatrix},$$

$$B = \begin{bmatrix} 0 \\ 1/J_1 \\ 0 \\ 0 \end{bmatrix}, \quad C = \begin{bmatrix} C_1 & 0 & 0 & 0 \\ 0 & C_2 & 0 & 0 \\ 0 & 0 & C_3 & 0 \\ 0 & 0 & 0 & C_4 \end{bmatrix}$$

and the output notation is as in Eq A.1-20.

### A.2.2 Modal Coordinate Representation

In the modal coordinate representation, plant damping is often approximated by assuming a viscous term for each mode, i.e.:<sup>1</sup>

$$\ddot{q}_j + 2\zeta_j \omega_j \dot{q}_j + \omega_j^2 q_j = \chi_{1j} T(t) \quad (\text{A.2-11})$$

which motivates a state space realization with

---

<sup>1</sup>This damping has a different form than that expressed in Eq's(A.2-6,-7) and in general is not literally representative of physical damping sources in the system. In order for viscous damping to exist and the modes to remain uncoupled, there must be an associated  $\dot{\theta}$  coefficient matrix  $C$  (Eq.(A.1-3)) which is proportional to either  $J$  or  $k$  - this is called *proportional damping*.

Thus damping will generally couple the modes to some extent so that an unforced system, initially experiencing single mode motion, will exhibit motion of the other mode(s) in time. With large influence of non proportional damping, the modal motion concept is wholly invalid. For small values of  $\zeta_j$  however, Eq.(A.2-10) is a useful approximation where the damping may be "visualized" as causing a decay of modal amplitude in the unforced plant.

$$A = \begin{bmatrix} 0 & 1 & 0 & 0 \\ -\omega_1^2 & -2\zeta_1\omega_1 & 0 & 0 \\ 0 & 0 & 0 & 1 \\ 0 & 0 & -\omega_2^2 & -2\zeta_2\omega_2 \end{bmatrix} \quad (\text{A.2-12})$$

and the remaining expressions and terms identical to Eq.(A.1-55). In the case  $k_2 = 0$  ( $\omega_1 = 0$ ), the 2,2 element in  $A$  becomes  $-c^*$  which is equal to  $-c/(J_1+J_2)$  with  $c$  being the damping coefficient associated with the rigid body motion. (i.e. the rigid body equation is  $(J_1+J_2)\ddot{\theta}_i + c\dot{\theta}_i = T$  ( $i=1,2$ ). Again, this approximation is only valid for small  $c$  or for  $c_1$  and  $c_2$  proportional to  $J_1$  and  $J_2$  –see note below. When these criteria are met, then  $c^* \approx (c_1+c_2)/(J_1+J_2)$  )

### A.2.3 Transfer Functions

From the Laplace transform of Eq's(A.2-8,9) we have:

$$\frac{\theta_1(s)}{T(s)} = \frac{J_2s^2 + c_2s + k_1 + k_2}{D(s)} \quad (\text{A.2-13})$$

$$\frac{\theta_2(s)}{T(s)} = \frac{k_1}{D(s)} \quad (\text{A.2-14})$$

where:

$$D(s) = J_1J_2s^4 + (c_1J_2 + c_2J_1)s^3 + (J_1(k_1+k_2) + J_2k_1 + c_1c_2)s^2 + (c_1(k_1+k_2) + c_2k_1)s + k_1k_2 \quad (\text{A.2-15})$$

The expanded transfer function forms resulting from Eq.(A.2-11) are:

$$\frac{\theta_1(s)}{T(s)} = \frac{\chi_{11}^2}{s^2 + 2\zeta_1\omega_1s + \omega_1^2} + \frac{\chi_{12}^2}{s^2 + 2\zeta_2\omega_2s + \omega_2^2} \quad (\text{A.2-16})$$

$$\frac{\theta_2(s)}{T(s)} = \frac{\chi_{11}\chi_{21}}{s^2 + 2\zeta_1\omega_1s + \omega_1^2} + \frac{\chi_{12}\chi_{22}}{s^2 + 2\zeta_2\omega_2s + \omega_2^2} \quad (\text{A.12-17})$$

where the  $\chi_{ij}$ 's may be obtained from Eq.(A.1-53) for small  $\zeta_j$ .



The above models are useful when the plant parameters  $J_i$ ,  $k_i$ , &  $c_i$  ( $i=1,2$ ) are known or are measurable explicitly. In many cases, the plant is identified via its natural frequencies, damping ratios, and gains. Either of the above transfer function types may be expressed in the form:

$$\frac{\theta_1(s)}{T(s)} = \frac{K_1 (s^2 + 2\zeta_z \omega_z s + \omega_z^2)}{(s^2 + 2\zeta_{p1} \omega_{p1} s + \omega_{p1}^2)(s^2 + 2\zeta_{p2} \omega_{p2} s + \omega_{p2}^2)} \quad (\text{A.2-18})$$

$$\frac{\theta_2(s)}{T(s)} = \frac{K_2}{(s^2 + 2\zeta_{p1} \omega_{p1} s + \omega_{p1}^2)(s^2 + 2\zeta_{p2} \omega_{p2} s + \omega_{p2}^2)} \quad (\text{A.2-19})$$

where the gains  $K_1$  &  $K_2$ , are nominally equal to  $1/J_1$  and  $k_1/J_1 J_2$  respectively (but may be measured more directly). Equations (A.2-18,-19) model the plant in terms of parameters which are either readily measured or derived and therefore are useful for practical implementation.

Again, for the case  $k_2 = 0$  ( $\omega_1 = 0$ ), the coefficient  $2\zeta_1 \omega_1$  (or  $2\zeta_{p1} \omega_{p1}$ ) becomes  $c^*$  which is nominally equal to  $c/(J_1 + J_2)$ . Thus the first denominator term in the right hand side of each of Eq's(A.2-16 through -19) becomes nominally equivalent to  $1/[(J_1 + J_2)s^2 + cs]$ .

Measurement of parameters to establish the explicit plant transfer functions for Model 205 is covered in Section 6.1 of this manual.

### A.3 One Degree of Freedom Plants

The dynamic models for the one degree of freedom (DOF) "free-clamped" plant (see Fig. A-1d) follow from Eq's(A.1-1 & A.2-8) by setting  $\theta_2 = 0$ . The results are stated below where the "rigid body" 1 DOF plant may be found by taking  $k_1 = 0$  in the appropriate equations. The undamped expressions are obtained by setting  $\zeta$  and  $c_1$  to zero.

The equation of motion is

$$J_1 \ddot{\theta}_1 + c_1 \dot{\theta}_1 + k_1 \theta_1 = T(t) \quad (\text{A.3-1})$$

which has the transfer function:

$$\frac{\theta_1(s)}{T(s)} = \frac{1}{J_1 s^2 + c_1 s + k_1} \quad (\text{A.3-2})$$

or

$$\frac{\theta_1(s)}{T(s)} = \frac{K_1}{s^2 + 2\zeta \omega s + \omega^2} \quad (\text{A.3-3})$$

The state space realization analogous to Eq (A.2-10) is comprised of the first 2x2, 2x1, 2x1, and 2x2 submatrices of the respective A, B, X, and C matrices in (A.2-10).

The modal coordinate state space realization has system matrix, A, that is the first 2x2 submatrix of Eq.(A.2-12) and with consistent B, C, and **q** matrices:

The characteristic root is  $\omega^2 = k_1/J_1$ , and the single modal weighting is  $\chi_{11} = 1/\sqrt{J_1}$ .

#### A.4 Three Degree of Freedom Plant (ECP Model 205a)

The dynamic models for the three degree of freedom (DOF) torsional apparatus are given below without derivation. They are however, a straightforward extension of the material in Sections A.1 and A.2. The analogous two DOF equations are given in brackets.

The damped plant model is shown graphically in Figure A-4. Note that the plant may also be configured into any of the two or one DOF types shown in Figure A-1 .

As before for the undamped plant:

$$J\ddot{\theta} + k\theta = T$$

with [A.1-4]

$$\theta = \begin{bmatrix} \theta_1 \\ \theta_2 \\ \theta_3 \end{bmatrix}, \quad J = \begin{bmatrix} J_1 & 0 & 0 \\ 0 & J_2 & 0 \\ 0 & 0 & J_2 \end{bmatrix}, \quad k = \begin{bmatrix} k_1 & -k_1 & 0 \\ -k_1 & k_1+k_2 & -k_2 \\ 0 & -k_2 & k_2 \end{bmatrix}, \quad T = \begin{bmatrix} T \\ 0 \\ 0 \end{bmatrix} \quad (\text{A.4-1})$$

which may be expressed in the state space form of Eq (A.2-10) with:

$$X = \begin{bmatrix} \theta_1 \\ \dot{\theta}_1 \\ \theta_2 \\ \dot{\theta}_2 \\ \theta_3 \\ \dot{\theta}_3 \end{bmatrix}, \quad A = \begin{bmatrix} 0 & 1 & 0 & 0 & 0 & 0 \\ -k_1/J_1 & -c_1/J_1 & k_1/J_1 & 0 & 0 & 0 \\ 0 & 0 & 0 & 1 & 0 & 0 \\ k_1/J_2 & 0 & -(k_1+k_2)/J_2 & -c_2/J_2 & k_2/J_2 & 0 \\ 0 & 0 & 0 & 0 & 0 & 1 \\ 0 & 0 & k_2/J_3 & 0 & -k_2/J_3 & -c_3/J_3 \end{bmatrix}, \quad (\text{A.4-1})$$

$$B = \begin{bmatrix} 0 \\ 1/J_1 \\ 0 \\ 0 \\ 0 \\ 0 \end{bmatrix}, \quad C = \begin{bmatrix} C_1 & 0 & 0 & 0 & 0 & 0 \\ 0 & C_2 & 0 & 0 & 0 & 0 \\ 0 & 0 & C_3 & 0 & 0 & 0 \\ 0 & 0 & 0 & C_4 & 0 & 0 \\ 0 & 0 & 0 & 0 & C_5 & 0 \\ 0 & 0 & 0 & 0 & 0 & C_6 \end{bmatrix}$$

with the output notation as in Eq (A.1-20).

The Eigenvalue expression [A.1-31] becomes:

$$\begin{bmatrix} k_1 - J_1 \omega^2 & -k_1 & 0 \\ -k_1 & k_1 + k_2 - J_2 \omega^2 & -k_2 \\ 0 & -k_2 & k_2 - J_3 \omega^2 \end{bmatrix} \begin{Bmatrix} \chi_1 \\ \chi_2 \\ \chi_3 \end{Bmatrix} = 0 \tag{A.4-2}$$

with characteristic equation:

$$J_1 J_2 J_3 \omega^6 - [J_1 (J_2 k_2 + J_3 k_1 + J_3 k_2) + J_2 J_3 k_1] \omega^4 + [J_1 k_1 k_2 + J_2 k_1 k_2 + J_3 k_1 k_2] \omega^2 = 0 \tag{A.4-3}$$

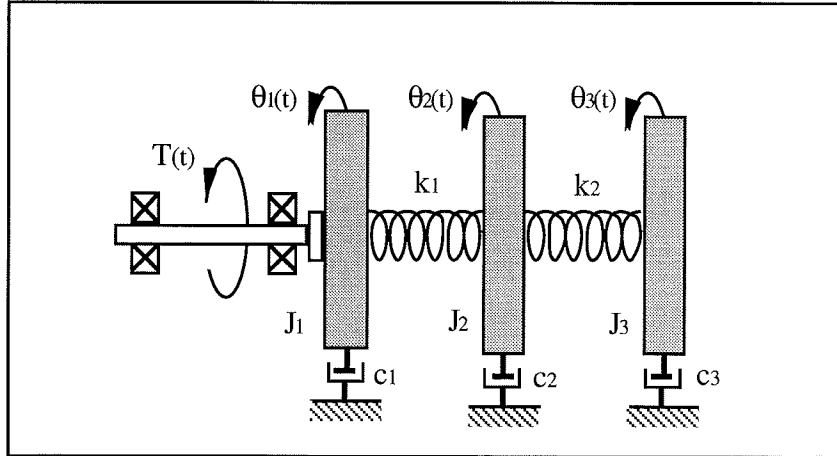


Figure A-4. Clamped-Free, 3 DOF (damped model)

which contains  $\omega^2$  as a factor and hence a rigid body mode ( $\omega = 0$ ) is present. Equations (A.4-2 & -3) are used to solve for the characteristic frequencies  $\omega$  and the amplitude ratios for each of the three modes. The ratio  $\chi_2/\chi_1$  is given by Eq(A.1-39) as before, and:

$$\frac{\chi_3}{\chi_1} = \frac{k_2(k_1 - J_1 \omega^2)}{k_1(k_2 - J_3 \omega^2)} \tag{A.4-4}$$

(Note that amplitude ratios are both equal to one for the rigid body mode.) The modal amplitudes are normalized by the 3x3 analog of Eq's(A.1-51,52).

Including the effects of damping (the undamped expressions are obtained via setting the  $\zeta$ 's and  $c^*$  to zero in the following equations) we have for the modal coordinate state space form [A.1-55, A.2-11]:

$$\begin{aligned} \dot{q} &= Aq + BT(t) \\ \theta &= Cq \end{aligned} \tag{A.4-5}$$

where

$$q = \begin{bmatrix} q_1 \\ \dot{q}_1 \\ q_2 \\ \dot{q}_2 \\ q_3 \\ \dot{q}_3 \end{bmatrix}, \quad A = \begin{bmatrix} 0 & 1 & 0 & 0 & 0 & 0 \\ 0 & -c^* & 0 & 0 & 0 & 0 \\ 0 & 0 & 0 & 1 & 0 & 0 \\ 0 & 0 & -\omega_2^2 & -2\zeta_2\omega_2 & 0 & 0 \\ 0 & 0 & 0 & 0 & 0 & 1 \\ 0 & 0 & 0 & 0 & -\omega_3^2 & -2\zeta_3\omega_3 \end{bmatrix},$$

$$B = \begin{bmatrix} 0 \\ \chi_{11} \\ 0 \\ \chi_{12} \\ 0 \\ \chi_{13} \end{bmatrix}, \quad C = \begin{bmatrix} \chi_{11} & 0 & \chi_{12} & 0 & \chi_{13} & 0 \\ \chi_{21} & 0 & \chi_{22} & 0 & \chi_{23} & 0 \\ \chi_{31} & 0 & \chi_{32} & 0 & \chi_{33} & 0 \end{bmatrix}$$

The plant transfer functions are:

$$\frac{\theta_1(s)}{T(s)} = \frac{N_1(s)}{D(s)} \tag{A.4-6}$$

$$\frac{\theta_2(s)}{T(s)} = \frac{N_2(s)}{D(s)} \tag{A.4-7}$$

$$\frac{\theta_3(s)}{T(s)} = \frac{N_3}{D(s)} \tag{A.4-8}$$

where:

$$N_1(s) = J_2J_3s^4 + [J_2c_3+J_3c_2]s^3 + [J_2k_2 + c_2c_3+J_3k_1+J_3k_2]s^2 + [c_2k_2+c_3k_1+c_3k_2]s + k_1k_2 \tag{A.4-9}$$

$$N_2(s) = k_1 [J_3 s^2 + c_3 s + k_2] \quad (\text{A.4-10})$$

$$N_3(s) = k_1 k_2 \quad (\text{A.4-11})$$

$$D(s) = J_1 J_2 J_3 s^6 + [J_1 J_2 c_3 + J_1 J_3 c_2 + J_2 J_3 c_1] s^5 + [J_1 (J_2 k_2 + J_3 k_1 + J_3 k_2 + c_2 c_3) + J_2 (J_3 k_1 + c_1 c_3) + J_3 c_1 c_2] s^4 + [J_1 (c_2 k_2 + c_3 k_1 + c_3 k_2) + J_2 (c_1 k_2 + c_3 k_1) + J_3 (c_1 k_1 + c_1 k_2 + c_2 k_1) + c_1 c_2 c_3] s^3 + [(J_1 + J_2 + J_3) k_1 k_2 + c_1 (c_2 k_2 + c_3 k_1 + c_3 k_2) + c_2 c_3 k_1] s^2 + [(c_1 + c_1 + c_1) k_1 k_2] s \quad (\text{A.4-12})$$

Note that this complicated expression for  $D(s)$  requires the measurement or estimation of eight dynamic parameters for its coefficients – some of which may be physically difficult to obtain .

The expanded transfer function forms which derive from Eq.(A.4-5) are [A.2-16,-17]:

$$\frac{\theta_3(s)}{T(s)} = \frac{\chi_{11}\chi_{31}}{s^2 + c^*s} + \frac{\chi_{12}\chi_{32}}{s^2 + 2\zeta_2\omega_2s + \omega_2^2} + \frac{\chi_{13}\chi_{33}}{s^2 + 2\zeta_3\omega_3s + \omega_3^2} \quad (\text{A.4-13})$$

$$\frac{\theta_2(s)}{T(s)} = \frac{\chi_{11}\chi_{21}}{s^2 + c^*s} + \frac{\chi_{12}\chi_{22}}{s^2 + 2\zeta_2\omega_2s + \omega_2^2} + \frac{\chi_{13}\chi_{23}}{s^2 + 2\zeta_3\omega_3s + \omega_3^2} \quad (\text{A.4-14})$$

$$\frac{\theta_3(s)}{T(s)} = \frac{\chi_{11}\chi_{31}}{s^2 + c^*s} + \frac{\chi_{12}\chi_{32}}{s^2 + 2\zeta_2\omega_2s + \omega_2^2} + \frac{\chi_{13}\chi_{33}}{s^2 + 2\zeta_3\omega_3s + \omega_3^2} \quad (\text{A.4-15})$$

The more practical forms expressed in terms of measurable frequencies, damping, and gains are [A.2-18,-19]:

$$\frac{\theta_1(s)}{T(s)} = \frac{K_1 (s^2 + 2\zeta_{z1}\omega_{z1}s + \omega_{z1}^2)(s^2 + 2\zeta_{z2}\omega_{z2}s + \omega_{z2}^2)}{s(s + c^*)(s^2 + 2\zeta_{p2}\omega_{p2}s + \omega_{p2}^2)(s^2 + 2\zeta_{p3}\omega_{p3}s + \omega_{p3}^2)} \quad (\text{A.4-16})$$

$$\frac{\theta_2(s)}{T(s)} = \frac{K_2 (s^2 + 2\zeta_z\omega_zs + \omega_z^2)}{s(s + c^*)(s^2 + 2\zeta_{p2}\omega_{p2}s + \omega_{p2}^2)(s^2 + 2\zeta_{p3}\omega_{p3}s + \omega_{p3}^2)} \quad (\text{A.4-17})$$

$$\frac{\theta_3(s)}{T(s)} = \frac{K_3}{s(s + c^*)(s^2 + 2\zeta_{p2}\omega_{p2}s + \omega_{p2}^2)(s^2 + 2\zeta_{p3}\omega_{p3}s + \omega_{p3}^2)} \quad (\text{A.4-18})$$

Parameter identification to establish the explicit plant transfer functions or state space realizations for Models 205 & 205a is covered in Section 6.1 of this manual.



## 6i. Instructor's Supplement To Experiments

This is the instructor's supplement to the experiments described in Chapter 6 of the main manual. It contains the expected experimental results and solutions to exercises as well as additional optional experiments and exercises and their solutions

This supplement is organized with section numbers consistent with those of the seven experiments in the main manual body. In addition to describing experimental results, Section 6.1i contains numerical models of three plant configurations. Appendix Ai contains several MATLAB® scripts useful in building numerical plant models and performing certain steps in the experiments.

### On Selection Of User Units:

The experiments described in Chapter 6 use (encoder) Counts as the system units of angular position. Other options are Degrees or Radians. The choice of units may vary based on the particular nature of the accompanying course work. The Counts option, for example, is most useful when the course incorporates elements of the hardware and data processing implementation where the counts correspond to encoder pulses and controller-internal register values. This set of units will tend to give students a more practical perspective of the data that they are obtaining and evaluating. Radians, are consistent with SI unit standards and are most directly related to the basic theoretical principles discussed. The instructor may modify the experiment instructions and solutions/expected results to be based on a different set of units by using the following relationships:

$$\begin{aligned} 1 \text{ revolution} &= 2\pi \text{ radians} \\ &= 360 \text{ degrees} \\ &= 16,000 \text{ encoder counts} \end{aligned}$$

Students should be instructed to select the corresponding units in User Units under the Setup menu.

### Rotational vs. Rectilinear Systems:

It is important that students recognize the dynamic equivalence of rotational and rectilinear dynamic systems. The students should not have the perception that the results obtained here pertain to the former but not the latter. Every principle studied here has a direct and intuitive analog in rectilinear systems. By the following parameter mapping the analogy is complete.

Rotational System Parameter	Rectilinear System Parameter
Inertia, $J$	Mass, $m$
Torsional Spring, $k$	Rectilinear Spring, $k$
Rotary Damping, $c$	Rectilinear Damping, $c$

On The Scope of Experiments

There are many control systems topics that relate to these experiments which are not explored in the manual, but which the instructor may wish to bring out. The methodologies presented here demonstrate some fundamental principles and behaviors, but are not represented to be necessarily superlative practical control solutions. They do in the least however, give the undergraduate student a hands-on introduction to control implementation, and the more advanced user a working orientation to the system from which much more general topics may be explored.

Note to instructors and advanced users:

If you or your students synthesize and implement a control structure that is of particular academic or instructional interest, please share it with us! Pending ECP review and your approval, it may be included in a future revision of this manual with credits of course to the inventor. For all earnest submittals, you will receive a complementary software and manual upgrade!

**6.1i System Identification**

The procedure given is for identifying the plant parameters in Eq's (5.1-1 through 5.1-8). For identifying a three disk plant (Model 205a only) or any plant where the middle disk is used, the inertia and damping parameters found in this procedure for the upper disk may be assumed to be the same for the middle one.

A representative plot of results from Step 6 is shown in Figure 6.1-1i.

Reasonable values for experimental results are on the order of:

- $\omega_{nd31} = 12 \text{ rad/s}$
- $\omega_{nd32} = 38 \text{ rad/s}$
- $\zeta_{d32} = 0.01$
- $\omega_{nd11} = 12 \text{ rad/s}$
- $\omega_{nd12} = 34 \text{ rad/s}$
- $\zeta_{d12} = 0.04$
- $k_a k_t k_p k_e = 1780 \text{ N-m-count/(V-rad)}$



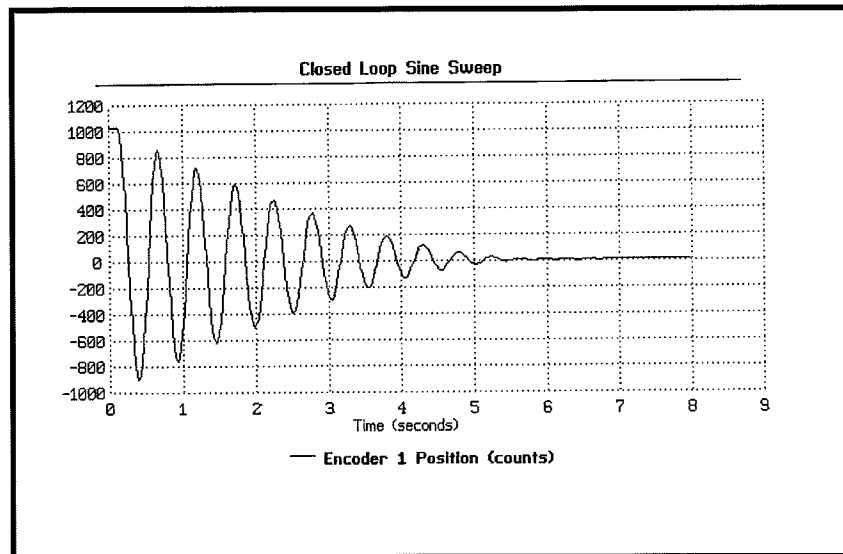


Figure 6.1-1i. Typical Response Used In Plant Identification

**Questions / Exercises:**

A. Values for calculated results (consistent with the values given above):

$J_m = 0.016825$  (exact for the nominal values given – includes inertia of 4 weights about their own c.g.).

$J_{d3} = 0.0019 \text{ kg-m}^2. (= J_m(\omega_{nd31})^2 / [(\omega_{nd32})^2 - (\omega_{nd31})^2])$

$J_{d1} = 0.0024 \text{ kg-m}^2.$

$c_{d3} = .001 \text{ N-m/rad/s} (= 2J_{d3}\zeta_{d32}\omega_{nd32})^1$

$c_{d1} = .007 \text{ N-m/rad/s}$

$k_{d3} = 2.7 \text{ N-m/rad} (= (\omega_{nd32})^2 J_{d3})$

$k_{d1} = 2.8 \text{ N-m/rad} (= (\omega_{nd12})^2 J_{d1})$

B. For the configuration shown in Figure 6.1-1b (this configuration is used extensively in this manual) and using the above parameter values, the desired transfer functions are obtained by substitution into Eq's(5.1-4,-5) using the following notation:

<sup>1</sup>Due to the nonlinear nature of the (largely Coulomb) damping, the resulting damping coefficients will vary with the inertia used in the free response tests. Here the value from the unloaded disk is used as it results in a lower apparent damping coefficient and hence is conservative from a system stability point of view. These damping coefficients and the resulting ratios may vary considerably as they are largely dependent on pulley tension and belt run-in. Their values are relatively low however and generally have a weak effect on system dynamics. The spring and inertia parameters will fall close to their nominal values and should be stable in time.

$$J_1 = J_{d1} + J_m/2 \cong 0.0108 \text{ kg-m}^2$$

$$J_2 = J_{d3} + J_m/2 \cong 0.0103 \text{ kg-m}^2$$

$$c_1 = c_{d1} \cong .007 \text{ N/rad/s}$$

$$c_2 = c_{d3} \cong .001 \text{ N/rad/s}$$

$$k_1 = k_{d1}k_{d3}/(k_{d1}+k_{d3}) \cong 1.37 \text{ N/rad}$$

$$k_2 = 0$$

$$k_{hw} = 17.4 \text{ (This value may vary significantly from system-to-system)}$$

C. The units of  $k_{hw}$  are N-m/rad.

#### Further Question (optional)

A. What are the poles and zeros, natural frequencies, damping, and gain coefficients of the transfer functions for the plant of Question B above?

*ans. (for values listed above):*

*Poles of  $D(s)$  @  $-0.21 \pm 16.13, -0.43$  (rad/s)*

*Roots of  $N_1(s)$  @  $-.097 \pm 11.5i$  (rad/s)*

*$\omega_{p2} = 16.134$  (rad/s),  $\zeta_{p2} = 0.013$*

*$K_1 k_{hw} = 1596$  (1/s)<sup>2</sup>*

*$K_2 k_{hw} = 200,600$  (1/s)<sup>4</sup>*

#### This section covered:

1. Derivation of inertia values and torsional spring constants using the classic frequency equations of a lightly damped oscillator.
2. Measurement of friction (modeled as viscous) using the logarithmic decrement.
3. Development of the system hardware gain and its measurement through known inertia acceleration.
4. Development of plant transfer function using the measured mechanical parameters and system hardware gain.

#### Alternative Method Of Plant Identification

Several other methods of plant identification are possible including those involving frequency domain modeling and those which find the modal shapes, damping, and frequencies. One such method is outlined below which will generally yield superior results to those from the method of

Chapter 6.1 for lightly damped systems. This method requires some manual skill, and is not amenable to a precise description of procedures for students.

### Procedure Outline

1. Set up the mechanism in whichever configuration is desired for subsequent controls testing.
2. Set up data acquisition per Steps 3 and 4 of Sect 6.1.
3. Manually excite modes of the system by rotating one disk back and forth by hand. (At the modal frequency, of course, very little effort is required to sustain oscillation, thus it is relatively easy to "feel" the mode and excite it at the proper frequency. Small errors in exciting the precise resonant frequency will manifest as harmonic modal frequencies – rigid body or oscillatory – which are easily distinguishable on the data plot.)
4. Acquire data as described in Step 5 of 6.1 to plot the unforced frequency decay. It is generally best to look at velocity to eliminate position drift effects. Measure modal frequencies and damping as described in Steps 5 & 9.
5. Repeat this step for the second mode if applicable. Alternatively, it is possible to deflect the inertias statically relative to one another, and release them suddenly. This will generally give components of multiple modes in the output unless the deflection is a mode shape. Again, however, the modal oscillations are usually well separated in frequency and easy to identify individually in a single plot.
6. The anti-resonant frequency(s) may be identified using the open loop sine sweep trajectory (as may be the resonant frequencies).<sup>1</sup> The "damping" of the zeros is a bit trickier to obtain. It may be calculated via the damping coefficients found under Sect 6.1 or estimated by the reduction in amplitude during a slow sweep through the anti-resonance and comparing with simulation.
7. The so-called rigid body damping,  $c^*$ , may be found by manually rotating the shaft at as constant a speed as possible and acquiring/plotting velocity data of the shaft spin-down (encoder #1 is best to use). Due to Coulomb friction, the velocity characteristic will be closer to linear than an ideal viscous exponential decay. By using a relatively high value of velocity (say  $\dot{\theta} = \pi$  rad/s) however, a conservatively low coefficient value may be obtained as:

$$c^* = \ddot{\theta} / \dot{\theta} \quad (1/s)$$

8. The system gains are best calculated using the results of Sect 6.1 for configurations with oscillatory modes, or may be measured via open loop step acceleration for rigid bodies.

### Scripts For Building Plant Models

Matlab® scripts for building plants #1, #2, & #3 are given in Appendix A.1i.

---

<sup>1</sup>A 1.0 Volt input is recommended and the sweep frequency range may be "zoomed" in to establish the precise anti-resonant frequency. For the final "zoom", it is recommended to set the sweep start and end frequencies  $\leq 0.1$  Hz apart and set the sweep time to  $\geq 60$  sec to minimize the transient effects associated with frequency change. It is best to acquire only the encoder data of interest and at a relatively low rate (say every 4 servo cycles) so that the data size is not excessive.

Numerical Plant Models

The following numerical models are of the three configurations shown in Figure 6.1-2i for a specific apparatus whose dynamic parameters and  $k_{hw}$  ( $= 17.4$  in this case) were used. The transfer functions are by the free modal frequency method described above, and the state space matrices derive from the indirect  $J, c, k$  measurements described in Section 6.1. There are slight differences between the corresponding model values (e.g. eigenvalues) between the two methods. These models will be used in examples later in this manual and should yield acceptable results when used for design of controllers for Model 205/205a in cases where the control is not highly sensitive to plant parameter changes. (In all cases, however, the constant  $k_a k_i k_p$  should be identified as the amplifier gain can vary significantly unit to unit.) For best results, an identification of each individual plant should be conducted. The state space realizations given are for the form of Eq (5.2-4) or the obvious lower order subsystems. In all cases, the given output is for the upper most disk.

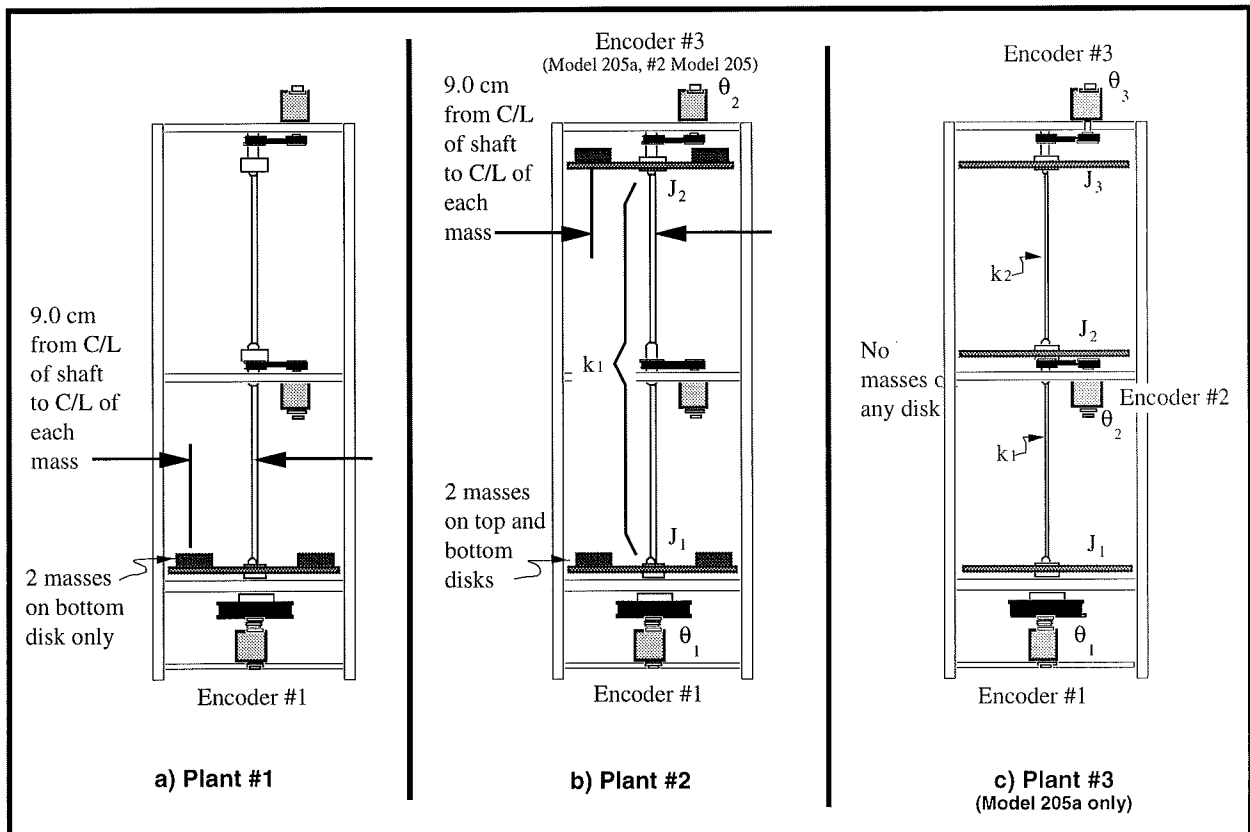


Figure 6.1-2i. Plant Model Configurations

1. Plant #1<sup>1</sup>

$$\text{TF:} \quad \frac{\theta(s)}{u(s)} = \frac{1600}{s(s+.83)} \quad (6.1-1i)$$

$$\text{SS:} \quad A = \begin{bmatrix} 0 & 1 \\ 0 & -0.83 \end{bmatrix}, \quad B = \begin{bmatrix} 0 \\ 1600 \end{bmatrix}, \quad C = [1 \ 0] \quad (6.1-2i)$$

2. Plant #2

$$\text{TF:} \quad \frac{\theta_1(s)}{u(s)} = \frac{k_{hw}N_1(s)}{D(s)} \quad (6.1-3i)$$

$$\frac{\theta_2(s)}{u(s)} = \frac{k_{hw}N_2(s)}{D(s)}$$

where:

$$k_{hw}N_1(s) = 1600((s+0.19)^2+11.15^2)$$

$$k_{hw}N_2(s) = 200,000$$

$$D(s) = s(s+0.69)((s+0.38)^2+15.71^2)$$

$$\text{SS:} \quad A = \begin{bmatrix} 0 & 1 & 0 & 0 \\ -126.9 & -0.648 & 126.9 & 0 \\ 0 & 0 & 0 & 1 \\ 133.0 & 0 & -133.0 & -0.971 \end{bmatrix}, \quad B = \begin{bmatrix} 0 \\ 1600 \\ 0 \\ 0 \\ 0 \end{bmatrix}, \quad C = [0 \ 0 \ 1 \ 0] \quad (6.1-4i)$$

3. Plant #3

$$\text{TF:} \quad \frac{\theta_1(s)}{u(s)} = \frac{k_{hw}N_1(s)}{D(s)} \quad (6.1-5i)$$

$$\frac{\theta_2(s)}{u(s)} = \frac{k_{hw}N_2(s)}{D(s)}$$

$$\frac{\theta_3(s)}{u(s)} = \frac{k_{hw}N_3(s)}{D(s)}$$

where:

$$k_{hw}N_1(s) = 6960((s+0.40)^2+23.1^2)((s+0.41)^2+60.1^2)$$

$$k_{hw}N_2(s) = 10.4 \times 10^6((s+0.42)^2+37.3^2)$$

$$k_{hw}N_3(s) = 1.51 \times 10^{10}$$

$$D(s) = s(s+1.60)((s+0.85)^2+35.2^2)((s+0.58)^2+63.9^2)$$

<sup>1</sup>In these transfer functions, u(s) is the output of the control algorithm. I.e. khw is included in the plant.

SS:

$$A = \begin{bmatrix} 0 & 1 & 0 & 0 & 0 & 0 \\ -1167 & -2.92 & 1167 & 0 & 0 & 0 \\ 0 & 0 & 0 & 1 & 0 & 0 \\ 1474 & 0 & -2895 & -0.526 & 1421 & 0 \\ 0 & 0 & 0 & 0 & 0 & 1 \\ 0 & 0 & 1421 & 0 & -1421 & -0.526 \end{bmatrix}$$

$$B = \begin{bmatrix} 0 \\ 6960 \\ 0 \\ 0 \\ 0 \\ 0 \end{bmatrix}, \quad C = [0 \ 0 \ 0 \ 0 \ 1 \ 0] \quad (6.1-6i)$$

## 6.2i Rigid Body PD & PID Control

This section first demonstrates the equivalence of  $k_p k_{hw}$  to a mechanical spring and  $k_d k_{hw}$  to a damper. It then shows the relationship of these to the natural frequency and damping ratio of the closed loop system. Parameters are selected to implement under-, over-, and critically damped systems and characteristic step responses are plotted. Integral action is then added and its effect on response, steady-state error, and stability are studied. These experiments may also be performed in the context of discrete time implementation where  $k_d$  must be divided by  $T_s$  and  $k_i$  multiplied by  $T_s$  when inputting parameters in the discrete time PID control window.

### Expected Results<sup>1</sup>:

- 1) In Step 3,  $k_p \approx 0.025$
- 2) In Step 7,  $\omega_n \approx 1$  Hz, after doubling  $k_p$ ,  $\omega_n \approx \sqrt{2}$  Hz.
- 3) In Step 8,  $k_d \approx 0.006$  for  $k_d k_{hw} = 0.1 \text{N-m/(rad/s)}$
- 4) In Step 11, gains for the respective under-, critical, and over-damped cases are approximately  $k_p = 0.10$ ,  $k_d = 0.003$ ,  $0.016$ , and  $0.03$ . Their step responses are shown in Figure 6.2-1i. The slower rise time with damping and oscillation in the underdamped case are clearly seen.
- 5) Sine sweeps for the three damping cases are shown in Figure 6.2-2i which shows the identical data plotted using the Linear time / Linear amplitude, and  $\log(w) / \text{Db}$  scaling options.
- 6) Figure 6.2-3i shows critically damped case with added integral terms  $k_i k_{hw} = 3 \text{N-m/(rad-sec)}$  and  $k_i k_{hw} = 9 \text{N-m/(rad-sec)}$ . The characteristic overshoot and zero steady state error are evident.

<sup>1</sup> These may vary according to a particular system's  $k_{hw}$ .

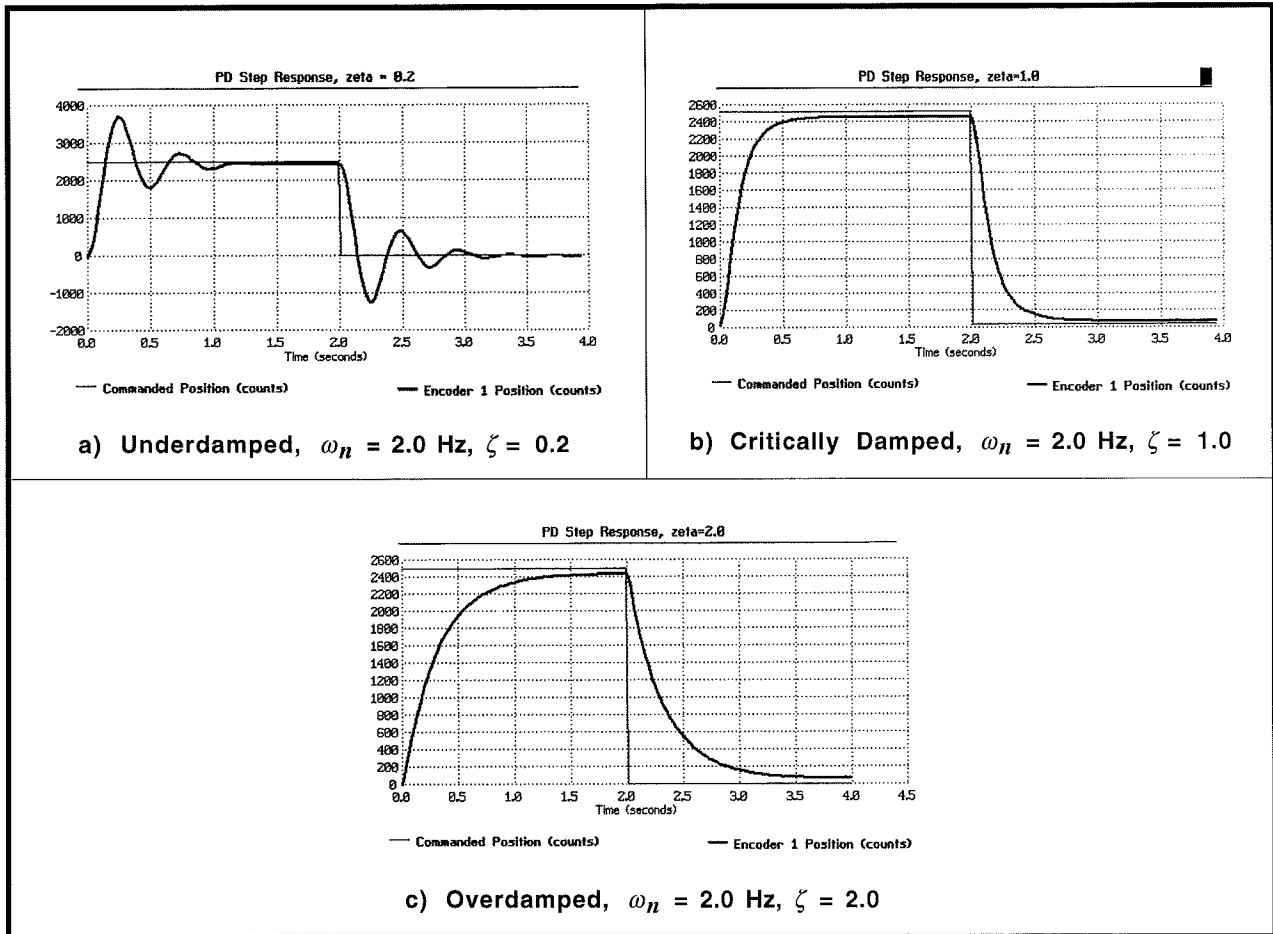
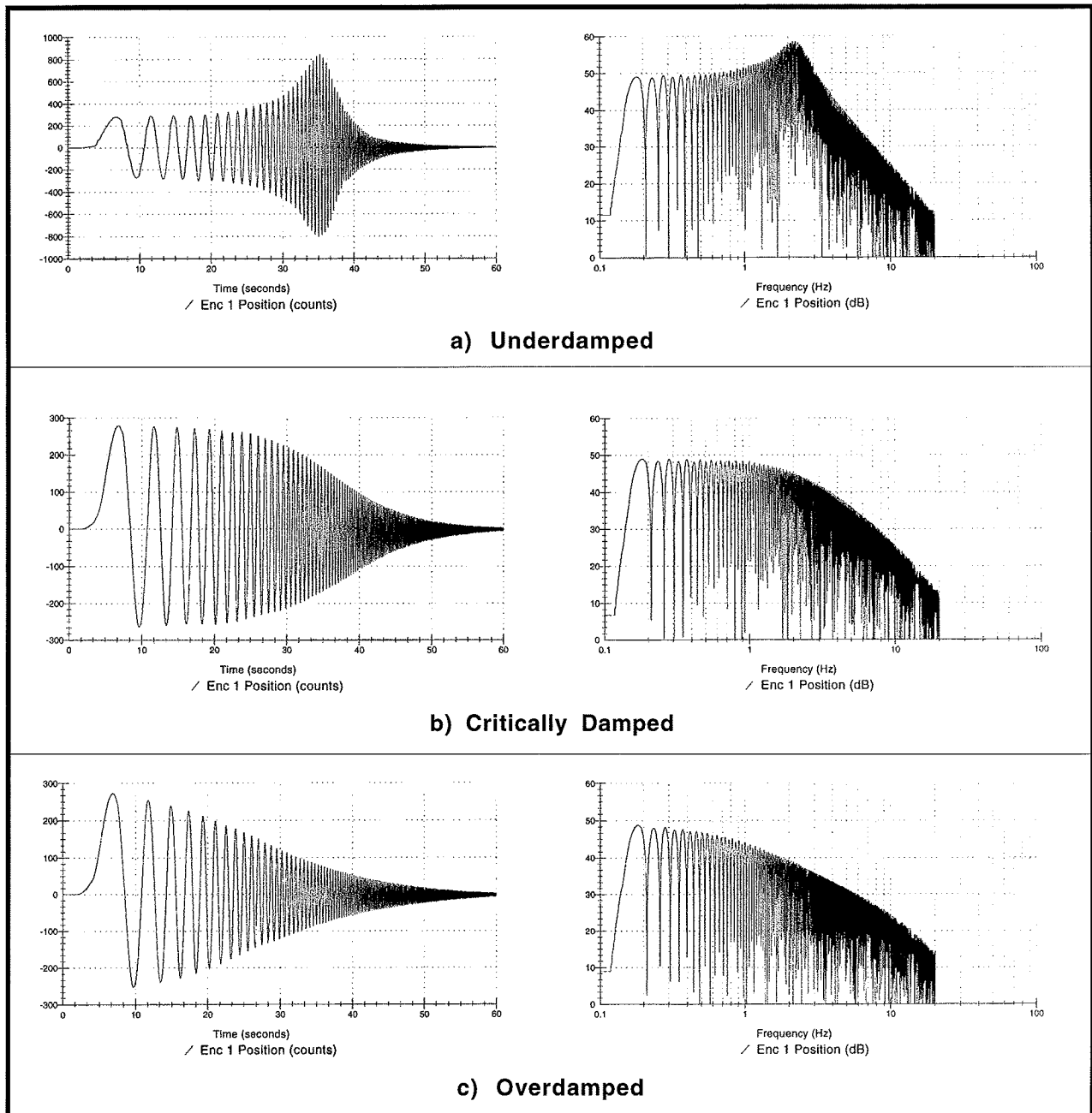


Figure 6.2-1i Typical Results of Step Response Tests

Note On Running Sine Sweep Tests. When running sine sweep trajectories, the output may be seen to drift or be biased at high frequency. This is normal and is associated with motor / amplifier cogging, commutation switching, and other practical drive effects and is most pronounced under relatively low gain control. It is often most apparent in the Db plots because the low amplitudes are graphically amplified due to the logarithmic scaling. The following should be considered in plotting experimental data.

1. If a bias is seen, this may usually be eliminated by selecting Remove DC Bias in the Setup Plot window.
2. If there is wandering or drift in the high frequency data, open the loop, then rotate the lower disk slightly (say 10 degrees), re-implement the controller, and rerun the sweep. It is often best to observe any wander resulting from a particular location. Once two locations are identified where the wander is of opposite sign, – positive going in one case, negative in the other – a position may usually be found between them in which the wander is minimal.

3. Bias and wander is essentially eliminated in viewing velocity and acceleration data. This data of course differs from the position data by  $\omega$  and  $\omega^2$  (+20 and +40 Db/decade) Plot velocity or acceleration.



**Figure 6.2-2i Representative Frequency Response Test Data Plotted With Linear Time / Amplitude & Log( $\omega$ ) / Db Amplitude Scalings**

Linear scaling best represents the data as students witness the test. The low frequency constant amplitude and  $1/\omega^2$  high frequency roll-off are evident. With log( $\omega$ ) / Db scaling, the amplitude of the system motion traces out the familiar Bode magnitude characteristics, thereby bridging from test results to theoretical concepts. Here the underdamped resonance frequency is read directly from the plot



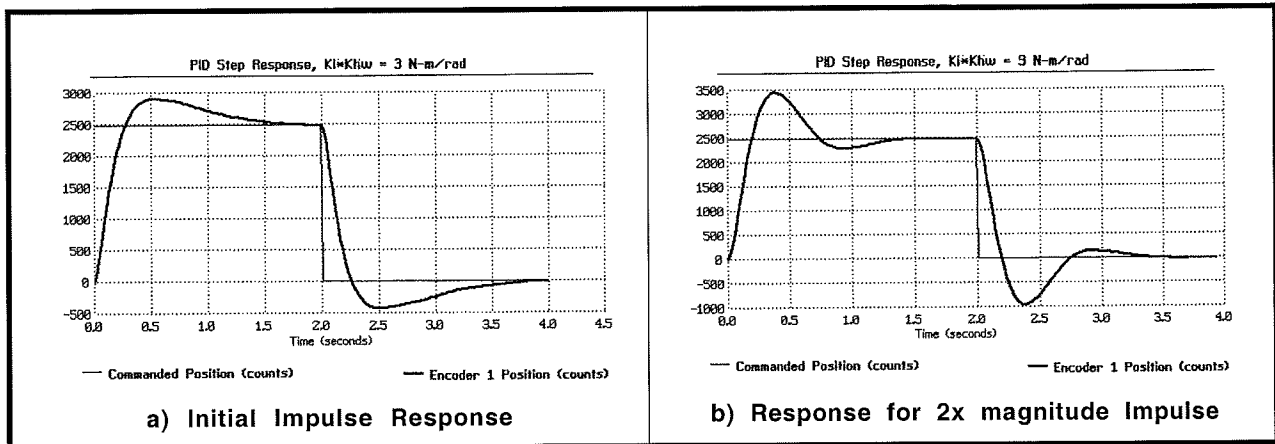


Figure 6.2-3i. Added Integrator Results in Overshoot & Zero Steady State Error

**Answers to Questions**

- A. Increased  $k_{hw}$  increases both  $\omega_n$  and  $\zeta$  by  $\sqrt{k_{hw}}$ .  $J$  reduces both  $\omega_n$  and  $\zeta$  by  $\sqrt{1/J}$ . “ $k_p$ ” increases  $\omega_n$  by  $\sqrt{k_p}$  and decreases  $\zeta$  by  $\sqrt{1/k_p}$ . “ $k_d$ ” does not affect  $\omega_n$  but increases  $\zeta$  proportionally. By replacing  $k = k_p k_{hw}$  and  $c = k_d k_{hw}$ , the transfer function of the plant of Fig. 6.2-2 is made identical to Eq. 6.2-2 except that the numerator is equal to  $1/J$  rather than  $k_p k_{hw}/J$ . Thus the PD controlled rigid body is dynamically the same as the spring/inertia/damper except for a scaling constant. (The system is in fact identical if the spring base is controlled by a prescribed angular position  $r(t)$  rather than being connected to inertial ground. The forward path derivative PD form is identical to the mechanical analog when both the damper and spring are connected to  $r(s)$ ).
- B. The S-plane diagram of the roots of Eq. 6.2-1 is shown in Fig. 6.2-4i. The roots are purely imaginary for  $\zeta=0$  corresponding to a pure oscillator. They become complex and lie along the circle  $|s| = \omega_n$  becoming more damped as  $\zeta$  increases. For  $\zeta \geq 1$  the roots are purely negative real corresponding to an exponential decay with no oscillation. As  $\zeta$  increases beyond 1, the response becomes slow as governed by the smaller magnitude root. The relative location of the roots in the s-plane is determined by  $\zeta$  while their dilation about the origin (time scaling) is determined by  $\omega_n$ .
- C. The oscillation in the underdamped step response has frequency  $\approx 2$  Hz corresponding to the approximate resonance in the frequency response. The overdamped and critically damped cases have no oscillations nor resonances. The bandwidth is greatest for the underdamped system and least for the overdamped one. This corresponds to the fastest and slowest rise times respectively.
- D. For all damping cases, the amplitude is constant and nominally equal to the input amplitude at low frequency. At high frequency, the shape is  $C/\omega^2$  ( $C$  is some constant) in the linear time and amplitude scaling and  $-40 \text{ Db/decade}$  in the  $\text{Log}(\omega)/\text{Db}$  scaling. These properties are shown by taking the steady-state frequency response amplitude found from  $|c(j\omega)|$  (Eq. 6.2-5) and evaluating as  $\omega$  tends to zero and infinity.
- E. Integral action eliminates steady state error to a step input. The transfer function between the disturbance and the output when the integrator is present is

$$\frac{\theta(s)}{T(s)} = \frac{s/J}{s^3 + (k_{hw}/J)(k_d s^2 + k_p s + k_i)} \quad (6.2-1i)$$

The final value for  $\theta$  is <sup>1</sup>

$$\lim_{s \rightarrow 0} \theta(s) = \frac{s/J}{s^3 + (k_{hw}/J)(k_d s^2 + k_p s + k_i)} u = 0 \quad (6.2-2i)$$

where  $u$  is the step magnitude. Without the integrator, the final value is

$$\lim_{s \rightarrow 0} \theta(s) = \frac{s/J}{s^3 + (k_{hw}/J)(k_d s^2 + k_p s)} u = \frac{u}{k_p k_{hw}} \quad (6.2-3i)$$

which is reduced according to the size of the proportional gain but never zero.

The integral term always results in an overshoot (linear, second order system) due to the integration of error during the period before the output initially reaches the step demand amplitude.

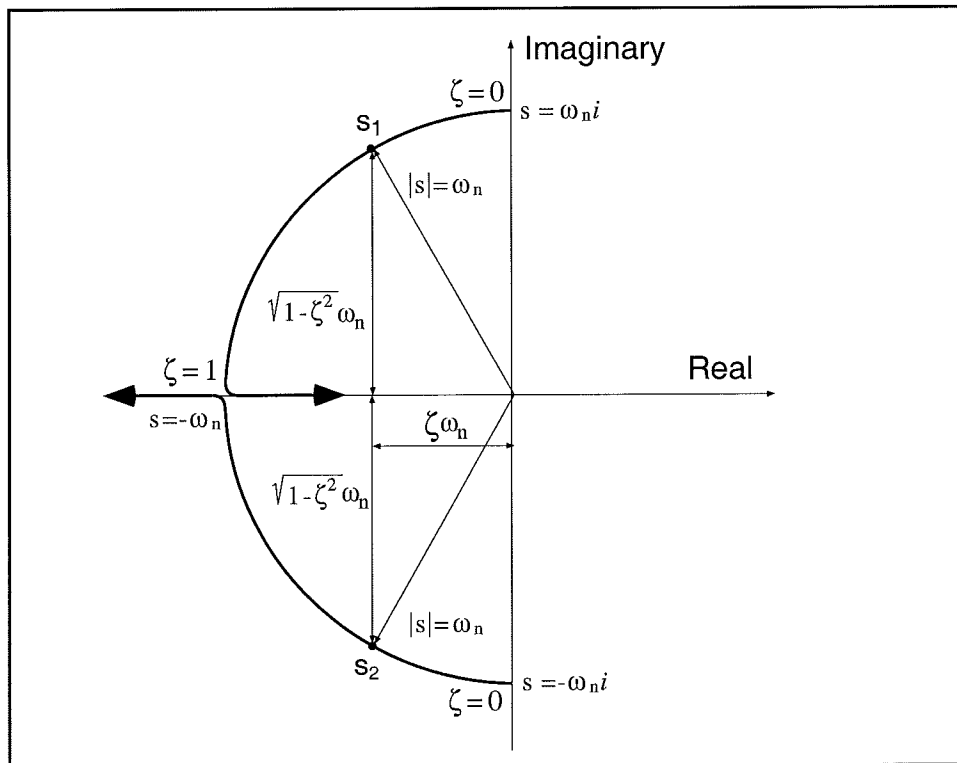


Figure 6.2-4i. Loci of Roots of Second Order Characteristic Equation

<sup>1</sup> It may be useful to point out to students at this point the concept of *static servo* stiffness which is the inverse of the final value of the unit step response of Eq. (6.2-1i). Here, the static servo stiffness is infinite with the integral control term and is  $k_p k_{hw}$  without that term. This topic is further addressed in the next several sections.

**Optional Exercises & Solutions**

A. What are the units of  $k_p k_{hw}$  and  $k_d k_{hw}$ ?

*ans.: N-m/rad and N-m/(rad/s) – same as for a torsional spring and damper respectively.*

B. What are the phase and gain margins under PD control?

*ans.: Gain margin is ideally infinite, however as the ratio  $k_p/k_d$  increases to large values phase margin becomes vanishingly small. In practical systems, there are time delays and nonlinearities which lead to instability when the ratio  $k_p/k_d$  is large. There are also discretization issues which affect the stability of all sampled data systems. For sufficiently large  $T_s$  the associated time delay leads to instability. (Conversely if  $T_s$  is too small, excessive noise is propagated due to numerical differentiation with finite sensor (and numerical processor-internal) quantization. (These topics are addressed in Section 6.8).*

C. Discuss via root locus arguments, the stability of the PID controlled rigid body when  $k_i \neq 0$ . In constructing the loci, assume that  $k_p$ ,  $k_i$  &  $k_d$  all increase proportionally.

*ans.: The locus of roots where  $k_p$ ,  $k_i$  &  $k_d$  all increase proportionally, begins at the triple integrator with one root tending toward  $-\infty$  and the other two toward the roots of  $(s^2 + (k_p/k_d)s + k_i/k_d)$ . The angles of departure of the three loci from the triple pole are 60, 180, and 300 deg and therefore the system is unstable at sufficiently low gains for all relative ratios of  $k_p$ ,  $k_i$  &  $k_d$ . Via the Routh-Hurwitz criterion, the requirement for closed loop stability is  $K_s k_p k_d > k_i$  where  $K_s$  is the system gain  $k_{hw}/J$ . Thus sufficient increase in relative magnitude of  $k_i$  leads to instability.*

D. Determine the sensitivity of the closed loop PD controlled system (assume reverse path  $k_d$ ) to changes in  $J$ . Plot the magnitude of this sensitivity as a function of frequency using the following control gain sets:<sup>1</sup>

$$\begin{aligned} k_p &= 0, & k_d &= 0 \text{ (same as open loop)} \\ k_p &= 0.01, & k_d &= 0.0051 \\ k_p &= 0.1, & k_d &= 0.016 \\ k_p &= 1, & k_d &= 0.051 \end{aligned}$$

Use the classical definition of the sensitivity of some function  $T(\alpha)$  to the parameter  $\alpha$ , i.e.

$$S_{\alpha}^{T(\alpha)} = \frac{d \ln T(\alpha)}{d \ln \alpha} = \frac{d T(\alpha)}{d \alpha} \frac{\alpha}{T} \quad (6.2-4i)$$

How does feedback control effect the sensitivity of the closed loop system to parameter changes? How does the magnitude of the control gains affect the sensitivity?

<sup>1</sup> These values correspond to incremental increases in  $\omega_n$  by  $\sqrt{10}$  with constant damping ratio ( $=1.0$ ) for the parameters used in this manual). The student should be able to show this.

ans.: Applying Eq.(6.2-4i) to Eq.(6.2-2) yields

$$S_J^{c(I)} = \frac{-Js^2}{Js^2 + k_{hw}(k_d s + k_p)} \quad (6.2-5i)$$

The magnitude of  $S_J^{c(I)}(j\omega)$  is plotted for the specified control gains in Figure 6.2-5i. The open loop system has a sensitivity of 1 (0 Db) at all frequencies. The low and medium frequency sensitivity (up to the neighborhood of the closed loop system bandwidth) is reduced by feedback control<sup>1</sup>. The sensitivity is increasingly reduced and brought to higher frequencies with increase in control gain. At frequencies beyond the neighborhood of the closed loop bandwidth sensitivity is unchanged by feedback control. (i.e. the high frequency closed loop attenuation characteristic is essentially the response of the inertia itself rather than that of the control action: hence the sensitivity to changes in  $J$  at these high frequencies is 1.)

### Optional Experiments

#### A. Frequency response phase measurements

The important concept of frequency response phase behavior is easily demonstrated with the experimental system. By exciting the system at a particular frequency<sup>2</sup> and plotting the Commanded Position and Encoder 1 Position data, the phase is found from the expression

$$\phi = -360^\circ \frac{t_{\omega_o}}{t_{\omega_i}} \quad (6.2-4i)$$

where  $t_{\omega_o}$  and  $t_{\omega_i}$  are measured from the data according to Figure 6.2-6i. Typically 10-20 cycles of sinusoidal input is sufficient to establish steady state. The students should “zoom” in to view a cycle of the data near the end of the maneuver. Typical test results for the three PD damping cases are shown in Figure 6.2-7i. These clearly demonstrate the effect of damping ratio on the output phase.

#### B. Tracking and frequency response with $k_d$ in forward vs. return path

It is instructive for students to compare the response of the system to a dynamic input with the derivative control term in the forward and return paths. Shown in Figure 6.2-8i is the response of the critically damped system under these two control types to a ramp input. From the figure it is seen that the return path derivative term results in significant following error but requires only modest control effort (actuator/amplifier power). The derivative in the forward path provides close tracking but requires relatively high peak control effort. These results may be correlated with experimental frequency responses of the two systems where the forward path  $k_d$  system is seen to

<sup>1</sup> It may be brought to students attention that the system bandwidth is typically the “useful” frequency range for practical systems. I.e. it is in this frequency band that sensitivity reduction is usually most important.

<sup>2</sup> The phase measurements may also be made from the frequency response (sine sweep) data but generally yields less accurate results due to the transient behavior associated with the changing input frequency.

have higher bandwidth and a reduced high frequency attenuation of -20 Db/dec. vs. -40 Db/dec. for the return path case.

A useful exercise for students is to find the steady state error ( $e_{ss}$ ) of each system to a ramp input. It is readily shown that

$$e_{ss} \text{ for ramp input with } k_d \text{ in reverse path} = Rk_d/k_p$$

$$e_{ss} \text{ for ramp input with } k_d \text{ in forward path} = 0$$

where  $R$  is the ramp constant.

Note: If forward path  $k_d$  is used, trajectories should not be specified such that they cause excessive control effort. E.g. for sine sweeps, the amplitude should not be greater than 100 counts.

- C. The results described in Optional Exercise C above regarding instability with increased  $k_i$  may be shown by slowly and successively increasing its value and implementing the resulting PID controller on the system. The system will become increasingly oscillatory and then unstable. Be certain that  $k_i$  is increased slowly and that the safety instructions of Section 2.3 are followed strictly during this procedure.

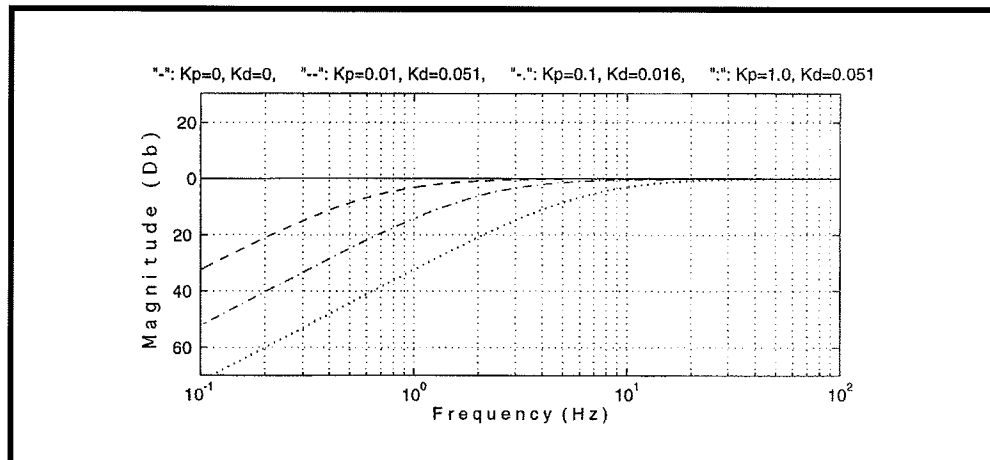


Figure 6.2-5i. Effect of Feedback Gain on Sensitivity To Inertia Changes

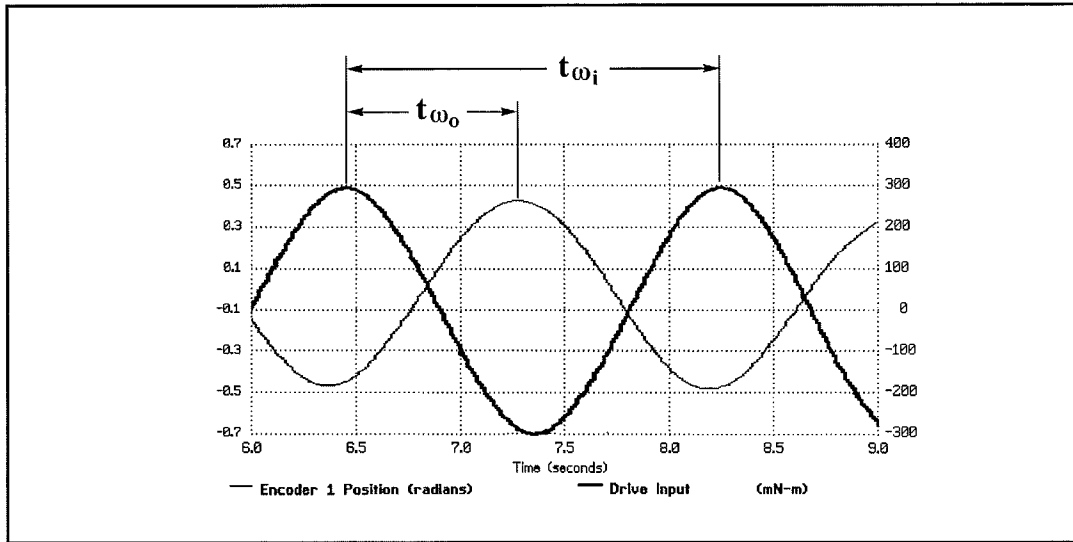


Figure 6.2-6i Phase Measurement Method<sup>1</sup>

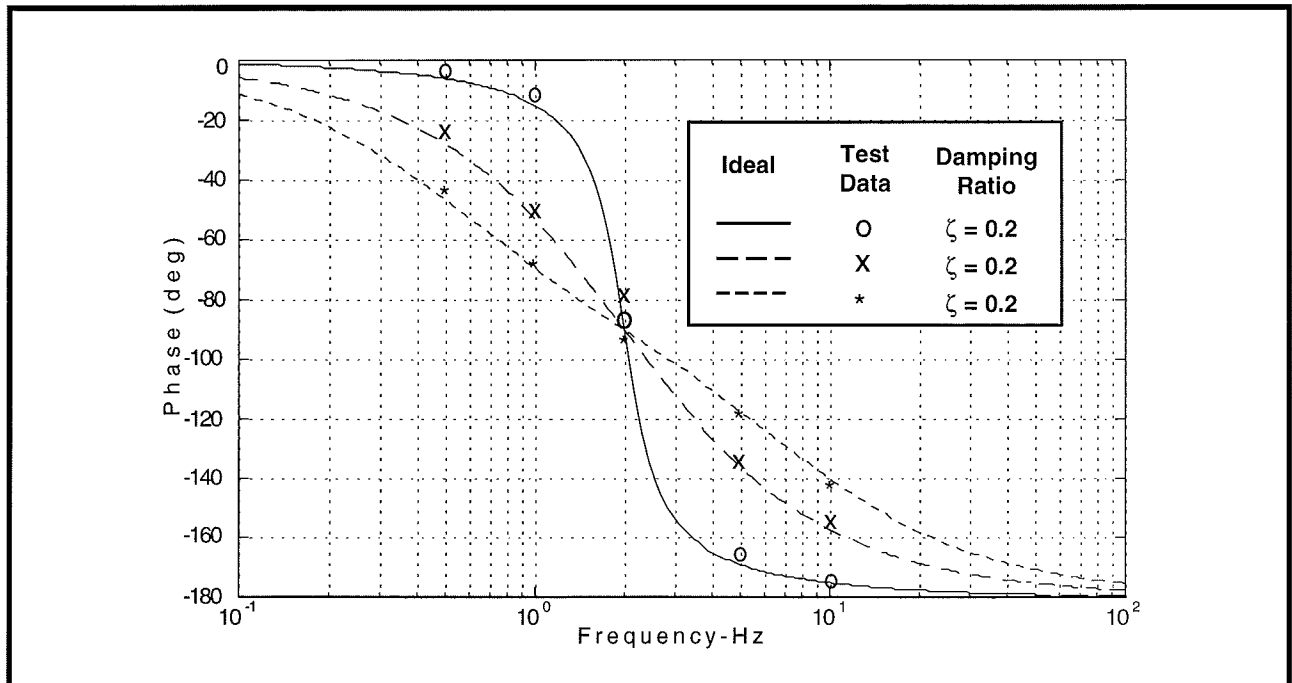


Figure 6.2-7i. Typical Phase Measurement Test Results Show Effect of Damping

<sup>1</sup> See also Eq. (6.2-4i)

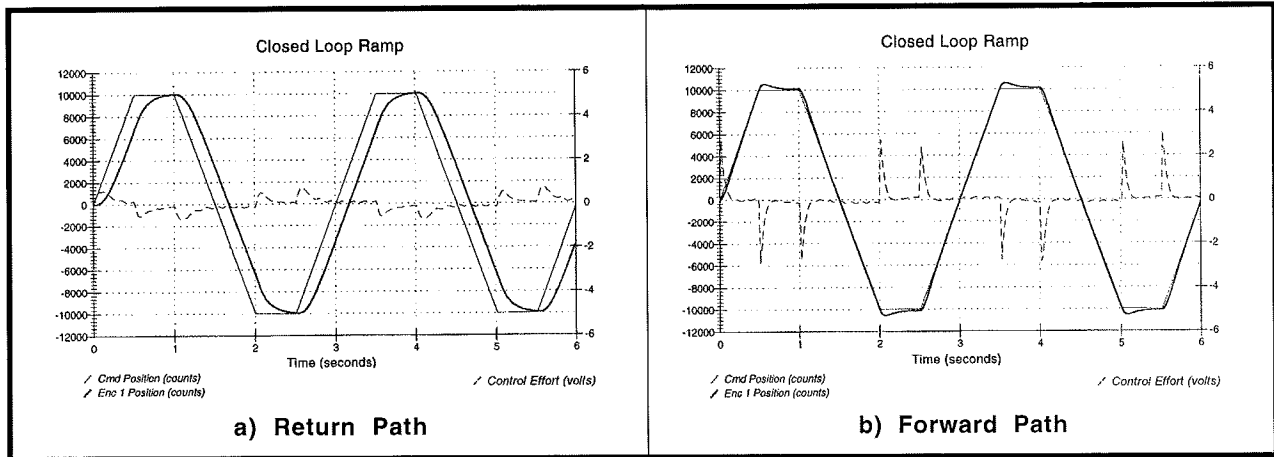


Figure 6.2-8i. Tracking Response Using Forward and Return Path Derivative Terms

**This section showed:**

1. The distinct actions of proportional and derivative control terms and their equivalence to mechanical springs and viscous dampers.
2. The effect of proportional and derivative control terms on the S-plane closed loop roots.
3. Pole Placement PD control design.
4. The effect of integral action and elimination of steady state error. (Static servo stiffness)
5. The characteristic under- critical, and overdamped PD step responses.
6. The frequency response magnitude shapes for the various damping cases and the characteristic low and high frequency gain slopes.
7. The frequency response phase characteristic of second order systems and the effect of damping ratio. (optional experiment)
8. The stability characteristics of the second order PD controlled systems and the effect of adding integral action. (optional exercise)
9. The difference between forward and reverse path derivative control and the effect on tracking performance, frequency response, and required control effort. (optional experiment)
10. Correlation between step (transient, time domain) and sine sweep (frequency domain) characteristics
11. The role of feedback control in reducing sensitivity to parameter changes. (optional exercise)

### 6.3i Disturbance Rejection of Various 1 DOF Controllers

#### Expected Results:

1. In Step 2b: The integral gain is:  $k_i = 2500 * J / k_{hw} = 1.6$  (using the value of  $k_{hw}$  in this manual, actual value may vary)
2. In Step 2c: The filter is:  $F(s) = \frac{6.28 + 5s}{6.28 + s}$
3. The plots of the disturbance effort and encoder 1 response are shown in Figure 6.3-1i. From the plots, it is seen that the PD controller had similar response amplitude at both low and high frequency. The PID system, was effective at attenuating low frequency disturbances, but actually amplified the high frequency one. The PD+lead/lag controller had similar response as the PD system at low frequency, but was effective at attenuating high frequency disturbance.

#### Answers to Questions

A. The open loop transfer functions for Controllers "a" and "b" are<sup>1</sup>:

$$\begin{aligned} \frac{N_{ol}(s)}{D_{ol}(s)} &= \frac{k_d s^2 + k_p s + k_i}{s} \frac{k_{hw}}{J s^2} && (6.3-1i) \\ &= \frac{1600(0.016s + 0.10)}{s^2} && \text{(Controller "a")} \\ &= \frac{1600(0.016s^2 + 0.10s + 1.6)}{s^3} && \text{(Controller "b")} \end{aligned}$$

For Controller "c", the expression is:

$$\begin{aligned} \frac{N_{ol}(s)}{D_{ol}(s)} &= (k_d s + k_p) \frac{N_f(s)}{D_f(s)} \frac{k_{hw}}{m s^2} && (6.3-2i) \\ &= \frac{1600(0.016s + 0.10)(5s + 6.28)}{s^2(s + 6.28)} \end{aligned}$$

For the closed loop expressions,  $\theta_1(s)/T_d(s)$ :

Controllers "a" & "b":

$$\frac{x_1(s)}{T_d(s)} = \frac{s}{J s^3 + k_{hw}(k_d s^2 + k_p s + k_i)} \quad (6.3-3i)$$

<sup>1</sup> These may vary according to a particular system's  $k_{hw}$ .



$$= \frac{91.7}{s^2 + 1600(0.016s + 0.10)} \quad (\text{Controller "a"})$$

$$= \frac{91.7s}{s^3 + 1600(0.016s^2 + 0.10s + 1.6)} \quad (\text{Controller "b"})$$

Controller "c":

$$\begin{aligned} \frac{\theta_1(s)}{T_d(s)} &= \frac{D_f(s)}{Js^2D_f(s) + k_{hw}(k_d s + k_p)N_f(s)} && (6.3-4i) \\ &= \frac{91.7(s + 6.28)}{s^3 + 134s^2 + 961s + 1005} \end{aligned}$$

- B. The Bode magnitude of the above transfer functions is given in Figure 6.3-2i. The correlation between the closed loop gain and the experimentally obtained disturbance attenuation at the two test frequencies is clear. The integrator in controller "b" provides large low frequency attenuation but has a high gain peak between one and two Hz making it ineffective at these frequencies. The lead-lag filter made no improvement over the PD controller at very low frequencies but was effective in the higher frequencies as predicted in the closed loop Bode response.

The correlation between the open and closed loop gains is also clear. The integrator is manifested as the -60 db/dec. low frequency slope and provides complete static disturbance attenuation (zero DC gain) in the closed loop. The low open loop gain slope near crossover correlates (significant phase lag also exists at this frequency) with the closed loop resonance near two Hz. The added gain from the lead-lag filter for frequencies beyond 0.1 Hz yields higher frequency attenuation in the closed loop.

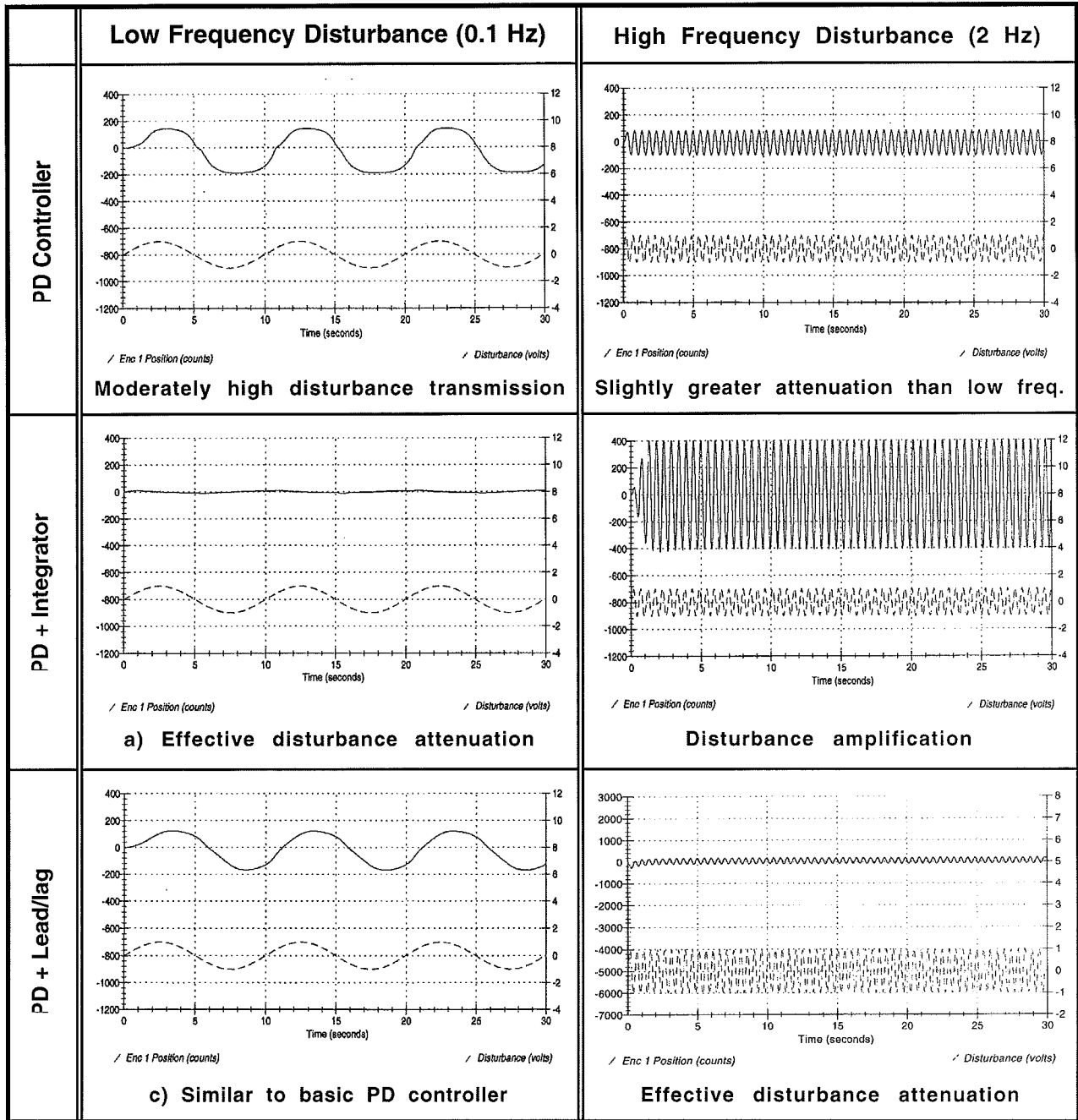
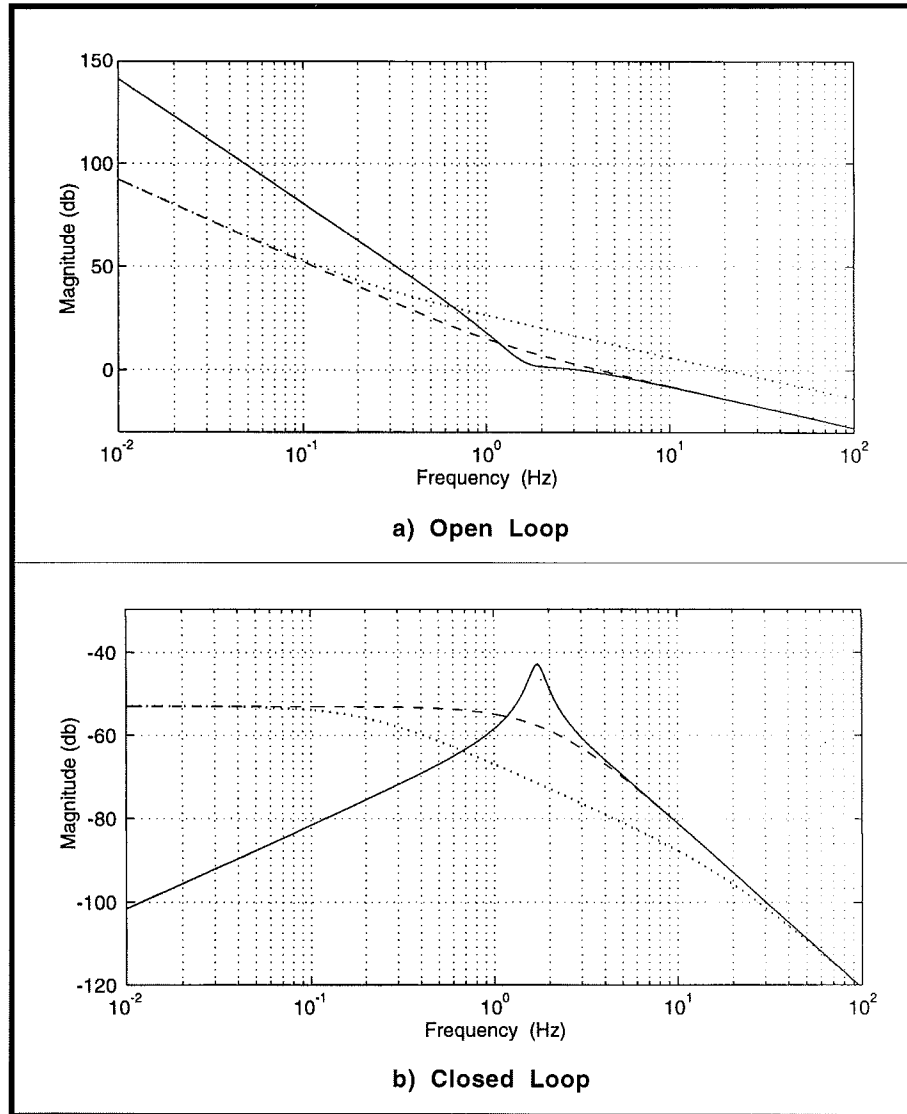


Figure 6.3-1i Experimental Results Show Frequency Dependence of Disturbance Attenuation For Three Controllers



**Figure 6.3-2i Transfer Functions of Disturbance to Output Give Underlying Basis For Experimental Results**

**This section showed:**

1. An integrator in the controller can be an effective way to attenuate disturbances at low frequencies due to the attendant infinite DC gain. It can however be deleterious for higher frequency disturbance attenuation.
2. Providing high open loop gain in the expected disturbance frequency band of interest is an effective attenuation approach (subject of course to the requirement for closed loop stability).
3. Disturbance attenuation properties may generally be predicted from the open loop frequency response. (The open loop frequency response also of course indicates other important properties such as bandwidth, stability, sensitivity to parameter changes and static stiffness.)

**6.4i Collocated PD Control With 2 DOF Plant**

This experiment illustrates the affect of dynamic coupling on the plant, characteristic differences between collocated and noncollocated dynamics, and the inherent controllability difficulties in the use of a collocated scheme when point of objective control is not at the sensor/actuator collocation.

Expected Results:

- 1) Step responses at  $\theta_1$  and  $\theta_2$  in Step 3 are shown in Figure 6.4-1ia where  $k_p = 1.0$ ,  $k_d = .09$  were selected.
- 2) In Step 4, the predominant feature in  $\theta_2$  is the lightly damped oscillation @ roughly 1.8 Hz. The relatively high PD gains have brought the closed loop poles very near the collocated zeros (roots of  $N_1(s)$ ); thus the oscillations are largely attenuated in  $\theta_1$ .
- 3) Step responses at  $\theta_2$  in Step 5 are shown in Figure 6.4-1ib where  $k_p = .06$ ,  $k_d = 0.015$  were selected. Here the oscillations in  $\theta_2$  are less severe than in the high gain case, but the response at  $\theta_1$  is much slower. Both disks have less static stiffness, and hence greater steady state error, than those of the higher gain controller of Step 3.

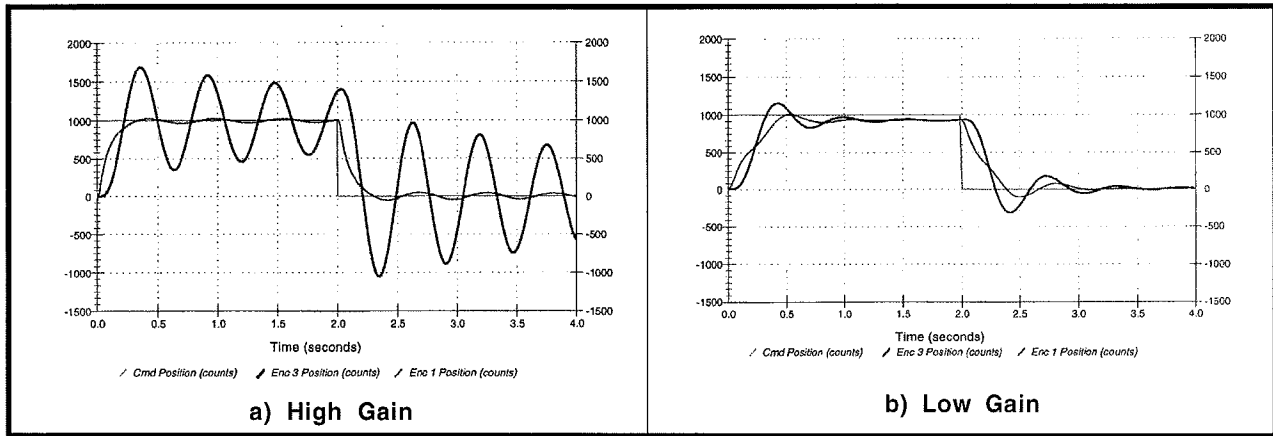


Figure 6.4-1i. Step Responses At  $\theta_1$  and  $\theta_2$  (Steps 3 & 5)

**Answers to Questions**

A. The closed loop poles for the gains above are roughly  $\{-21, -2.0, -0.05 \pm 1.8i\}$  (Hz, from Step 3), and  $\{-1.4 \pm 0.3i, -0.5 \pm 1.9i\}$  (Hz, Step 5). The closed loop zeros are identical to the open loop ones with the additional zero at  $-k_p/k_d$ . The high PD gains in Step 3 have brought the closed loop poles very near the lightly damped collocated zeros. This pole pair is not canceled in the  $\theta_2$  output. To reduce the oscillatory response, the proportional gain must be greatly decreased resulting in the more damped poles in Step 5. The oscillations are also reduced by the slower system response due to the lower frequency real poles. (The system begins to attenuate below the complex pole frequency so that the oscillatory mode is not well excited - see Figure 6.4-6i.) A view of the root loci of this system for various ratios  $k_d/k_p$  is shown in Figure 6.4-2i. Notice that the poles remain close to the imaginary axis for high and low values of  $k_d/k_p$ .

B. The transfer function is

$$\frac{\theta_2(s)}{r(s)} = \frac{(k_p + k_d s) k_{hw} N_2 / D(s)}{1 + (k_p + k_d s) k_{hw} N_1(s) / D(s)} \quad (6.4-1i)$$

The Nyquist plot is shown in Figure 6.4-3i<sup>1</sup>. As can be seen in the figure, the phase margin for both systems is roughly 60 degrees. The gain margin is infinite in both cases. Because the denominator is unchanged by the choice of output location, the stability margins are identical for  $\theta_1(s)/r(s)$ . (It is worth mentioning to the students that in practical systems there are issues such as sensor phase lag and sampling delays that eventually lead to instability at sufficiently high gain. There are also issues such as drive saturation and noise propagation that limit the practical bandwidth. See Section 6.8.)

<sup>1</sup> The “loops” in the figure are associated with the resonant poles and zeros.

C. Static servo stiffness is

$$T_{d1}/\theta_1 = k_p k_{hw} \text{ (N-m/rad)} \tag{6.4-2i}$$

The static servo stiffness at  $\theta_1$  couples in series with the torsional spring and reduces the effective stiffness at  $\theta_2$  according to:

$$T_{d2}/\theta_2 = (k_p k_{hw})k_I / (k_p k_{hw} + k_I) \tag{6.4-3i}$$

With integral action, the static servo stiffness is infinite, and the stiffness at  $\theta_2$  in this case is  $k_I$ .

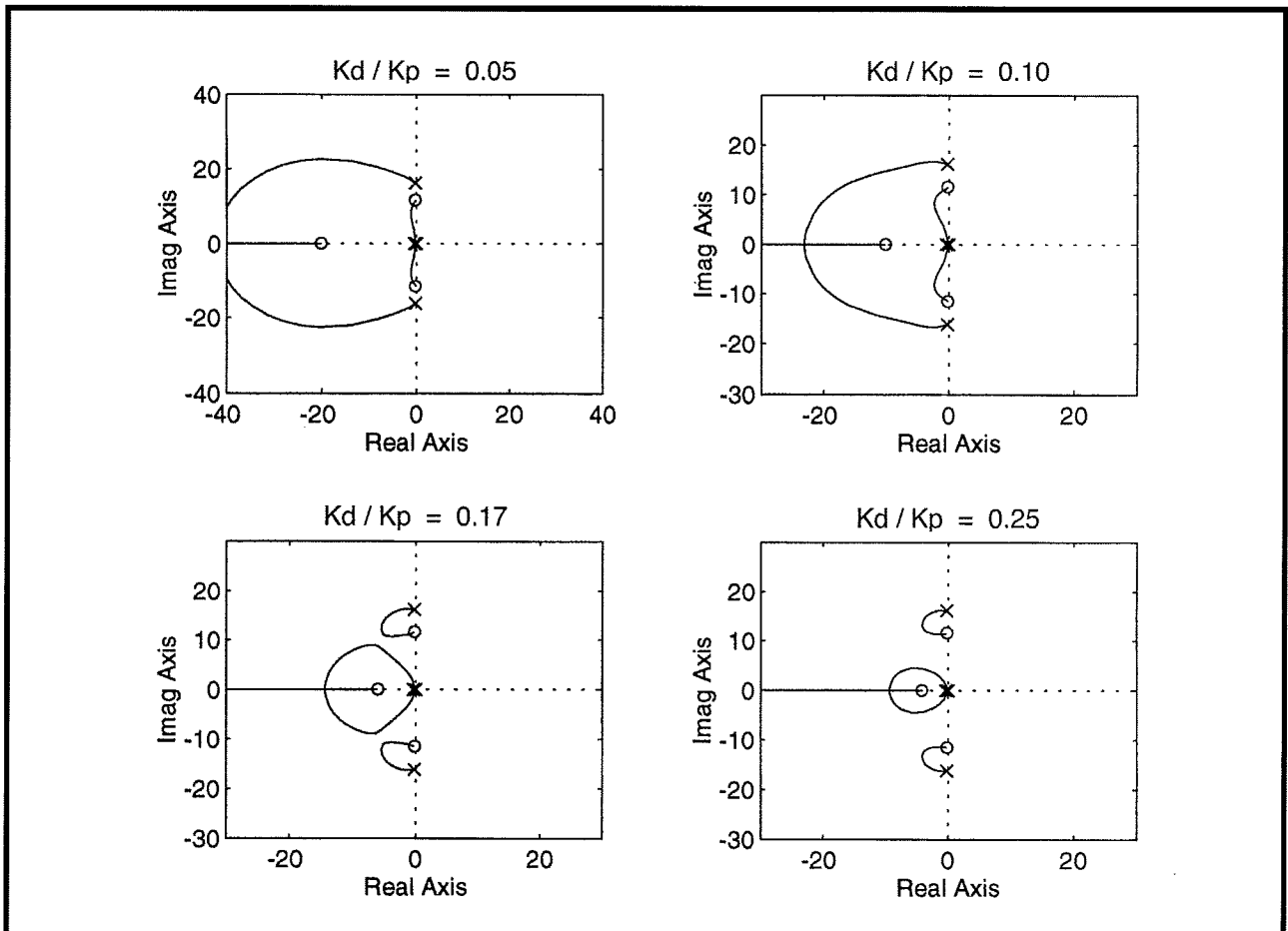


Figure 6.4-2i. Root Loci For Various  $k_d/k_p$

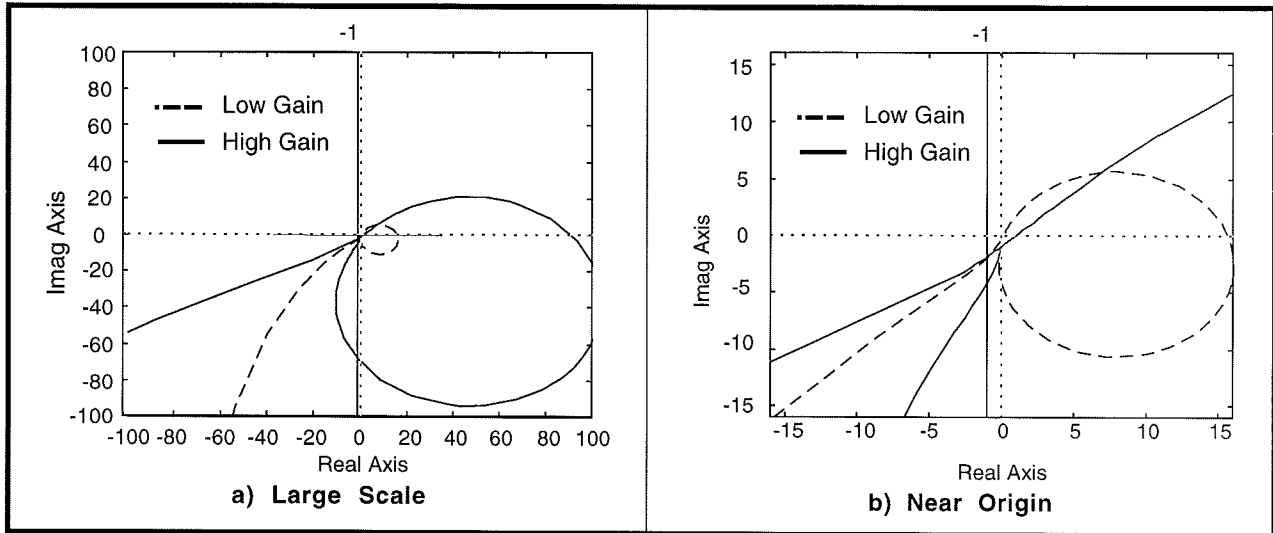


Figure 6.4-3i. Nyquist Plots Show Large Phase Margins and Infinite Gain Margins

**Optional Exercise & Solution**

A. Determine the sensitivity of the open loop transfer functions at the collocation and noncollocation ( $\theta_1(s)/T(s)$  and  $\theta_2(s)/T(s)$  respectively) to changes in  $J_1$  and  $J_2$ . Determine the sensitivity of the closed loop PD controlled system  $\theta_2(s)/r(s)$  of this experiment under low and high gain. Plot the magnitude of the sensitivity as a function of frequency for each case. Discuss the physical reasons for the salient features of the curves by considering the behavior of the respective transfer functions at low, medium (i.e. near pole or zero frequencies or system bandwidth), and high frequency.

*ans.:*

Open Loop:

Applying Eq.(6.2-4i) to Eq's.(5.1-4,-5) with  $k_1=k, k_2=0$  yields

$$S_{J_1}^{(Col(J_1))collocated} = \frac{-J_1(J_2s^4+c_2s^3+ks^2)}{D(s)} \tag{6.4-4i}$$

$$S_{J_2}^{(Col(J_2))collocated} = \frac{J_2(s^2D(s)-k_{hw}N_1(s)(J_1s^4+c_1s^3+ks^2))}{D(s)} \tag{6.4-5i}$$

at the collocation and

$$S_{J_1}^{(Col(J_1))noncollocated} = \frac{-J_1(J_2s^4+c_2s^3+ks^2)}{D(s)} \tag{6.4-6i}$$

$$S_{J_2}^{(c_{o1}(J_2))_{\text{noncollocated}}} = \frac{-J_2(J_1 s^4 + c_1 s^3 + k s^2)}{D(s)} \quad (6.4-7i)$$

at  $\theta_2$ . The magnitude for each of these as a function of frequency for the parameter values Section 6.1i is shown in Figures 6.4-4i.

At the collocation, the open loop sensitivity to both inertias is low at low frequency. Here the magnitude is governed by friction (i.e. it responds approximately as  $1/((c_1+c_2)\omega)$ ). At the zero in  $N_1(s)$  ( $\triangleq \omega_z$ ), the plant is highly sensitive to  $J_2$  ( $\omega_z = \sqrt{k/J_2}$ ), but is insensitive to  $J_1$  (because  $J_1$  is motionless at this frequency). At the pole frequency ( $\triangleq \omega_p$ ), the collocated plant is sensitive to both  $J_1$  and  $J_2$  (because  $\omega_p$  is strongly dependent on them). At high frequencies the plant becomes insensitive to  $J_2$  but has a sensitivity of 1 to  $J_1$  (because the response approaches that of  $1/J_1\omega^2$ ).

At the noncollocation, the open loop sensitivity to  $J_1$  is the same as for the collocated case. This is because  $J_1$  only appears in  $D(s)$  which is common for both locations. The physical reasons given for the shape of  $S_{J_1}^{(J_2)}(j\omega)$  above apply here as well. For our specific parameter set, ( $J_1 \approx J_2$ ;  $c_1, c_2$  small) and the symmetry of the particular plant configuration results in the sensitivities to both inertias being of nearly identical shape.

As for a physical interpretation of  $S_{J_2}^{(J_1)}(j\omega)$ , the sensitivity of the system pole  $\omega_p$  to  $J_2$  follows from the arguments above. The insensitivity at  $\omega_z$  is more subtle. Here, the zero in the sensitivity expression is dependent on  $J_1$  (not  $J_2$ )<sup>1</sup> and its occurrence very near  $\omega_z$  is an artifact of the particular parametric symmetry of the plant. For clarity we'll call this insensitive root  $\omega_{z\alpha}$ . Now, the plant can be factored as

$$\frac{\theta_2(s)}{T(s)} = \frac{k_{hw}k}{J_2(J_1 s^2 + c_1 s + k)s^2 + (c_2 J_1)s^3 + (J_1(k) + c_1 c_2)s^2 + (c_1 + c_2)ks} \quad (6.4-8i)$$

For low friction, the first term in the denominator of Eq.(6.4-8i) approaches zero at  $s = j\omega_{z\alpha}$ . Neglecting friction, the plant with output at  $\theta_2$  behaves as

$$\frac{\theta_2(\omega_{z\alpha})}{T(\omega_{z\alpha})} = \frac{k_{hw}k}{J_1 \omega_{z\alpha}^2} \quad (6.4-9i)$$

i.e. as a rigid body of inertia  $J_1$  at the frequency  $\omega_{z\alpha}$ . Physically, the motion at  $J_1$  is the superposition of its responses to the drive torque  $T(\omega_{z\alpha})$  and the spring torque (caused the relative displacement between  $\theta_2$  and  $\theta_1$ ) which we'll define as  $T^*(s)$ .

<sup>1</sup> Whereas  $\omega_z$  is dependent on  $J_2$  not  $J_1$ .



Now observe that  $T^*$  also acts equally and oppositely on  $J_2$  and that  $\omega_{z\alpha}$  is a zero of the transfer function  $\theta_2/T^*$ .<sup>1</sup>  $J_2$ , therefore does not follow the motion at  $\theta_1$  associated with the spring displacement, but only the motion associated with  $T(\omega_{z\alpha})$ . Its response is then that of  $J_1$  if it were acted on by  $T(\omega_{z\alpha})$  only, i.e., that given by Eq.(6.4-9i).

Closed Loop

The closed loop sensitivities at  $\theta_2$  are as follows

$$S_{J_1}^{(ccl(J_1))noncollocated} = \frac{-J_1(J_2s^4 + c_2s^3 + ks^2)}{D(s) + (k_d s + k_p)k_{hw}N_1(s)} \tag{6.4-10i}$$

$$S_{J_2}^{(ccl(J_2))noncollocated} = \frac{-J_2(J_1s^4 + (c_1 + k_d k_{hw})s^3 + (k + k_p k_{hw})s^2)}{D(s) + (k_d s + k_p)k_{hw}N_1(s)} \tag{6.4-11i}$$

Their magnitude as a function of frequency is shown in Figure 6.4-5i for the low and high gain collocated control of this section. Under low gain, the sensitivity to  $J_1$  and  $J_2$  at the open loop resonance is damped and there is an amplification of sensitivity at the lightly damped closed loop pole. Under high gain control, the sensitivity to  $J_1$  is reduced, but to  $J_2$  is essentially unchanged except at the resonant pole where it is increased by nearly 10x. In both cases, the feedback control has generally reduced sensitivity at frequencies below the system bandwidth. At low frequencies the respective sensitivities behave as  $J_1s^2/k_pk_{hw}$  and  $J_2(k + k_pk_{hw})s^2/kk_pk_{hw}$ .

Sensitivity to inertia changes is easily demonstrated by changing inertias and obtaining the characteristic experimental responses (e.g. step and sine sweep). See Section 6.9.

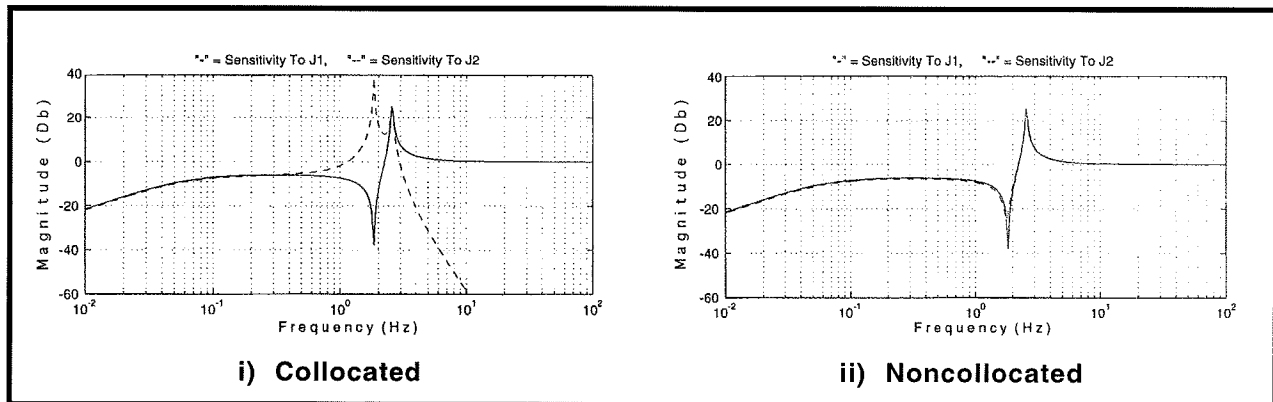


Figure 6.4-4i Sensitivity of Open Loop Plant To Inertia Changes

<sup>1</sup> And hence  $\theta_2/T^*$  is insensitive to  $J_2$ .

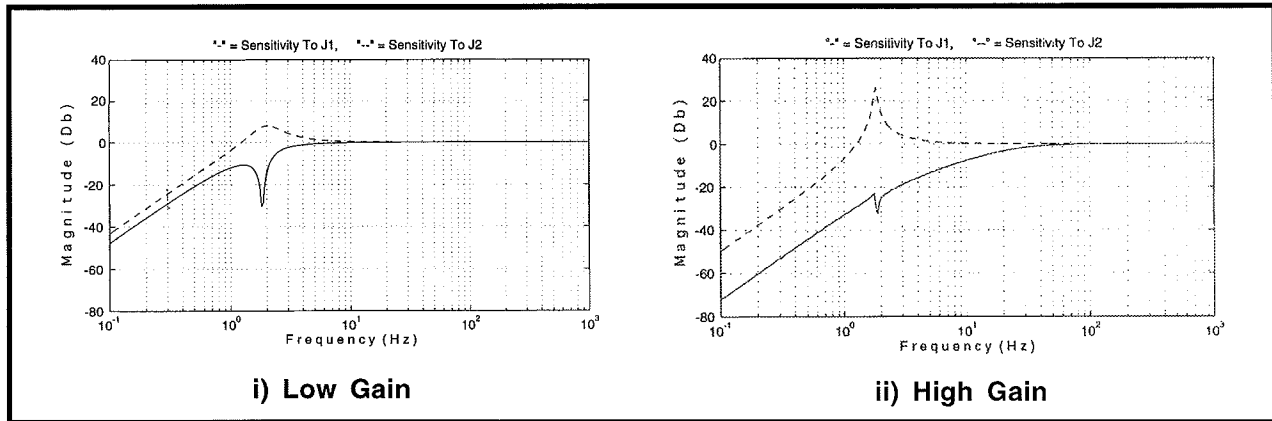


Figure 6.4-5i Sensitivity To Inertia Changes at  $\theta_2$  Under Collocated PD Control

### Optional Experiments

#### A. Frequency response measurements

It is illustrative to demonstrate frequency response behavior via sine sweeps of the closed (& open) loop systems. Shown in Figure 6.4-6ia is the output at  $\theta_1$  and  $\theta_2$  with sweep frequency of 0.1 to 10 Hz and 100 count amplitude for the high gain PD controller from Step 3. Note the flat shape (near pole-zero cancellation) of the collocated response, and the resonance in the noncollocated one. This corresponds to the much larger oscillation in the  $\theta_2$  step response than that of  $\theta_1$ . With the lower gain controller (Figure 6.4-6ib), the resonance is much less pronounced.<sup>1</sup> The corresponding step response oscillations are attenuated both because poles become more damped and the system bandwidth rolls off ahead of these poles. Note: Here and in subsequent sine sweep plots, the “Remove DC Bias” plotting option should be selected for  $\theta_2$  to minimize distortion of the very low amplitude shape at high frequency.

Other properties of discrete multi-DOF flexible structures and other high order, systems are visible from the plots, namely: flat low frequency response (type 0 system), the collocated plant zero - unaffected by closed loop control, the high frequency attenuation of -40 Db/decade<sup>2</sup> (2 pole excess) at the collocation and -80 Db/decade (4 pole excess) at the first noncollocation.

#### B. Tracking Response to Sawtooth (Ramp) Input

Shown in Figure 6.4-7ia are the  $\theta_1$  and  $\theta_2$  responses to a 10,000 count, 10,000 count/sec ramp trajectory (2 rep's) for the controller in Step 3 (Note that depending on the gains selected, this trajectory could cause a software limit to guard against over-deflection of the torsional shaft. If so, the ramp rate should be reduced.) Note the relatively good tracking at the collocation and poor tracking with large overshoot in the noncollocated output. The noncollocated response for the softer control of Step 5

<sup>1</sup> In Figure 6.4-6ib the input amplitude was increased to 200 counts to offset the effects of friction at low frequency for this low gain controller.

<sup>2</sup> The -40dB/decade asymptote was not approached at the frequencies tested in the high gain collocated case.

(Figure 6.4-7ib) shows even greater phase lag, but a generally better behaved (albeit still relatively poor) response at  $\theta_2$ .

C. Stability Margins

Comparison of the stability margins in this and the next section is also a very useful exercise. Generally speaking, the phase and margins of collocated control can be made greater than those for noncollocated control, but have poorer performance at the noncollocation (outer disk). As shown in Fig. 6.4-2i above, the closed loop roots stay in the LHP for all values of  $k_p$  and  $k_d$ . Phase margin may become small in the higher gain cases however and instability may result from unmodeled phase lags.

D. Control Effort

In all experiments, it is insightful to consider control effort and to examine the price paid in power consumption and component size (i.e. cost) in providing high gain tracking. In some cases the effects of DAC saturation are also evident.

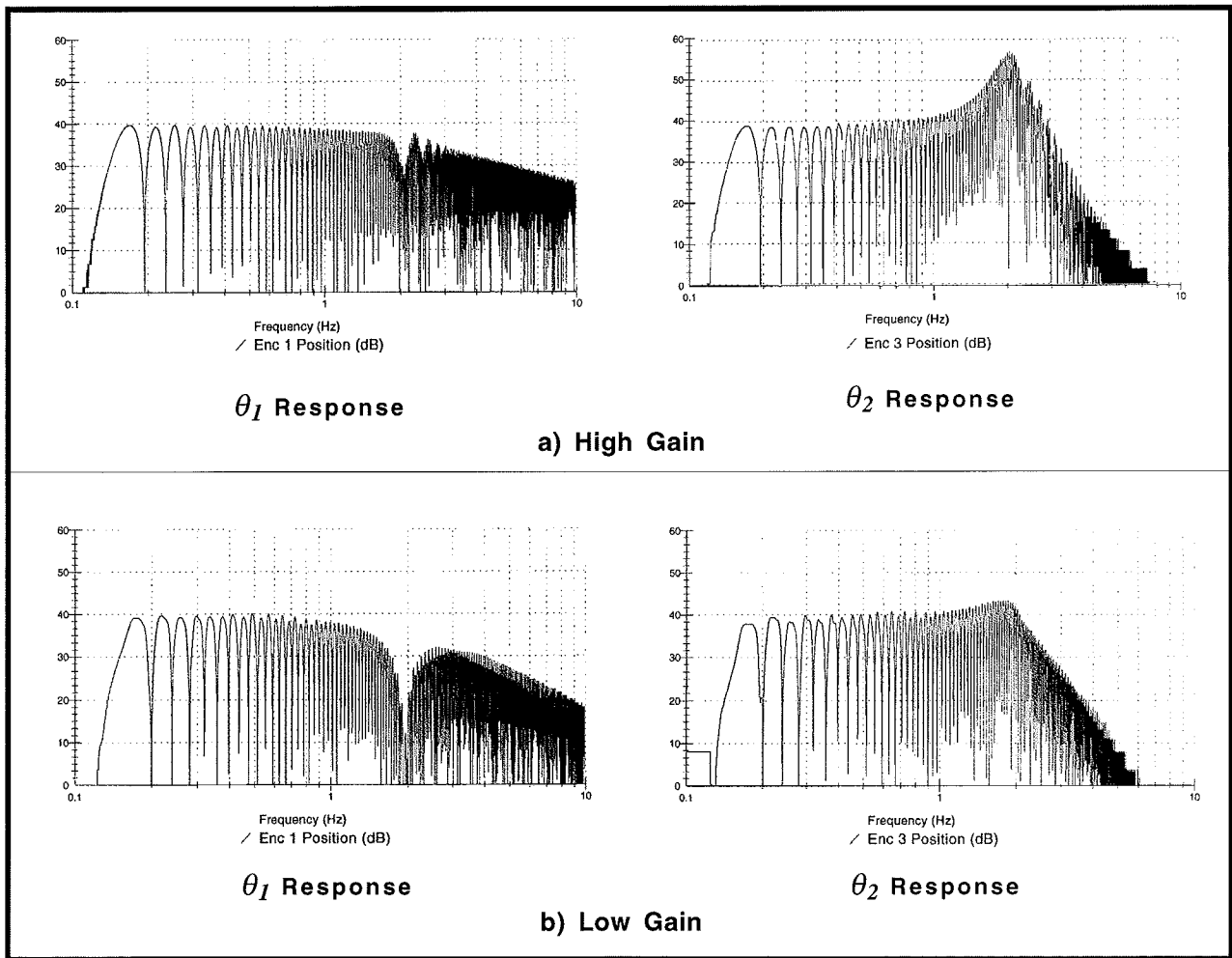


Figure 6.4-6i Sine Sweep Test Data

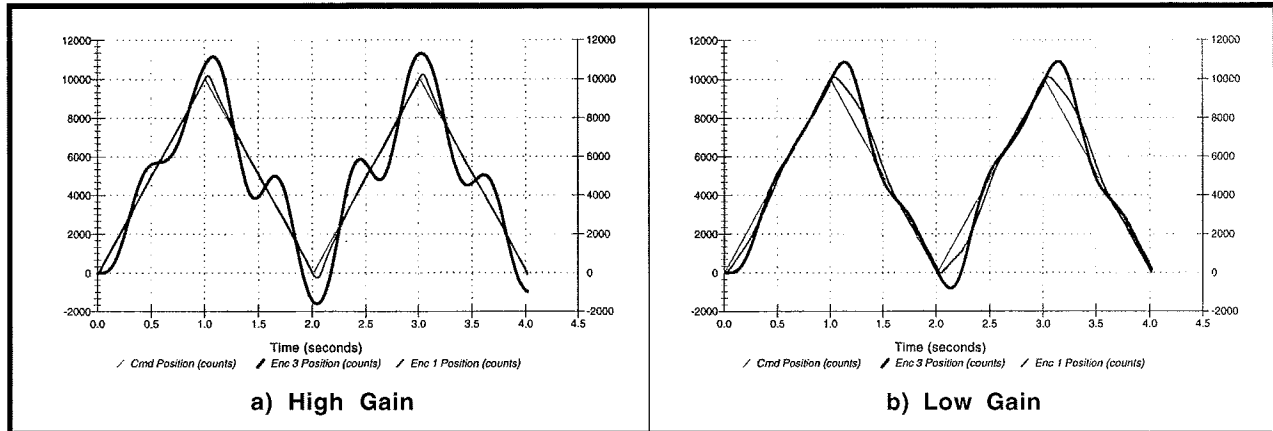


Figure 6.4-7i. Ramp Following At  $\theta_1$  and  $\theta_2$

### This section showed:

With respect to low order collocated control:

1. High gain control may be effective for flexible systems where the control objective is at the actuator location ( $\theta_1$ ); but may be largely ineffective for control of the noncollocation ( $\theta_2$ ) due to flexible plant oscillations.
2. Plant oscillations may be damped via lower gain control, but at the expense of collocated performance and system stiffness.
3. The static stiffness at the collocation is the same as that of a rigid body. At the noncollocation, it is equal to the collocated static servo stiffness in series with the structural (the torsion rod in this case) stiffness .
4. Collocated PD control is ideally stable for all gains but has lightly damped closed loop poles at both low and high gain.
5. The high gain system frequency response is well flattened at the collocated output but has a sharp resonance at  $\theta_2$ . This correlates with the step and ramp responses at these outputs. The low gain frequency response has lower bandwidth and reduced resonance at  $\theta_2$  corresponding to slower tracking but with less oscillation. (optional exercise)
6. The plant sensitivity to inertia changes is relatively high at low to mid frequencies, and particularly large at the resonant poles and zeros. Closed loop collocated control generally lowers the low-mid frequency sensitivity but can result in relatively high sensitivity to changes in  $J_2$  under high control gains. (optional exercise)

**6.5i Noncollocated PD + Notch filter.**

This experiment illustrates an approach often used in noncollocated structural control where a collocated rate feedback loop is first closed to improve plant stability. An outer loop is then closed about the location where control is desired. This approach generally yields superior performance over purely collocated schemes in cases with significant structural flexibility.

Expected Results:

- 1) The root locus of the plant given in Eq (6.1-3i) is shown in Figure 6.5-1i where  $k_v = 0.010$  is selected as providing the greatest damping.

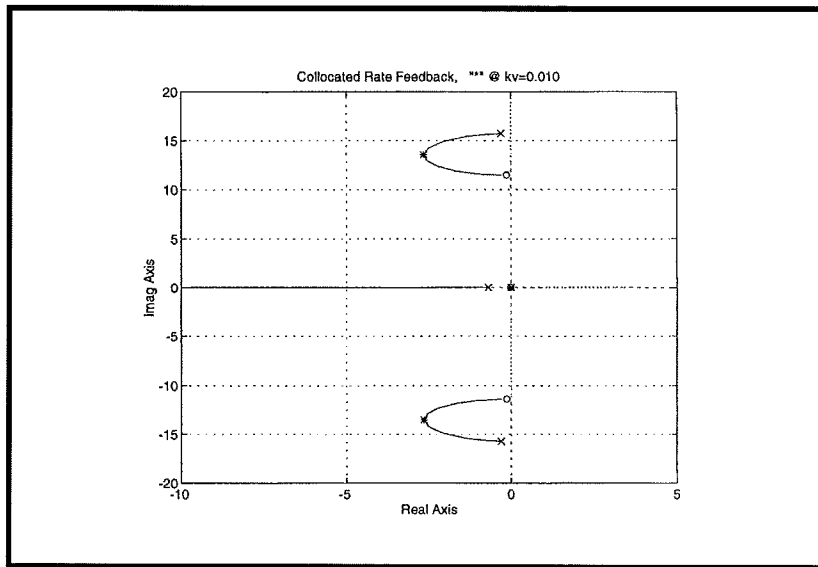


**Figure 6.5-1i. Collocated Rate Feedback Root Locus**

- 2) In Step 5, a step response for  $k_p=0.06$ ,  $k_d=0.001$  is shown in Figure 6.5-2i. The steady state error here is comparatively high and is similar to the low gain collocated PD control design.

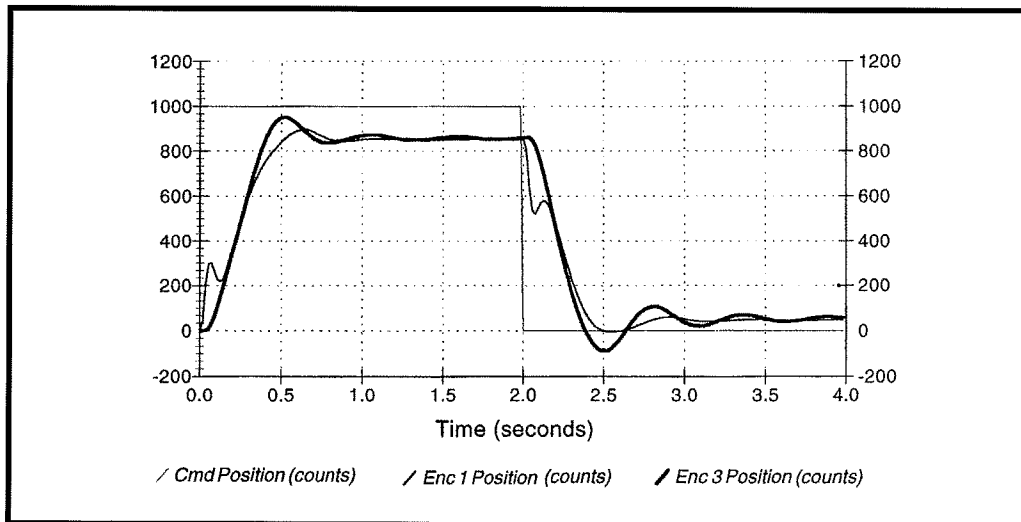


**Figure 6.5-2i. Step Response At  $\theta_1$  and  $\theta_2$**

**Answers to Questions**

A. Expected values (consistent with others in this manual) are approximately:

$$k_v = 0.01$$

$$N_n = 1,333,000 ((s+2.91)^2 + 13.3^2)$$

$$D_n = ((s+44.4)^2 + 44.4^2)((s+177)^2 + 177^2)$$

A response meeting the performance specification (see Figure 6.5-2i) was found using:

$$k_p = 0.06, k_d = 0.001$$

B. The specified transfer function is

$$\frac{\theta_2(s)}{r(s)} = \frac{k_p k_{hw} N_2 N_n(s) / D_n(s) D^*(s)}{1 + (k_p + k_d s) k_{hw} N_2 N_n(s) / D_n(s) D^*(s)} \quad (6.5-1i)$$

The open loop Bode plot is shown in Figure 6.5-3i. As can be seen in the figure, the phase margin is roughly 60 degrees and the gain margin is approximately 20 Db. (It is worth mentioning to the students that in practical systems there are unmodeled effects such as sensor phase lag and sampling delays that eventually lead to instability at sufficiently high gain. There are also issues such as drive saturation and noise propagation that limit the practical bandwidth. See Section 6.8.

C. The static stiffnesses are readily found by referring to the static system diagram of Figure 6.4-4i. At equilibrium and in the absence of static friction, the drive torque  $T_u$  is equal and opposite to the disturbance torque regardless of which inertia the disturbance acts on. We also have that

$$\text{for disturbances at } J_1: \theta_2 = \theta_1 \quad (6.5-2i)$$

$$\text{for disturbances at } J_2: \theta_2 = \theta_1 + T_{d2}/k \quad (6.5-3i)$$

where  $k$  is the spring constant. From these, we have the static stiffness expressions<sup>1</sup> and their values for the parameters listed above:

$$\frac{T_{d1}}{\theta_1} = \frac{T_{d1}}{\theta_2} = k_p k_{hw} \frac{n_0}{d_0} = k_p k_{hw} \quad (= 1.0 \text{ N-m/rad}) \quad (6.5-4i)$$

$$\frac{T_{d2}}{\theta_1} = k_p k_{hw} \frac{n_0 k}{d_0 k - k_p k_{hw} n_0} = k_p k_{hw} \frac{k}{k - k_p k_{hw}} \quad (= 4.4 \text{ N-m/rad}) \quad (6.5-5i)$$

$$\frac{T_{d2}}{\theta_2} = k_p k_{hw} \frac{n_0}{d_0} = k_p k_{hw} \quad (= 1.0 \text{ N-m/rad}) \quad (6.5-6i)$$

<sup>1</sup> Note that the notch filter has unity gain as specified in the student's section.

Because the control effort and the disturbance both act on  $J_1$  when the disturbance is at the lower disk, no torque is acting on  $\theta_2$  at equilibrium; ideally then  $\theta_2$  follows  $\theta_1$  exactly (Eq. 6.5-2i). In the case of disturbances at the upper disk, a differential displacement of the upper disk occurs due to the shaft compliance (Eq. 6.5-3i). Since the static control gains act on  $\theta_2$  only for this scheme, the upper disk stiffnesses for torques at the upper and lower disk are identical. Eq. (6.5-5i) shows that the lower disk will undergo reverse motion in response to disturbances on the upper disk whenever  $k_p k_{hw} > k$ , i.e. whenever the outer loop proportional gain is higher than the spring constant.

The stiffness  $T_{d1}/\theta_1 = k_p k_{hw}$  is the same expression as for the collocated PD case. The stiffness  $T_{d2}/\theta_2$  is reduced in the collocated case (see Eq. 6.4-3i) because the torsional spring acts in series with the proportional control action. Because the gain here is similar to that of the low gain collocated PD design, and because the proportional term in that design is smaller than the spring constant the steady state errors at  $\theta_1$  and  $\theta_2$  are expected to be of similar magnitude (and relatively high) for these two designs.

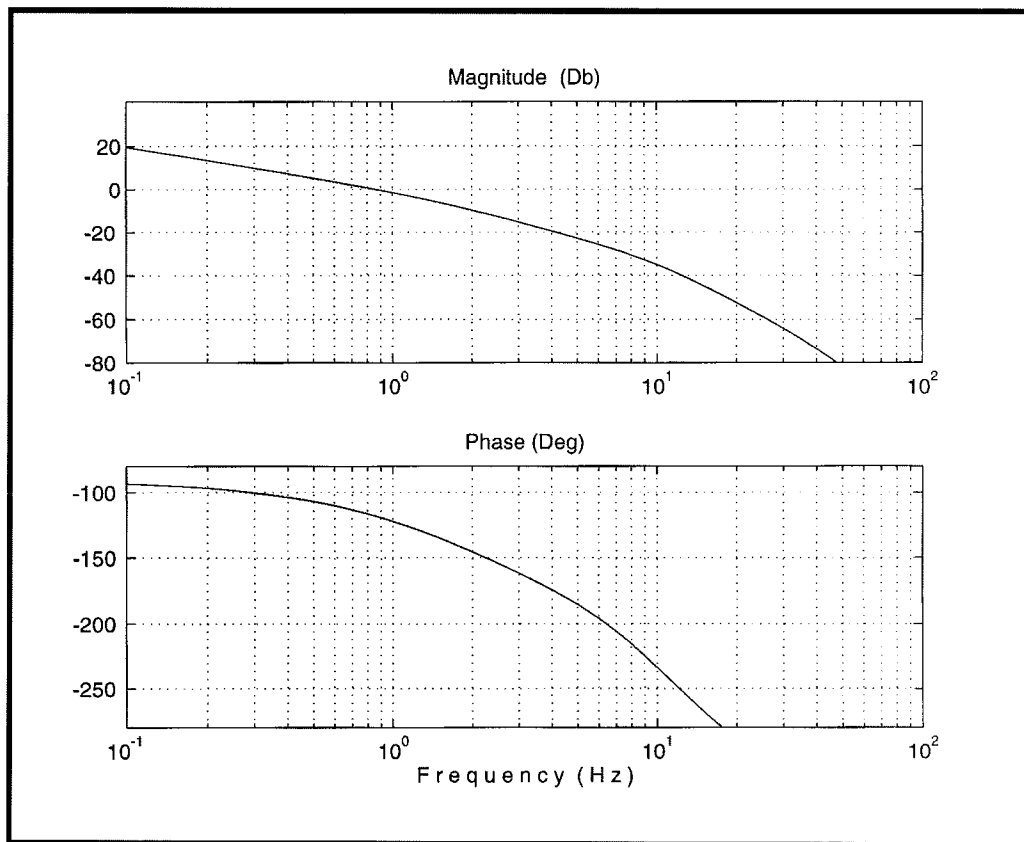


Figure 6.5-3i. Open loop Bode Plot For Stability Analysis

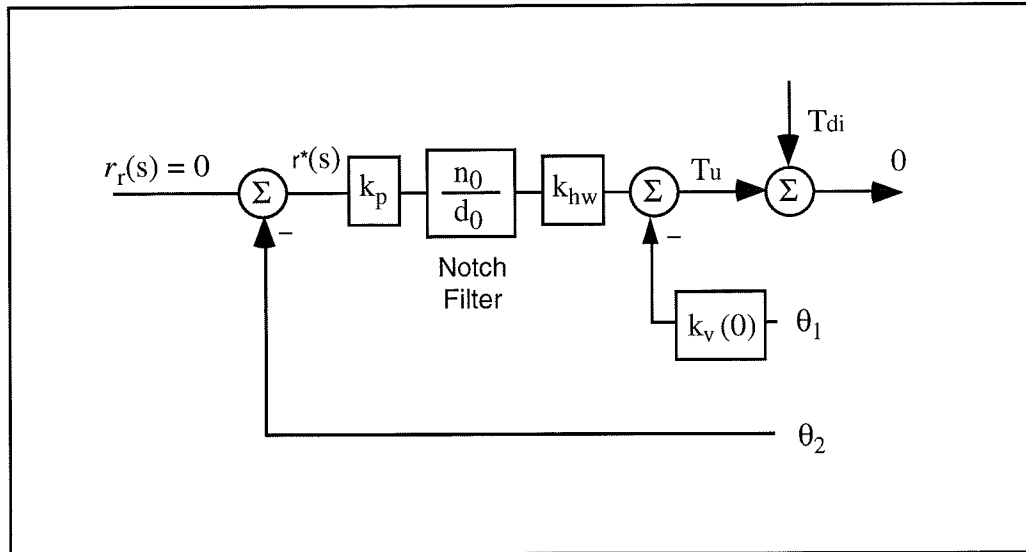


Figure 6.5-4i. Block Diagram of Static System State

**Optional Exercise**

- A. Determine the sensitivity of the closed loop transfer function,  $\theta_2(s)/r(s)$  of this experiment, to  $J_1$  and  $J_2$  using your final gain values from Step 5. Plot the magnitude of the sensitivity as a function of frequency for each case. What is the role of the collocated rate feedback in reducing sensitivity at the open loop resonant frequency? How do the sensitivities to  $J_1$  and  $J_2$  compare at low frequency? How do the sensitivities compare with those of the previous PD control at the  $\theta_2$  output and the noncollocated plant?

ans.:

The sensitivities are:

$$S_{J_1}^{c(j_1)} = \frac{-D_n(s)J_1(J_2s^4 + c_2s^3 + ks^2)}{D^*(s)D_n(s) + N_2(k_d s + k_p)k_{hw}N_n(s)} \tag{6.5-7i}$$

$$S_{J_2}^{c(j_2)} = \frac{-D_n(s)J_2(J_1s^4 + (c_1 + k_v k_{hw})s^3 + ks^2)}{D^*(s)D_n(s) + N_2(k_d s + k_p)k_{hw}N_n(s)} \tag{6.5-8i}$$

The collocated rate feedback control gains damp the sensitivity to both inertias at the open loop resonant frequency. This is because the damped resonant frequency<sup>1</sup> is a common term in  $D^*(s)$  and  $N_n(s)$  and hence in the denominator of both sensitivity expressions. The collocated rate feedback also damps the resonant zero in  $S_{J_2}^{c(j_2)}(s)$  resulting in increased sensitivity in the neighborhood of 2 Hz (see Figure 6.5-5i). Here there is no constant gain term at the  $\theta_1$  output and hence the sensitivity to

<sup>1</sup> It would be very lightly damped if not for the collocated rate feedback.



changes in  $J_1$  are essentially the same as for  $J_2$  at low frequency. That is, they behave as <sup>1</sup>

$$(J_i / k_{hw} k_p) s^2 \tag{6.5-9i}$$

( $i=1,2$ ) at low frequency and hence have reduced sensitivity as compared with the noncollocated plant due to the proportional gain. As compared with the collocated PD control, the sensitivities here are approximately the same as for the low gain collocated PD controlled system due to the similarity in gains of the two systems. The sensitivity to  $J_1$  is higher than the high gain collocated design at low and mid frequency due to the comparatively low PD gains here. The sensitivity to  $J_2$  is approximately the same except for near the undamped resonance in the collocated control case where it peaks sharply.

Sensitivity to inertia changes is easily demonstrated by changing inertias and obtaining the characteristic experimental responses (e.g. step and sine sweep). See Section 6.9.

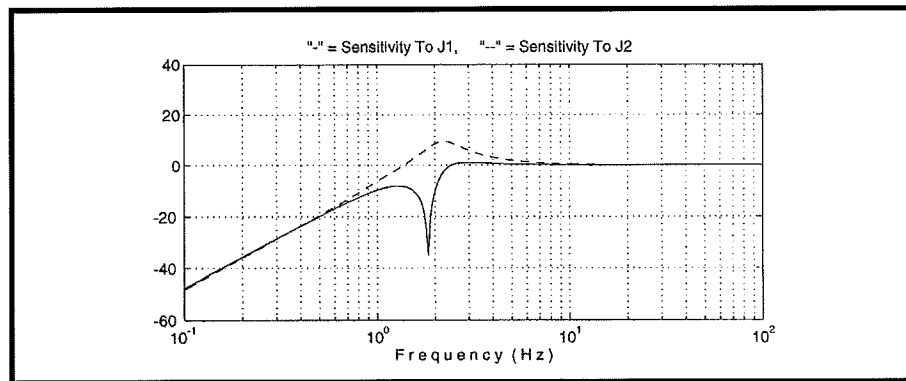


Figure 6.5-5i Sensitivity To Inertia Changes for PD+Notch Filter Experiment

**Optional Experiments**

A. Frequency response measurements

Shown in Figure 6.5-6i is the sweep output at  $\theta_1$  and  $\theta_2$  with sweep frequency of 0.1 to 10 Hz and 400 count amplitude for the design described above. Note the sharp anti-resonance due to the plant zero of the collocated response. The noncollocated response shows the system bandwidth to be approximately 1.5 Hz. It is seen that notch antiresonance has somewhat overcompensated for the damped resonance in  $G^*(s)$  at 2.1 Hz. The sine sweep maneuver for this particular design is sensitive to position drift due to motor cogging torque and amplifier nonlinearities. See the comments in Section 6.2i regarding mitigating these effects in the sine sweep data.

<sup>1</sup> Recall  $N_2 = k$  and  $d_0/n_0 = 1$ . The noncollocated plant low frequency sensitivity is

### B. Tracking Response to Sawtooth (Ramp) Input

Shown in Figure 6.5-7ia and -7ib are the  $\theta_1$  and  $\theta_2$  responses to a 10,000 count, 10,000 count/sec ramp trajectory (2 rep's) for the system in this section. Here the tracking at  $\theta_2$  is significantly improved over the collocated control case. Substantial phase lag and amplitude error however are still apparent. In contrast to the collocated control case, the tracking at  $\theta_2$  is generally closer than at  $\theta_1$ . This is because the system "automatically" compensates for the "adverse" plant dynamics to minimize the error at  $\theta_2$ . This will be more evident in the controllers that follow.

### C. Experimental Stability Margin

It is instructive to demonstrate to students the pending instability of the system as gain is increased. This should only be done under the laboratory supervisor's immediate oversight. While the system is designed with software and hardware safeguards (see Section 2.3), it should never be assumed that these will be effective.

During any stability tests, the user should always double check that the masses are secure, keep all persons well clear of the mechanism, and assign a responsible individual to keep their finger on the red "off" button on the controller box and to turn off the system immediately if speed or shaft deflections become large or loud "buzzing" occurs. After implementing the controller, contact the mechanism only using a long, slender non-sharp object (e.g. a ruler) to displace it and determine stability.

The procedure is to follow the instructions in Step 4 of the experiment in this section except to incrementally and uniformly increase gains  $k_p$  and  $k_d$ . For the parameters given above and for the particular system used in this manual, pending instability (large sustaining oscillations) was found at  $k_p=0.3$ ,  $k_d=0.005$  (i.e. the two gains were increased uniformly). This yields a gain margin of 5 (14 Db) for the original design, which is 6 Db less than the analytical prediction. It may be explained to students that in practice the available stability margins are generally less than the analytical prediction due to unmodeled phase lags in sensors, actuators, and data processing.

Phase margin may be shown by decreasing the sampling rate. For the particular system in this manual, pending instability occurred at  $T_s = 65$  ms which is roughly 20 degrees at  $\omega_c=0.9$  Hz and 70 degrees at the instability oscillation frequency (3.5 Hz) (Note that here the sampling related phase lag affects the inner collocated loop, and the transformed discrete time control algorithm dynamics as well.)

### D. Integral Action

The addition of integral action to the noncollocated control may be demonstrated. This results in a zero steady state error to a step input, but generally significant overshoot in tracking maneuvers. Shown in Figure 6.5-8i are the step and ramp responses when a value of  $k_i=0.04$  is added to the controller described above. This is easily implemented via the PID+Notch controller dialog box in the ECP Executive program. The remainder of the control setup including setting  $k_v$  and  $k_d$  should be done in the Generalized Form dialog box as described in Step 4 of the Student's instructions for this section.

E. Control Effort

In all experiments, it is insightful to consider control effort and to examine the price paid in power consumption and component size (i.e. cost) in providing high gain tracking. In some cases the effects of DAC saturation are also evident.

F. Collocated PD+Notch

The same notch filter may be applied to the collocated loop and PD gains at  $\theta_1$  be applied. This is easily done via the PD+Notch dialog box and selecting Encoder 1 for feedback. (The user should still augment the collocated loop with rate feedback in order for the notch filter zeros to be applicable. This should be done via the Generalized form dialog box. It is recommended that any additional derivative term be added in the return path if step response is to be measured. This is to reduce the anomalous response characteristics due to DAC saturation.)

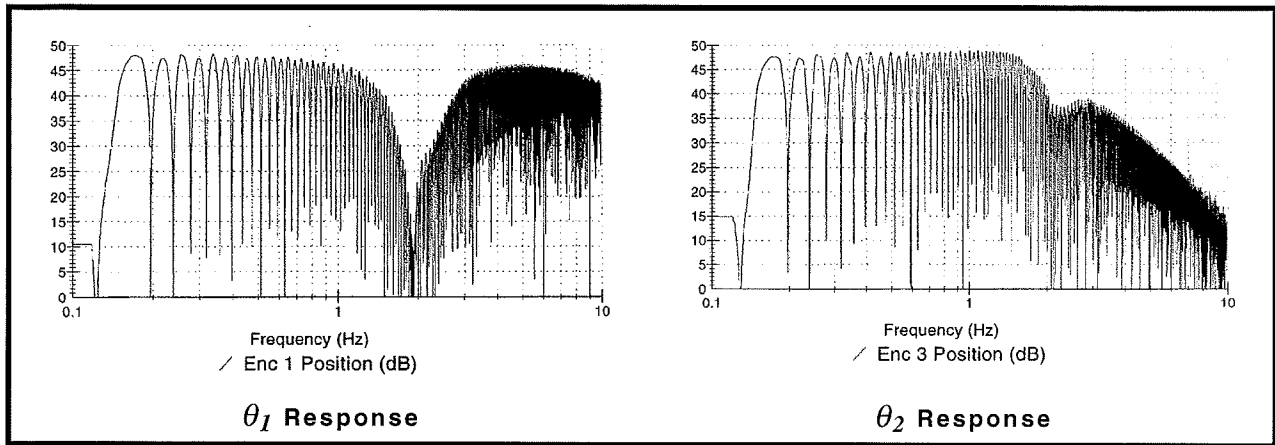


Figure 6.5-6i Sine Sweep Data

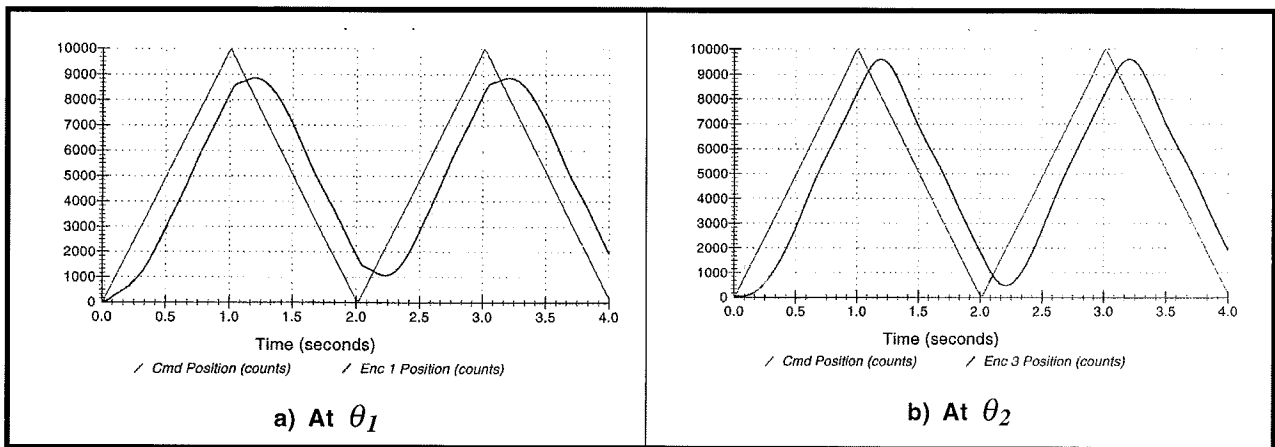


Figure 6.5-7i. Ramp Following At  $\theta_1$  and  $\theta_2$

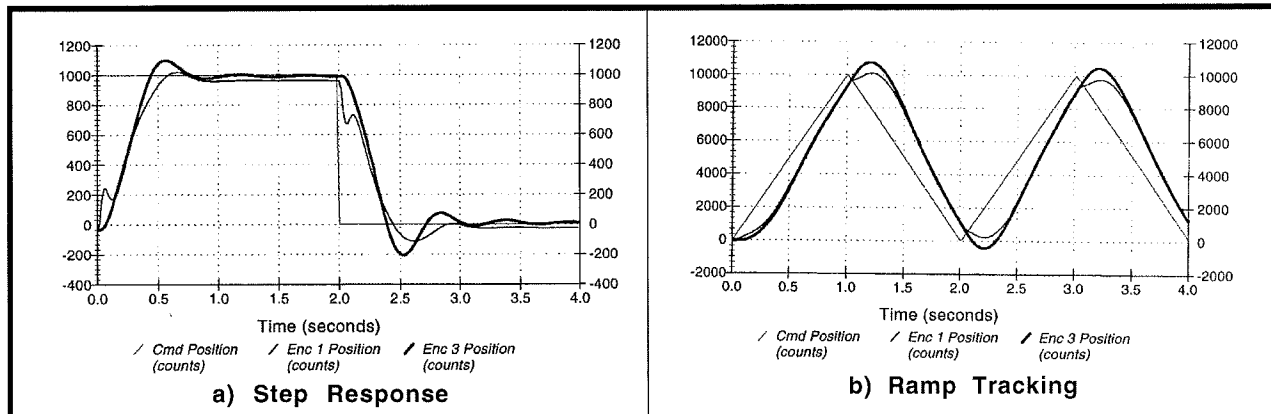


Figure 6.5-8i. Addition of Integral Action Eliminates Steady State Error but Causes Tracking Overshoot

### This section showed

1. Collocated rate feedback is useful in damping open loop plant resonances.
2. A notch filter may be employed to further reduce the transmission of flexible plant oscillations and provide improved step and tracking responses compared to the collocated scheme.
3. Sensitivity to changes in  $J_2$  is reduced from the collocated control scheme but is still limited by the relatively low control gain.
4. Attainable control gain magnitude is limited by the modest gain margins of the open loop system
5. The static stiffness at both outputs is proportional to  $k_p$ . Which is in turn limited by the gain margin of the system.
5. The noncollocated frequency response is better flattened through the system bandwidth than for the collocated control. This correlates with the reduced oscillations in the transient responses. The bandwidth is limited however by the relatively low control gain and hence the step rise time and ramp following lag are still moderately large. (optional exercise)
6. Steady state error to a step input may be eliminated by addition of integral action. This may not be suitable for tracking applications however because of the attendant overshoot. (optional exercise)

### 6.6i Successive Loop Closure / Pole Placement Design For 2 DOF Plant

This approach has the advantage that by closing the high gain collocated loop, system sensitivity to nonideal such effects as motor and amplifier Nonlinearities and Coulomb friction at  $\theta_1(s)$  is reduced. The success of the approach depends greatly on the ability to attain sufficiently high bandwidth at the collocation so that the assumption of unity gain (and zero phase lag) through the ensuing system bandwidth is valid. Because it utilizes pole placement, success also strongly depends on the accuracy and validity of the pseudo-plant model  $N_2/N_1$ . In cases where this model is not well known or involves significant Nonlinearities, this approach may be inappropriate.

This general approach may be successfully employed using other methods of control design about the outer loop (e.g. Bode design, linear quadratic,  $H_\infty$ ,  $\mu$ -synthesis, or QFT). The outer loop controller may be either a forward path cascade or return path/prefilter type. State space controllers are easily expressed in one of these forms.

#### Important Notes on Safety, Performance, and Noise Reduction:

1. The laboratory staff should always be on hand when students implement their controllers. This is particularly important during the testing of higher gain designs such as the ones here.
2. For a dynamic filter design in general, and pole placement in particular, it is important to maintain high numerical precision. Students should work in high precision and enter  $S(s)$  and  $R(s)$  in at least 6 significant digits. Use of only 4 digits has been shown to yield significantly altered results.
3. Due to the high associated gains, this approach is robust against model uncertainty and Nonlinearities at the collocation. Because the remaining plant is "well behaved" and closely approximated by its linear model between  $\theta_1$  and  $\theta_2$ , the approach here may be employed with success. In order to get the best possible model of  $\theta_2(s)/\theta_1(s)$ , the user may wish to identify that portion of the plant directly.  $\theta_2(s)/\theta_1(s)$  is found precisely by clamping the lower disk and measuring the free oscillation frequency ( $\approx \omega_n$ ) and damping ratio ( $\approx \zeta$ ) of the upper disk as per Section 6.1. We then have that

$$\frac{N_2(s)}{N_1(s)} = \frac{\omega_n^2}{s^2 + 2\zeta\omega_n s + \omega_n^2} \quad (6.6-1i)$$

4. If controller noise is excessive and all other elements of the procedure have been performed correctly. It may be necessary to further lower the low pass filter pole. This may be made as low as 5 Hz but reduced performance of the closed loop system will result due to the lower inner loop bandwidth. Whenever audible noise is present, it is always a good idea to try several other sampling frequencies to find the least noisy one.

#### Expected Results:

See answers to questions for expected control design values

- 1) In Step 3,  $b_f = a_f = 240$

- 2) Under the high gain collocated control, the lower disk is quite stiff ( $k_p k_{hw} \approx 40$  N-m/rad) while the upper disk stiffness is essentially that of the torsion rod ( $\approx 1.3$  N-m/rad).
- 3) In Step 8,  $k_{pf} = (r_0 n_{10} + s_0 n_{20}) / n_{10}$  where  $n_{i0}$  ( $i=1,2$ ) is the constant term in  $N_i$ . In this case  $n_{20} = n_{10}$  so that  $k_{pf} = (r_0 + s_0)$
- 4) Typical step response plots are shown in Figure 6.6-1i. The  $\theta_2$  rise time is relatively rapid with only slight overshoot. The steady state error is also low. The first disk moves quickly to accelerate the second disk, then reverses motion to minimize overshoot.

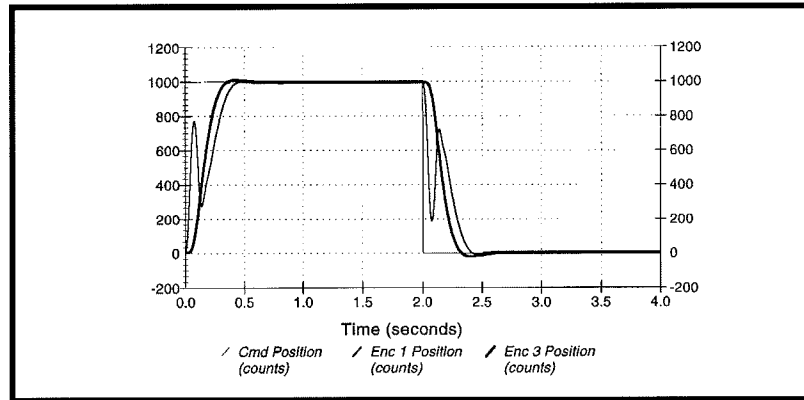


Figure 6.6-1i. Step Response At  $\theta_1$  and  $\theta_2$  Shows Relatively High System Performance. Lower Disk Leads, Then Reverses, To Minimize Error In Upper Disk.

**Questions:**

A. Expected values (consistent with others in this manual) are on the order of:

$$k_p = 2.5, k_d = 0.056$$

$$a_f = b_f = 240$$

$$e_0 = 600, e_1 = 13.3, g_0 = 240, g_1 = 1$$

$$s_0 = -7.968143, s_1 = 3.492598, r_0 = 37.67107, r_1 = 1$$

$$k_{pf} = 29.70$$

B. The full and reduced order (design) closed loop transfer functions are:

$$\frac{\theta_2(s)}{r_1(s)} = \frac{a_f k_{pf} k_{hw} N_2 (k_d s + k_p)}{R(s)(D(s)(s+a_f) + a_f k_{hw} N_1(s)(k_d s + k_p)) + S(s) a_f k_{hw} N_2 (k_d s + k_p)} \quad (6.6-1i)$$

$$\left( \frac{\theta_2(s)}{r_1(s)} \right)_{\text{design}} = \frac{k_{pf} N_2}{R(s) N_1(s) + S(s) N_2} \quad (6.6-2i)$$

The simulated frequency responses for the two expressions are given in Figure 6.6-2i. Both magnitude and phase are essentially identical through the system bandwidth and the assumption of unity gain in  $c(s)$  is valid.

- C. The full and reduced order open loop transfer functions for the outer loop are respectively

$$\left(\frac{\text{Num}_{ol}}{\text{Den}_{ol}}\right)_{\text{reduced order}} = \frac{N_2S(s)}{N_1R(s)} \quad (6.6-3i)$$

$$\left(\frac{\text{Num}_{ol}}{\text{Den}_{ol}}\right)_{\text{full order}} = \frac{a_f k_{hw}(k_d s + k_p) N_2 S(s)}{(s + a_f) D(s) R(s) + a_f k_{hw}(k_d s + k_p) N_1 R(s)} \quad (6.6-4i)$$

The Bode plots of these are shown in Figure 6.6-3i. The phase margin in each case is approximately 70 degrees, and the gain margin is approximately 16 Db for the full order case and infinite for the reduced order one.

- D. As in the previous section the static system block diagram is constructed (Figure 6.6-4i). As before

$$\text{for disturbances at } J_1: \theta_2 = \theta_1 \quad (6.6-5i)$$

$$\text{for disturbances at } J_2: \theta_2 = \theta_1 + T_{d2}/k \quad (6.6-6i)$$

where  $k$  is the spring constant. From these, we have the static stiffness expressions and their values (for the parameters in this manual):

$$\frac{T_{d1}}{\theta_1} = \frac{T_{d1}}{\theta_2} = k_p k_{hw} \left(1 + \frac{s_0}{r_0}\right) \quad (= 34 \text{ N-m/rad}) \quad (6.6-7i)$$

$$\frac{T_{d2}}{\theta_1} = k_p k_{hw} \frac{k(r_0 + s_0)}{r_0 k - k_p k_{hw} s_0} \quad (= 4.4 \text{ N-m/rad}) \quad (6.6-8i)$$

$$\frac{T_{d2}}{\theta_2} = k_p k_{hw} \frac{k(r_0 + s_0)}{r_0(k + k_p k_{hw})} \quad (= 1.1 \text{ N-m/rad}) \quad (6.6-9i)$$

By comparing Eq's (6.6-7i) and (6.6-9i) it is seen that for this system, the upper disk is less stiff than the lower disk for all  $k_p > 0$ . Eq. (6.6-6i) shows that the lower disk will undergo reverse motion in response to disturbances on the upper disk whenever  $k_p k_{hw} s_0 > r_0 k$ . This occurs whenever the outer loop control gain  $s_0/r_0$  is high relative to the spring  $k$ . The particular values for  $T_{d2}/\theta_1$  and  $T_{d2}/\theta_2$  are coincidentally nearly identical to those of the collocated PD control case. Note that  $T_{d1}/\theta_1$  is more than thirty times higher however and hence this design is much more resistant to friction and other low frequency disturbances at the base disk.

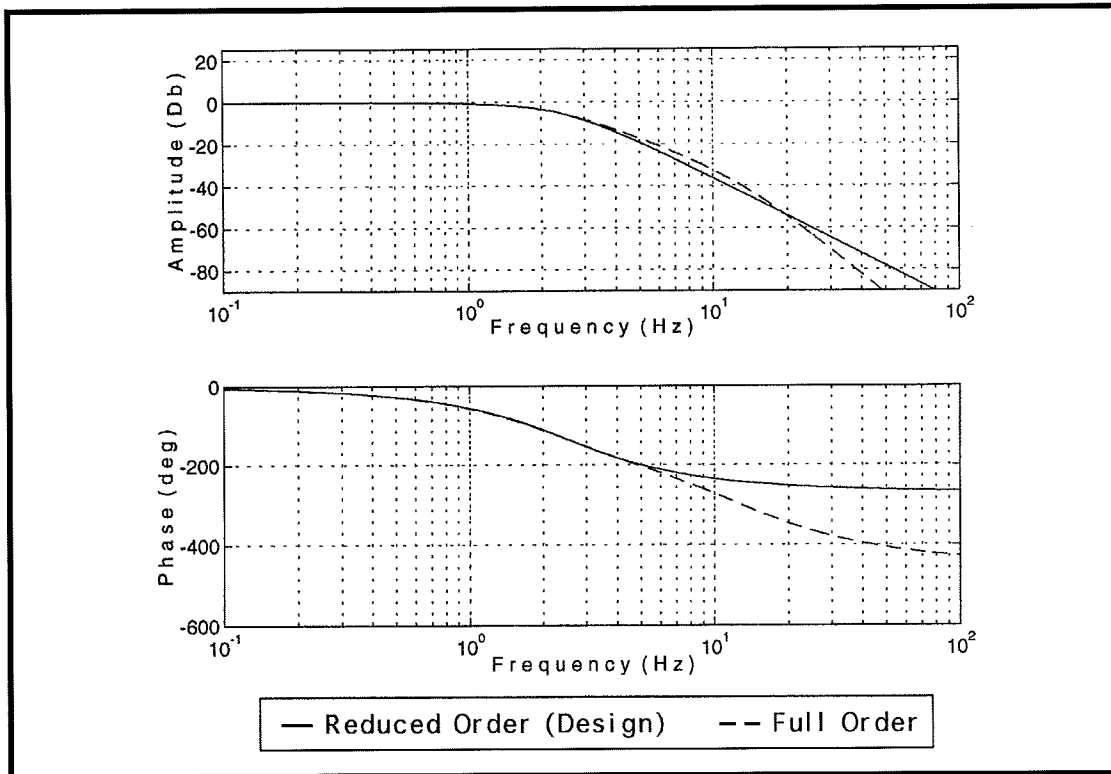


Figure 6.6-2i. Frequency Response of Reduced and Full Order Closed Loop Transfer Functions are Essentially Identical Through System Bandwidth

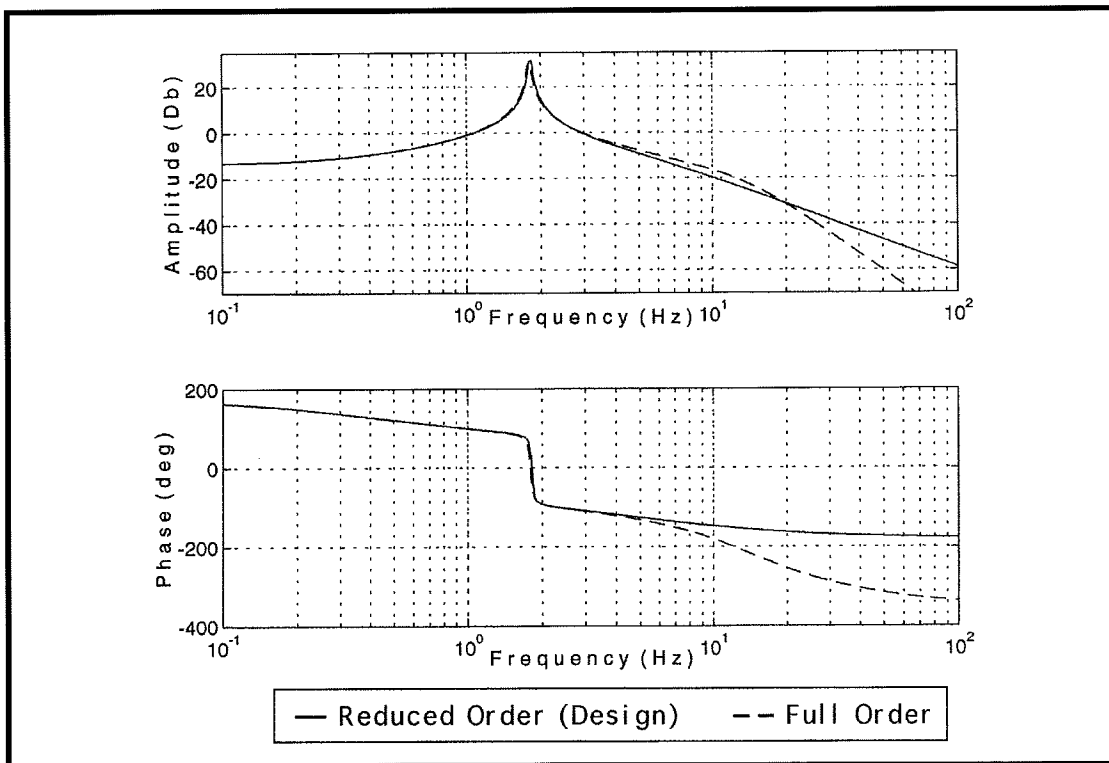


Figure 6.6-3i. Reduced and Full Order Open Loop Transfer Functions. Systems Have Similar Phase and Gain Margins



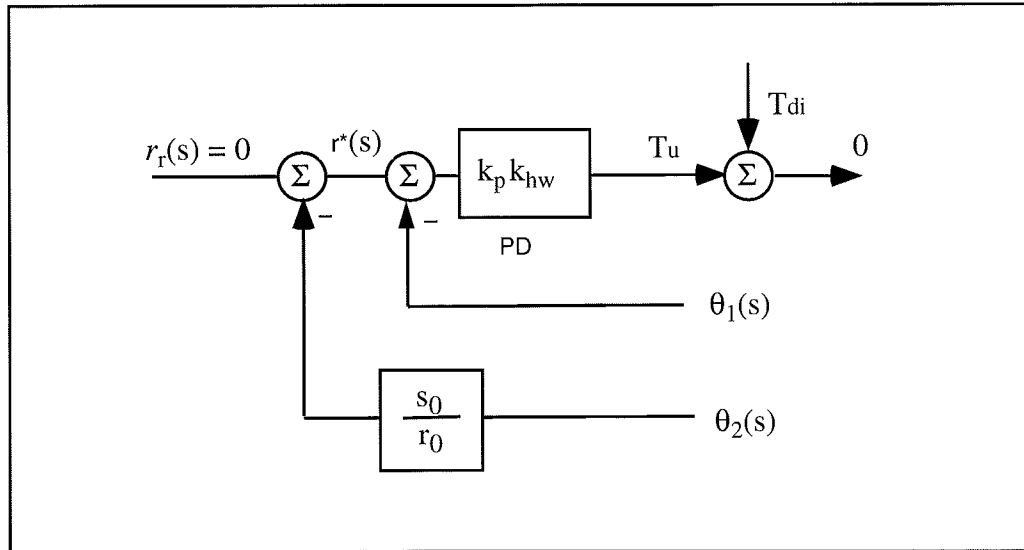


Figure 6.6-4i. Static System Block Diagram

**Optional Exercise & Solution**

A. Determine the sensitivity of the closed loop transfer function to  $J_1$  and  $J_2$ . You may ignore the low pass noise filter in your analysis. How do the collocated control gains reduce the sensitivity to  $J_1$ ? Do these gains reduce the sensitivity to other parameter changes at the collocation? How does the sensitivity to changes in  $J_2$  compare with the high gain collocated PD controlled system and noncollocated PD+Notch filter designs of prior sections?

ans.: The sensitivities are:

$$S_{J_1}^{c(01)} = \frac{-R(s)J_1(J_2s^4 + c_2s^3 + ks^2)}{R(s)D(s) + R(s)N_1(s)(k_d s + k_p)k_{hw} + S(s)N_2(k_d s + k_p)k_{hw}} \quad (6.6-10i)$$

$$S_{J_2}^{c(02)} = \frac{-J_2R(s)(J_1s^4 + (c_1 + k_d k_{hw})s^3 + (k + k_p k_{hw})s^2)}{R(s)D(s) + R(s)N_1(s)(k_d s + k_p)k_{hw} + S(s)N_2(k_d s + k_p)k_{hw}} \quad (6.6-11i)$$

The PD control gains increase the values of the coefficients of the low order and constant terms in the denominator of Eq. (6.6-10i), and hence reduce the sensitivity to changes in  $J_1$  at lower frequency. It is easily shown that this also holds for other parameters associated with the collocation. The PD gains also increase the lowest orders in the numerator in Eq.(6.6-11i), however and hence do not necessarily reduce sensitivity to  $J_2$ . This is reflected in the plot of Figure 6.6-5i, where the sensitivity to  $J_1$  changes is strong below the system bandwidth; but the sensitivity to changes in  $J_2$  is not particularly low. It is however significantly reduced with respect to the open loop and PD controlled systems, and is dramatically lower than that of the PD+ notch system at mid frequencies..

Sensitivity to inertia changes is easily demonstrated by changing inertias and obtaining the characteristic experimental responses (e.g. step and sine sweep). See Section 6.9.

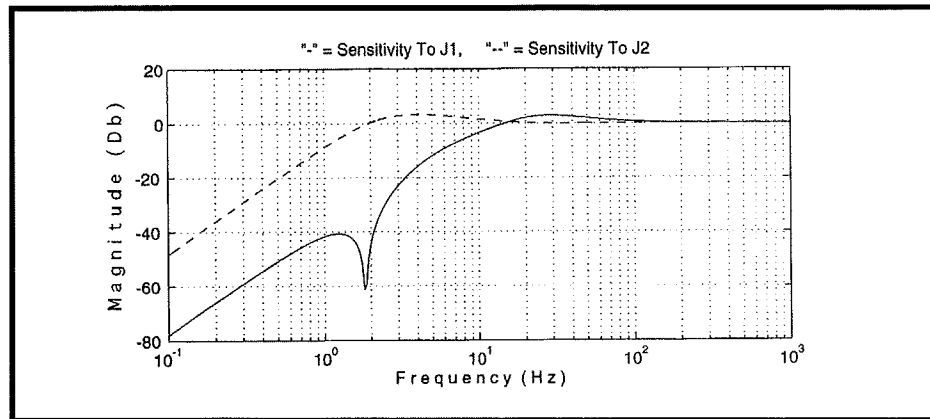


**Figure 6.6-5i. Control Scheme Provides Generally Large Reduction in  $J_1$  Sensitivity & Moderate Reduction in  $J_2$  Sensitivity**

### Optional Experiments & Expected Results

#### A. Frequency response measurements

Shown in Figure 6.6-6ia is the sweep output at  $\theta_1$  and  $\theta_2$  with sweep frequency of 0.1 to 10 Hz and 100 count amplitude. Note the signature of the plant zero but otherwise relatively flat shape of the collocated response out to the inner loop bandwidth. The noncollocated response is flat out to the outer loop design bandwidth. This shape agrees with the simulated Bode response shown in Figure 6.6-2i.

#### B. Tracking Response to Sawtooth (Ramp) Input

Shown in Figure 6.6-7ia and -6ib are the  $\theta_1$  and  $\theta_2$  responses to a 10,000 count, 10,000 count/sec ramp trajectory (2 rep's). Note the irregular shape in  $\theta_1$  as it leads and makes dynamic corrections to minimize the error in  $\theta_2$ .

#### C. Simulated Step Response

The simulated step response using the  $c(s) = 1$  assumption is shown in Figure 6.6-8i. This shape is identical (by design) to that of the specified third order polynomial and is closely approximated by the experimental data shown in the same figure. This close agreement further demonstrates the usefulness of this approach for this class of control problems.

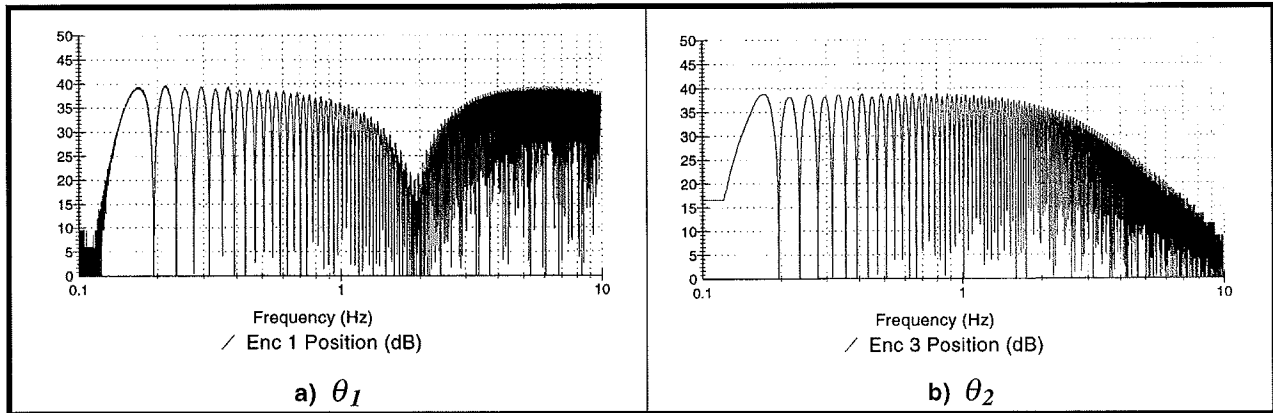


Figure 6.6-6i. Experimental Frequency Response Shows Plant Zero in  $\theta_1$  and Flat Response in  $\theta_2$  To Design Bandwidth

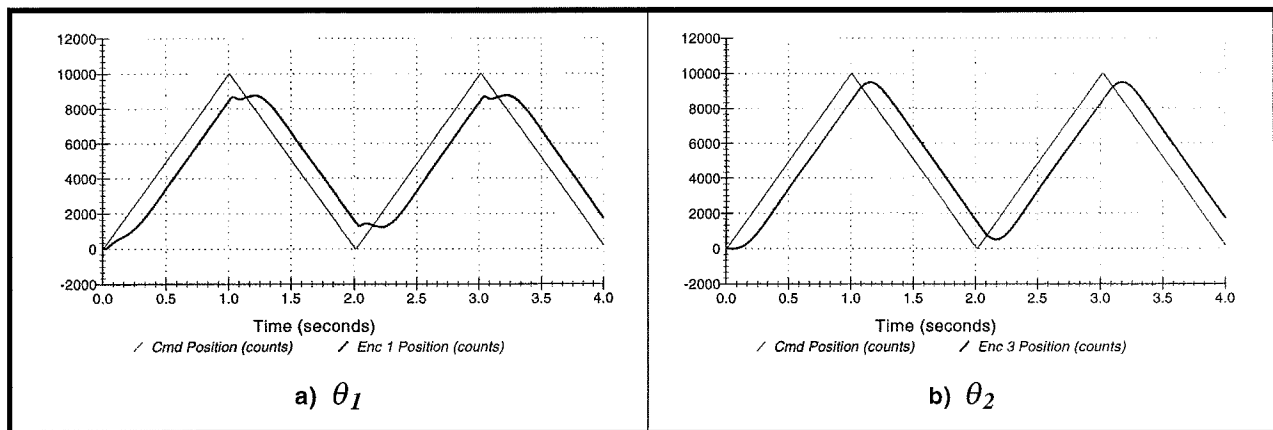


Figure 6.6-7i. Ramp Following Shows Dynamic Corrections in  $\theta_1$  To Minimize Errors at  $\theta_2$

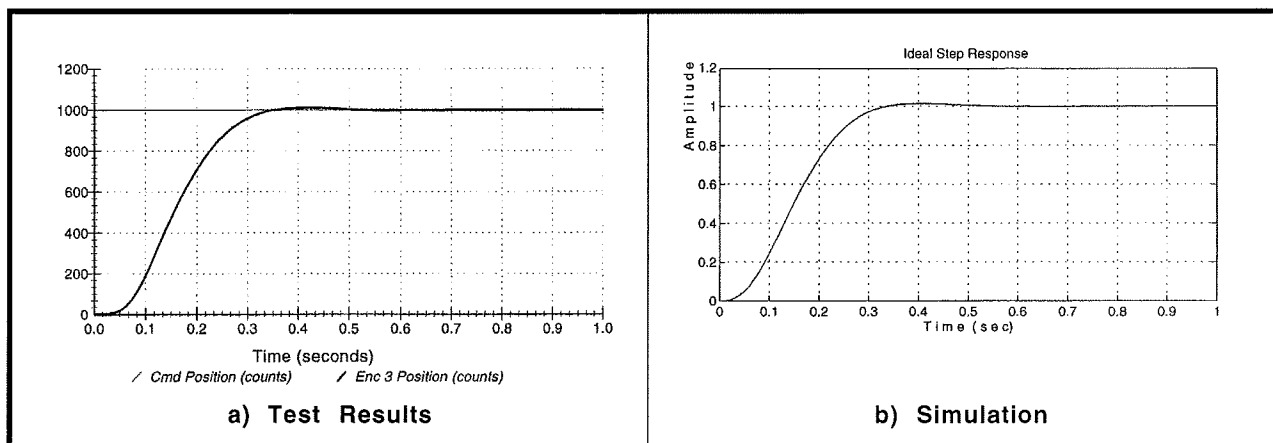


Figure 6.6-8i. Experimental Step Response Closely Follows Design Simulation

**This section showed:**

1. The concept of successive loop closure for SIMO systems.
2. High gain inner loop control may be used to desensitize the system to nonlinear and uncertain parameters at the collocation. The outer loop may then be closed by any of several methodologies.
3. The technique of pole placement design.
4. Some salient properties of flexible structure frequency responses.
4. Relatively high performance characteristics of frequency response, step and ramp response, and static stiffness.
5. Strong sensitivity reduction to  $J_I$  due to high PD gains at the collocation and moderate sensitivity reduction at the noncollocation by this control scheme.

6.7i LQR Control

Expected Results:

A typical step response from experimental Step 5 is shown in Figure 6.7-1i. Here the response at  $\theta_2$  is faster than for all previous controllers, but with more overshoot than in the pole placement design (due to the selected closed loop poles of the latter). As with the pole placement design, the motion at  $\theta_1$  first leads  $\theta_2$  in order to accelerate it; then undergoes a direction reversal to reduce the overshoot.

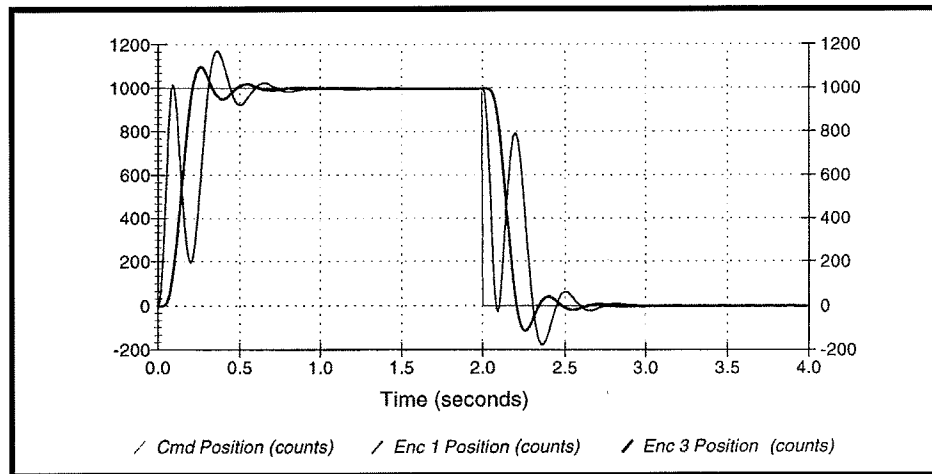


Figure 6.7-1i. LQR Experimental Step Response

Answers to Questions / Exercises

- A. Using the numerical plant of Eq. (6.1-6i) the poles of the closed loop transfer function for the specified values of  $r$  are plotted in Figure 6.7-2i.<sup>1</sup> (The roots asymptotically approach a fourth order Butterworth distribution as  $r$  becomes small.) A suitable controller from these which meets the closed loop pole specification is the case of  $r = 1.0$  which has a corresponding controller:

$$K = [ 0.717 \quad 0.0294 \quad 0.283 \quad 0.0847 ] \tag{6.7-1i}$$

- B. The closed loop transfer function is

$$\frac{\theta_2(s)}{r(s)} = \frac{k_{pf}k_{hw}N_2}{D(s) + k_{hw}N_1(s)(k_1+k_2s) + k_{hw}N_2(k_3+k_4s)} \tag{6.7-2i}$$

<sup>1</sup>Scripts for LQR synthesis using MATLAB® are included in Appendix Ai.

The open loop transfer function for phase and gain margin analysis is

$$\left(\frac{N(s)}{D(s)}\right)_{\text{open loop}} = \frac{k_{hw}(N_1(s)(k_1+k_2s) + N_2(k_3+k_4s))}{D(s)} \quad (6.7-3i)$$

The Bode plot of Eq 6.7-3i is shown in Figure 6.7-3i. Here, by the Nyquist stability criterion, the magnitude must stay above the 0 Db line at the second (positive going) crossing of the -180 degree phase curve to avoid clockwise encirclement of the -1 point. Thus the gain margin is 10 Db. The phase margin is 55 degrees.

C. The static stiffnesses may be found by a static block diagram similar to Figure 6.6-4i and using Eq's (6.6-5i, -6i). Using the notation of Section 6.6, we have

$$\frac{T_{d1}}{\theta_1} = \frac{T_{d1}}{\theta_2} = k_{hw} (k_1 + k_3) \quad (= 17.4 \text{ N-m/rad}) \quad (6.7-4i)$$

$$\frac{T_{d2}}{\theta_1} = k k_{hw} \frac{k_1 + k_3}{k - k_3 k_{hw}} \quad (= -4.9 \text{ N-m/rad}) \quad (6.7-5i)$$

$$\frac{T_{d2}}{\theta_2} = k k_{hw} \frac{k_1 + k_3}{k + k_1 k_{hw}} \quad (= 1.3 \text{ N-m/rad}) \quad (6.7-6i)$$

Again, because the control effort and the disturbance both act on  $J_1$  when the disturbance is at the lower disk, no torque is acting on  $J_2$  at equilibrium. The torque for a unit displacement is equal to the sum of the feedback gains times the forward path gain,  $k_{hw}$ . For disturbances at the upper disk, again, the upper disk is less stiff than the lower disk for all control gains. Eq. (6.7-5i) shows that the lower disk will undergo reverse motion in response to disturbances on the upper disk whenever  $k_3 k_{hw} > k$ . For the design given above this is indeed the case, and the lower disk moves in reverse direction as it attempts to regulate against the upper disk disturbance.

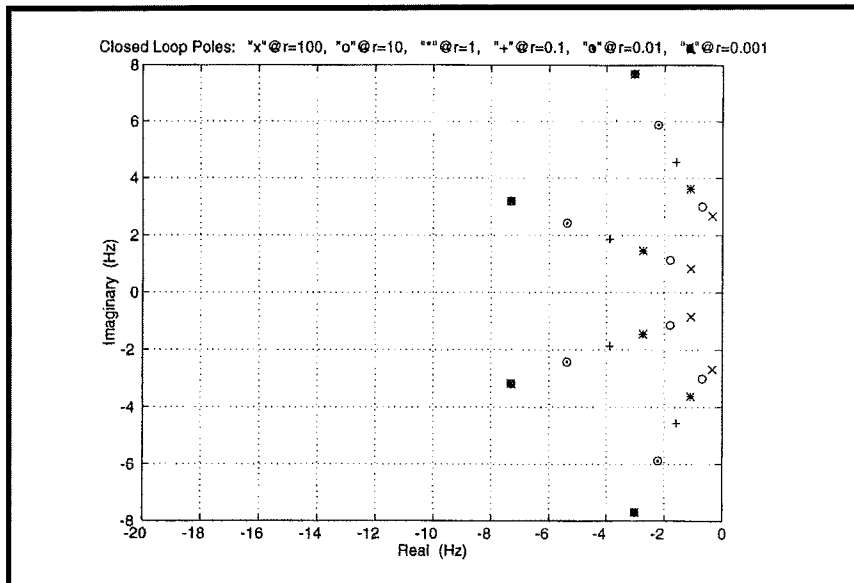


Figure 6.7-2i. Closed Loop LQR Pole Locations For Various Control Effort Weights

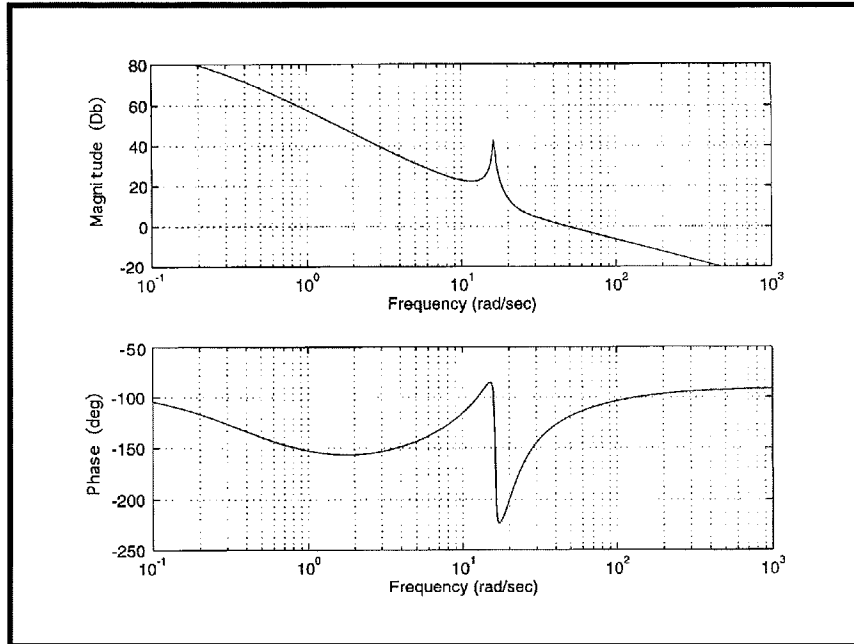


Figure 6.7-3i. Open Loop Frequency Response for Stability Margin Analysis

**Optional Exercise & Solution**

- A. Determine the sensitivity of the closed loop transfer function to  $J_1$  and  $J_2$ . Plot the magnitude of the sensitivities as a function of frequency. How do the sensitivities compare with those of previous noncollocated controllers?

ans.: The sensitivities are:

$$S_{J_1}^{c(J_1)} = \frac{-J_1(J_2s^4 + c_2s^3 + ks^2)}{D(s) + N_1(s)(k_2s + k_1)k_{hw} + N_2(k_4s + k_3)k_{hw}} \quad (6.7-7i)$$

$$S_{J_2}^{c(J_2)} = \frac{-J_2(J_1s^4 + (c_1 + k_2k_{hw})s^3 + (k + k_1k_{hw})s^2)}{D(s) + N_1(s)(k_2s + k_1)k_{hw} + N_2(k_4s + k_3)k_{hw}} \quad (6.7-8i)$$

As seen in Figure 6.7-4i, the LQR controller provides strong sensitivity reduction to changes in  $J_1$ . This reduction is less than for the successive loop / pole placement design however. The sensitivity to changes in  $J_2$  has been reduced slightly more than for the pole placement approach at low frequency but is significantly increased (by roughly a factor of two) near the crossover frequency. The sensitivity to changes in  $J_2$  is improved from the PD + Notch Filter design at lower frequency but is roughly the same at the crossover frequencies of the respective systems. This frequency is higher of course in the LQR system.

Sensitivity to inertia changes is easily demonstrated by changing inertias and obtaining the characteristic experimental responses (e.g. step and sine sweep). See Section 6.9.

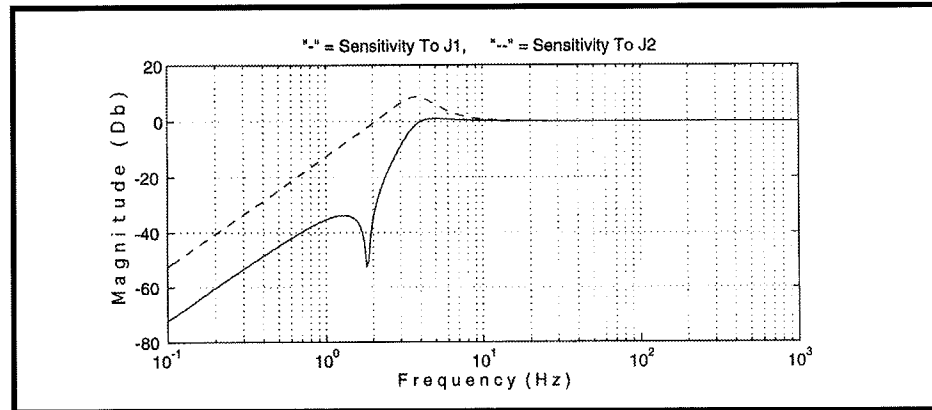


Figure 6.7-4i. LQR System Sensitivity To Inertia Changes

### Further Optional Experiments

#### A. Frequency response measurements

Shown in Figure 6.7-5ia is the sweep output at  $\theta_1$  and  $\theta_2$  with sweep frequency of 0.1 to 10 Hz and 100 count amplitude. Here, the collocated magnitude is relatively high including a rise following the zero (due to the derivative lead) out to roughly 4 Hz. The noncollocated response is flat out to the outer loop design bandwidth of 3 Hz.

#### B. Tracking Response to Sawtooth (Ramp) Input

Shown in Figure 6.7-6ia and -6ib are the  $\theta_1$  and  $\theta_2$  responses to a 10,000 count, 10,000 count/sec ramp trajectory (2 rep's). Note the irregular shape in  $\theta_1$  as it leads and then makes dynamic corrections to minimize the error in  $\theta_2$ . The  $\theta_2$  tracking here more closely follows the reference input than in the previous designs. This is consistent with the relatively flat, high bandwidth frequency response.

#### C. Simulated Step Response

The simulated and experimental step responses are shown in Figure 6.7-7i. The agreement is generally close. As in the successive loop / pole placement approach, the relatively high collocated loop gain desensitizes the system to uncertainty & nonlinearity in parameters at the collocation. This is where most uncertainty in this type of plant typically exists; therefore this agreement may be viewed as the result of the effectiveness of the control in desensitizing the system rather than of the plant behaving particularly close to the ideal model.



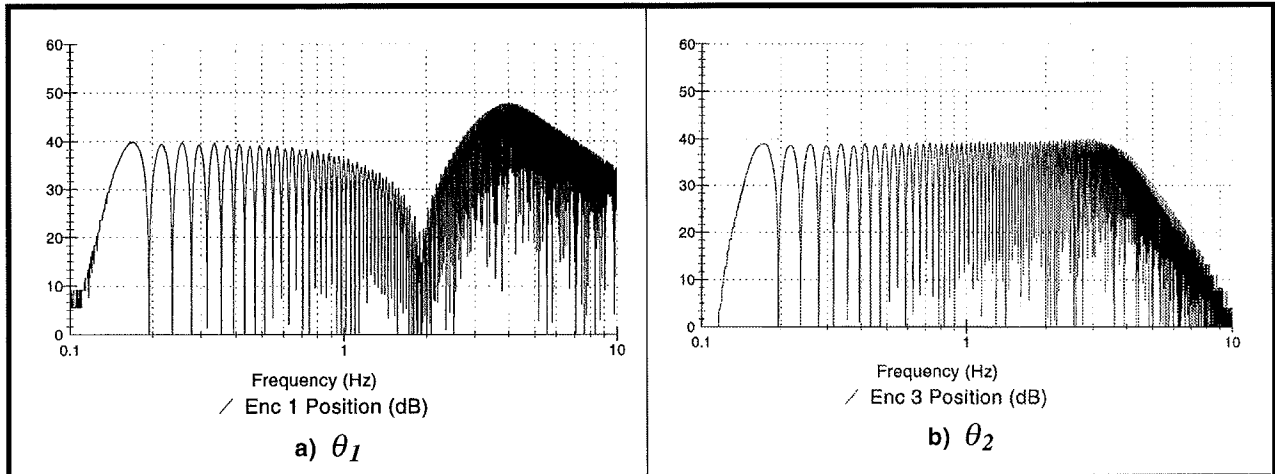


Figure 6.7-5i. LQR Experimental Frequency Response Shows Comparatively High Bandwidth

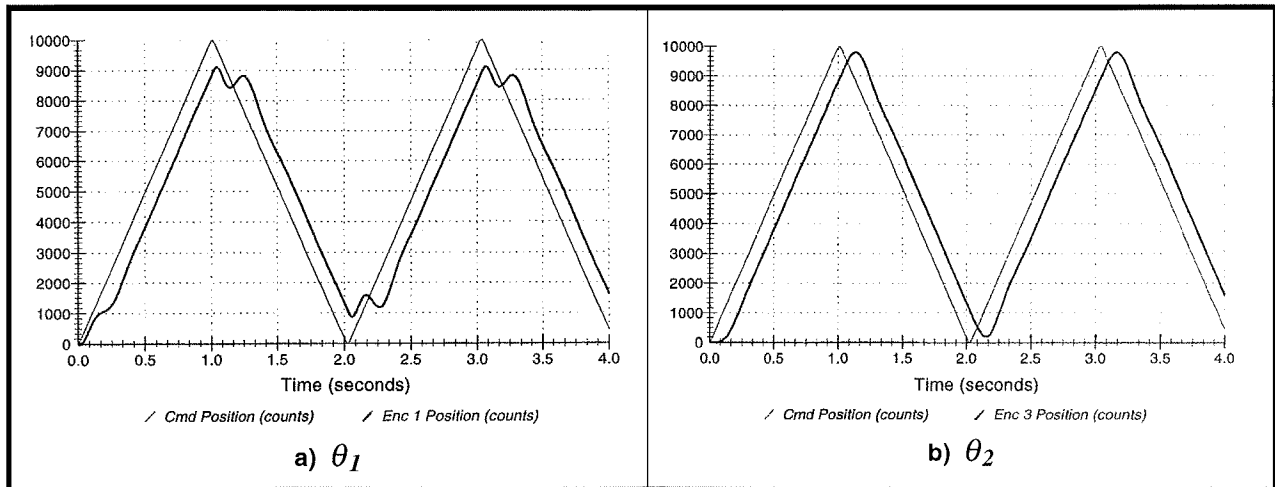


Figure 6.7-6i. Tracking Response: Dynamic Corrections in  $\theta_1$  Minimize Errors at  $\theta_2$

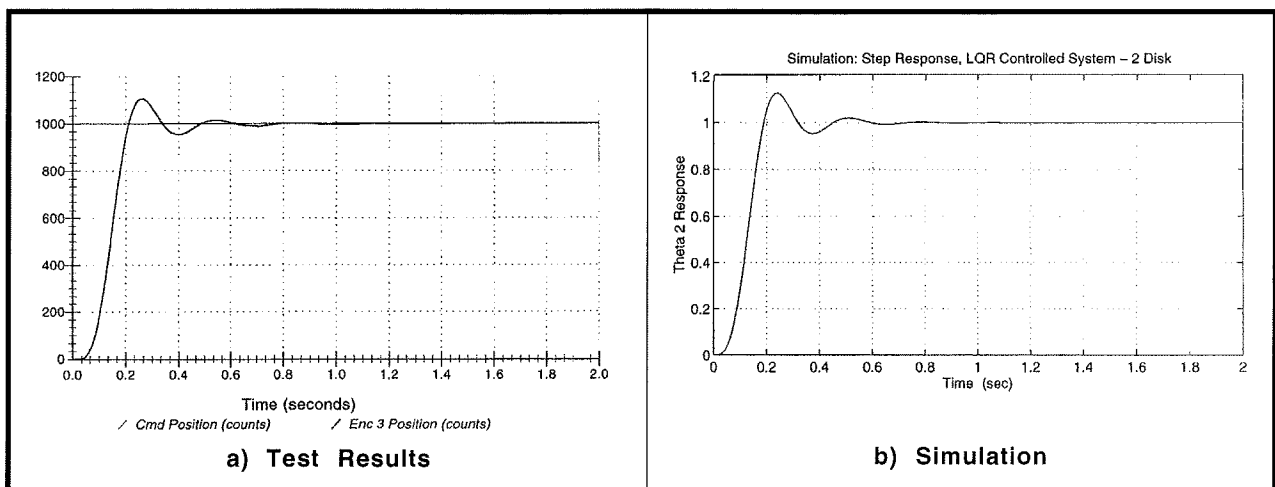


Figure 6.7-7i. Experimental LQR Step Response Compared with Design Simulation

**This section showed:**

1. LQR design synthesis and control implementation
2. With sufficiently high resolution / low noise sensors, rate may be effectively measured by differentiating position data (process imbedded in real-time controller).
- 3 Full state feedback LQR control is effective in providing comparatively high performance and ample stability margins. Here "performance" is stated with respect to low sensitivity to parameter changes, fast and close tracking performance ( also flat, high bandwidth noncollocated frequency response), and high static stiffness.

## 6.8i Practical Control Implementation

### 6.8.1 Effect of Drive Saturation

#### Expected Results:

#### Qualitative Changes in Step Response For High Bandwidth Controller

Figure 6.8-1i shows the three specified responses using forward path derivative action. In the first, there is a rapid rise time and overshoot. The second more closely resembles the ideal return path derivative response (see Figure 6.8-2i) and the third shows a considerably slowed response due to DAC saturation. (See "Answers to Questions" for further discussion)

#### Effect on Stability For Certain Higher Order Systems

#### Important Note

The following procedure must be followed carefully in order to assure there is no risk of injury or equipment damage. For this reason, it is not included in the student's instructions and it is recommended that it be performed as a classroom demonstration by the instructor or qualified laboratory technician. It does provide a valuable lesson on the effects of saturation on stability and may serve as an introduction to nonlinear system limit cycles.

#### Procedure

- 1 Install the upper and lower disks only on the mechanism and secure two 500 g. brass weights to each at the a 9.0 cm position. Thus setup the apparatus as per

- Figure 6.1-1b. Verify that the disk and mass attachment screws are securely tightened (but not over torqued).
- 2 Input the controller designed in Section 6.6 (Successive Loop / Pole Placement approach)<sup>1</sup>. It is important to verify that all parameters are properly set prior to exiting the Generalized Form dialog box. Implement this algorithm and verify that the system is stable (i.e. "Safety Check" the controller - see Section 2.3). Setup to acquire Encoder 1, Commanded Position, and Control Effort every 1 servo cycle.
  - 3 Perform a 500 count step maneuver and plot the data. Increase the step size in 500 count increments and observe the amount and degree of DAC saturation. Increase the step size until a limit cycle of constant or slightly increasing amplitude is observed. Discontinue control immediately (Abort Control button) upon observing increasing limit cycle amplitude. Plot and save the data.

Shown in Figure 6.8-3i are the initial 500 step response where there is no appreciable effect of DAC saturation and a 4000 count step in which a limit cycle of increasing amplitude is induced. Here the saturation causes not only a change in the response shape, but more significantly system instability.<sup>2</sup>

---

<sup>1</sup> In many systems, the parameters found Section 6.6i of this manual will suffice for this experiment in lieu of those designed using system specific parameters.

<sup>2</sup> It should be pointed out, that a step input is unnecessarily harsh and is almost never used under normal operations (it may be used for system characterization) in industrial applications involving servo motion control or power sensitive hardware elements. Such discontinuous inputs may occur however as unexpected disturbances and therefore the sensitivity of a particular controller to them - including DAC saturation effects - should be considered for practical applications.

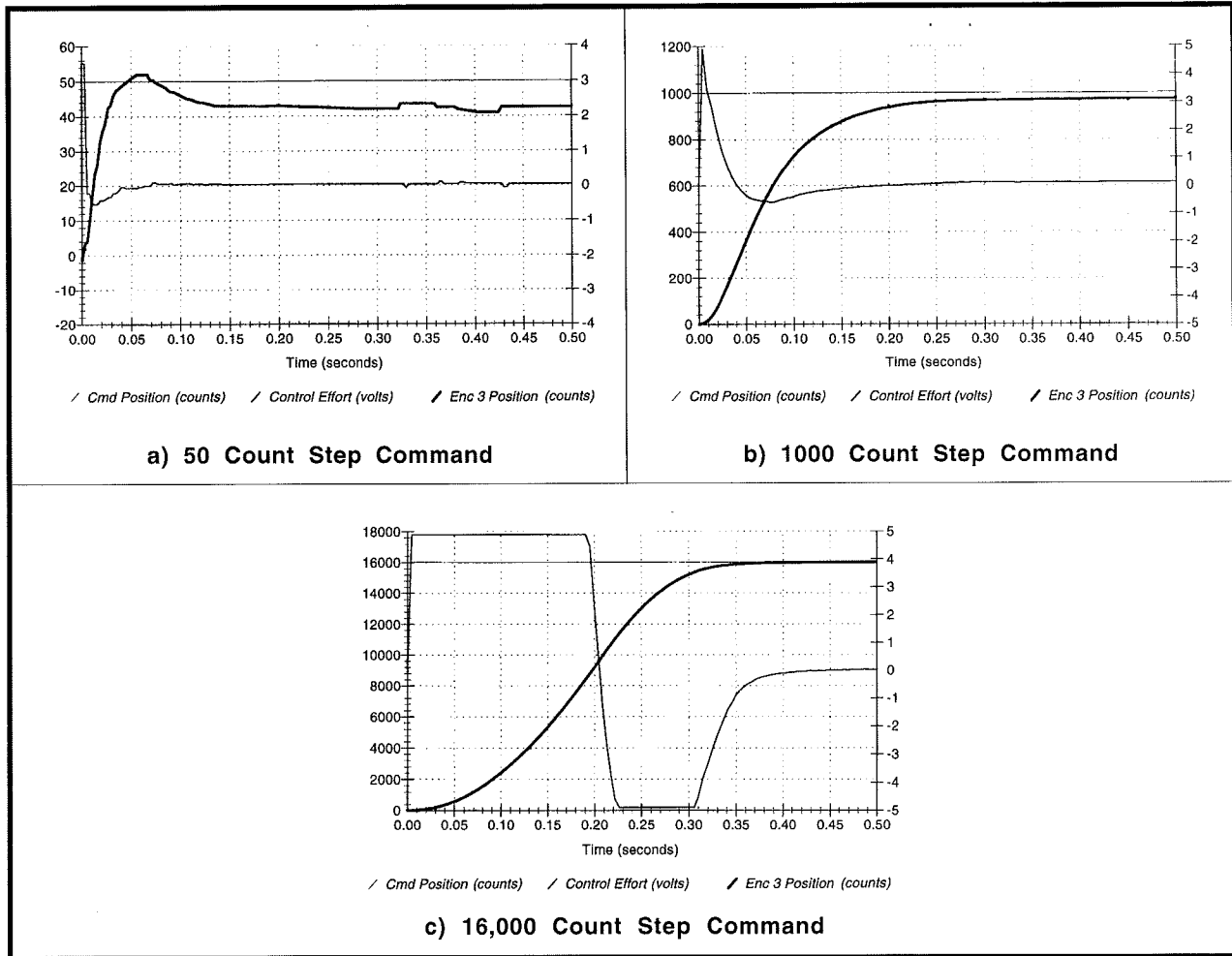


Figure 6.8-1i. DAC Saturation Test Results: Increased Amplitude Causes Greater Saturation and Changes Response Shape

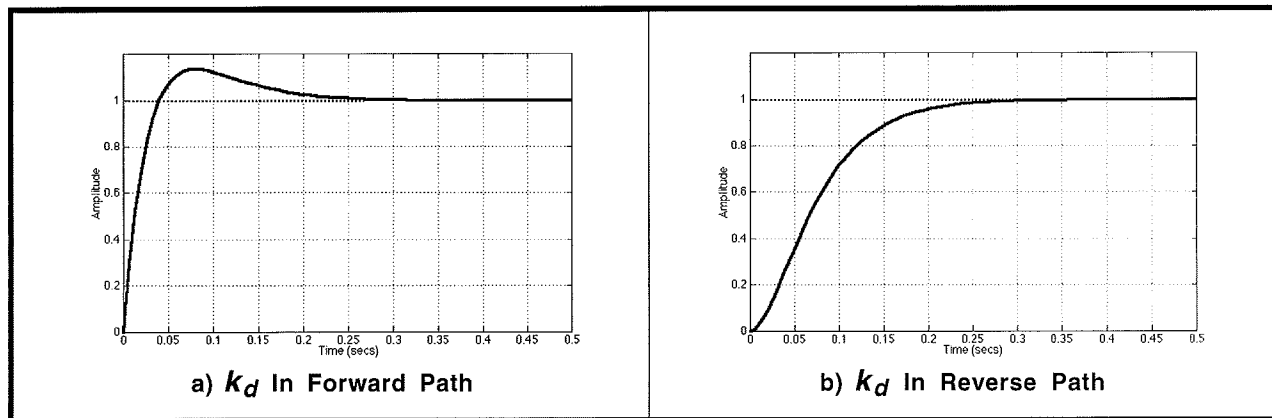


Figure 6.8-2i. Ideal Step Responses

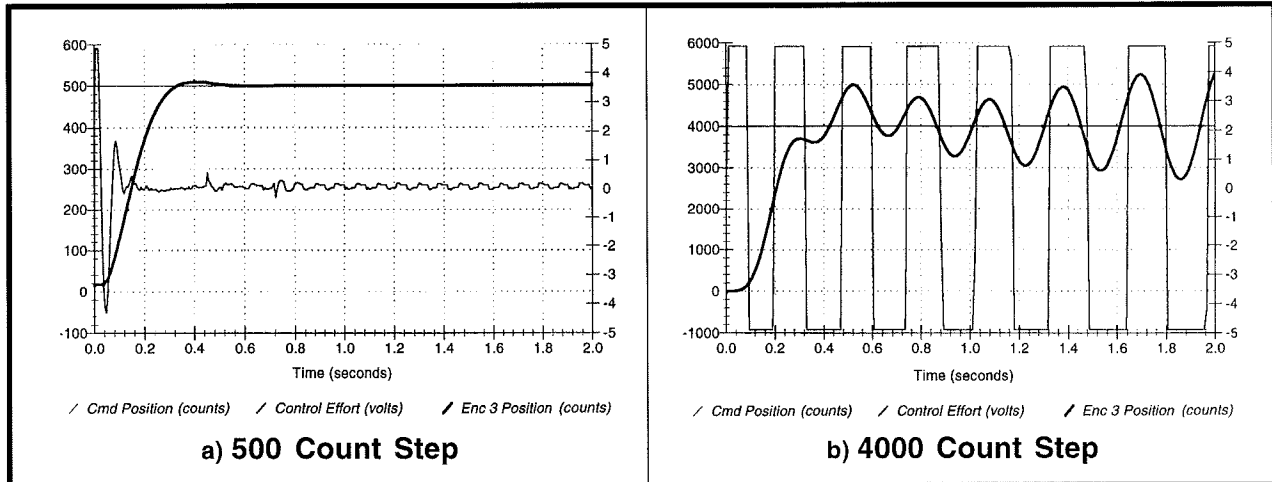


Figure 6.8-3i. Saturation Induced Limit Cycle Instability

**Answers to Questions / Exercises:**

- A. From Figure 6.8-1i: the 50 count step response shows rapid rise time and significant overshoot, the 1000 count response shows slower rise time and no overshoot. The ideal forward and reverse path unit step responses are shown in Figure 6.8-2i. At 50 count amplitude, the experimental system more closely follows the ideal forward path response because the DAC is not saturated. At 1000 counts the initial impulsive torque – associated with (backwards) differentiation of the initial discontinuity – is grossly truncated due to DAC saturation. After the initial change, the input is constant and the derivative action acts only on the return path signal. Hence at 1000 counts, the system responds essentially as the ideal return path differentiated one.
- B. The 16,000 count response is relatively slow compared with those above. The control effort is saturated for nearly 200 ms indicating that the system is producing less torque than the ideal linear one. Because there is a nominally constant (maximum available) torque during this period, there is a nominally constant acceleration resulting in a parabolic shape. Another parabolic shape of negative curvature occurs in the period from 0.23 to 0.30 sec as the system decelerates.
- C. Increased controller bandwidth and increased input acceleration increase the likelihood that saturation will occur and increase its extent if it does. Input amplitude (for a given maximum acceleration) does not in itself cause saturation. If the amplitude of an input trajectory is increased while the duration is held constant, peak commanded acceleration will increase and so will the likelihood of saturation.

**6.8.2i Effect of Discrete Time Sampling**

1. In Step 3: Experimental instability occurs for sample periods greater than about 60 ms. The plots showing the sampling rate induced oscillations for Steps 3 and 4 are shown in Figure 6.8-4.
2. In Step 2: Experimental instability occurs for sample periods greater than about 10 ms.

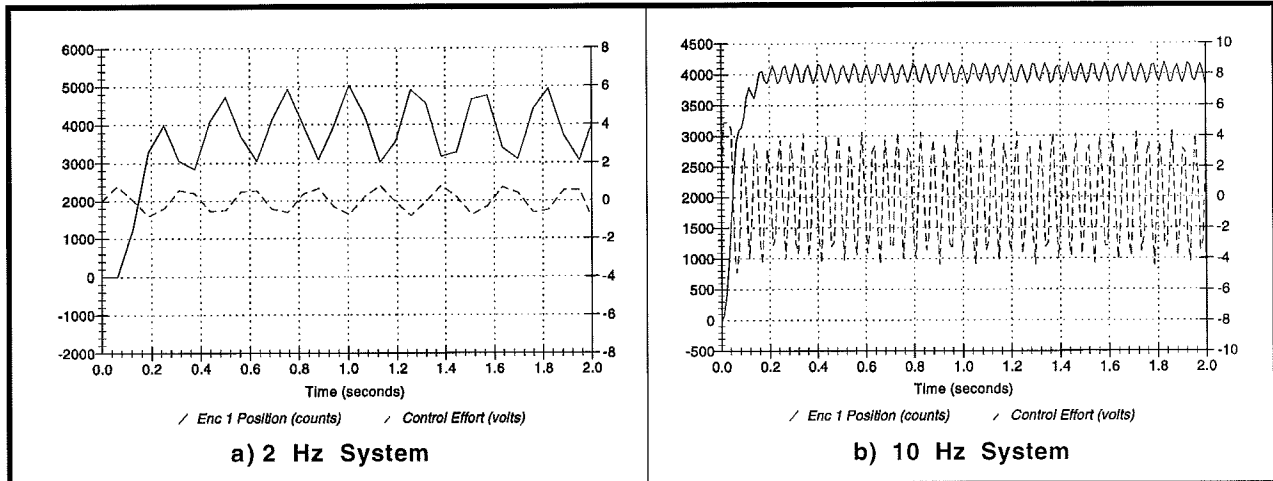


Figure 6.8-4i. Sample Rate Induced Limit Cycle Instability

**Answer to Exercise:**

D. Phase margins are both  $76^\circ$  (1.33 radians) and occur at 26 and 129 rad/s for the respective 2 and 10 Hz systems. Using the approximation by way of Eqs.(6.8-1, -2)<sup>1</sup>, we would expect instability when  $T_s\omega$  is roughly equal to the phase margin (PM) at the critical frequency. I.e. at:

$$T_s \approx PM/\omega \tag{6.8-1i}$$

$\approx 51 \text{ ms for the 2 Hz system}$

$\approx 12 \text{ ms for the 10 Hz system}$

From Figure 6.8-4, the oscillations associated with impending instability are at approximately 4 Hz (25 rad/s) and 20 Hz (126 rad/s) respectively. These correspond to the approximate critical frequency for each system. The increased sampling period has caused sufficient phase lag according to Eq. (6.8-2) to nearly encircle the -1 point and result in Nyquist instability.

Approximations similar to the pure time delay of Eq.(6.8-1) give rise to a often used rule of thumb that the sample frequency should be at least 1 decade higher than the open loop crossover frequency  $\omega_c$ . In many cases however, one should consider the continuous time phase margin in order to be certain that the thumb's rule is sufficiently conservative. For the pure time delay approximation,  $36^\circ$  of lag is levied when sampling at  $10\omega_c$  – i.e. a substantial and in some cases destabilizing amount. For sampling two decades higher than  $\omega_c$ , the phase loss is only  $3.6^\circ$ , which is negligible in most systems.

<sup>1</sup>In most industrial implementations, sampling related phase lag is not less than that of a zero order hold which has one half the phase lag of a pure time delay for a given  $T_s$ . Generally the sample and hold process is the dominant phase lag source and hence at modest sample rates Eq 6.8-1 tends to be conservative. For high sample rates, other non  $T_s$  related phase lags including those in analog signal and power processing may become significant hence the non conservative prediction for the 10 Hz system.

It may be mentioned to students that well before increases in  $T_s$  cause instability, they cause significant changes in plant dynamics – e.g. measurable changes in natural frequency and damping for the simply controlled system studied here. These topics are more rigorously studied in the context of z-domain and discrete time linear systems analyses and are readily supported by the Model 205 system and Executive software.

#### 6.8.6i Effect of Sensor Quantization

It is important that students shut down (via Abort Control) the system promptly after inducing quantization noise and that the sampling rate is lowered not more than one increment at a time when identifying  $T_s$  for noise onset. Operating the system for any time greater than a second or two while in a “strong noise” condition could damage the drive components.

1. In Step 6: Noise onset should be at 0.884 – 1.768 ms.
2. In Step 7: Noise onset should be at 2.652 ms  $\pm$  1  $T_s$  increment (0.884 ms).

**Answer to Question:**

- E. The higher minimum  $T_s$  for quantization noise onset with greater  $k_d$  is consistent with the associated control torque quantization as defined in Eq.(6.8-5).







**This section showed:**

1. High bandwidth forward path control (e.g. a differentiator) and high input acceleration (i.e. abruptly changing input trajectories) can lead to drive saturation.
2. Drive saturation can significantly reduce the system response time and alter the response shape. In higher order systems, it can lead to limit cycle instability.
3. The phase lag associated with discrete-time sampling can lead to performance changes and instability when continuous-time techniques are exclusively employed.
4. The maximum sample period to induce instability,  $T_{smax}$ , for many servo systems is approximately:  $T_{smax} = PM/\omega$ . This value should be reduced by a factor of 2 or more to furnish adequate phase margin and a more close approximation of continuous time performance.
5. Sensor quantization noise increases with high frequency gain and with increased sampling frequency.

**6.9i Sensitivity To Parameter Changes (optional)**

Experiments are easily performed that vary parameters of the plant or controller and measure the effect on system behavior. Examples of such parameters are: the system gain (e.g. via a forward path gain in the general form controller), spring constant (via moving the upper disk to the center location), and friction (either via the collocated control loop or the optional disturbance drive at other outputs). Presented below are the step and sine sweep responses of the various control systems studied in this manual as upper disk inertia,  $J_2$ , is varied. This is a practical parameter to study because in a large class of industrial applications the noncollocated inertia or "payload" may vary greatly.

Here the inertia is varied from approximately 1/2x to 2x of the nominal value. For 1/2 nominal, the two brass weights are set at 5.7 cm from the shaft centerline. For 2x, an additional set of weights is placed at a radius of 9.0 cm (this falls short of 2x by 9%.)

The results are given in Figures 6.9-1i and -2i. Note that for the Pole Placement and LQR low inertia cases, the step size has been reduced to 500 counts and the sine sweep amplitude to 100 counts. This is to eliminate a high frequency limit cycle instability in the Pole Placement system (low inertia case) due to DAC saturation. The system remains stable for inputs that result in control effort within the linear DAC range of  $\pm 5$  V. The input amplitudes for the LQR system under low inertia were reduced because the system is near its stability limit (i.e. near instability of the linear system). This system becomes unstable for approximately 20% further inertia reduction.

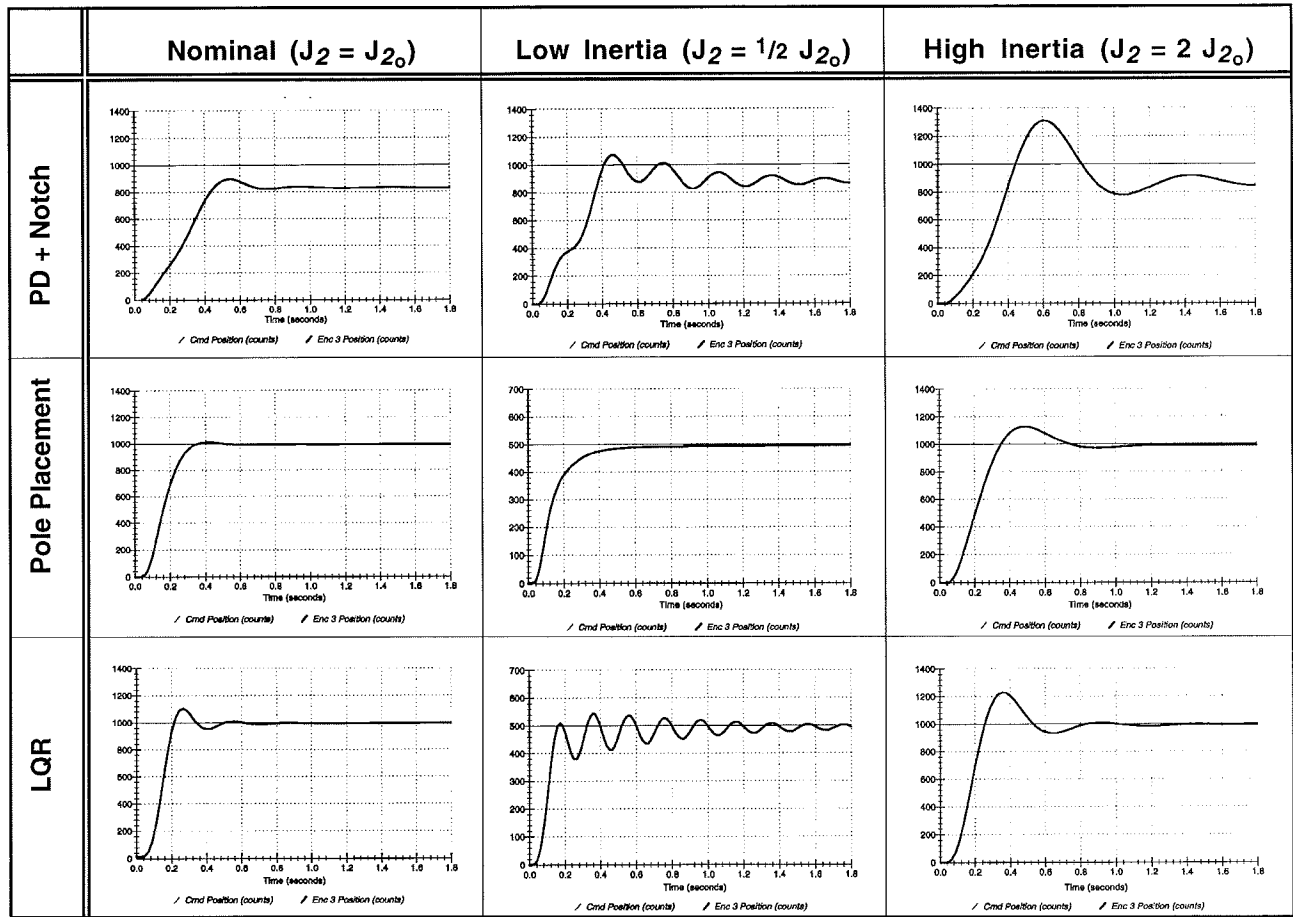


Figure 6.9-1i. Step Responses of Various Systems With Changing Inertia

In reviewing the plots, it is seen that all systems have faster response / higher bandwidth for reduced inertia (higher plant gain) and slower response / lower bandwidth (lower plant gain) for increased inertia. In general, the PID+notch filter design is most strongly affected by the inertia change followed by the LQR system, and then the successive loop / pole placement design.

In reviewing the plots of  $S_{J_2}^{c(J_2)}(\omega)$  from the respective control design experiments, the results of these plots are interpreted. The highest sensitivity occurs in the neighborhood of the system crossover frequency. With addition of inertia the greatest amplitude change occurs below the nominal crossover, with reduced inertia it occurs above. (It is this high frequency (~ 5Hz) resonance that leads to instability with further reduced inertia in the LQR system.) The high frequency amplitude is seen to scale linearly with inertia (sensitivity = 1) and the low frequency amplitude is seen to be independent of inertia (sensitivity = 0). The bandwidth, resonances, and low frequency amplitude of the frequency response plots in Figure 6.9-2 are readily correlated with the rise time, steady state amplitude, and oscillation features respectively of the step response plots of Figure 6.9-1.

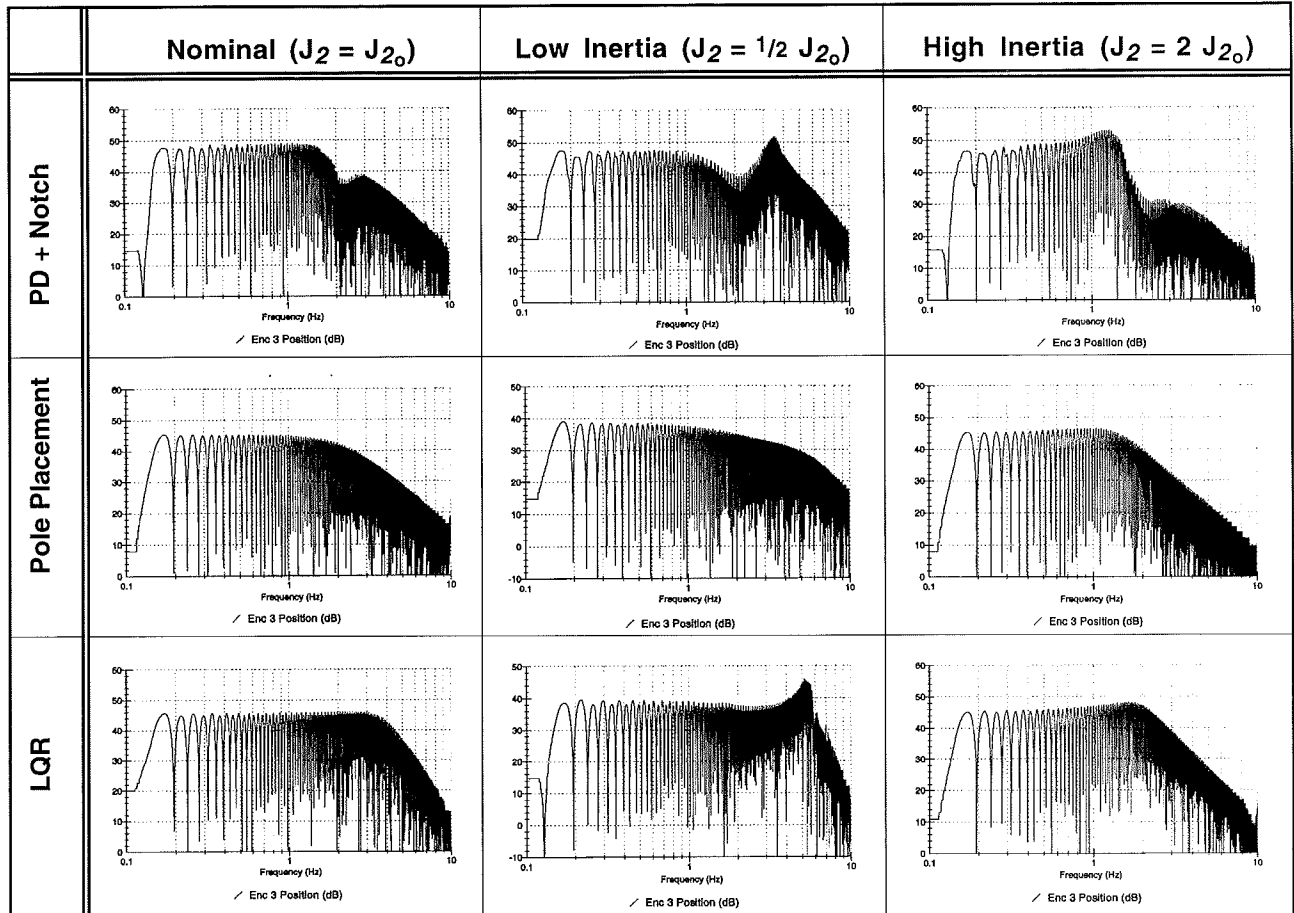


Figure 6.9-2i. Frequency Responses of Various Systems With Changing Inertia

### 6.10i Effect Of Output Disturbance on Multi-DOF Systems (optional)

The effect of an output disturbance torque on the multi-DOF systems is an important factor on evaluating system performance in many applications. Using the optional disturbance drive, it is straightforward to implement such a torque on the Model 205 plant at any of the outputs (inertia disks).

Shown in Figure 6.10-1 is the effect of low and high frequency disturbances (1 V amplitude) introduced at  $\theta_2$  (noncollocation) for the three controllers studied above. The response to low frequency disturbances torque is in agreement with the static stiffness relationships found in the above sections. Here, the pole placement design is the least stiff (i.e. at low frequency), and the LQR design shows negative displacement in  $\theta_1$  as predicted by those relationships. The higher frequency responses are in order of least attenuation to greatest according as follows: PD+Notch, Pole Placement, and LQR. This order follows the succeeding higher closed loop bandwidth for the three systems.

Tracking performance for the three systems under a spatially dependant disturbance is shown in Figure 6.10-2i (8000 count ramp at 8000 counts/second, 1 V sinusoidal disturbance at 4 cycles per revolution). Here, the PD+Notch system shows large disturbance in both  $\theta_1$  and  $\theta_2$ ; the Pole Placement system shows moderate disturbance effect at  $\theta_1$  but is successful in attenuating most of the effect at  $\theta_2$ . The LQR system shows the least effect at  $\theta_1$  and is the most effective in attenuating most of the effect at  $\theta_2$ .

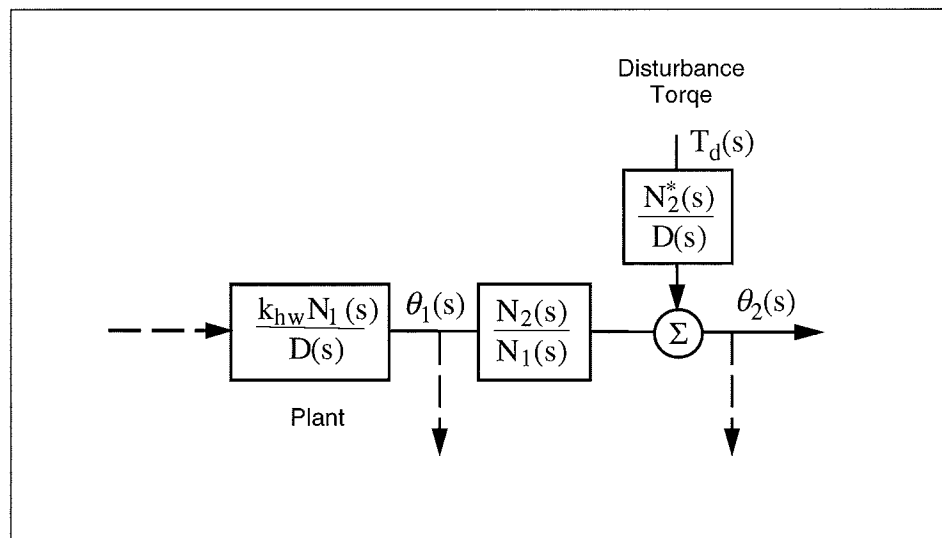


Figure 6.10-1i. Model of Disturbance At Noncollocated Output

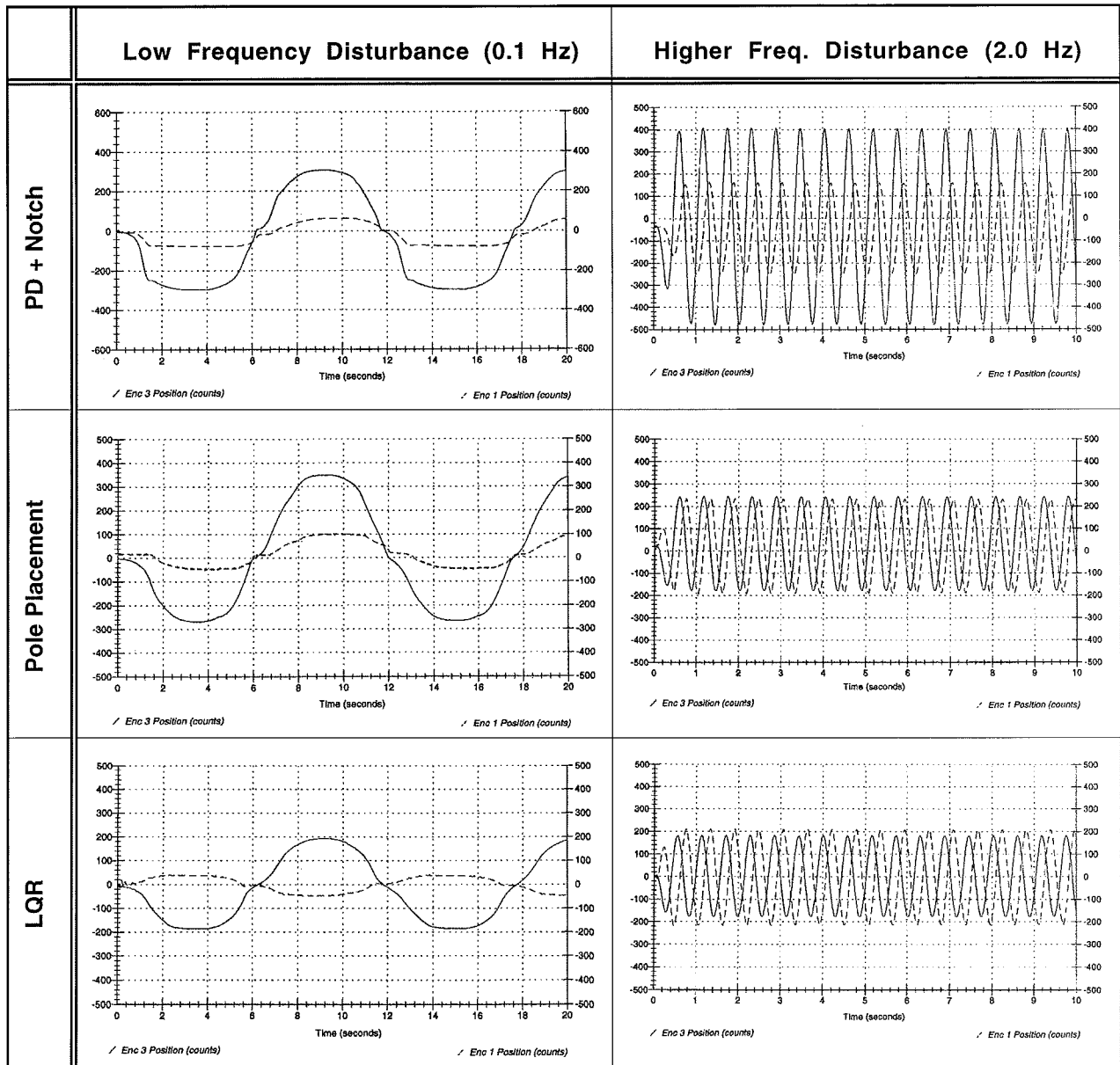


Figure 6.10-1i. Disturbance Transmission Of Three Control Systems At Low And High Frequency (Disturbance Torque At  $J_2$ )

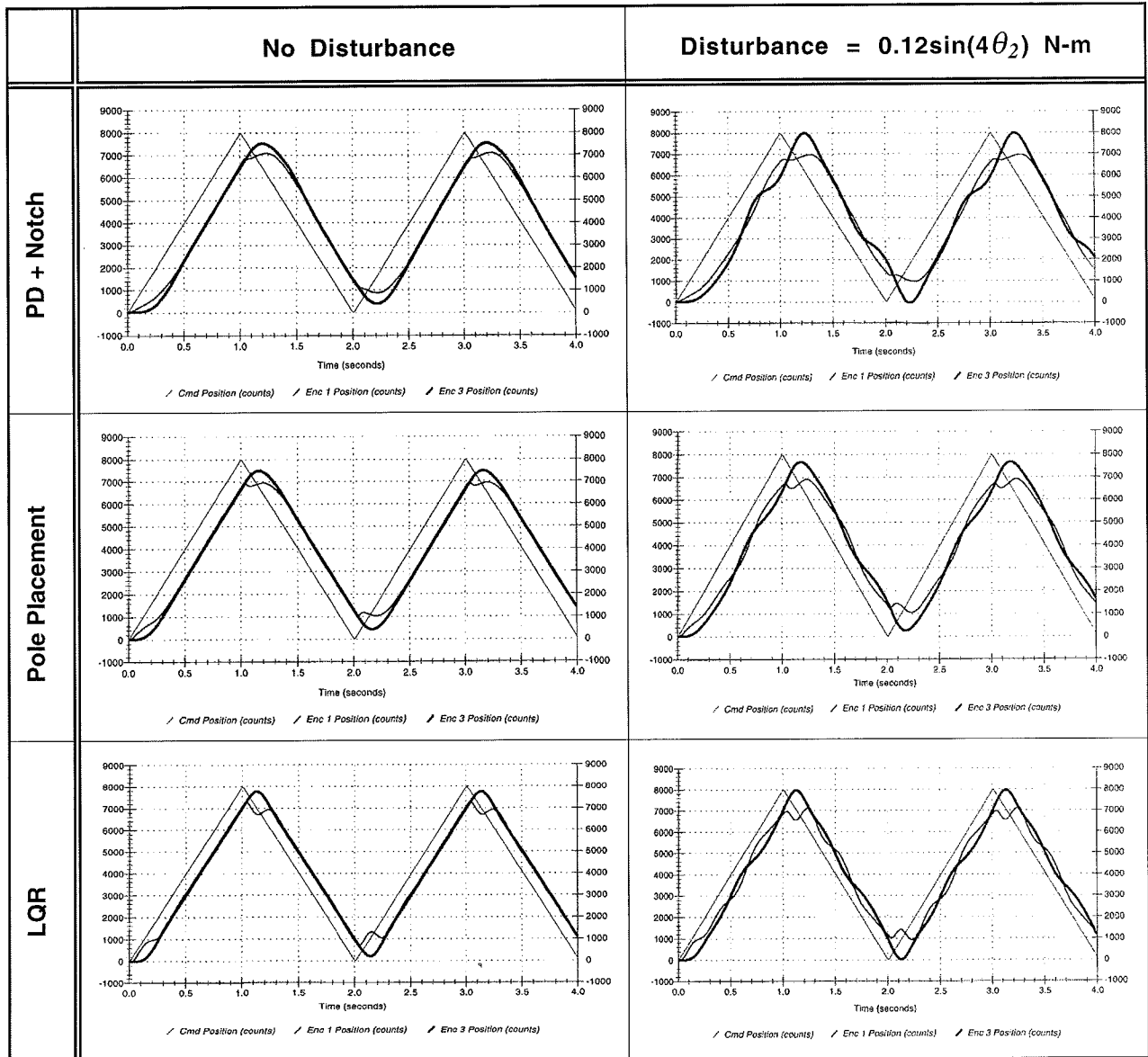


Figure 6.10-1i. Tracking Performance Of Three Control Systems Under Position Dependant Disturbance (Disturbance Torque At  $\theta_2$ )

### 6.11i Suggestions For Other Experiments

The following experiments are readily supported by the ECP control system, rectilinear apparatus, and certain system options where applicable. Still others are possible.

- 1) Dynamics: Many aspects of coupled discrete inertia systems may be demonstrated on this system. These may be done with the controls package (i.e. this manual and accompanying Controls Executive software) but is most effectively demonstrated using the dynamics & vibrations system option (Dynamics Executive software and accompanying experiments):
  - a) The interrelationship between stiffness and inertia and the modal shapes and frequencies may be analyzed, then demonstrated. (See Appendix A, main manual)
  - b) Unforced transient and harmonic response of 1, 2, and 3 DOF systems.
  - c) Characteristic responses of type 0, 1, and 2 systems
  - d) Linearity principles: Proportionality, superposition, and the convolution integral. These are dramatically demonstrated in experiments in the Dynamics manual.
  - e) Mode shapes and zeros may be vividly demonstrated by exciting the plant at the respective frequencies (use sine trajectory). By illuminating the plant with a strobe light at a frequency slightly different than the driven one, the plant will appear to slowly move through the modal shape (or the response shape at a zero frequency).
  - f) Viscous friction may be added via rate feedback, the optional disturbance drive, or approximated by the dashpot at various damping constants.
  - g) Base motion dynamics (i.e. the system boundary motion is prescribed such as in structural/seismic systems.)
  - h) The plant may be identified by modal techniques with data gathered via the encoders.
  
- 2) Digital Control
  - a) Demonstrate limitations of continuous time analysis & design assumptions by increasing  $T_s$  on a continuous time designed controller until performance is visibly altered and/or instability is immanent (usually seen as output oscillation).
  - b) Demonstrate that a significantly larger  $T_s$  can be accommodated by designing in discrete rather than continuous time.
  - c) Demonstrate digital controller implementation by simulating a controller response to an indicial input then implementing the controller and seeing the same. This may be accomplished via the general controller form by setting feedback or "downstream" gains to zero. Then perform a closed loop move (e.g. step response ) while collecting data at the appropriate node (See Figure 4.1-1).<sup>1</sup>

---

<sup>1</sup>It is a good idea to do this check on any complicated controller before implementing it.



- 3) System Robustness. In addition to the noncollocated inertia robustness tests in Section 6.9i, the following are readily demonstrated.
  - a) Change system gain (e.g. via a forward path gain in the general form controller); spring constant, or collocated inertia.
  - b) Continue changing parameters until instability is approached (often instability only occurs via inertia reduction).
  - c) Design robust controllers and test comparatively with nonrobust designs.

- 4) Disturbance Rejection

Controllers may be tested for their disturbance rejection capability. This is best implemented using the optional disturbance drive but may also be introduced manually or by ad hoc apparatus. One such possible device is a small motor (e.g. battery operated) temporarily attached to one disk and revolving an eccentric inertia. (Note that ECP is not responsible for the equipment or human safety of any such setup. The guidelines of Section 2.3 must be followed at all times). The control rejection properties at various disturbance frequencies may be tested in this way

- 5) Tracking Performance

- a) Feedforward design for improved tracking performance is readily implemented through the Setup Feedforward box under Setup Control Algorithm.
- b) Trajectories may be optimized for characteristics such as rapid response, minimum tracking error, or minimum peak control effort. The user may select from the library of geometric trajectories, or develop and implement custom shapes via User Defined in the Trajectory Configuration dialog box.

- 6) Advanced Control

The general control form supports virtually any linear controller up to and including seventh order (e.g. observer based, LQG/LTR,  $H_\infty$ , QFT).<sup>1</sup> The data acquisition, trajectory generation, and file management features of the system provide for rapid implementation and system characterization. The optional user-written algorithm for of the Executive software supports fully general control forms such as nonlinear, adaptive, fuzzy logic, variable structure, etc.

---

<sup>1</sup>The authors for example, have had good luck designing high performance and robust noncollocated controllers for this system using the loop shaping techniques and algorithms found in the MATLAB® Robust Control Toolbox. The approach for noncollocated control is generally to use collocated rate feedback and then close the high performance or robust loop through the noncollocated encoder.

Closing Note:

The control designs given here are in no sense optimized, but rather are designed to demonstrate certain fundamental principles of control. The user is invited to implement other designs or invent other approaches. We would be most appreciative if you shared them with us at ECP. Pending ECP review and your approval, it may be included in a future revision of this manual with credits of course to the inventor. For all earnest submittals, you will receive a complementary software and manual upgrade!

## Appendix Ai. Useful Scripts

Listed in this appendix are Matlab® scripts for building the numerical plant models, and some LQR related design work from Section 6.7. These are not represented as being numerically or methodologically optimal, but may be useful to some users.

### A.1i Plant Model Builder

The following script builds models of configurations 1, 2, and 3 of Section 6.1i (see Figure 6.1-2i). Parameter values used here are for a specific measured plant. For more precise results, use the identified values for your plant. Use only the script portion for one configuration at a time (i.e. Plant #1, #2, or #3).

```

%%%%%%%%%%%%%%%%%%%%%%%%%%%%%%%%%%%%%%%%%%%%%%%%%%%%%%%%%%%%%%%%%%%%%%%% Hardware Gain, khw %%%%%%%%%%%%%%%%%%%%%%%%%%%%%%%%%%%%%%%%%%%%%%%%%%%%%%%%%%%%%%%%%%%%%%%%%
kc=10/32768;
kaktkp=0.70;
ke= 16000/2/pi;
ks=32;
khw=kc*kaktkp*ke*ks

% Use any the following to build Plant #1,2,or3.

%%%%%%%%%%%%%%%%%%%%%%%%%%%%%%%%%%%%%%%%%%%%%%%%%%%%%%%%%%%%%%%%%%%%%%%% Plant #1 %%%%%%%%%%%%%%%%%%%%%%%%%%%%%%%%%%%%%%%%%%%%%%%%%%%%%%%%%%%%%%%%%%%%%%%%%
J=.0109;
cstr=.948;
N=khw/J;
D=[1 cstr 0];
% State Space model:
A1=[0 1];
A2=[0 -cstr];
Aol=[A1;A2];
B=[0 khw/J]';
C=[1 0];%For theta output

%%%%%%%%%%%%%%%%%%%%%%%%%%%%%%%%%%%%%%%%%%%%%%%%%%%%%%%%%%%%%%%%%%%%%%%% Plant #2 %%%%%%%%%%%%%%%%%%%%%%%%%%%%%%%%%%%%%%%%%%%%%%%%%%%%%%%%%%%%%%%%%%%%%%%%%
% By J,c,k identification:
J1=.0108;J2=.0103;
c1=0.007;c2=0.001;
k1=1.37;
N1=khw/J1*[1 c2/J2 k1/J2];
N2=khw*k1/(J1*J2);
D=[J1*J2 (c1*J2+c2*J1) (k1*(J1+J2)+c1*c2) (k1*(c1+c2)) 0]/(J1*J2);

% By Frequency based identification:
wp=15.71;zp=0.024;

```

```

wz=11.15;zz=.017; %Use zz=abs(imag(zero(N1))/abs(zero(N1))), where N1 is as
above
cstr=0.69;
N1=khw/J1*[1 2*zz*wz wz^2];
N2=khw*k1/J1/J2;
D=conv(conv([1 0],[1 cstr]),[1 2*zp*wp wp^2]);

% State Space model:
A1=[0 1 0 0];
A2=[-k1/J1 -c1/J1 k1/J1 0];
A3=[0 0 0 1];
A4=[k1/J2 0 -k1/J2 -c2/J2];
Ao1=[A1;A2;A3;A4];
B=[0 khw/J1 0 0]';
C=[0 0 1 0];%For theta2 output

%%%%%%%%%%%%%%%%%%%%%%%%%%%%%%%%%%%%%%%%%%%%%%%%%%%%%%%%%%%%%%%%%%%%%%%% Plant #3 %%%%%%%%%%%%%%%%%%%%%%%%%%%%%%%%%%%%%%%%%%%%%%%%%%%%%%%%%%%%%%%%%%%%%%%%%
% By J,c,k identification:
J1=.0025;J2=.0018;J3=J2;
c1=0.007;c2=0.001;c3=c2;
k1=2.7;k2=2.6;
N1=khw*[J2*J3 (J2*c3+J3*c2) (J2*k2+J3*k1+J3*k2+c2*c3) (c2*k2+c3*k1+c3*k2)
k1*k2]/J1/J2/J3;
N2=khw*k1*[J3 c3 k2]/J1/J2/J3;
N3=khw*k1*k2/J1/J2/J3;
D=[J1*J2*J3, (J1*J2*c3+J1*J3*c2+J2*J3*c1), (J1*(J2*k2+J3*k1+J3*k2+c2*c3)+J2*(J3*k
1+c1*c3)+J3*c1*c2), (J1*(c2*k2+c3*k1+c3*k2)+J2*(c1*k2+c3*k1)+J3*(c1*k1+c1*k2+c2
*k1)+c1*c2*c3), (J1+J2+J3)*k1*k2+c1*(c2*k2+c3*k1+c3*k2)+c2*c3*k1, (c1+c2+c3)*k1*
k2,0]/J1/J2/J3;

% By Frequency based identification:
wp1=35.18;zp1=0.032;
wp2=63.9;zp2=0.012;
wz1=23.1;zz1=.023;
wz2=60.1;zz2=.009;
wz=37.3;zz=.015;
cstr=1.6;
N1=khw/J1*conv([1 2*zz1*wz1 wz1^2],[1 2*zz2*wz2 wz2^2]);
N2=khw*k1/J1/J2*[1 2*zz*wz wz^2];
N3=khw*k1*k2/J1/J2/J3;
D=conv(conv(conv([1 0],[1 cstr]),[1 2*zp1*wp1 wp1^2]),[1 2*zp2*wp2 wp2^2]);

% State Space model:
A1=[0 1 0 0 0 0];
A2=[-k1/J1 -c1/J1 k1/J1 0 0 0];
A3=[0 0 0 1 0 0];
A4=[k1/J2 0 -(k1+k2)/J2 -c2/J2 k2/J2 0];
A5=[0 0 0 0 0 1];
A6=[0 0 k2/J3 0 -k2/J3 -c3/J3];
Ao1=[A1;A2;A3;A4;A5;A6];
B=[0 khw/J1 0 0 0 0]';
C=[0 0 0 0 1 0];%For theta3 output

```

### A.2i Notch Filter Designer

The following provides tools for the notch filter scheme of Section 6.5. It first solves for the desired collocated rate feedback, then for the notch filter. You should first run “Plant Model Builder”. Because there is much interaction in the various steps, these routines should be run in the groupings shown rather than in a continuous script.

```
%Perform root locus to select collocated rate feedback gain, Kv
[RL,Kv]=rlocus(conv([1 0],N1),D)

%Example Below Selects Kv = 0.01, change as per your design
Kv=0.01;
Dstr=D+[0 conv([Kv 0],N1)]
rtemp=roots(Dcol);

%The below assumes the lightly damped roots in Dcol are rtemp(2:3). The user
should verify and change the indices in rtemp below if necessary
Ntmp=poly(rtemp(2:3))

Dn=poly(2*pi*([10/sqrt(2)*[-1-i;-1+i];40*[-1-i;-1+i]]))
%Remove any imaginary part artifacts
Dn=real(Dn)
%Scale Nn for unity notch filter DC gain
Nn=Ntmp*Dn(5)/Ntmp(3)

%Check full system open loop Bode for stability margins
kd=0.001;
kp=0.060;
Nol=kp*Nn*N2;
Dol=conv(Dn,Dstr);
%Check Closed Loop Bode & Step response
Ncl=Nol;
Dcl=conv(Dstr,Dn)+[0 0 0 0 0 Nol]
```

### A.3i Successive Loop / Pole Placement Designer

The following script solves for the proportional and derivative gains for the inner loop of the controller of Section 6.6. The user specifies the desired closed loop poles of the outer loop based on the assumption that the inner loop has unity gain. The script then solves the diophantine equation to find the outer loop controller  $S(s)/R(s)$ . You should first run “Plant Model Builder”.

```
% PDPOLPLC.M
% This script first solves for the PD gains kp & kd for the collocated inner
% loop, then S(s)/R(s) for pole placement control of theta
% You must first run Plant Builder

% INNER LOOP PD CONTROL
% Input desired natural frequency, wnhz (Hz), and damping ratio, z
wnhz=10;
```

```

wn=wnhz*2*pi;
z=1;

% Calculate kp & kd.
kp=wn^2*J1/khw
kd=2*z*sqrt(J1*kp/khw)

% For mechanical parameter forms of Nstr, & Dstr: (Comment out if not used)
Nstr=k1/J2
Dstr=[1 c2/J2 k1/J2]

% OUTER LOOP POLE PLACEMENT CONTROL
% Input desired closed loop poles, pi to construct desired closed loop
denominator, Dcl:
% Specify wclhz (Hz) for poles at 135, 180, & 225 deg.
wclhz=2.5,
wcl=wclhz*2*pi;
p1=-wcl/sqrt(2)*(1+i);
p2=-wcl/sqrt(2)*(1-i);
p3=-wcl;
% The following is for third order Butterworth poles. These provide a faster
rise time
% but with more overshoot than the above; decomment if preferred (Poles at
120, 180, & 240 deg.)
%p1=-wcl/2*(1+sqrt(3)*i);
%p2=-wcl/2*(1-sqrt(3)*i);
%p3=-wcl;
%Create specified closed loop denominator
Dcl=poly([p1;p2;p3]);
% Solve Diophantine Equation for S(s) & R(s) via Sylvester matrix
SYLVa=toeplitz([Dstr zeros(1,1)],zeros(1,2));
SYLVb=toeplitz([[0 0 Nstr] zeros(1,1)],zeros(1,2))
SYLV=[SYLVa SYLVb];
SR=SYLV\Dcl';
S=SR(3:4)';
R=SR(1:2)';
kpf=(R(2)*Dstr(3)+S(2)*Nstr)/Nstr
% For discrete implementation use Sd(z) & Rd(z)
%[Sd,Rd]=c2dm(S,R,ts,'tustin')

%Plot simulation of idealized (c(s)=1) closed loop system
t=0:.02:2.5;
Ncli=kpf*Nstr;
Dcli=[0 0 conv(Nstr,S)]+conv(Dstr,R);
stepi=step(Ncli,Dcli,t);
plot(t,stepi),grid,pause

```

## A.2i LQR Synthesis

The script below is useful in LQR design and in comparing experimental step responses with the ideal continuous time ones.

```
% The following generates a family of LQR controllers and plots the
% resulting closed loop poles. You must have first generated the
% A,B, & C matrices.

Q=C'*C;

Klqr1=lqr(Aol,B,Q,100);
Klqr2=lqr(Aol,B,Q,10);
Klqr3=lqr(Aol,B,Q,1);
Klqr4=lqr(Aol,B,Q,.1);
Klqr5=lqr(Aol,B,Q,.01);
Klqr6=lqr(Aol,B,Q,.001);

Pcl1=eig(Aol-B*Klqr1)/2/pi;
Pcl2=eig(Aol-B*Klqr2)/2/pi;
Pcl3=eig(Aol-B*Klqr3)/2/pi;
Pcl4=eig(Aol-B*Klqr4)/2/pi;
Pcl5=eig(Aol-B*Klqr5)/2/pi;
Pcl6=eig(Aol-B*Klqr6)/2/pi;

% Plot Roots
axis([-8,1,-8,8])
plot(Pcl1,'x')
hold;
plot(Pcl2,'o');
plot(Pcl3,'*');
plot(Pcl4,'+');
plot(Pcl5,'. ');
plot(Pcl5,'o');
plot(Pcl6,'*');
plot(Pcl6,'o');
title('LQR Controller, Closed Loop Poles For Various Control Effort Weights')
xlabel('Real (Hz)')
ylabel('Imaginary (Hz)')
grid;
hold;
pause
% User may define labels, frequencies in Hz.
% Stike any key to continue

% Continuous time step responses:
t=0:.02:2;
%Must multiply by sum of proportional gain terms (this becomes the prefilter
%gain). Given is for the two disk case. For three disks, Klqrj(5)
%(j=1,...,6) must be added to the step response coefficient sum.
```

```
steplq1=(Klqr1(1)+Klqr1(3))*step([Aol-B*Klqr1],B,C,0,1,t);
steplq2=(Klqr2(1)+Klqr2(3))*step([Aol-B*Klqr2],B,C,0,1,t);
steplq3=(Klqr3(1)+Klqr3(3))*step([Aol-B*Klqr3],B,C,0,1,t);
steplq4=(Klqr4(1)+Klqr4(3))*step([Aol-B*Klqr4],B,C,0,1,t);
steplq5=(Klqr5(1)+Klqr5(3))*step([Aol-B*Klqr5],B,C,0,1,t);
steplq6=(Klqr6(1)+Klqr6(3))*step([Aol-B*Klqr6],B,C,0,1,t);

%Example Step Response Plot
axis([0,2,0,1.2]);
plot(t,[steplq1 steplq3 steplq5]);
title('Step Response, LQR Controlled System')
xlabel('Time (sec)')
ylabel('Theta 2 Response')
grid
```